

A  
T H E S I S  
entitled

THE GEOCHEMISTRY AND MINERALOGY OF SOME  
FERROMANGANESE OXIDES AND ASSOCIATED  
DEPOSITS FROM THE INDIAN  
AND ATLANTIC OCEANS

submitted for the degree of  
DOCTOR OF PHILOSOPHY  
in the

FACULTY OF SCIENCE OF THE UNIVERSITY OF LONDON

by

STEWART ANTHONY MOORBY

Royal School of Mines,  
Imperial College

October 1978

A B S T R A C T

Ferromanganese nodules and encrustations from sites throughout the Indian Ocean have been analysed for Mn, Fe, Co, Ni, Cu, Zn, Pb, Ca and Al and in some cases Cd, Cr and Ti also, by atomic absorption spectrophotometry. The mineralogy of these deposits has also been investigated using X-Ray diffraction techniques. A suite of Indian Ocean sediment samples, many of them from the same sites at which nodules were recovered, have also been analysed for the same elements by the same chemical techniques. Nodules and associated sediment samples from detailed traverses across two different Indian Ocean basins have in addition been subjected to a series of selective chemical attacks.

Different trends in the composition of the ferromanganese-oxides occur in samples from sea-mounts, the mid-ocean ridge and basin areas. The observed trends and possible reasons for them are discussed. An attempt is made to account for these variations in terms of environments of deposition as defined by element source and availability, rate and type of sedimentation and authigenic oxide mineralogy.

The principal manganese minerals present are todorokite and  $\delta$ -MnO<sub>2</sub>. These minerals are found to develop preferentially in different environments and the reasons for this observation are discussed.

Regional variations in the chemical composition of surface sediments also occur in the Indian Ocean which are broadly similar, but not nearly so marked, as those seen in the ferromanganese-oxide deposits.

The variations observed in the chemical partitioning of major and trace elements between the fractions examined is complex for both nodules

and sediments and no simple relationship links the partitioning of elements in nodules with their partitioning in the same fraction of associated sediments.

A suite of ferromanganese-oxide samples from several sites in a small area of the north-east Atlantic Ocean have also been analysed chemically and mineralogically by the same techniques. The bulk chemistry of these deposits is rather different to the Indian Ocean deposits, as is their chemical partitioning. The authigenic minerals present are similar but goethite is much more abundant than in Indian Ocean samples. The reasons for the observed chemical and mineralogical variations are discussed.

## A C K N O W L E D G M E N T S

The work presented in this thesis was carried out during the period October 1973 to September 1976 in the Applied Geochemistry Research Group of the Royal School of Mines at Imperial College. The project was under the general direction of Professor J.S. Webb and was supervised throughout by Dr. D.S. Cronan to whom I would like to express my gratitude.

Many other people have given help and guidance during the project. In particular I would like to thank:

The Master, officers and scientists on R.R.S. Shackleton on legs 5 and 7 of the Indian Ocean cruises 1975 during which many samples were obtained from the north-west Indian Ocean.

Dr. J. Swallow of the Institute of Oceanographical Sciences, Wormley, for kindly allowing me to participate in leg 7 of the R.R.S. Shackleton Indian Ocean cruises and for donating ship time to allow samples to be collected.

The Scripps Institution of Oceanography, University of California and the Lamont-Doherty Geological Observatory for generously providing many of the nodule and sediment samples used.

Dr. H. Backer of Preuesag, for kindly providing nodule and sediment samples from the Central Indian and Madagascar Basins, collected during cruises of the research vessel "Valdivia" in the Indian Ocean.

Professor J.S. Cann, University of East Anglia, for providing nodule samples from the north-east Atlantic Ocean.

Sincere thanks are due to Mr. R. Curtis for his invaluable help in



the problems of analysis of the samples by X-Ray diffractometry.

Particular thanks are also due to the technical staff of the Applied Geochemistry Research Group for carrying out chemical analyses.

Members of the department both past and present for useful advice and discussion, particularly the following:- Mr. M. Horder, Dr. A. Horowitz, Dr. M. Thompson, Mr. T. Thompson.

Mrs. Richardson for assistance with photographic work.

Miss J. Turner for help with reproducing diagrams.

Miss C. Fetherston and particularly Miss P. Beavan for typing the manuscript.

The work was supported by a Natural Environment Research Council grant for which I am most grateful.

TABLE OF CONTENTS

ABSTRACT	Page (i)
ACKNOWLEDGEMENTS	(iii)
CONTENTS	(v)
LIST OF FIGURES	(x)
LIST OF TABLES	(xiv)
LIST OF PLATES	(xvi)

INTRODUCTION

PART ONE 1

<u>SECTION 1</u>	GEOLOGY OF THE INDIAN OCEAN	2
(i)	Introduction	2
(ii)	Structure and evolution	3
(iii)	Sedimentation:-	12
(a)	Sedimentation rates	13
(b)	Sediment type	23
 <u>SECTION 2</u>	 OCEANOGRAPHY	 31
(i)	Ocean currents	31
(ii)	Biological productivity	37
 <u>SECTION 3</u>	 SAMPLE DISTRIBUTION AND MORPHOLOGY	 44
(i)	Distribution	44
(ii)	Morphology:-	47
(a)	Size	50
(b)	Shape	53
(c)	Shape and texture of surface	59
(d)	Internal features	65

<u>SECTION</u>		Page
<u>4</u>	MINERALOGY	74
(i)	Introduction	74
(ii)	Mineralogy of the ferromanganese phases of Indian Ocean samples:-	80
	(a) Mineralogy of the manganese phases	81
	(b) Mineralogy of the iron phases	82
(iii)	Other minerals	82
(iv)	Discussion	84
(v)	Conclusions	97
<u>5</u>	BULK GEOCHEMISTRY OF FERROMANGANESE OXIDE DEPOSITS	99
(i)	Introduction	99
(ii)	Local variations in sample compositions:-	100
	(s) Compositional variations within single samples	101
	(b) Compositional variations between samples from the same site	101
(iii)	Mineralogical influence on composition	112
(iv)	Inter-element associations	114
(v)	Areal variability	125
(vi)	Geochemistry of north-west Indian Ocean samples	143
<u>6</u>	BULK GEOCHEMISTRY OF SEDIMENTS	151
(i)	Introduction	151
(ii)	Sediment type	153
(iii)	Geochemistry:-	154
	(a) Treatment of data	154
	(b) Comparison of composition of sediment in contact with nodule and additional sediment from the same horizon	156
	(c) Comparison of composition of surface sediment with sediment from depth	158
	(d) Inter-element associations	162
	(e) Regional geochemistry of surface sediments	165
(iv)	Nodule-sediment interrelationships	181

<u>SECTION</u>		Page
<u>SECTION 7</u>	PARTITION GEOCHEMISTRY	192
(i)	Introduction	192
(ii)	Element partition:-	195
	(a) Average partition in nodules	196
	(b) Average partition in sediments	200
	(c) Range of partition values	201
	(d) Discussion	203
(iii)	Comparison of partition in nodules and sediments from different basins:-	210
	(a) Element partition in nodules	210
	(b) Discussion	213
	(c) Element partition in sediments	219
	(d) Discussion	221
(iv)	Individual element partition along the traverses:-	224
	(a) Variation in nodule partition along the traverses	227
	(b) Variation in sediment partition along the traverse	255
	(c) Nodule-sediment interrelationships	260
(v)	Discussion	260
 <u>SECTION 8</u>	 REGIONAL GEOCHEMISTRY	 265
 <u>SECTION 9</u>	 DISCUSSION	 282
(i)	Regional geochemistry:-	282
	(a) Major elements: source influences	282
	(b) Major elements: mineralogical influences	290
	(c) Minor elements	292
(ii)	Summary and conclusions	298
 <u>PART TWO</u> 		
 <u>SECTION 10</u>	 SAMPLE LOCATION AND DESCRIPTION	 301
(i)	Introduction	301

<u>SECTION 10</u> (Continued)	Page
(ii)(a) Setting and general geology	301
(b) Sedimentation	305
(c) Sample location	306
(iii) Sample morphology	307
<u>SECTION 11</u> MINERALOGY	311
(i) Introduction	311
(ii) Mineralogy of the ferromanganese phases	314
(iii) Other minerals	316
(iv) Discussion	317
<u>SECTION 12</u> GEOCHEMISTRY	319
(i) Introduction	319
(ii) Compositional variation of samples from the same station	319
(iii) Inter-element associations	322
(iv) Regional geochemistry	326
(v) Partition geochemistry:-	328
(a) Average partition values in all samples	332
(b) Variation in element partition with depth	335
<u>SECTION 13</u> DISCUSSION	337
REFERENCES	347
APPENDICES	364
<u>APPENDIX 1</u> Chemical Analytical Techniques	365
(i) Sample preparation	365
(ii) Bulk chemical attack	366
(iii) Selective leach techniques	367
(iv) Analytical precision and accuracy	369
(v) Selective attacks on minerals and synthetic phases	370

<u>APPENDIX 1</u> (Continued)	Page
(vi) Correction procedure for Ca interference	373
<u>APPENDIX 2</u> Mineralogical Analysis	377
(i) Sample preparation	377
(ii) Analysis	377
(iii) Problems of identification of $\delta$ -MnO <sub>2</sub> in samples containing todorokite	378

LIST OF FIGURES

Figure		Page
1	Map of the Indian Ocean showing the main geographical and physiographic features	4
2	Rates of sedimentation in surface sediments of the Indian Ocean	14
3	Thickness of unconsolidated sediments in the Indian Ocean	18
4	Clay mineral provinces in the Indian Ocean	25
5	Distribution of surface sediment type in the Indian Ocean	28
6	Major bottom currents in the Indian Ocean	33
7	Primary phytoplankton productivity in the Indian Ocean	38
8	Total zooplankton biomass in the Indian Ocean	39
9	Carbonate critical depth and lysocline variation in the Indian Ocean	42
10	Distribution of ferromanganese nodules in the Indian Ocean	45
11	Ferromanganese oxide sample sites in the Indian Ocean	49
12	Distribution of todorokite in Indian Ocean ferromanganese oxide samples	85
13	Distribution of birnessite in Indian Ocean ferromanganese oxide samples	88
14	Distribution of $\gamma\text{-MnO}_2$ in Indian Ocean ferromanganese oxide samples	91
15	Distribution of Indian Ocean ferromanganese oxide samples containing no identifiable manganese phase	94
16	Distribution of goethite in Indian Ocean ferromanganese oxide samples	96
17	Variation in chemical composition of morphologically similar samples from the same sample station	104

Figure		Page
18	Variation in chemical composition of morphologically dissimilar samples from the same sample station	107
19	Scatter plot for Mn - Fe -(Ni x 10)	132
20	Scatter plot for Mn - Fe -(Cu x 20)	133
21	Scatter plot for Mn - Fe -(Zn x 100)	134
22	Scatter plot for Mn - Fe -(Co x 50)	136
23	Scatter plot for Mn - Fe -(Pb x 100)	137
24	Scatter plot for Mn - Fe -(Cu + Ni) x 10	139
25	Scatter plot of average values of Mn, Fe and (Ni + Cu) for different physiographic regions of the Indian Ocean	140
26	Scatter plot for Mn - Fe -(Co + Pb) x 50	141
27	Scatter plot of average values of Mn, Fe and (Co + Pb) for different physiographic regions of the Indian Ocean	142
28	Compositional variations with depth in north-west Indian Ocean ferromanganese oxide deposits	148
29	Distribution of sediment sample sites in the Indian Ocean	152
30	Regional variation of Mn in Indian Ocean sediments	167
31	Regional variation of Fe in Indian Ocean sediments	168
32	Regional variation of Co in Indian Ocean sediments	169
33	Regional variation of Ni in Indian Ocean sediments	170
34	Regional variation of Cu in Indian Ocean sediments	171
35	Regional variation of Zn in Indian Ocean sediments	172
36	Regional variation of Pb in Indian Ocean sediments	173
37	Regional variation of Ca in Indian Ocean sediments	174
38	Regional variation of Al in Indian Ocean sediments	175
39	Compositional variations in Madagascar Basin surface sediments	178
40	Compositional variations in Central Indian Basin surface sediments	180



Figure		Page
41	Variation on Mn values in nodules and associated bulk sediments	183
42	Variation of Fe values in nodules and associated bulk sediments	184
43	Variation of Co values in nodules and associated bulk sediments	185
44	Variation of Ni values in nodules and associated bulk sediments	186
45	Variation of Cu values in nodules and associated bulk sediments	187
46	Mean partition values in Indian Ocean nodules and sediments	197 - 198
47	Mean partition values in nodules from the Central Indian and Madagascar Basins	211 - 212
48	Mean partition values in sediments from Central Indian and Madagascar Basins	217 - 218
49	Sample sites in the Madagascar Basin	225
50	Sample sites in the Central Indian Basin	226
51	Mn partition in Central Indian and Madagascar Basin nodules and sediments	228 - 229
52	Fe partition in Central Indian and Madagascar Basin nodules and sediments	230 - 231
53	Co partition in Central Indian and Madagascar Basin nodules and sediments	232 - 233
54	Ni partition in Central Indian and Madagascar Basin nodules and sediments	234 - 235
55	Cu partition in Central Indian and Madagascar Basin nodules and sediments	236 - 237
56	Zn partition in Central Indian and Madagascar Basin nodules and sediments	238 - 239
57	Pb partition in Central Indian and Madagascar Basin nodules and sediments	240 - 241
58	Cd partition in Central Indian and Madagascar Basin nodules and sediments	242 - 243
59	Cr partition in Central Indian and Madagascar Basin nodules and sediments	244 - 245
60	Ca partition in Central Indian and Madagascar Basin nodules and sediments	246 - 247

Figure		Page
61	Al partition in Central Indian and Madagascar Basin nodules and sediments	248 - 249
62	Ti partition in Central Indian and Madagascar Basin nodules and sediments	250 - 251
63	Regional variation of Mn in Indian Ocean ferromanganese oxide deposits	266
64	Regional variation of Fe in Indian Ocean ferromanganese oxide deposits	268
65	Regional variation of Ni in Indian Ocean ferromanganese oxide deposits	270
66	Regional variation of Cu in Indian Ocean ferromanganese oxide deposits	272
67	Regional variation of Zn in Indian Ocean ferromanganese oxide deposits	274
68	Regional variation of Co in Indian Ocean ferromanganese oxide deposits	277
69	Regional variation of Pb in Indian Ocean ferromanganese oxide deposits	278
70	Regional variation of Ca in Indian Ocean ferromanganese oxide deposits	279
71	Regional variation of Al in Indian Ocean ferromanganese oxide deposits	280
72	Mn/Fe ratios of Indian Ocean ferromanganese oxide deposits	285
73	Map of Atlantic Ocean showing location of sample area	303
74	Bathymetric map of Horseshoe Sea-Mount area showing sampling localities	304
75	Distribution of Mn minerals in north-east Atlantic Ocean samples	313
76	Range in bulk composition of samples from the north-east Atlantic Ocean	321
77	Element variation with depth in Atlantic Ocean ferromanganese oxide samples	325
78	Mean partition values in Atlantic Ocean ferromanganese oxide samples	329
79	Means and standard deviations of element partitions in Atlantic Ocean ferromanganese oxide samples	330

LIST OF TABLES

Table		Page
1	Diffraction patterns of the manganese phases recognised in Indian Ocean ferromanganese oxides	78
2	Frequency of occurrence of manganese minerals in Indian Ocean ferromanganese oxides	81a
3	Results of heating experiments carried out on sample 91 GBX	81a
4	Powder patterns of selected ferromanganese oxide samples	82a
5	Powder patterns of selected ferromanganese oxide samples containing goethite	82c
6	Average depth and depth range of various authigenic phases in Indian Ocean ferromanganese oxides	86a
7	Comparison of average composition with composition of outer layer of an encrustation from the mid-Indian Ocean Ridge	102
8	Average composition of samples of different mineralogy	113
9	Table of correlation coefficients for Indian Ocean ferromanganese oxide samples	116
10	Minimum values of correlation coefficients significant at the 95% and 99% confidence levels	117
11	Average compositions and compositional ranges of samples from various physiographic regions of the Indian Ocean	126-129
12	Correlation coefficients for north-west Indian Ocean ferromanganese oxide samples	146
13	Comparison of composition of sediments associated with ferromanganese oxide deposits	157
14	Composition of sediments from different horizons at the same sample site	159
15	Correlation coefficients for Indian Ocean sediments	163
16	Average composition of surface sediments from different physiographic regions of the Indian Ocean	166

Table		Page
17	Comparison of metal ratios in nodules and sediments and average sediment thicknesses in different physiographic regions of the Indian Ocean	188
18	Material present in pelagic nodules and sediments	193
19	Summary of compositional trends observed in Indian Ocean ferromanganese oxide deposits	295
20	Summary of compositional variability of Indian Ocean ferromanganese oxide deposits in relation to mineralogy, element source and type of substrate	297
21	Diffraction patterns of the manganese phases recognised in Atlantic Ocean ferromanganese oxides	312
22	Mineralogical composition of Atlantic Ocean nodules and encrustations	315
23	Correlation matrices for Atlantic Ocean ferromanganese oxides	323
24	Comparison of average composition of Atlantic Ocean ferromanganese oxide samples analysed in the present study with previously published data	344

LIST OF PLATES

Plate		Page
1a	Sample SH 1301D	51
1b	Sample SH 1301D	51
2	Sample SH 1301D	52
3	Sample SH 1301D	52
4	Sample CIRCE 116D	54
5	Sample AB 387C	54
6	Sample 101GBD	56
7a	Sample ANTP 109D	58
7b	Sample ANTP 109D	58
8	Sample ANTP 109D	60
9a	Sample ANTP 153D	62
9b	Sample ANTP 153D	62
10	Sample AB 384B	64
11	Sample AB 367C	64
12a	Sample SH 1307D	66
12b	Sample SH 1307D	66
13	Sample SH 1317D	68
14	Sample ANTP 113D	68
15	Sample 85GK	70
16	Sample AB 384C	70
17	Sample RC 14/D4	72
18	Sample SH 73:178.4	309
19	Sample SH 73:178.3	309

## I N T R O D U C T I O N

Ferromanganese nodules have been a source of interest and controversy ever since their discovery during the Challenger Expedition of 1873 - 1876, reported by Murray and Renard (1891). Research work on these deposits, however, was rather sporadic until the late 1950's and early 1960's when more detailed sampling of the deposits in all three major world oceans revealed their vast extent and highlighted their significance as possible ore deposits.

Despite the great amount of work which has now been carried out in this field, many basic problems pertaining to marine ferromanganese-oxide deposits remain unsolved. Among the unsolved geochemical problems which these deposits still pose are the relative importance of the sources of major and trace elements in the authigenic phases, the rates and mechanisms of growth of the deposits and the way in which the minor elements are incorporated into the deposits. Many major reviews of the subject, covering one or more of these problems, are to be found in the literature and the reader is referred to the following as giving fuller accounts of these problems: Murray and Renard (1891); Goldberg (1954); Goldberg and Arrhenius (1958); Goldberg (1961); Arrhenius (1963); Arrhenius and Bonatti (1965); Bonatti and Nayudu (1965); Mero (1965); Bonatti, Kraemer and Rydell (1972); Cronan (1976).

The problem of the ultimate source of the Mn and Fe in the deposits has been a source of disagreement since the earliest times (see Murray and Renard, 1891). The two major proposals are, on the one hand, that these metals are derived predominantly from continental run-off as

proposed by Renard (in Murray and Renard, 1891) and on the other that submarine volcanism supplies the bulk of these metals as first suggested by Murray (in Murray and Renard, 1891). Whilst some early workers tended to support one or other of these sources, others suggested that both sources may be of importance (e.g. Arrhenius, Mero and Korkisch, 1964). More recent work (Bonatti, Kraemer and Rydell, 1972; Elderfield, 1976; Lyle, 1976) has tended to show that any one of several major sources may be predominant depending on the area of the ocean floor under consideration.

In order to consider fully the problems of the geochemistry of ferromanganese oxide deposits it has become obvious that factors other than their geochemistry must be considered. Thus in recent years much detailed work has been done on specific aspects of the deposits. Since the pioneering investigations of Buser and Grutter (Buser and Grutter, 1956; Grutter and Buser, 1957) the mineralogy of the authigenic Mn and Fe phases of the deposits has received detailed examination by many workers (e.g. Andrushchenko and Skornyakova, 1969; Herzenberg and Riley, 1969; Burns and Brown, 1972; Giovanoli et al, 1973). This work has been reviewed in some detail by Burns and Burns (1977).

The internal structure of nodules and inter-element associations on a microscopic scale within single samples has also been examined in detail (Sorem, 1967; Andrushchenko and Skornyakova, 1969; Cronan and Tooms, 1969; von Heimendahl et al, 1976). Attempts have also been made to find relationships between the chemical composition of nodules and encrustations and other factors such as their mineralogy (Crerar and Barnes, 1974), their growth rates (Heye and Marchig, 1977), the rate of accumulation of accompanying sediment (Price and Calvert, 1970), the physical properties of the substrate (Horn et al, 1973) and the chemical composition of the underlying sediment (Calvert and Price, 1977), whilst yet others have tried to discover the mechanisms by which the trace metals are incorporated in the deposits (Burns, 1976).

A comprehensive study of the geochemistry and mineralogy of marine ferromanganese oxide deposits therefore, cannot be confined simply to these two features of the deposits, if satisfactory answers are to be found to the various problems which are raised. Consideration, then, must also be given to the factors affecting the geochemistry and mineralogy of the deposits. Thus factors such as rate and type of sedimentation, chemical composition of accompanying sediment, element source and degree of oxygenation of the bottom environment must all be examined in order to assess their effect on nodule and encrustation geochemistry and mineralogy. Although the amount of research being carried out on these topics has greatly increased in recent years our knowledge of some of these factors is still limited, particularly in the Indian Ocean.

In this thesis therefore, several topics of a non-geochemical nature are described and discussed as a background to the work so that their effects on the geochemistry and mineralogy of the deposits can be assessed. Thus Sections 1, 2 and 3 deal with the oceanography and geology (including sedimentology) of the Indian Ocean and the morphology and internal structure of the deposits. Sections 4 and 5 deal with the mineralogy and bulk geochemistry of the deposits whilst Section 6 deals with the bulk geochemistry of some associated sediments. In Section 7 an examination is carried out of the chemical partitioning of the elements between various fractions in nodules and sediments and of whether any correlations exist between the two types of deposit. In Section 8 the regional bulk geochemistry of Indian Ocean ferromanganese oxides is examined by combining data from this thesis with that from previous studies, thus providing the most detailed picture yet obtained of the regional geochemistry of these deposits in the Indian Ocean. An attempt is made in Section 9 to account for the variations observed in terms of the various factors examined in the preceding Sections.



In the second part of this thesis (Sections 10 to 13) a brief examination is made of several ferromanganese oxide deposits from the north-east Atlantic Ocean and an attempt made to account for their geochemical and mineralogical variations in terms of the same factors as those used in Part 1 of this thesis. A comparison is made of the composition of these deposits with deposits elsewhere in the Atlantic Ocean reported in the literature and the differences in chemical partitioning between these deposits and those from the Indian Ocean are discussed.

PART ONE

## SECTION 1

### GEOLOGY OF THE INDIAN OCEAN

#### (i) INTRODUCTION

The Indian Ocean is the smallest of the world's three major oceans, covering an area of about 75 million square kilometres, and stretching from the coasts of Arabia, India and south-east Asia in the north to south of latitude 55°S where it merges with the Southern Ocean. The African continent marks its western boundary whilst the eastern extremity is bounded by Australia and the complex Indonesian Archipelago. The ocean is marked by a peculiarly large number of island groups, Madagascar, Rodriguez, Réunion, Mauritius and the Seychelles, Amirantes, Farquhar and Comoro groups in the west; the Chagos and Laccadive Island groups in the central northern area; the Cocos and Christmas Island groups in the east and the Prince Edward, Crozet, New Amsterdam, Heard and Kerguelen Islands in the south and south-west. Geographically it is the most remote of the three major oceans from the main centres of marine research, in the U.S.A. and Europe, and as a result has received less study in the past, than have the Atlantic and Pacific Oceans.

## (ii) STRUCTURE AND EVOLUTION

The Indian Ocean is the most structurally complex and least understood of the major world oceans. An important feature of this ocean is the large number of continental fragments it contains, such as the Seychelles Islands, Madagascar, the Agulhas, Kerguelen-Heard, Broken and Naturaliste Plateaux. All these fragments have to be accounted for in any structural reconstruction of the history of the Indian Ocean. Fortunately there is another characteristic of the Indian Ocean, which is helpful in piecing together its history and that is the almost complete lack of ocean trenches which are presently active or have been active in the past. This means that much of the sea-floor formed at the ridges in the past must still exist and as more data become available it should prove possible to put together more and more accurate reconstructions of the ocean's pre-Quaternary history.

### Active Ridges

At the present time, the major structural features of the Indian Ocean are conveniently revealed by the 1 k.m. and 4 k.m. bathymetric contours, as can be seen from figure 1. The most marked and continuous structural feature of the Indian Ocean, and one which has a profound effect on the ocean's oceanography, stratigraphy, and geochemical characteristics, is the mid-ocean ridge system. This lies predominantly in the western part of the ocean. At 70°E, between the equator and 20°S, it runs approximately north-south, but to the north of this it swings to the north-west and runs into the Gulf of Aden and the Red Sea. This north-west part of the ridge system is called the Carlsberg Ridge. South of 20°S and to the east of Mauritius, Réunion and Rodriguez

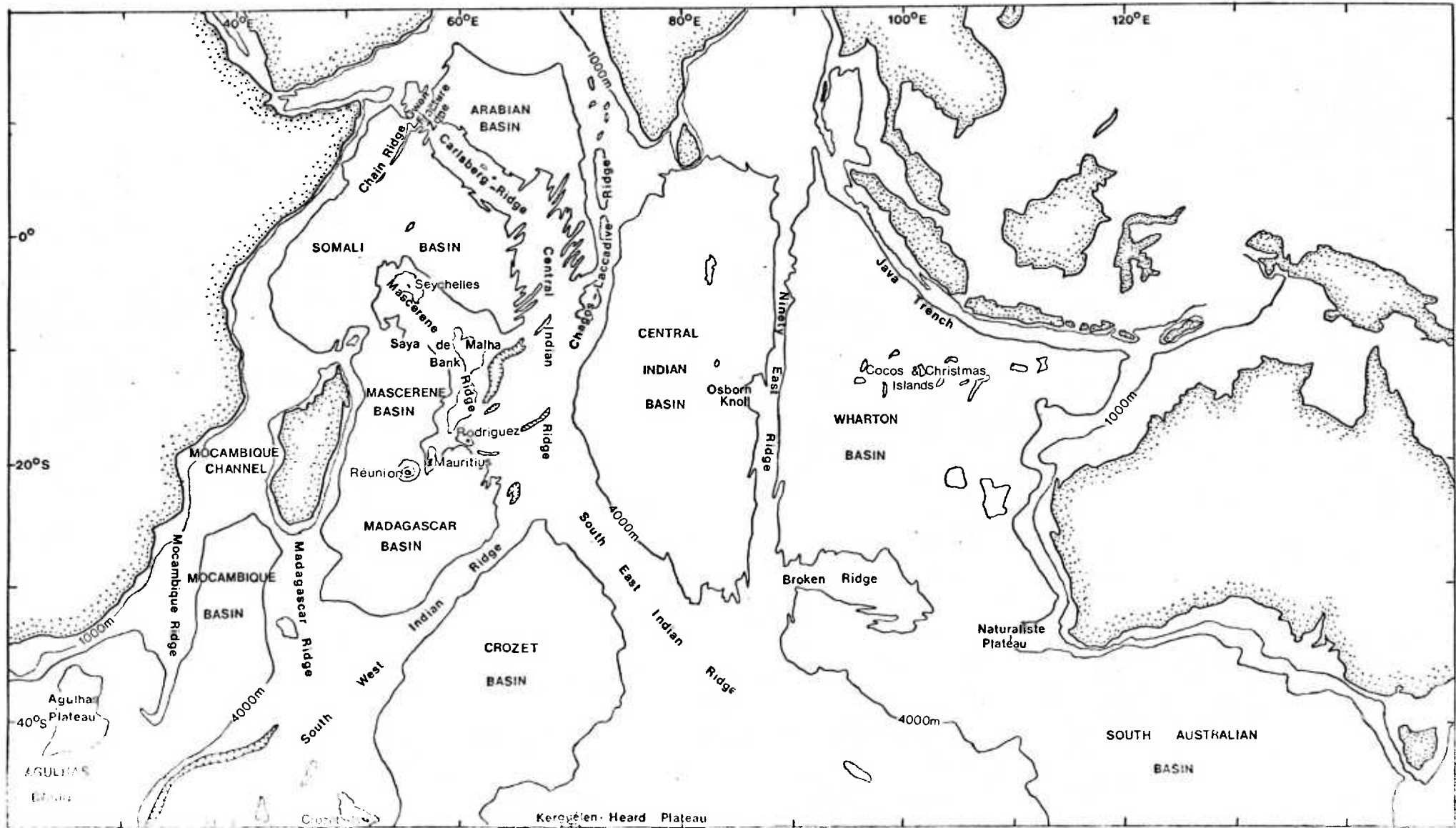


Figure 1. Map of the Indian Ocean basin, its main geotectonic and physical features.

Islands the ridge bifurcates into a south-west and a south-east trending component, forming an RRR-type triple junction (McKenzie and Sclater, 1971)

Although apparently north - south trending, magnetic surveys of the Central Indian Ridge (Fisher, Sclater and McKenzie, 1971) have shown that this section is in fact a complex set of an echelon north-west - south-east trending spreading centres and north-east - south-west fracture zones. This feature is also clearly marked by the 4 k.m. bathymetric contour. Magnetic analyses of the south-east Indian ridge (Sclich and Patriat, 1971; Weissel and Hayes, 1971) show this to be a simpler ridge with somewhat fewer fracture zones. However, the south-west Indian Ridge appears to have many north-north-east - south-south-west trending fracture zones which dominate the sections of an echelon spreading centres (Bergh, 1971). This ridge appears to have been the least volcanically active, slowest-spreading of the three ridge axes during the last 20 million years (McKenzie and Sclater, 1971) and like the Central Indian Ridge has a more rugged topography than the south-east branch, the comparative smoothness of which is typical of more rapidly spreading ridges (Menard, 1967).

#### Inactive Ridges

Within the Indian Ocean there are several ridges which are not seismically active and which do not appear to be spreading centres, being intra-plate features rather than plate margins. The most striking of these ridges is the Ninety East Ridge. This ridge is remarkable in its length and topography, stretching 4800 k.m. almost due north - south and splitting the eastern Indian Ocean into two distinct basin areas (see figure 1). According to Laughton, McKenzie and Sclater (1972) the Ninety East Ridge

formed originally as a simple transform fault formed by the rapid northward movement of Greater India during the late Cretaceous and early Tertiary. Francis and Raitt (1967) suggest that its topographic expression is due simply to uplift of volcanic crust along the fault and not to volcanism and this idea is backed up by gravity studies over the feature (Le Pichon and Talwani, 1969). Luyendyk and Davies (1974) suggest a more complicated three-phase origin for this ridge. North of  $7^{\circ}\text{S}$  they regard the ridge as being the trace of a volcanic point source. Between  $7^{\circ}\text{S}$  and the Osborn Knoll they suggest the ridge was formed by volcanism along a "leaky" part of the transform fault boundary. South of the Osborn Knoll the ridge formed originally as a volcanic trace, then became overprinted by volcanism along the transform fault boundary formed by the southward jump of the south-east Indian Ridge which occurred some 35 to 40 million years ago (Laughton, Matthews and Fisher, 1971). According to McKenzie and Sclater (1971) the northward extension of the Ninety East Ridge has been consumed by the same trench which consumed the Tethyan Oceanic crust north of India.

To the west of the Ninety East Ridge lies the Chagos-Laccadive Ridge. This ridge is also a north - south trending feature, lying at about  $70^{\circ} - 75^{\circ}\text{E}$  and stretching from  $10^{\circ}\text{S}$  to  $15^{\circ}\text{N}$  where it runs close to India, sub-parallel with the coast. This ridge, and the Mascarene Ridge to the south-west are both equidistant from the Central Indian Ridge and the ridge-associated fracture zones all terminate against these two features. On the assumption that the Central Indian Ridge has spread symmetrically the Mascarene and Chagos-Laccadive Ridges must have been contiguous at the start of spreading on this ridge (McKenzie and Sclater, 1971). As the Central Indian Ridge became volcanically active the Chagos-Laccadive

and Mascarene Ridges began to form, either by volcanic events along the "leaky" transform fault which formed the western analogue of the Ninety East Ridge or by drift over a hot-spot area. Some segments of the ridge however, especially the Maldive Islands segment, may be microcontinents rifted away from India during the early phases of movement of the Indian Plate (Avraham and Bunco, 1977).

The origins of the Mozambique, Madagascar and Rodriguez Ridges are not clear. Laughton, Matthews and Fisher (1971) suggest that the Mozambique and Madagascar Ridges are continental fragments and Kutina (1975) has suggested that they are horst structures formed by the subsidence of the intervening Mozambique Channel and Basin area which occurred as early as the Lower Jurassic (175 m.y. B.P.). According to Laughton, Matthews and Fisher (1971) the Rodriguez Ridge was formed by left-lateral movements along a west-north-west - east-south-east trending fracture zone in the late Tertiary, during the same hiatus which formed the volcanic islands of Réunion, Mauritius and Rodriguez.

#### Continental Fragments

The Indian Ocean is unique in the number and complexity of fragments of continental crust entrapped within it. The largest of these and most problematical in terms of origin is Madagascar. Most reconstructions of Gondwanaland place Madagascar against the East African coast between the equator and 10°S (Dietz and Holden, 1970; McElhinney, 1970; McElhinney and Luck, 1970) however no satisfactory explanations of its subsequent movement have been produced. According to Smith and Hallam (1970) Madagascar had moved to its present position by the mid-Cretaceous, however, no magnetic anomalies or fracture zones have been found in the western Indian Ocean which might lend



weight to this theory. Kutina (1975) has presented a very strong argument, using geological evidence, to suggest that Madagascar has not moved from its present position with respect to Africa since the break-up of Gondwanaland.

Another important continental fragment lies to the north-east of Madagascar, this is the Seychelles Plateau. Like Madagascar, it is predominantly of pre-Cambrian age and the islands in the Seychelles group form the only granitic mid-oceanic islands in the world (Baker, 1963). Much of its movement seems to have occurred early in the Indian Ocean's history and its arrival at its present position and its fit in the reconstruction of Gondwanaland are still not fully understood.

Other areas of the Indian Ocean floor which have supposedly continental crustal structure are Broken Ridge (Francis and Raitt, 1967), Kerguelen-Heard Ridge (Laughton, McKenxie and Sclater, 1972) and the Agulhas Plateau (Laughton, Matthews and Fisher, 1971). According to Johnson et al (1976) only the south-eastern part of the Kerguelen Plateau has a continental structure and this was at one time contiguous with the Broken Ridge structure. These two features separated during an early phase of spreading on the south-east Indian Ridge 20 million years ago.

It is still not known how the Agulhas Plateau fits in to the original fragmentation of Gondwanaland and its continental structure has even been questioned by Le Pichon and Heirtzler (1968) who detected large magnetic anomalies across it.

#### Continental Margin Area

The structure of the continental margins bordering the Indian Ocean shows marked differences between northern and southern areas. In western Australia, south-east Africa and Antarctica the margins are typical of inactive margins found elsewhere in

the world, with well-defined shelves and steep slopes. Off East Africa the margin is downwarped and has considerable sediment thickness (see figure 3) making the true edge of the continent hard to determine. In the Arabian Sea and Bay of Bengal a similar situation occurs, with large-scale depression and modification of the crust (Curry & Moore, 1971). Intense earthquake activity in the Java Trench areas and its island-arc structure show this area to be one of subduction, consuming the oceanic crust of the Wharton Basin, generated to the south. This appears to be the only presently active subduction zone in the Indian Ocean.

A more detailed survey of Indian Ocean structure is beyond the needs of this thesis and reference should be made to the detailed discussions of this subject given by McKenzie and Sclater (1971) and Laughton et al (1971) for fuller accounts of particular aspects.

#### Evolution of the Indian Ocean

It is sufficient here to give merely a brief résumé of the ocean's evolution. Fuller accounts of this topic are given by McKenzie and Sclater (1971), Laughton et al (1972), Luyendyk and Davies (1971) and Johnson et al (1976).

The oldest magnetic anomalies so far identified in the Indian Ocean crust are only about 75 million years old and detailed reconstruction can only be carried back this far. Prior to this plate movements have to be inferred from polar wandering curves of the continents and interpretation is therefore very conjectural.

Initial movements within Gondwanaland (comprising South America, Africa, India, Australia and Antarctica) began during the Upper Permian (McElhinney & Luck, 1970) when Africa and Antarctica jointly moved northward away from the other continents. It is not

known exactly when Africa and Antarctica parted or when India began its northward flight from Antarctica, however the former is thought to have happened in the late Jurassic, 140-120 m.y. B.P., (McElhinney, 1970) and the latter in the early Cretaceous, 120 to 110 m.y. B.P., (Johnson et al, 1976). In the Upper Cretaceous the evolution of the ocean was dominated by the rapid northward migration of India, by as much as 17 c.m. per year, causing an oceanic part of the Indian Plate to be transferred to the Antarctic-Australian Plate (Johnson et al, 1976). This period of spreading produced much of the northern Central Indian Basin and southern part of the Crozet Basin and continued to the end of the Palaeocene (about 50 m.y. B.P.). Thus whilst most of the Wharton Basin is of Cretaceous age, the Central Indian Basin south of the equator is Palaeocene to Miocene in age. At about this time Australia and Antarctica began to separate, with the inception of the South-East Indian Ridge. The Australian, Antarctic and Indian Plates continued to spread at a slow rate until the early Oligocene (32 m.y. B.P.) when the separate Indian and Australian plates became united by sealing of the transform fault now forming the Ninety East Ridge. More recently south-east Asia appears to have rotated westwards across the sea-floor generated by India's northward flight, and to have arrived at its present position no more than 10 million years ago, consuming part of the Indian Plate in the Java Trench system. The ocean floor to the south-east of the Java Trench in the northern Wharton Basin has been shown to be the oldest part of the Indian Ocean floor (Dietz and Holden, 1971; Luyendyk and Davies, 1974) probably at least as old as the late Jurassic (Heirtzler et al, 1973). An interesting and not yet satisfactorily explained feature of this part of the ocean is the broad chain of isolated seamounts trending east-west which form

the Cocos and Christmas Island groups. The area is weakly seismically active and this has led Sykes (1970) to propose that this may be the site of a nascent island arc system, but the evidence is far from clear.

In the western Indian Ocean the main spreading centre between 75 and 45 million years ago lay to the north of the Seychelles. This generated the sea floor which now forms the Arabian Basin and part of the Somali Basin. Thus the extensive sea-mounts in the Northern Somali Basin, if they were formed at the ridge crest and have since migrated due to subsequent sea floor spreading, must be Eocene in age and 40 to 50 million years old. This northern spreading centre was linked to the one south of India by the Mascarene-Chagos-Laccadive Ridge which at this time was a complementary transform fault to the Ninety East Ridge, facilitating the northward movement of India. The northern spreading centre was terminated in the north-west by the Owen Fracture Zone - Chain Ridge structure (Laughton et al, 1972). Between about 55 and 35 million years B.P. relatively little new oceanic crust was produced in the western Indian Ocean, and in the south western part of the ocean this quiescent period lasted until 20 million years B.P., however some considerable movement along transform faults is likely to have occurred.

In the last 35 million years the African, Indian and Antarctic Plates have all moved apart along the slow-spreading Carlsberg Ridge (1.2 cm./year/limb), the Central Indian Ridge (2.3 cm. / year/limb), the faster spreading South-East Indian Ridge (3 cm. / year/limb) and the very slow-spreading, highly fractured, South West Indian Ridge (<1 cm. /year/limb). The Madagascar Basin now forms part of the Somalian Plate but magnetic lineations south of Réunion Island show that much of this basin formed as part of the

Antarctic Plate (McKenzie & Sclater, 1971). The south-west Indian Ridge must therefore have broken through the Antarctic Plate, splitting off the Madagascar Basin and transferring it to the Somalian Plate. Contrary to what might be expected therefore the floor of the Madagascar Basin ages from north-east to south-west where at its oldest it is at least early Palaeocene in age (65 million years B.P.). It appears that very little contribution to the floor of this basin has been made by spreading along the south-west Indian Ridge. To the north of the Madagascar Basin, the Mascarene Basin has not shown any clear magnetic lineations and McKenzie and Sclater (1971) regard this part of the ocean floor as being older than late Cretaceous. To the south-east of the Madagascar Basin, the northern part of the Crozet Basin appears to have been produced almost exclusively from spreading along the south-east Indian Ridge rather than the south-west branch, and north of about  $35^{\circ}\text{S}$  is of Palaeocene and younger age.

The evolution of the Indian Ocean south and west of the Madagascar Ridge is extremely uncertain, however it seems that several continental fragments may occur in this area and that the Mozambique Basin and Channel area may be graben-type structures rather than having been formed by sea-floor spreading (Kutina, 1975).

### (iii) SEDIMENTATION

As with many aspects of the Indian Ocean, study of its sediments has not been as detailed as that carried out in the other major oceans. However, two sedimentary parameters appear to be of great importance in controlling the distribution and composition of marine ferromanganese nodules, these are sedimentation rate and sediment type (Price & Calvert, 1970;

Greenslate et al, 1973; Horn et al, 1973; Lyle et al, 1977). These parameters and their variability throughout the Indian Ocean are examined in the following discussion.

(a) Sedimentation Rates

Early studies of sedimentation rates in the Indian Ocean (Baranov & Kuzima, 1958; Starik et al, 1958; Goldberg & Koide, 1963) all involved very limited numbers of samples. Moreover these are not directly comparable studies since the Russian workers age-dated their samples using total Th content of the sample whilst Goldberg and Koide tried to eliminate Th introduced by land-derived detrital minerals. Furthermore, Goldberg and Koide re-calculated their data on a biogenic carbonate-free and silicate-free basis and so their figures are not indicative of total sediment accumulation rates. However all three groups of workers agreed that sedimentation rates in the Indian Ocean seemed to be intermediate between those observed in the south Pacific and those observed in the north Pacific and Atlantic Oceans. A later study, using 40 core samples, by Opdyke and Glass (1964) confirmed these findings, and observed sedimentation rates in pelagic areas of between 3 mm. and 7 mm. per thousand years. However, on elevated ridge areas they observed sedimentation rates of 10 mm. to 20 mm. per thousand years.

As a result of the International Indian Ocean Expedition in the early 1960's much more material became available for study, seismic studies revealed the thickness of unconsolidated sediments throughout the ocean and sedimentation rates were calculated using isotopic and magnetic reversal techniques on the many cores collected. Using this information it became possible to compile a map showing variation in total sedimentation rates throughout the Indian Ocean, and this is shown in figure 2. From this map

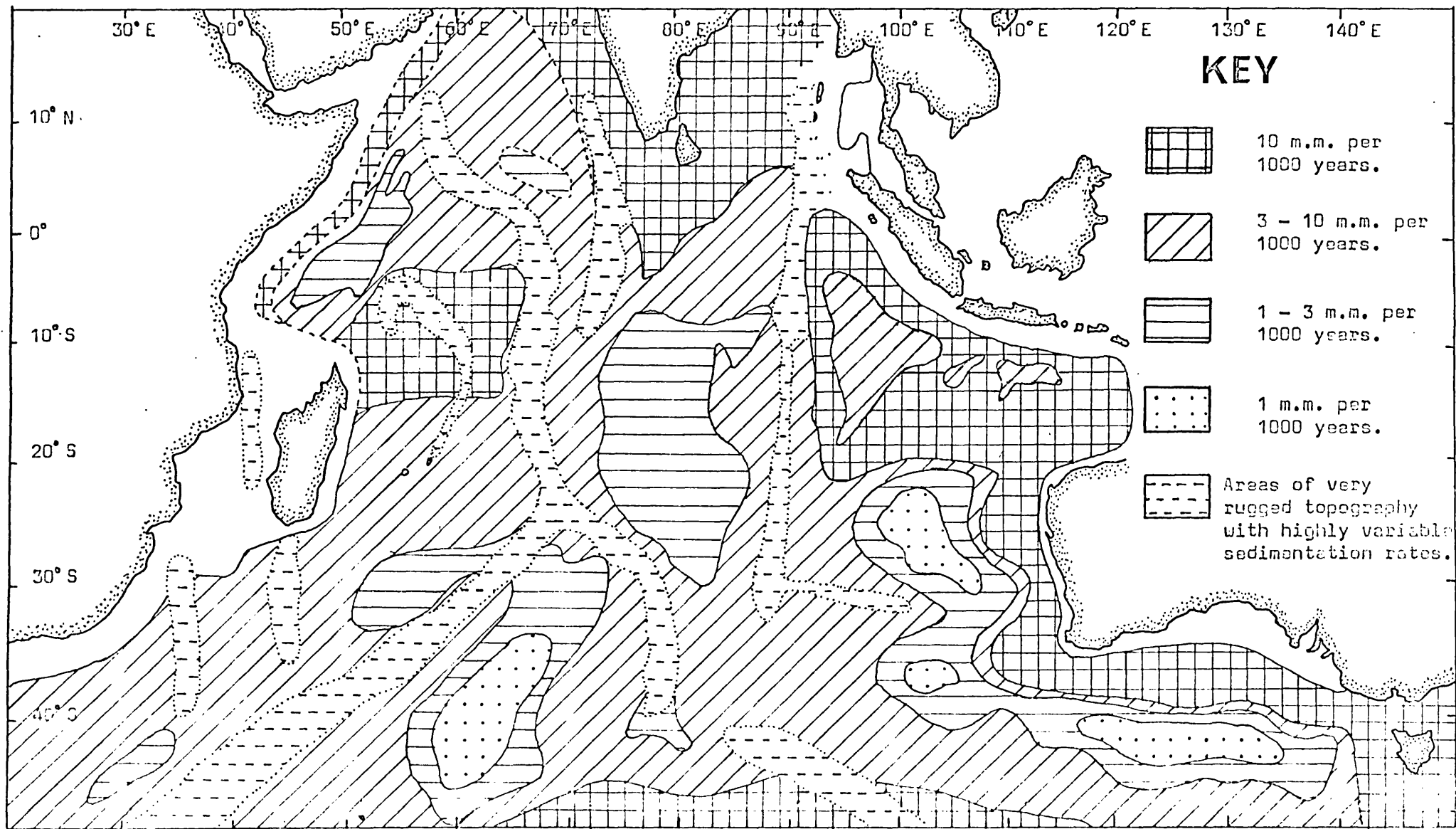


**FIGURE 2** Rates of sedimentation in surface sediments of the Indian Ocean (adapted from Udintsev et al, 1970)

it can be seen that there are three areas of the Indian Ocean with high sedimentation rates (i.e. greater than 10 mm. per thousand years). The largest of these, and the area where sedimentation is the most rapid of all, lies in the northern part of the ocean forming a wide band around the coastline of India. This area of high sedimentation stems from the huge input of terrigenous material brought down by the great Indian rivers, especially the Indus and the Ganges, which supply, respectively, 435 million tons and 1450 million tons of sediment per year to the Indian Ocean (Rateev et al, 1969). A thin belt of the ocean floor receiving equally rapid sedimentation extends from this northern area down the east coast of Africa and Arabia. It is likely that a thin strip of rapid sedimentation girdles the whole of Africa and Madagascar but no details of sedimentation rates in this near-coastal area are known at present.

A second zone of rapid sedimentation occupies the southern part of the Somali Basin and the northern Mascarene Basin, stretching over the intervening Seychelles Plateau and Saya de Malha Bank. In view of its geographical position this area is not likely to be receiving large amounts of continental run-off except perhaps in the extreme south-west. The high sedimentation rate therefore is probably due to rapid deposition of biogenic carbonate material in an area of the sea-floor which is above the carbonate compensation depth (C.C.D.) and lies beneath a zone of high biological productivity (see Section 2).

A third area of high sedimentation rates occupies much of the northern part of the Wharton Basin and from here stretches in a thin band round the coast of Australia thence southwards into the Antarctic zone of high biological productivity. The high sedimentation rates in the Wharton Basin are difficult to account for,



particularly since much of the ocean floor here is well below the carbonate compensation depth. Continental run-off is unlikely to be a major contribution to the sediments of the Wharton Basin since no large rivers drain into it from Australia and much of the run-off from the Indonesian Archipelago is likely to be trapped in the Java Trench system. However, the northern part of the basin is characterised by many sea-mounts and these may have a significant, though local effect on sedimentation rates due to slumping down their flanks. This mechanism was put forward by Opdyke and Glass (1969) as an explanation for the sedimentation rates of up to 20 mm. per thousand years which they observed in this basin.

Apart from the Wharton Basin, low sedimentation rates are typical of the deep basin areas below carbonate compensation depth and beyond the limits of transport of land derived material by turbidity currents. Such provinces occur in the northern Somali Basin and distal parts of the Arabian Abyssal Plain, in central and southern areas of the Central Indian Basin, in southern parts of the Madagascar and Wharton Basins and much of the Crozet Basin. The areas with the lowest sedimentation rates occur in the Crozet Basin and parts of the southern Wharton and South Australian Basins. These areas appear to be areas of strong bottom current activity and there is evidence that sediment erosion rather than deposition may be occurring at the present time in these areas (Kolla et al, 1976; Kennett and Watkins, 1975). Bottom current activity may also be a cause of low sedimentation rates in the southern part of the Madagascar Basin (Kolla et al, 1976c). No data on sedimentation rates are available for the Mozambique Channel area although in view of the large rivers draining into this area sedimentation rates are likely to be high.

However, there is evidence of strong bottom current activity in the area (Vincent, 1972; Kolla et al, 1976c) and these currents may markedly affect sedimentation rates producing local provinces of slow- or even non-deposition.

Most of the elevated regions of the Indian Ocean, especially the mid-ocean ridge system, are characterised by high sedimentation rates (Opdyke and Glass, 1969), mainly by virtue of their being above the carbonate compensation depth, and thus receiving large amounts of biogenic carbonate débris. However, because of the very rugged nature of the topography of these regions sedimentation rates can fluctuate wildly over comparatively short distances, rendering any measurement of an average sedimentation rate for such areas almost meaningless.

The thickness of accumulated sediment is obviously a function of sedimentation rate and time. Thus if the age of the oceanic crust in a particular locality is known it can be roughly ascertained whether or not present rates of sedimentation are similar to those which operated in the past. Ewing et al (1969) compiled a map of unconsolidated sediment thickness in the Indian Ocean using seismic profile data (see figure 3). From this diagram it can be seen that areas with thick accumulations of sediment generally correspond to areas with rapid sedimentation rates. This is especially marked in the area of the ocean fed with sediment by the Indus and Ganges rivers. According to Ewing et al (1969), 40% of the total volume of sediment on the Indian Ocean floor is to be found in the huge abyssal fans produced by these two rivers. At its thickest the Ganges cone is more than 3 km. thick and Ewing et al (1969) have estimated that sedimentation rates on the cone since the mid-Miocene have been as high as 170 mm. per thousand years.

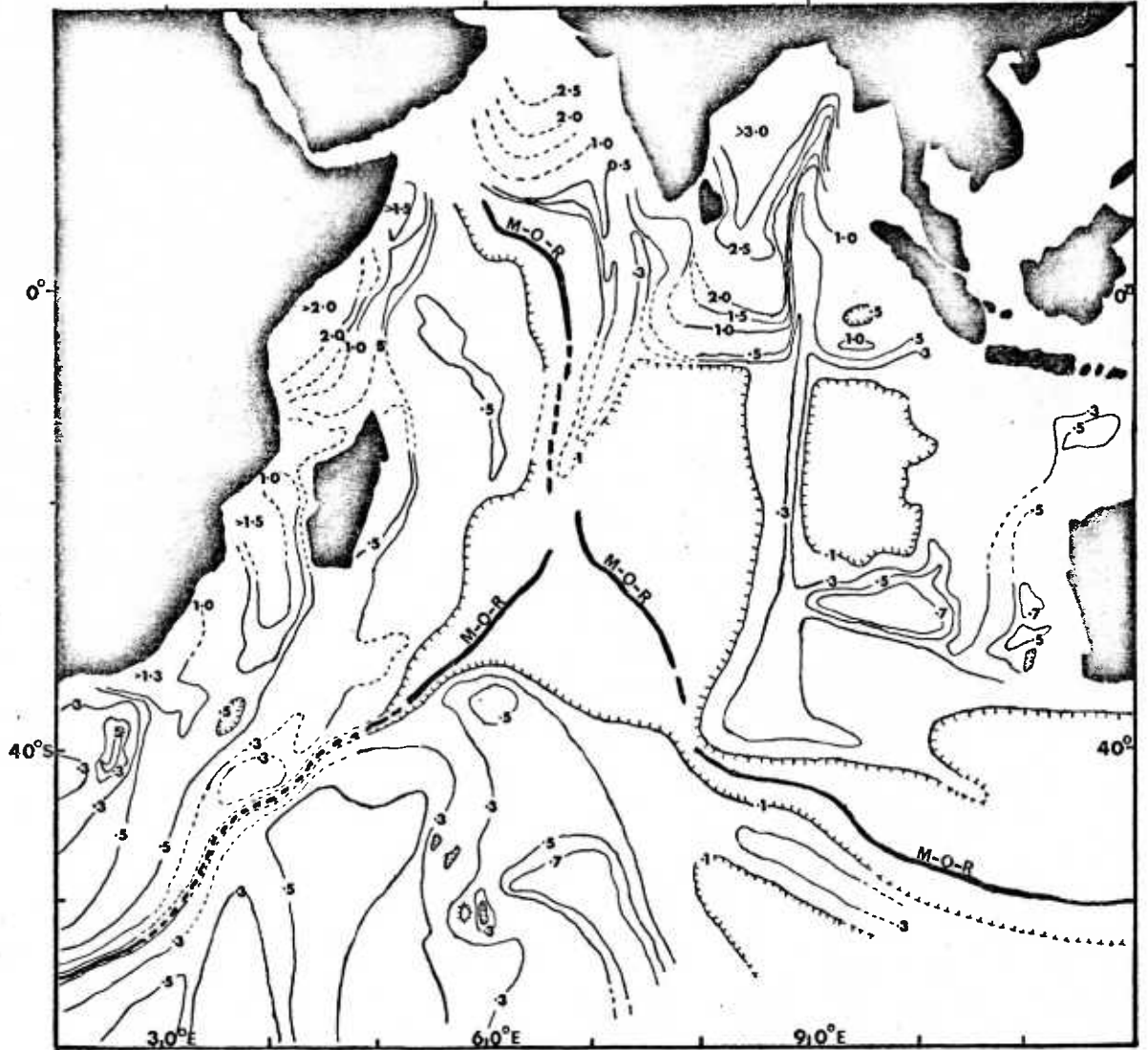


**FIGURE 3** Thickness of unconsolidated sediments in the Indian Ocean measured by seismic reflection studies (from Ewing et al 1969).

Contours in seconds of travel time (1 sec.  $\approx$  100 m. of sediment).

There are some regions with comparatively thick sediment cover but where sedimentation rates are at present very low, this applies in particular to the south-western part of the Crozet Basin and the southern Wharton Basin. Evidence from cores taken in the vicinity of Australia, however (Payne and Conolly, 1972; Watkins and Kennett, 1973) shows that there has been a marked increase in bottom current velocity around Australia during the last 3.5 million years. This current, produced by an increased supply of Antarctic Ocean Bottom Water (AABW) has caused widespread winnowing and erosion of sediments in the South Australian and southern Wharton Basins (Kennett and Watkins, 1975). This comparatively recent change in sedimentation pattern is reflected in the low sedimentation rates measured over the last three-quarters of a million years and shown in figure 2, but is in contrast to the generally higher sedimentation rates which must have been operating prior to this, as evinced by the total sediment thickness which is shown in figure 3. The low sedimentation rates presently occurring in the Crozet Basin may be partly due to similar scouring action by AABW flowing northward in this basin (Kolla et al, 1976c). According to Ewing et al (1969) the area of thicker sediment cover at about 40°S in the western Crozet Basin is a small abyssal plain formed by intermittent slumping of material from the Crozet Plateau to the south-west.

The generally high sedimentation rates in much of the Indian Ocean west of 65°E are in agreement with the fairly thick sediment accumulations present in much of this region. Similarly the low sedimentation rates occurring in the southern parts of the Central Indian and Madagascar Basins are in agreement with the thin sedimentary accumulations there, even allowing for the fact that parts

of these basins are as old as Palaeocene age.

Of the basin areas of the Indian Ocean, only the northern part of the Wharton Basin appears to have sediment thicknesses too small to be a result of prolonged sedimentation at the rates which are currently occurring. This is particularly so in view of the fact that this part of the ocean floor is amongst the oldest in the Indian Ocean, being at least late Cretaceous in age and therefore over 70 million years old.

Another example of apparent disequilibrium is provided by the mid-ocean ridge system. According to Ewing et al (1969) the mid-ocean ridge system is largely sediment-free for distances of up to 100 km. from the ridge crest. According to these authors this provides proof of the relatively young age of the crust along the ridge system. However, many sediment samples have been recovered by research vessels from areas on the ridge, even very near the ridge crest itself. Several nodules analysed in this study came from the mid-ocean ridge and these must obviously have been underlain by sediment. Thus it seems that sediment cover does exist on the ridge and that whilst it may be thin or absent in many places it occurs in thick ponded accumulations in others. Indeed Opdyke and Glass (1969) found that sedimentation rates on the mid-ocean ridge were amongst the highest observed in the Indian Ocean. The failure of Ewing et al (op. cit.) to detect sediments on the ridge probably results from their very irregular distribution and also from the problems of detecting thin sediment cover by seismic techniques in areas of rugged topography.

Apart from the Wharton Basin and the areas where recent bottom current scour has been shown to be taking place, present sedimentation rates over much of the ocean do not seem to be

markedly in conflict with the thickness of accumulated sediment. However, it is dangerous to assume from this that sedimentation rates and conditions have been uniform throughout the geological past. For example Luyendyk and Davies (1974) have shown that a wide-spread sedimentary hiatus seems to have occurred in the Indian Ocean in the Oligocene Period and this lasted in some localities up until less than 10 million years ago (late Miocene). During this period unconformities were formed due to non-deposition and to dissolution of carbonate sediments. This hiatus occurs at many of the D.S.D.P. sites in the Indian Ocean and in cores examined by other workers (Opdyke and Glass, 1969). Whilst Luyendyk and Davies (1974) have emphasised the danger of drawing regional conclusions on the evidence of single core stations, Davies et al (1975) have used palaeo-reconstructions of the Indian Ocean together with D.S.D.P. site information to construct maps showing the areas of the Indian Ocean floor affected by this hiatus. At its most widespread it seems to have affected all the basins of the Western Indian Ocean, the Central Indian Basin and the Wharton Basin, however in each of these basins the stratigraphic record shows that the hiatus commenced and terminated at different times.

Since periods of very slow or even negative accumulation of sediments are likely to be particularly favourable for the growth of nodules, it is tempting to try and tie in such sedimentary hiatuses to the initiation and development of the main nodule fields in the Indian Ocean. Such a study has been attempted on a local scale in the south-west Pacific by Pautot and Melgouan (1974). These authors found a nodule field sitting on sediments in which there had been an Oligocene to Quaternary hiatus and they suggested that this hiatus and periods of nodule growth were closely connected

with pulses of AABW, which had affected the area in the past. A similar conclusion was reached by Kennett and Watkins (1975) for the nodule pavement in the south-east Indian Ocean.

One problem in attempting to carry out such a study on a large scale is the determination of the likely maximum and minimum ages of particular nodule fields. Using the slowest reliable estimates of nodule accumulation rates, 1 m.m. per million years (Ku and Broecker, 1969; Krishnaswami et al, 1972), then the largest pelagic nodules investigated in this study are not likely to be more than 20 million years old. Even assuming such a slow growth rate many of the samples investigated must be much younger than the oceanic crust underlying them, indicating that the growth of these samples did not begin until some considerable time after the formation of the underlying crust. Higher growth rates however have been calculated by many other workers (Grant, 1967; Heyo, 1975; Sugimura et al, 1975) and these infer a maximum age of Indian Ocean nodules of only about 3 million years. The large discrepancy between these two estimates and the fact that no age-dating work was carried out on the samples used in this investigation, means that no correlations can be realistically postulated between nodule development and sedimentary hiatuses in the Indian Ocean. Only when nodule accumulation rates can be more accurately ascertained will it be possible to fully investigate any relationships which may exist between sedimentary hiatuses, bottom current activity and nodule growth. In addition, much more information must be gathered on the stratigraphic history and the nature of bottom current activity in many areas of the Indian Ocean.

(b) Sediment Type

Very little regional investigation of sediment type in the Indian Ocean was carried out until the late 1960's, when, as a result of the International Indian Ocean Expedition, abundant samples became available. The early ocean-wide studies by Griffin et al (1968) and Rateev et al (1969) were limited by the relatively small numbers of samples used. Moreover, these studies were concerned primarily with the clay-mineral assemblages of the surface sediments rather than with overall sediment type. Later work carried out by Goldberg and Griffin (1970), Vankatarathnam and Biscaye (1973) and Kolla et al (1976) was more detailed but again concentrated specifically on the clay-mineral assemblages. A study of the clay-mineral fraction of sediments provides no knowledge of overall sediment composition and therefore of the relative importance of different types of sediment. However, with only one or two exceptions, such as rapidly-deposited carbonate-oozes, clay minerals do form a significant, if not major, component of deep-sea sediments and a knowledge of the clay mineral assemblage of samples therefore proves a useful guide to the relative importance of parameters such as aeolian transport, continental run-off and submarine volcanism as suppliers of material to the sea-bed. Griffin et al (1968) showed that the marked bipolar and latitudinal distribution of clay minerals seen in the Pacific and Atlantic Oceans does not seem to occur in the Indian Ocean, although Rateev et al (1969) found some evidence of such a distribution. Vankatarathnam and Biscaye (1973) suggested that the lack of marked latitudinal variations was due to the asymmetry of the continents surrounding the Indian Ocean, most of the land lying to the north and west of the ocean. Based on the distribution of characteristic mineral

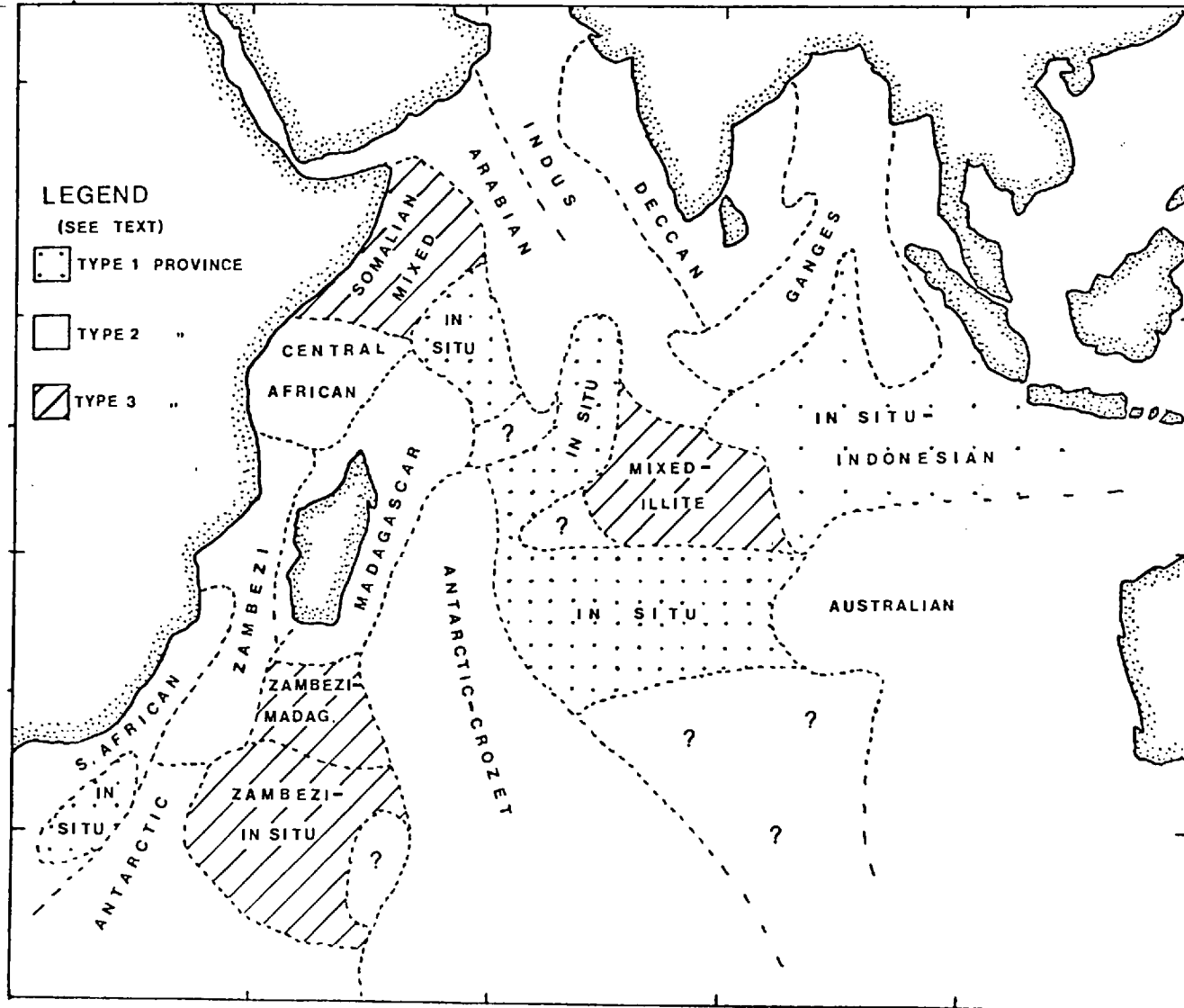


assemblages Kolla et al (1976b) recognised three different types of sedimentary province in the Indian Ocean. These were as follows:-

Type 1. - Montmorillonite-rich provinces, the montmorillonite being derived from the alteration of in-situ basalts, and showing no evidence of long-distance transport of material. The main areas of this type are the southern part of the Central Indian Basin, parts of the Central Indian Ridge, the north-eastern Somali Basin and a small area on the Agulhas Plateau off southern Africa (see figure 4).

Type 2. - Provinces enriched in a particular mineral or minerals, which have been derived from continents or submarine volcanic areas and which show evidence of long-distance sediment transport. This group includes the Arabian, Indus, Deccan and Ganges Provinces in the northern Indian Ocean, the Central African, Madagascar, Zambezi and South African provinces in the west and the Antarctic and Antarctic-Crozet Provinces in the south and the Australian and Indonesian Provinces in the east. The Indus and Ganges provinces are illite-rich and contain clays primarily derived from the run-off of these rivers. The Deccan province is formed by the products of run-off of the southern Indian rivers. The Arabian Province, which includes much of the Carlsberg Ridge, contains appreciable palygorskite and shows evidence of appreciable aeolian transport of material. The Zambezi Province sediments are thought to be kaolinite-rich in addition to containing abundant illite, although the mineral composition of the sediments brought down by this river is not known accurately at present. However, the Zambezi is the only major river currently entering the western Indian Ocean and the 100 million tons of sediment per year which it supplies, whilst

FIGURE 4 Clay mineral provinces in the Indian Ocean (adapted from Kolla et al 1976b).



nothing like as large as that supplied by the Ganges (1450 million tons) or the Indus (435 million tons) (Rateev et al, 1969), nevertheless exerts a significant influence on sediment type and distribution in the western Indian Ocean. The Central African and Madagascar Provinces are kaolinite-rich, inferring that much of the material is derived from run-off from the kaolinite-rich soils of East Africa and Madagascar. Lack of knowledge of ocean currents in these areas precludes an accurate knowledge of the processes of distribution of this material however. The Australian province is also kaolinite-rich but since there is very little river drainage from western Australia much of the material must be transported to the ocean by the south-east trade-winds. By contrast, the illite-rich south African Province derives its material mainly from run-off from South African soils. The Antarctic Province is also illite-rich, much of this material appears to have been derived from the Antarctic Continental margin and to have been transported northwards by the AABW.

The Antarctic-Crozet Province is montmorillonite-rich and occupies the Crozet Basin, part of the South-West Indian Ridge and the eastern parts of the Madagascar and Mascarene Basins. This pattern of montmorillonite-rich sediments results from the transport of montmorillonite-rich clays from the volcanic regions of the Crozet and Kerguelen Plateaux by AABW. The continuation of this province north of the South-West Indian Ridge indicates that this current is able to traverse the ridge (see Section 2).

Another montmorillonite-rich province is the Indonesian Province. In part this is a north-eastward extension of the montmorillonite province in the southern Central Indian Basin but east of  $80^{\circ}\text{E}$  there appears to be a gradually increasing contribution to the sediment of Indonesian tephra, transported

partly by north-east trades and partly by equatorial surface currents.

Type 3. - This type of province contains no clay mineral in particularly high amounts and the origin of the sediment is therefore more obscure, probably resulting from the ad-mixing of material from several other provinces. Provinces of this type include areas east of the Horn of Africa (Somalian Province), south of Madagascar (the Zambezi-Madagascar and Zambezi-in-situ Provinces) and the central part of the Central Indian Basin (mixed-illite Province). Lack of accurate knowledge of bottom currents in these areas prevents detailed understanding of the relative importance of other sedimentary provinces in supplying material to these areas.

Maps of surface sediment-type in the Indian Ocean have been compiled by Luyendyk and Davies (1974) and Udintsev et al (1975). The map compiled by Luyendyk and Davies is based on the fairly limited regional data obtained from D.S.D.P. drilling sites throughout the ocean whereas that by Udintsev et al (figure 5) is based on many hundreds of cores collected during the International Indian Ocean Expedition and is the one used in the following discussion.

Both maps are in broad agreement although several differences of note do occur. Of the more important differences, Luyendyk and Davies (1974) infer a greater terrigenous influence in Mozambique Channel and Arabian Abyssal Plain sediments than that shown by Udintsev et al (figure 5). In view of the large amounts of terrigenous materials entering the Mozambique Channel, as discussed above, the area of predominance of this type of material indicated in figure 5 does seem surprisingly small and may have to be modified as a result of future work.

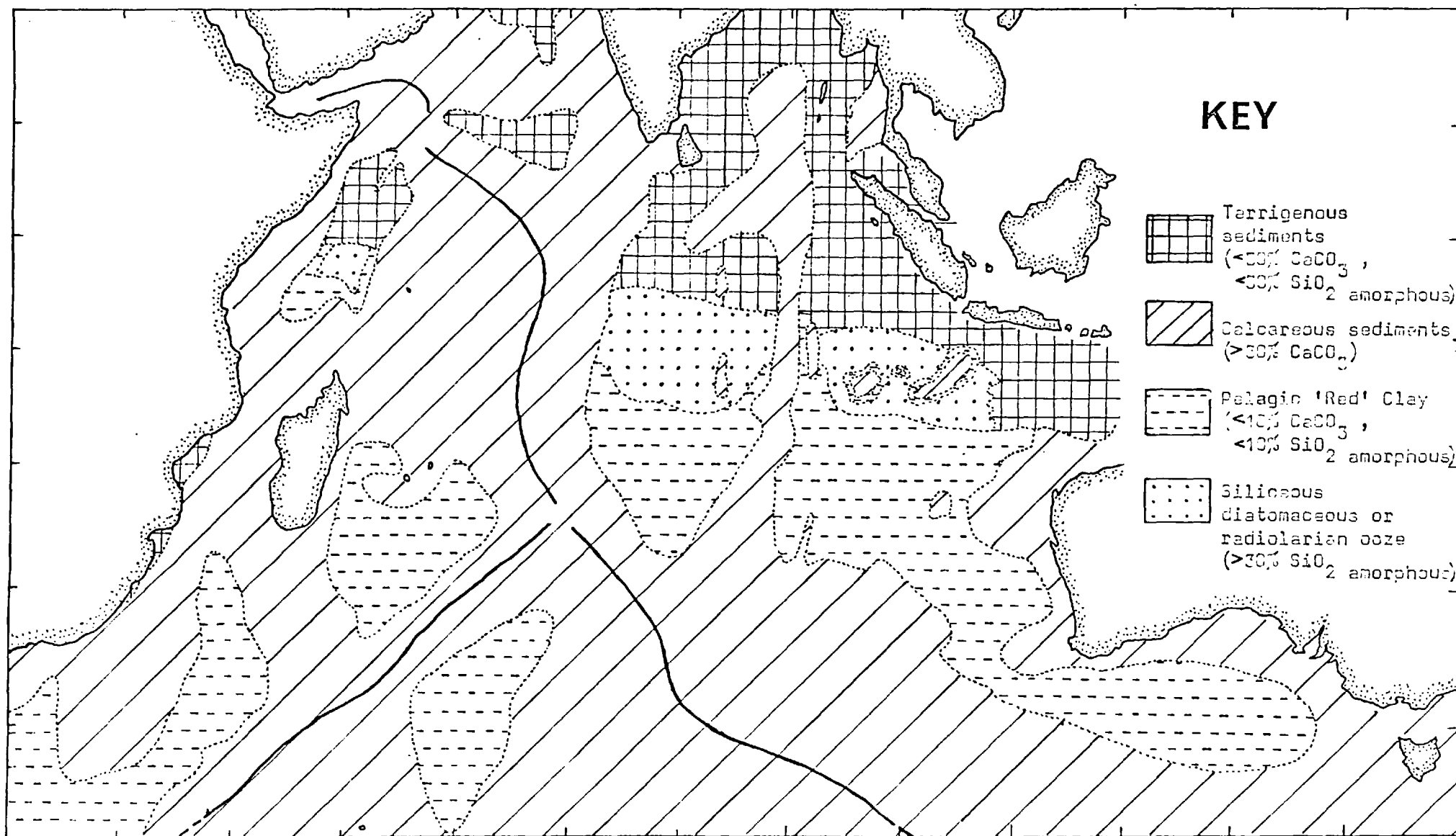


FIG. 1. Distribution of surface sediment type in the Indian Ocean (adapted from Ujintsev et al 1975).

Luyendyk and Davies (1974) also infer a larger area of siliceous ooze occurrence in the Wharton Basin than that suggested by Udintsev et al (1975) (figure 5). According to Luyendyk and Davies siliceous ooze covers the whole of the northern Wharton Basin stretching right up to the Java Trench system and running along its whole length, whereas Udintsev et al suggests that siliceous ooze has a more limited occurrence in the Wharton Basin. The only other major difference between the two interpretations is the classification of Crozet Basin sediments as siliceous by Luyendyk and Davies whereas, according to Udintsev et al, these sediments are pelagic clays. Most of these discrepancies can probably be accounted for by the different proportions of each of the four investigated components which was regarded by each of the authors as being the minimum required before a sediment could be classed as being of a particular type. The relative proportions used by Udintsev et al (1975) are given on figure 5, but Luyendyk and Davies (1974) do not indicate what criteria they used to classify their samples and therefore no confirmation can be gained of this explanation for the observed difference.

Apart from the areas already mentioned, terrigenous sediments in the Indian Ocean occur in three separate areas, all in the northern Indian Ocean. Two of these areas are small pockets of terrigenous sediment lying below the carbonate compensation depth (C.C.D.) in the deepest parts of the Somali Basin and the Arabian Abyssal Plain. The third area is much larger, occurring both below and above the C.C.D. and stretching southwards in two lobes from the Bay of Bengal. The western lobe extends to about 5°S but the eastern lobe extends slightly further south and also occupies a wide strip off the Indonesian

Archipelago as already discussed.

Siliceous ooze sediments form an even smaller proportion of the total surface sediment of the Indian Ocean and occur only in three isolated patches in the deepest parts of the tropical ocean. All three patches lie immediately to the south of areas of predominantly terrigenous material, one in the Somali Basin, one in the Central Indian Basin and one in the Wharton Basin. Pelagic "red"-clay sediments occur in all the major basins below the carbonate compensation depth and thus are found in the Moçambique, Madagascar, Mascarene, Crozet and South Australian Basins, in the Somali Basin and in much of the southern Wharton Basin, extending from the latter into the South Australian Basin. The rest of the Indian Ocean floor, including vast areas in the western and southern ocean is at or above the C.C.D. and consequently is covered by carbonate oozes. The areas with sediments containing greater than 30% calcium carbonate, shown in figure 5, agree very well with the map of calcium carbonate distribution in Indian Ocean sediments produced by Kolla et al (1976a) from over 1200 surface sample analyses. These authors found the most carbonate-rich sediments (greater than 85% calcium carbonate) occurred in a fairly narrow belt stretching from the Seychelles-Mascarene Plateau in the north-west to east of the Kerguelen-Heard Plateau in the south-east; where the belt is also at its widest. Sediments equally high in carbonate occur in small areas on the southern part of the Ninety East Ridge, on the Madagascar and Moçambique Ridges and on the Agulhas Plateau.

## SECTION 2

### OCEANOGRAPHY

#### (i) OCEAN CURRENTS

As was discussed briefly in the preceding section, ocean currents, particularly bottom currents, by their influence on the bottom environment, seem to play an important role in the development of marine ferromanganese nodules. In order to investigate this role more fully, detailed knowledge of present-day and palaeo-bottom currents is needed and for many areas of the Indian Ocean, no such information is available at present.

It appears from the work of several authors, however, that the most important source of major bottom currents in the Indian Ocean is Antarctic Bottom Water (AABW) (Payne and Conolly, 1972; Kennett and Watkins, 1975; Kolla et al, 1976c). Wherever this water finds its way northwards into the Indian Ocean it has a very marked effect on the bottom environment. Where the bottom current is very strong it can erode the surface sediment by winnowing action (Watkins and Kennett, 1977); where current velocity slackens it can re-deposit suspended material (Burckle et al, 1974) and in all areas it has a marked effect on carbonate dissolution rates because of its marked undersaturation in calcium carbonate (Kolla



et al, 1976a). The production of this current of very cold bottom water has occurred progressively over the last 60 million years as Antarctica has become increasingly glaciated, (Kennett et al, 1974). Fluctuations in the strength and activity of AABW are likely to have occurred in the past due to variations in climate and the effects of sea-floor spreading on the bottom environment. In particular, the global deterioration of climate over the last 2 to 3 million years has increased the activity of this current since the late Pliocene (Watkins and Kennett, 1973).

Le Pichon (1960), Wyrski (1971), Kennett and Watkins (1975) and Kolla et al (1976c) have shown that AABW finds its way into the Indian Ocean by three main routes, (see figure 6).

1. A westerly route from the Atlantic-Indian Basin, via relatively deep passages in the Atlantic-Indian Ridge, into the Agulhas and Moçambique Basins.

2. A central route from the eastern Atlantic-Indian Basin directly into the Crozet Basin.

3. An easterly route from the South Indian Basin, via passages in the South-East Indian Ridge into the South Australian then Wharton Basins.

The circulation and spreading of each of these three tongues of bottom water has been described by Kolla et al (1976c) and is summarised in figure 6.

The Source of AABW in the western Indian Ocean is the Atlantic-Indian Basin from whence the water traverses the Atlantic-Indian Ridge through two passages, one at  $20^{\circ}$ - $25^{\circ}$ E and the other, major, passage at  $35^{\circ}$ E. Some of this bottom water spreads between the Agulhas Plateau and the South African coast but most passes northwards along the western side of the Moçambique Basin to about  $25^{\circ}$ S where the shallow Moçambique Channel appears to prevent further

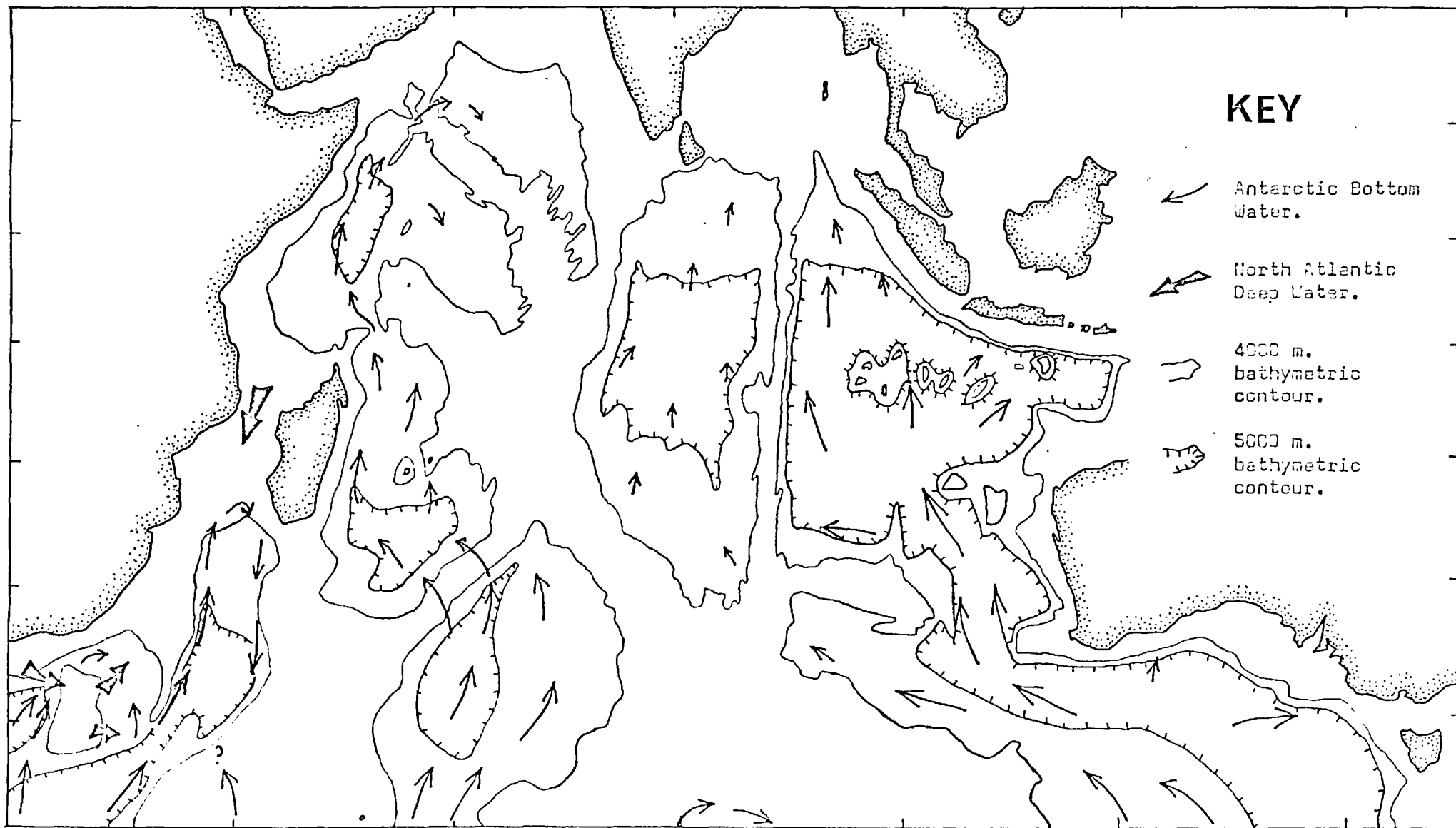


FIGURE 1 Major Bottom Currents in the Indian Ocean (from Kolla et al. 1976c).

progress and the current returns southwards along the eastern side of the Moçambique Basin. Temperature and salinity data obtained in the Moçambique and Madagascar Basins (Wyrтки, 1971; Warren, 1974) suggest that no significant transfer of AABW occurs between the two basins.

In the Crozet Basin strong northward flowing bottom currents caused by spreading AABW have been inferred from evidence of erosional features, sediment reworking, turbidity and direct current measurement. This tongue of bottom water appears to traverse the South-West Indian Ridge and flow into the Madagascar Basin. This theory is borne out by bottom-water potential temperature evidence (Wyrтки, 1971). An area of sediments extending from the Crozet into the Madagascar Basin, which is particularly low in carbonate (Kolla et al 1976e) and contains Antarctic diatoms (Burckle et al, 1974) also indicates that AABW is able to pass through the South-West Indian Ridge from the Crozet Basin. Warren (1974) and Kolla et al (1976c) suggest that such a passage exists at about  $26^{\circ}$ - $29^{\circ}$ S and  $60^{\circ}$ - $64^{\circ}$ E. That this passage is a major one, allowing substantial flow of AABW is indicated by the very marked effects which the current has on the floor of the Madagascar Basin, producing erosional features and giant ripple-marks (Ewing et al, 1968). From the Madagascar Basin AABW flows northwards into the Mascarene Basin and then into the Somali Basin. Bottom potential temperatures and salinity measurements (Wyrтки, 1971) indicate that AABW traverses the Carlsberg Ridge through a passage in the region of the Chain Ridge and then flows into the Southern Arabian Basin. However, the vigour of the AABW in the Somali Basin and more especially the Arabian Basin, is greatly diminished compared to the southern basins.

In the South Indian Basin AABW flows westwards from its source in the Ross Sea area until it reaches the Kerguelen Plateau, where

it turns northwards then eastwards. Some AABW traverses the South-East Indian Ridge through a passage at about  $120^{\circ}$ - $125^{\circ}$ E and enters the South Australian Basin where it travels westwards. Intense erosional and other features indicative of strong bottom current activity show that this bottom water spreads into the Wharton Basin via the narrow deep gap between the Naturaliste Plateau and the Broken Ridge (Kennett and Watkins, 1975). The bottom water temperature in the whole of the Wharton Basin is cold (Wyrтки, 1971) however, Kolla et al (1976c) found little evidence of bottom current activity north of about  $25^{\circ}$ S in this basin. This may be because the AABW entering the Wharton Basin is less vigorous than that in the south-western Indian Ocean. This could be partly due to its circuitous route from its source and the fact that during its passage over the South-East Indian Ridge it appears to become admixed with significant amounts of Antarctic Circumpolar Water, making it warmer and more saline (Kolla et al, 1976c). Another reason for the apparent lack of bottom current activity in the Wharton Basin is that this basin forms a very large, wide, deep area and the AABW may therefore spread uniformly everywhere over the basin floor rather than behaving as a stronger current confined to a narrow, deep region.

According to Kolla et al (1976c) some AABW may spill over from the South Australian Basin into the Central Indian Basin via a deep gap between the Broken Ridge and the South-East Indian Ridge. The Ninety East Ridge seems to form an effective barrier to AABW flowing into the Central Indian Basin from the Wharton Basin, although small amounts may be able to pass through some of the deeper gaps in this ridge. However, the deep-water temperatures in the entire Central Indian Basin are the highest of any Indian Ocean basin at corresponding latitudes (Wyrтки, 1971) and this indicates that this basin is receiving much less AABW than any other Indian Ocean Basin.

This is confirmed by the apparent lack of sea-floor features indicative of bottom current activity in this basin.

Thus most of the strong bottom current activity associated with AABW occurs in the south-western part of the ocean. The basins of the eastern Indian Ocean, except for the southern part of the Wharton Basin, show little evidence of strong bottom current activity at the present time.

#### Other Currents

Strong bottom current activity occurs in several areas of the Indian Ocean which are at depths too shallow for the current to be caused by AABW. For example, the high current velocities measured over the Agulhas Plateau are caused by bottom water which is quite warm and saline and low in silica (Wyrтки, 1971). According to Kolla et al (1976c) this current is caused by North Atlantic Deep Water (NADW). This current flows across the Agulhas Plateau then continues eastwards, mixing with Circumpolar Deep Water, and northwards, travelling both east and west of Madagascar. West of Madagascar the NADW does not penetrate north of  $19^{\circ}\text{S}$  (Vincent, 1972) because the sea-floor here shoals to less than 3000m. preventing further progress. In fact it appears that at about  $19^{\circ}\text{S}$  the NADW turns and flows southwards again in a similar manner to AABW in this region (Kolla et al 1976c). These authors also report a southward flowing bottom water in the Bengal Basin area but they do not attribute this to AABW. Bottom current indications in many other localised shallow areas of the ocean are also likely to be caused by water masses other than the AABW. For example, the considerable sediment erosion which has occurred on the Naturalists Plateau is thought to be due (Wyrтки, 1971) to Circumpolar Deep Water admixed with North Atlantic Deep Water.

Unless detailed work is carried out in each region, the source

of bottom currents in localised, shallow areas of the ocean cannot be established. However, it is obvious that on an ocean-wide basis, by far the most important water mass in terms of its effect on the bottom environment is Antarctic Bottom Water.

#### (ii) BIOLOGICAL PRODUCTIVITY

Greenelate et al (1973) suggested that the nodule distribution and composition might be affected by surface biological productivity of the overlying ocean and these workers have inferred that the biogenic debris forms an important source of trace metals, especially of Ni and Cu in bottom waters. It is thus worth examining the biological productivity of the Indian Ocean briefly.

Remarkably little was known about regional variations in biological productivity in the Indian Ocean until the late 1960's when the many samples collected during the International Indian Ocean Expedition were studied. This work has enabled maps showing the variation in primary phyto- and zoo- plankton to be compiled for the Indian Ocean. Figure 7 shows the variation in phytoplankton productivity in the Indian Ocean, and it is immediately obvious that the most productive areas of the ocean are the coastal areas of India, Arabia and parts of Africa and Indonesia. These regions are areas of upwelling (Krey, 1973) where "young" nutrient-rich water is brought to the surface, encouraging high productivity. There are also areas of comparatively high productivity beneath the west-wind drift system in the southern half of the ocean (Krey, 1973) and to a lesser extent in the equatorial current region. However, this equatorial region of enhanced productivity is displaced slightly to the south of the equator and is very narrow and not nearly so marked as the belts seen in the Atlantic and Pacific Oceans, which are symmetrical about the equator (Koblitz-Mishke

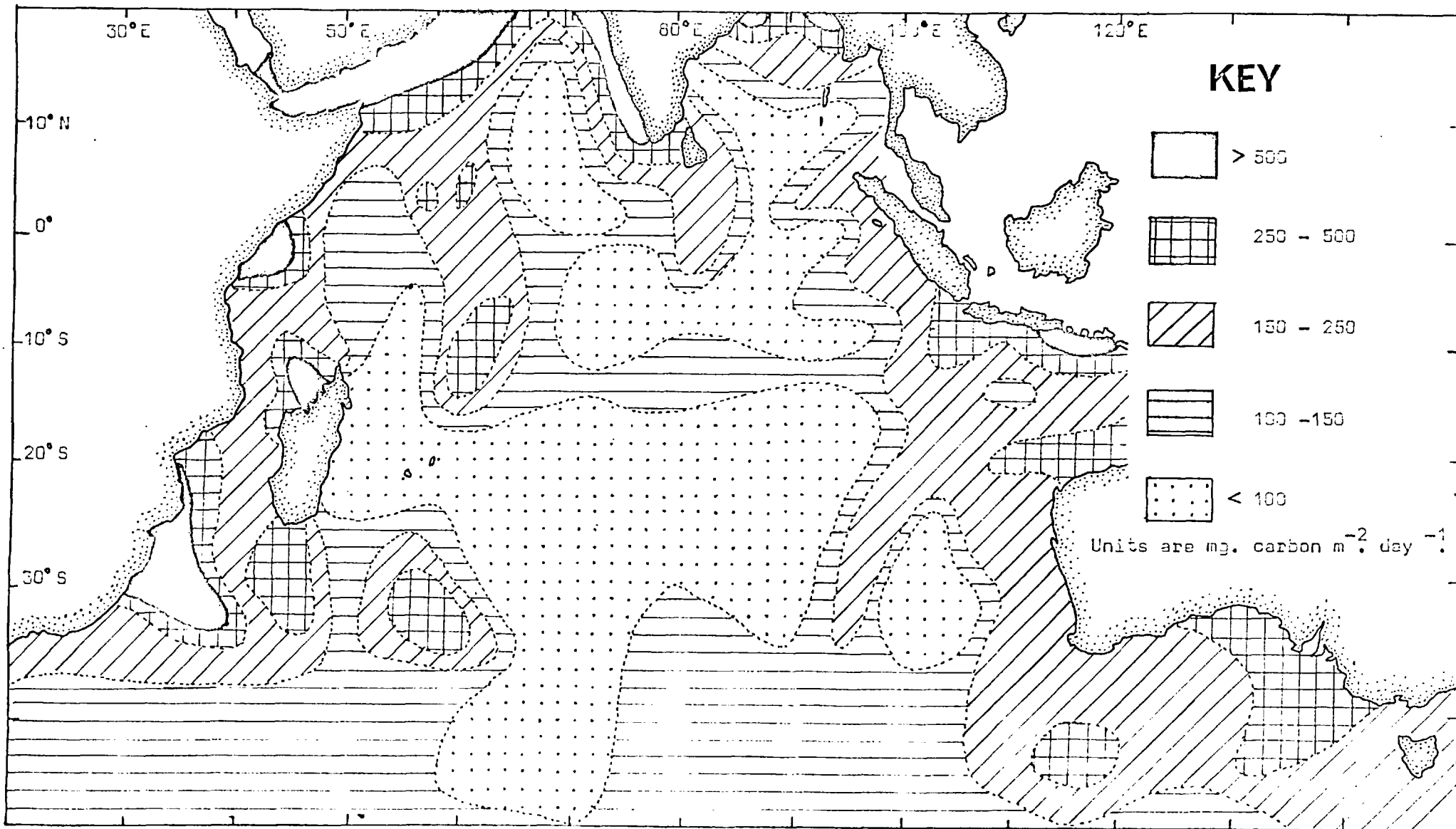


FIGURE 7 Primary phytoplankton productivity in the Indian Ocean (from Pohlitz-Nichke et al. 1977).

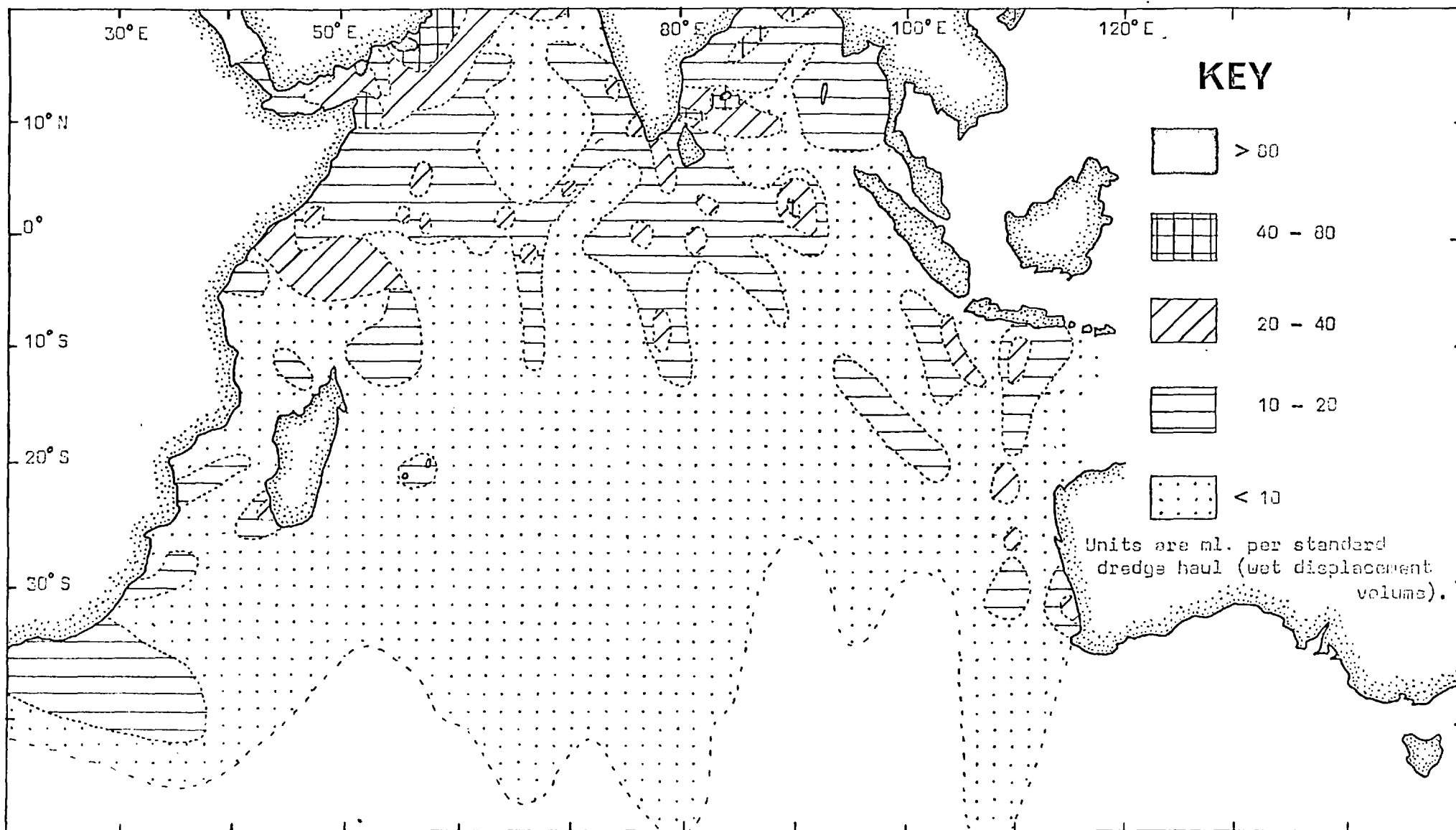


FIGURE 2. Total zooplankton biomass in the Indian Ocean (from Rao 1973).



et al, 1970). Areas of low productivity occur throughout much of the Central Indian Ocean south of  $15^{\circ}\text{S}$  and also in a smaller region between the equator and  $10^{\circ}\text{S}$ , to the south of Sri Lanka. According to Krey (1973) these are the "desert" regions of "old" water, where surface currents are weak, the thermocline well-developed and upwelling of fresh nutrient-rich water therefore at a minimum.

The map of total zoo plankton productivity in the Indian Ocean compiled by Rao (1973) (figure 8) is based on less detailed sampling, especially south of  $10^{\circ}\text{S}$ , and this is reflected in the rather patchy nature of the map. However, it is again obvious that the regions of extensive upwelling off the coasts of India, Arabia and parts of Africa and Indonesia are the most productive areas. The findings of Rao (1973) are in general agreement with those of earlier work (Panikkar, 1968) although an equatorial region of enhanced productivity weakly defined by Rao's data was not detected by Panikkar.

The lack of a marked equatorial zone of high biological productivity in the Indian Ocean is in contrast to the productivity patterns observed in the Atlantic and Pacific Oceans (for example see Koblentz-Mishke et al, 1970). An explanation for this unique feature of the Indian Ocean is provided by the behaviour of the Equatorial Undercurrent. This current flows eastwards in a narrow, well-defined belt beneath the equator in all three major oceans, with the core of the current at a depth of 50 - 150 m. (Sharma, 1968). This current is associated with upwelling in equatorial regions and it is this upwelling of fresh, nutrient-rich water which is responsible for the high biological productivity in equatorial ocean waters. The Equatorial Undercurrent persists throughout the year in the Atlantic and Pacific Oceans, however the Indian Ocean is unique in its exposure to the seasonally-varying

monsoon-wind system and these winds cause the Equatorial Undercurrent in the Indian Ocean to disappear during the south-west monsoon period (May to October) and reappear during the north-east monsoon (November to April) (Sharma, 1968). During the south-west monsoon the equatorial region of the ocean is in fact one of sinking water whilst upwelling occurs to the north and south. This phenomena agrees well with the seasonal variation in zooplankton productivity observed by Panikkar (1968). He showed that productivity in the equatorial Indian Ocean is low during the south-west monsoon but high during the north-east monsoon when the region reverts to one of upwelling as the Equatorial Undercurrent becomes re-established. Thus when average productivity of the equatorial region for the whole year is compiled no marked region of high productivity is observed. In addition to the seasonal nature of the Equatorial Undercurrent in the Indian Ocean, Krauss and Taft (1964) and Swallow (1964) have shown that, in contrast to its markedly symmetric behaviour in the Atlantic and Pacific Oceans the Equatorial Undercurrent is displaced southwards by as much as  $3^{\circ}$  of latitude in this ocean.

Despite the rather limited nature of the equatorial zone of high biological productivity in the Indian Ocean, Kolla et al (1976c) have shown that increased carbonate rain in the equatorial regions depresses the carbonate critical depth (depth at which the calcium carbonate content of sediments falls below 10%) to more than 5100 m. between  $10^{\circ}\text{N}$  and  $10^{\circ}\text{S}$ . However, these authors state that this depression of the carbonate critical depth (C.Cr.D.) may be due to other factors apart from enhanced productivity.

According to the theories of Greenslate et al (1973) and Piper and Williamson (1977) the C.Cr.D. and lysocline are important factors in controlling the regional compositional variation of

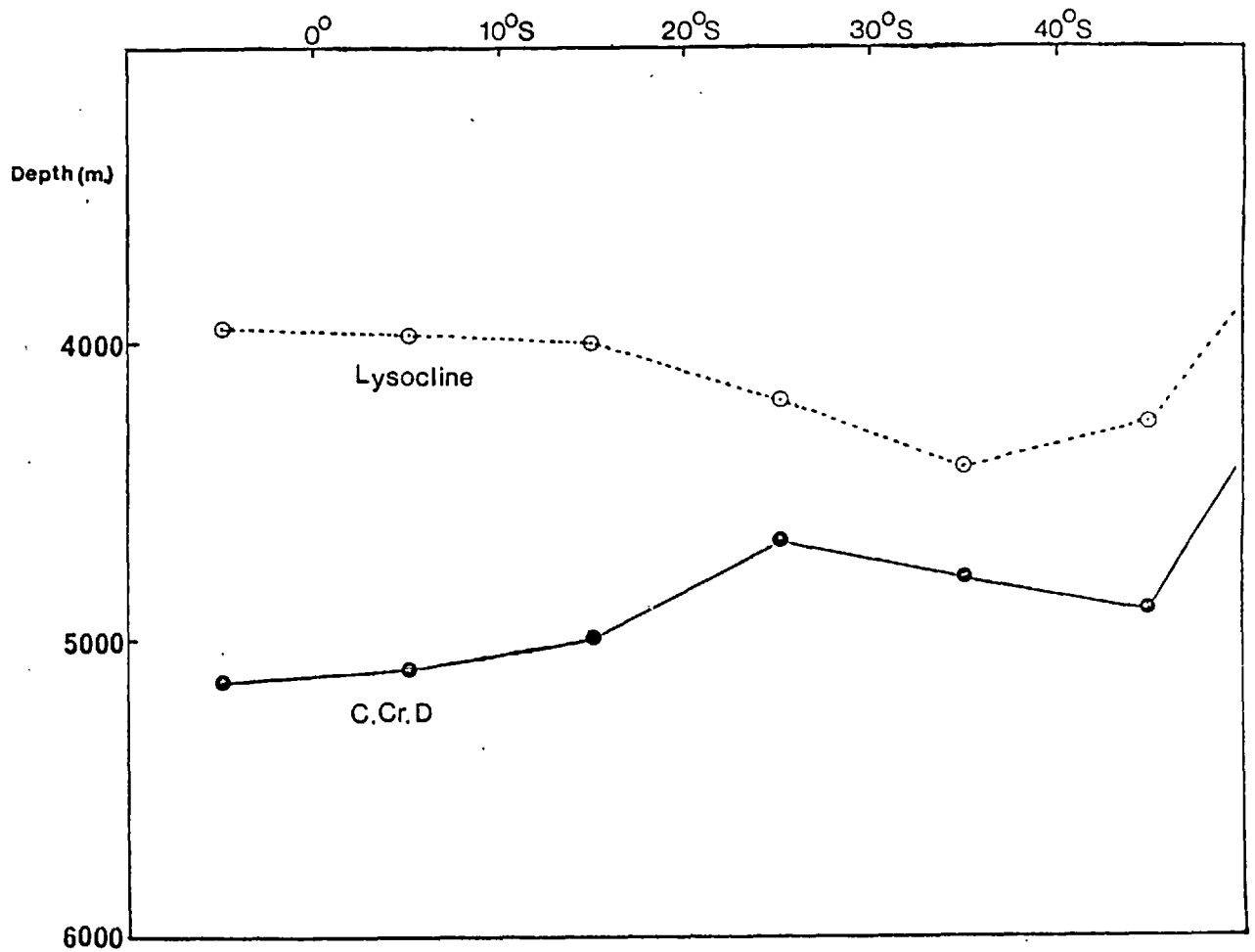


FIGURE 9 Carbonate critical depth and lysocline variation in the Indian Ocean (from Kolla et al 1976a).

ferromanganese nodules since significant dissolution of carbonate débris occurs between these depths. This dissolution process leads to the release into the deep waters of trace metals contained in the carbonate organisms. Figure 9 shows the variation in depth of the C.Cr.D. and lysocline with variation in latitude throughout the Indian Ocean, excluding areas where dilution by terrigenous material seriously affects these parameters. In such areas the C.Cr.D. and lysocline occur at shallower depths. For example between  $0^{\circ}\text{N}$  and  $10^{\circ}\text{N}$  in the Somali Basin the C.Cr.D. is at 5100 m., whilst in the northern Arabian Basin it is at 4800 m. and in the Ganges Cone area of the Central Indian Basin it is at 4500 m., and at 4800 m. between  $0^{\circ}\text{S}$  and  $10^{\circ}\text{S}$ .

According to Kolla et al (1975c) excluding areas where dilution by terrigenous material is occurring, the variations with latitude of the C.Cr.D. and the lysocline are similar in the Indian Ocean to those observed in the Atlantic and Pacific Oceans and are caused partly by variations in surface productivity and partly by factors such as deep water turbulence and degree of undersaturation. Since these latter two parameters are markedly affected by AABW it appears that this body of water has far reaching effects on the bottom and near-bottom environment over and above its sediment-transport and bottom erosional features.

### S E C T I O N 3

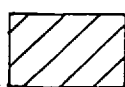
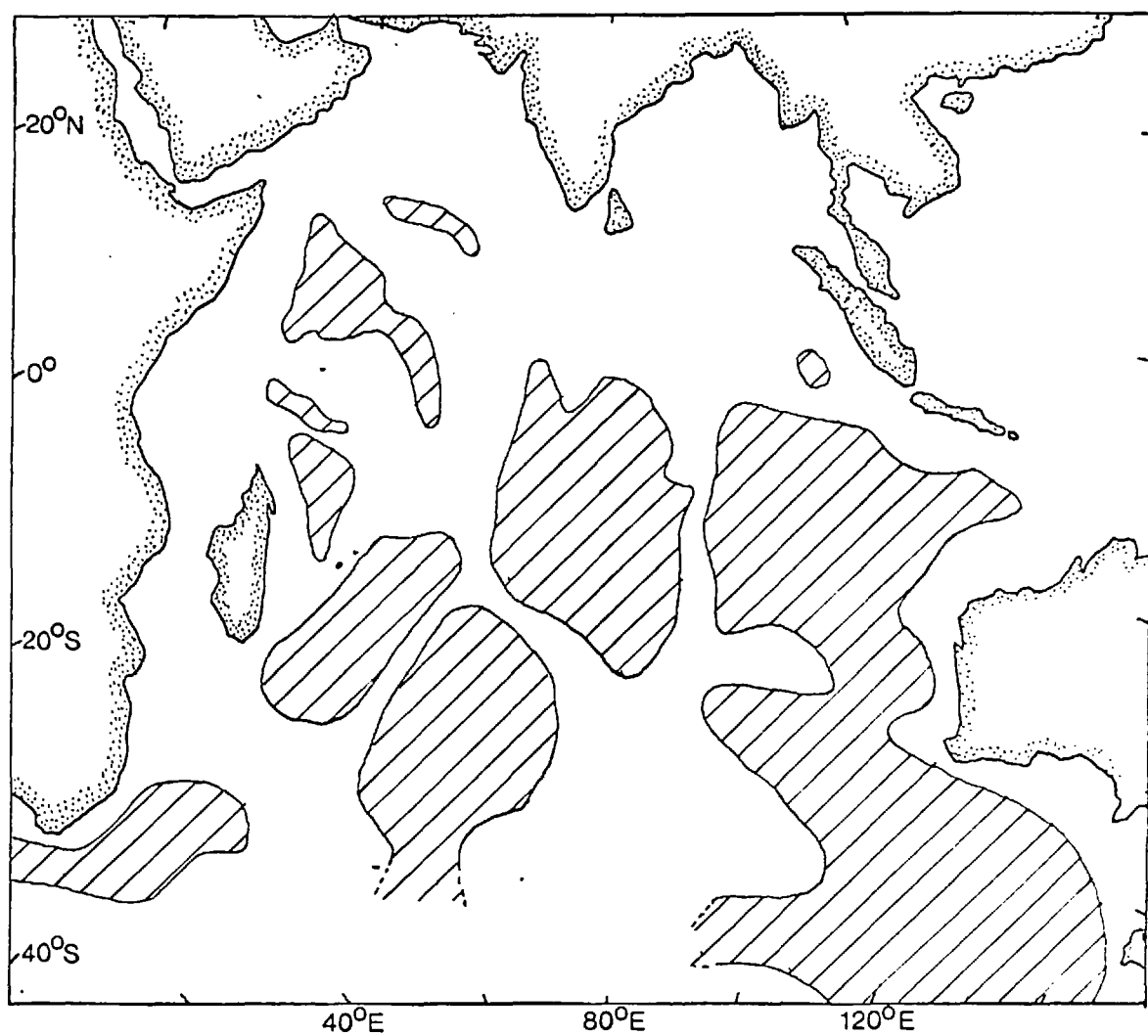
#### SAMPLE DISTRIBUTION AND MORPHOLOGY

##### (i) DISTRIBUTION

Whilst the distribution of ferromanganese nodules in the Pacific Ocean is relatively well known, information on nodule coverage of the Indian Ocean has until recently been much less abundant, due to the comparative paucity of research carried out in this ocean.

The first detailed sampling of ferromanganese-oxides in the Indian Ocean (Bezrukov, 1962, 1963) revealed extensive deposits of nodules in many parts of the southern Indian Ocean. Later, more detailed work in comparatively small areas revealed highly variable degrees of nodule coverage often over quite small distances, in regions such as the Carlsberg Ridge (Laughton, 1967) and off southern Africa and Madagascar (Vincent, 1972). Much more knowledge of nodule coverage was gained as a result of the International Indian Ocean Expedition and using data from this and earlier sources a map of nodule coverage of the Indian Ocean has been drawn up (Udintsev et al, 1975) and is shown on figure 10. From this diagram it can be seen that the most extensive areas of nodule coverage have been found to be predominantly in the southern part of the Indian Ocean in areas of comparatively slow sedimentation. According to Bezrukov

FIGURE 10 Distribution of ferromanganese nodules in the Indian Ocean (from Udintsev et al, 1975).



Areas with abundant nodule coverage.

and Andrushchenko (1973) nodules are most abundant in areas of the Indian Ocean floor with slow sedimentation rates and with dissected hilly relief where the height of the hills above the depressions reaches several tens or even hundreds of metres. Bottom photography has shown that nodules are particularly abundant in the Crozet Basin (Udintsev, 1975) and Central Indian Basin (Backer, pers. comm.). In areas of rapid sedimentation such as the continental margins and flat abyssal accumulative plains nodules appear to be rare or absent. Most of the samples examined in this study came from regions which are known to have extensive nodule coverage but several samples were obtained from the Mozambique Channel area where, according to Vincent (1972), nodule coverage is at best patchy. In the whole of the Indian Ocean this is the only area of rapid sedimentation near the continents from which nodules have been recovered. The presence of nodules in what would seem to be a relatively unfavourable environment may be a result of localised scouring of the sediments by bottom currents which, as already discussed, are particularly strong in this area.

Encrustations have been found in all areas of the Indian Ocean where bare rock is exposed on the sea-bed. This type of deposit is therefore particularly common along the mid-ocean ridge system and other areas of rugged topography swept clear of sediment such as isolated sea-mounts and aseismic ridges. The encrustations examined in this study came from all three types of environment but those from the mid-ocean ridge system formed the largest percentage of the total. Whilst encrustations are the most common type of ferromanganese-oxide deposit on the mid-ocean ridge there are many narrow valley areas with ponded sediments from which nodules have been recovered (Glasby, 1970; this study).

Only in three cases were nodules and encrustations collected

from the same station site. In one case the nodule and encrustations came from separate coring and dredging operations respectively, on the same large sea-mount. At station RC14/D4 on a Madagascar Basin sea-mount and at station ANTP109D on the south-west Indian Ridge both nodule and encrustation samples were collected in the same sampling operation. The very rugged topography at both these sites is likely to cause rapid changes in bottom environment even over the short distances traversed by the respective dredging operations. Glasby (1970) commented on the difficulty in assessing the influence of microtopography of the bottom environment on the morphology of ferromanganese-oxides, because of the inherent problems of bottom sampling using dredging techniques. However, Glasby (1970) was able to show that in a limited area on the flanks of the Carlsberg Ridge, samples from near the base of the ridge system consisted predominantly of nodules with very few crusts, whilst those from the southern Massif area of the ridge itself were mainly encrustations with limited numbers of nodules. This conclusion fits the general observations made in this study concerning the distribution of nodules and encrustations with respect to the nature of the bottom topography viz.; encrustations are confined mainly to elevated areas of rugged topography whilst nodules occur mainly in the sediment-floored basins of more gentle topography. This conclusion leads to the suggestion that at stations RC14/D4 and ANTP109D the nodules were picked up at greater depths during the dredging operations whilst the encrustations were recovered from more elevated, rugged areas later in the dredging operations.

#### (ii) MORPHOLOGY

A total of 116 ferromanganese-oxide samples from sites



throughout the Indian Ocean were examined during the course of this investigation. The sample sites are plotted in figure 11. The samples came from a wide range of bottom environments and tend to show a wide range of physical characteristics.

The most obvious morphological division of marine ferromanganese oxides is into nodules on the one hand and encrustations on the other. Whilst it can be argued that nodules are simply a special type of encrustation, in which growth has occurred on all sides of the substrate rather than just one, the division between nodules and encrustations is an important one on genetic grounds as will be discussed later.

Many authors (Cronan & Tooms, 1969; Crerar & Barnes, 1974; Calvert & Price, 1976) have suggested that variations in the bottom environment may cause variations in the chemical and mineralogical composition of marine manganese nodules. Few authors however, have investigated the role of environmental factors in controlling the morphology of these deposits although such a study has been carried out, with some success, in a freshwater lake (Sozanski & Cronan, 1976). Goodell et al (1970), working on samples from the Southern Pacific and Atlantic Oceans recognized four different morphological types of concretion on the basis of type of nuclei, thickness of deposit and external shape. They suggested that morphology was dependant on the nature and proximity of element source and the rate of accretion. However as suggested by Cronan (1976), it seems likely that the shape and nature of the nucleus is also an important factor in determining the shape of nodules particularly where the overlying ferromanganese-oxide layers are thin.

Meylan (1974) developed a method of rapid field classification of manganese nodules which defined samples in terms of size, shape and surface texture. However this field description system is rather



too basic for a study of this type and ignores such important features as the nature of the nucleus and internal growth features. Compared to the amount of work published on the internal features of nodules, very little attention has been paid to external features. This is perhaps surprising since, if as suggested by Goodell et al (1970), nodule morphology is partly controlled by element source, it may in turn reflect compositional trends.

In describing the ferromanganese-oxide samples analysed in this study four major parameters were recognised; size, shape, surface texture and nature of core and internal structure.

#### (a) Size

The nodules studied varied greatly in size, ranging from fragments less than 1 cm. in size to nodules with a maximum diameter of more than 2.5 cm. Most nodules however had an average diameter of between 3 cm. and 6 cm. No overall size could be given to encrustations since these were obviously broken off from deposits of larger size by the dredging operations. The thickness of the encrusting ferromanganese-oxides however varied from coatings 1 mm. or less in thickness to crusts more than 5 cm. in thickness (Plate 1 (a)). Heye (1975) made a study of fractures in nodules and reached the conclusion that they were an ageing feature and that nodules therefore eventually completely break up due to the increasing development of fractures within them. He argued that this process therefore set a limiting age and size for nodules and explained the fact that the largest nodules in the Pacific Ocean came from continental margin areas not pelagic areas since growth rates are faster in the former than in the latter (Ku and Glasby, 1972). This also

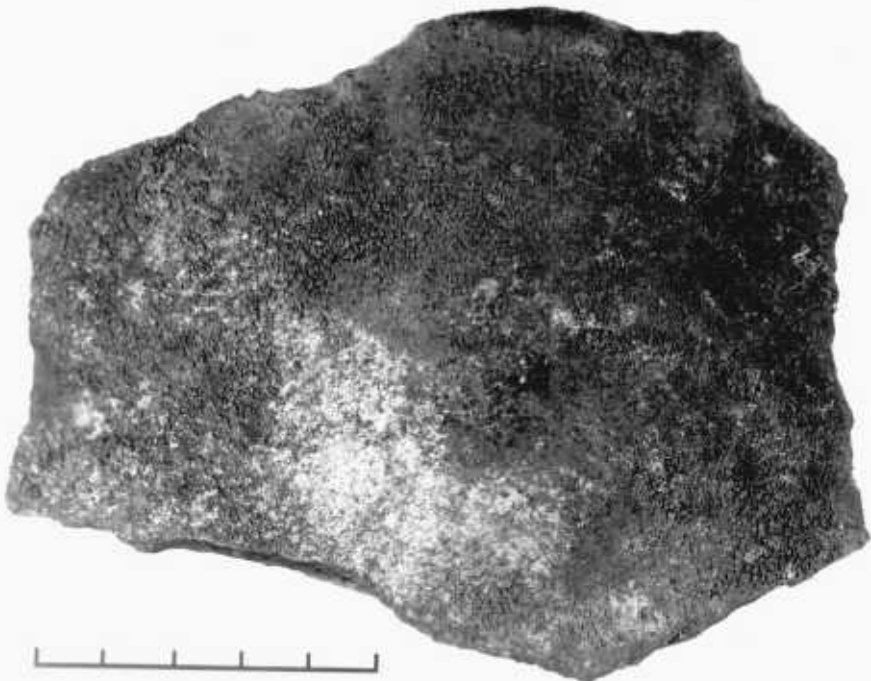
**SH 130 1D**



**CMS**

PLATE 1b

**SH 130 1D**



**CMS**

# SH 130 1D



PLATE 3

# SH 130 1D



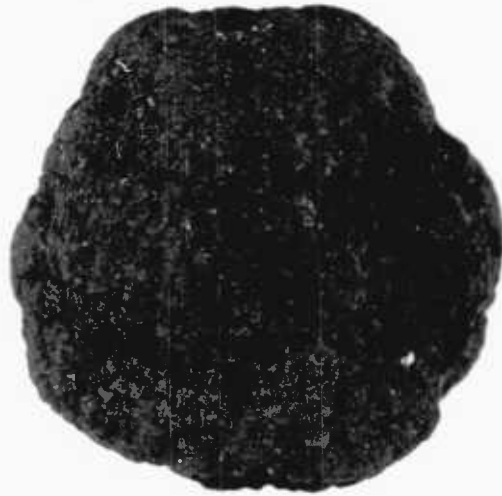
agrees with the observations made in this study, the largest nodules being recovered from the continental margin areas off South Africa and Madagascar.

It was noticeable that, whilst nodules varied greatly in size over the Indian Ocean as a whole, no large size variations were observed in nodules from a single dredge haul or even between samples from closely spaced sampling stations. In contrast to the findings of Cronan and Tooms (1967) no distinct population subsets of nodules were identified at any Indian Ocean sampling site on the basis of size. It was interesting to note that the Cu-Ni-rich nodules from the Central Indian Basin were of very similar diameter (2 - 4 cm.) to those in the Pacific ore-grade belt (Friedrich et al, 1974).

#### (b) Shape

The shape of the samples investigated was even more variable than their size. Unfortunately, in quite a few cases the samples had broken up during recovery and since not all the fragments were present the original shape could not be recognised. Many nodules were fairly nearly spherical in shape (e.g. plates 4, 5 and 17), however some nodules were slightly or noticeably flattened (see plates 6, 7 and 9). In general, a slightly flattened shape was particularly characteristic of nodules from the Central Indian and Wharton Basins. Some nodules showed slight surface irregularities (plates 7 and 9). These are probably caused by a small secondary nucleus of growth becoming attached to the main nodule during its growth. Irregularities in nodule shape can also be caused, when the encrusting layers are thin, simply by irregularities in the shape of the nucleus or substrate. However as the concretionary layers become thicker any irregularities tend to become smoothed

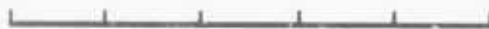
CIRCE116D



CMS

PLATE 5

AB387C



CMS

out. This phenomenon is well seen in sample AB384C (plate 16). Other types of irregular nodule are formed by the adhering together during growth of several nuclei producing a polynodule, often with a wide variety of different nuclei and therefore shape (see plate 10). This type of irregular nodule was found in various areas of the Indian Ocean but was particularly common in the Madagascar Basin. A possible reason for this is that the high bottom current velocities in this basin cause small accreting nodules to roll together and coalesce. Highly irregular nodules have been reported from other areas with high bottom current activity (Goodell et al, 1970; Glasby, 1972). However, Payne and Connally (1972) and Kennett and Watkins (1975), studying large areas of extensive nodule deposits underlying the highly active Antarctic Circumpolar Current found that spherical nodules were more prominent than irregular nodules in most areas. High bottom current velocity may therefore not be the major factor influencing the formation of irregular nodules and some other factor such as the availability of large numbers of small nuclei may be of prime importance.

At one station off the west coast of Madagascar samples of highly unusual shape were recovered (see plate 11) together with a small fairly regularly-shaped nodule. These samples were encrustations around a thin cylindrical core which was brown in colour and very hard and rich in iron. It is postulated that these samples are encrustations around iron nails which have become completely oxidised and, in some cases, partly dissolved away. They were recovered from an area much used by shipping for at least the last two hundred years. If they are this old, a growth rate of at least 3 mm. per 100 years would have been necessary for them to have grown to their present size. Whilst this rate is



PLATE 6

101GBD

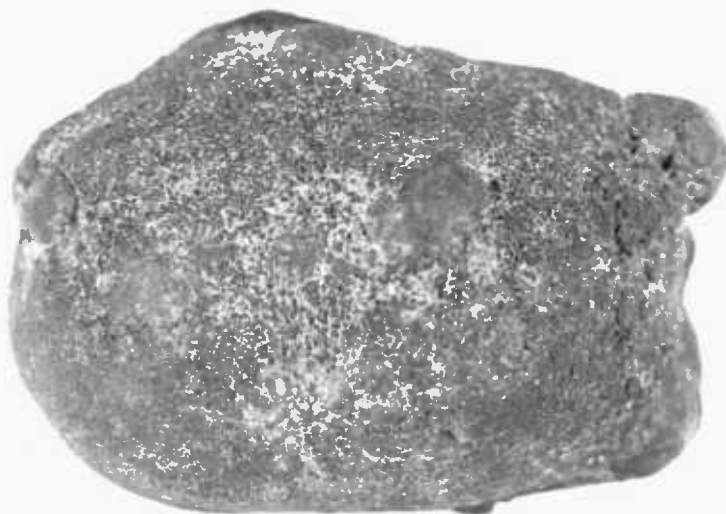


at least two orders of magnitude higher than most estimates of deep-sea nodule accretion rates (Ku and Broecker, 1969; Tooms et al, 1969; Bhat et al, 1973; Heye, 1975), shallow water continental margin-type nodules are thought to accrete at rates as high as several millimetres per 100 years (Mero, 1965; Tooms et al, 1969; Ku and Glasby, 1972). Furthermore, rapid growth of ferromanganese oxides may occur around iron-rich objects due to the ability of iron to initiate and catalyse the oxidation and precipitation of manganese oxides (Burns and Brown, 1972). Proof of this was found by Goldberg and Arrhenius (1958) who recovered casings from naval shells from the Pacific Ocean which were already thickly coated with ferromanganese oxides.

The shape of ferromanganese crusts tends to be controlled by the surface shape of the substrate, where the crust is thin. Plate 14 shows a sample consisting of a thin encrustation around a highly altered montmorillonite- and phillipsite-rich substrate, which illustrates this point. However, in almost all samples examined where the encrustation was thick, the surface shape tended to be much smoother (for example see plates 1 (a) and 12 (a)).

No major variations in sample shape were observed at many stations at which abundant material was recovered. However, some stations sited in areas of very rugged bottom topography produced material of very varied type, shape and thickness. For example plates 7 and 8 show the two markedly different samples recovered at station ANTP 109D on the flanks of the south-west Indian Ridge. Plates 1, 2 and 3 also show material collected within the same dredge haul, in this case on the flanks of the Carlsberg Ridge. Plates 1 and 2 show crusts of markedly different thickness. The sample in plate 2 consists of a thin crust on

ANTP109D



CMS

ANTP109D



CMS

an angular fragment of relatively fresh basalt whilst that in plate 1 is a 5 to 6 cm. thick crust with no substrate attached. Thus within the same small areas it appears that some substrates have been exposed to favourable conditions for ferromanganese-oxide deposition for much longer periods than others. This is probably a result of submarine erosional processes which in this type of rugged volcanic environment will continually produce new fragments of basalt about which accretion can take place. The three fragments shown in plate 3 show granular accreting surfaces over the whole of their outside area. Their extremely angular shape points to the conclusion that they are fragments of a pre-existing nodule or encrustation which after breaking up have begun to accrete as separate nodules. However, close inspection of their internal structure showed them to be almost featureless and gave no clear evidence to back up this hypothesis.

(c) Shape and Texture of surface

The surface textures of the nodules and encrustations examined varied from smooth and polished to coarsely granular. Raab (1972) and Calvert (pers. comm.) have noted that in Pacific Ocean nodules a granular surface texture tends to develop on that part of the nodule which is in contact with the sediment, whilst the upper parts of nodules, which are in direct contact with sea-water, tend to have smooth surfaces. This has led Calvert to believe that a granular surface texture on ferromanganese nodules suggests their growth by element precipitation from interstitial pore waters at, or very near, the sediment-water interface. A smooth surface texture on the other hand indicates accretion by direct precipitation from sea-water. In this

PLATE 8

ANTP109D



CMS

investigation several encrustations were examined which had a granular surface texture (for example, see plates 1 (b), 2 and 12 (b)), yet these deposits must, by their very nature, have accreted by direct precipitation from sea-water. The nature of the surface texture of samples does not therefore appear to be a reliable guide to the way in which these deposits accreted, at least in the case of Indian Ocean samples. This may be the case because, whatever the original nature of the surface texture of a sample, it may be altered by subsequent changes in the bottom environment. This is illustrated by some nodules from the Mozambique Channel (see plate 5). These samples have generally smooth to polished surfaces but have granular surfaces wherever depressions occur in the outer surface (see centre of right-hand nodule in plate 5). It is postulated that the whole surface of the nodules was originally granular but that strong bottom currents perhaps operating when conditions were otherwise unfavourable for nodule growth, have subsequently physically corroded the nodules. This process may be effected by the abrasive action of the suspended sediment load in the bottom current. It is interesting to note that many samples from areas of strong bottom current activity at present, such as the Mozambique Channel and Madagascar Basin, tend to have smooth surfaces (see plates 5, 8 and 10). By contrast, samples from areas where bottom currents are not strong, such as the Central Indian Basin, have very granular surfaces (see plate 6).

Haye (1975), in a detailed study of Pacific Ocean nodule structures and growth rates, reached the conclusion that rough, "gritty" or "knobby" outer surfaces on nodules simply indicated accretion under favourable circumstances whilst smooth surfaces (but ones with no gloss or polish) were formed as a result of growth under unfavourable circumstances. He studied only one nodule from

# ANTP 153D



CMS

# ANTP 153D



CMS

the Indian Ocean. This had a smooth, shiny surface and age dating of the nodule indicated that no growth had occurred for at least the last  $3 \times 10^5$  years. Heye suggests that the shiny surface is therefore due to mechanical or chemical erosion.

Heye and Marchig (1977) reach the conclusion that the granular knobbly layers within nodules are fast-accreted layers, and they also found that these layers were enriched in Mn, Ni and Cu. More massive internal layers, those which produce a smooth surface texture, tend to be depleted in these metals and are thought to have accreted more slowly. If these theories are correct then the Cu-Ni-rich pelagic nodules in the Pacific and Indian Oceans are likely to have grown relatively quickly unless growth has consisted of short bursts of rapid growth interspersed with long periods with no growth. However, several workers (Ku and Broecker, 1969; Tooms et al, 1969; Bhat et al, 1973) have shown that pelagic nodules in general appear to grow very slowly and Heye himself alludes to this theory in an earlier study, (Heye, 1975). The surface texture of nodules and encrustations and its implications as to rates and modes of growth must therefore be regarded as another unsolved problem of these marine deposits.

The surface shape of the ferromanganese oxide deposits varied from regular to highly botryoidal and cavernous. As with the surface texture, surface shape tended to be fairly similar in samples from the same locality, but showed rather more variation over small distances than did surface texture. In general encrustations, especially where thick, tended to have a more regular surface than nodules. Some nodules (see plate 5) had a very regular surface, however more commonly they showed some departure from regularity such as the presence of knobbly lumps



AB384B



PLATE 11

AB367C



(plates 6 and 7) which if large gave the whole nodule an irregular shape. Some nodules, especially from the Central Indian Basin, had a very cavernous surface (see plates 4 and 6). This surface structure was also a feature of some encrustations (see plate 2). However, in contrast to nodules, only rarely did thick encrustations have an irregular surface such as that seen in sample SH1317D (plate 13).

No definite, marked regional trends were observed in the surface shape or texture of the samples analysed in this study, but many areas were so sparsely sampled that inter-regional comparisons were not feasible. Despite this, some general trends were observed in the more well-sampled areas. Nodules from the south-west part of the Indian Ocean i.e. from the Crozet, Madagascar and Mozambique Basin areas had generally smoother surfaces, were less friable and were browner in colour than nodules from the central and eastern areas of the ocean. Nodules from these regions tended to be blacker in colour, to be rather friable and to have granular cavernous surfaces whilst being generally regular in shape. Interestingly, the Cu-Ni-rich nodules from the Central Indian Basin (see Section 5) were very similar in colour, size and surface texture to the deposits of similar chemical composition in the north-east Pacific Ocean although some nodules from the latter region appear to be generally more discoidal in shape, Raab (1972). However sampling in the Central Indian Basin has been comparatively sparse and more detailed sampling and study may show even greater physical similarities between these chemically similar nodule deposits.

#### (d) Internal Features

The internal structure of marine ferromanganese-oxide

SH 1307D



CMS

SH 1307D



CMS

deposits is complex and has received much more study than the external features, mostly using microscope techniques (Arrhenius, 1953; Mero, 1965; Soren, 1967; Cronan and Tooms, 1968; Andrushchenko and Skornyakova, 1969; Glasby, 1970; Bezrukov and Andrushchenko, 1973, Shterenberg et al, 1975). The detailed study of Pacific Ocean nodules by Andrushchenko and Skornyakova (1969) revealed at least five major different types of structure in the ferromanganese oxide phase, whilst Bezrukov and Andrushchenko (1973) in a detailed study of Indian Ocean nodules recognised seven structural types, which were similar to those observed by Andrushchenko and Skornyakova (1969) in the Pacific. The five main structures recognised by both groups of workers were:-

1. Concentrically banded collomorphic structures
2. Collomorphic globular structures
3. Parallel laminar and shelly laminar structures
4. Dendritic structures
5. Cataclastic structures

Most earlier workers had described features similar to some or all of the features listed above. Andrushchenko and Skornyakova (1969) and Bezrukov and Andrushchenko (1973) found that structures of type 1 and 2 were the most common features in Pacific and Indian Ocean nodules. No microscopic investigations were carried out on the samples investigated in this study and detailed internal structures were therefore not examined. However, major structural features could be recognised with the naked eye and it appeared that in the samples examined structures of type 1 and type 2 were again the most common feature.

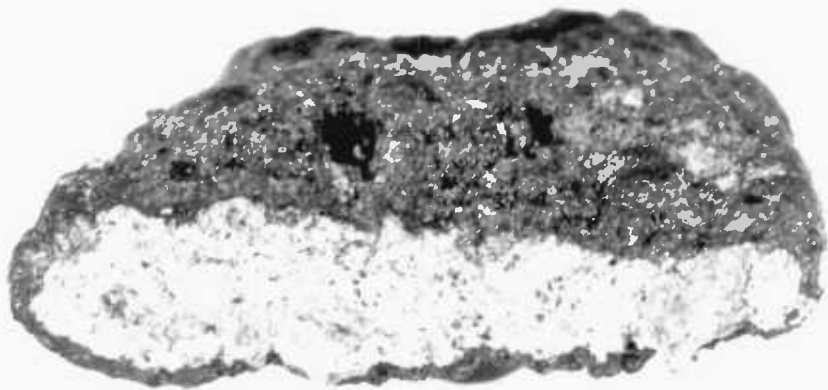
Concentric banding was clearly developed in many samples (for example see plate 15) however this type of structure was

SH 13 17D



CMS

ANTP113D

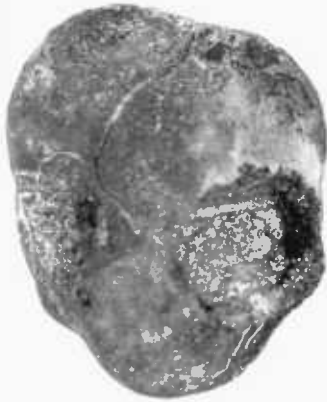


CMS

not always visible throughout the whole thickness of the oxide layer. The not infrequent observation of a particular ferromanganese-oxide-rich layer at the same horizon throughout the whole of the nodule indicates that deposition has often occurred equally on all sides of the sample and this argues strongly for the idea that at least some nodules do roll around somewhat on the ocean floor during growth, although the mechanisms causing this movement are unknown at present.

Most nodules showed a core of some type. In a few cases this was of biological origin such as shark's teeth but nodules from all areas of the ocean more commonly displayed a core of volcanic origin. Many of the encrustations examined had no substrate attached and it was therefore not possible to say with certainty what this might have been. However, in view of the type of environment from which most crusts were recovered the most likely substrate is volcanic rock of some sort, usually basalt. Coatings and thin slab-shaped crusts however were more commonly found with other than basaltic substrates. Some coatings on coral and limestone slabs were recovered and thin slab-shaped concretions around compacted sediment and phosphatic deposits were also observed, albeit rarely. In most cases where the substrate was recovered with the encrustation it appeared relatively fresh and there was usually a clearly marked boundary, between the encrusted material and the overlying oxide layers. In some nodules also the core material was fresh and unaltered but in most nodules where the oxide layer had attained an appreciable thickness, alteration of the core had occurred. This process of alteration of volcanic nuclei appears to continue until the core is completely altered and often begins to be replaced to a greater or lesser extent by ferromanganese-oxide

85GK



CMS

AB384C



CMS

material. Plates 14 to 17 show samples with cores displaying progressive increase in alteration and replacement. Plate 14 shows an encrustation which still has a clearly recognisable core of silicate material, whilst plate 15 shows small nodules in which the cores are beginning to show signs of replacement by oxide material. The nodule in plate 16 has a core showing extensive replacement by ferromanganese oxide material whilst in sample RC14/D4 (plate 17) the core is no longer visible, having been completely replaced by dendritic ferromanganese oxides. This sample is interesting in that its internal structure is entirely of this rather uncommon dendritic type and there is no indication of how large the original core was. Cronan (1976, quoting Sorem) suggests that dendritic formations are indicative of post-depositional migration and recrystallisation of manganese oxides within the deposit whilst Glasby (1970) suggests that banded structures are also an ageing feature, forming from recrystallisation of originally more globular structures. If this is so, the question remains as to whether dendritic growth structures are ageing products which occur after an earlier process of concentric layer formation or as an alternative to it, in response to rather different physico-chemical conditions.

Cracks were a common feature in many nodules examined. However, many of these may simply be contraction cracks due to the sample losing much of its interstitial adsorbed water during storage. The cracks were of two types, radial and concentric. Radial cracks were more common but some concentric breakage also occurred, in some cases causing shells of ferromanganese oxide material to be shed from the outer surface of the nodule (see plate 5). The preponderance of radial cracks over concentric ones was noted in Pacific Ocean nodules by Raab (1972) who



PLATE 17

**RC 14 / D 4**

CMS

interpreted the former as shrinkage cracks due to ageing. A much more detailed study of fractures in nodules was carried out by Heye (1975), who produced mathematical models for the development of both types of crack. Heye argues that cracks within nodules are self-propagating features and eventually result in the complete break-up of nodules on the sea bed. The intensity of cracks within a nodule can therefore be used as a rough guide to its comparative age. As suggested by Sorem (1973) much information can probably be gained from nodule internal structure concerning many aspects of their palaeo-environment but such a goal can only be achieved when much more attention and research has been focussed on this subject.

## S E C T I O N 4

### MINERALOGY

#### (i) INTRODUCTION

Since the pioneering investigations of Buser and Grutter (1956), the mineralogy of marine ferromanganese-oxide deposits has been a source of continued controversy. Much of this stems from the fact that the positive identification of the phases present in these deposits is extremely difficult because of their very small particle size and poor degree of crystallinity.

Three distinct manganese phases were originally found in manganese nodules by Buser and Grutter (Buser & Grutter, 1956; Grutter & Buser, 1957; Buser, 1959). They termed these phases "10Å manganite", "7Å manganite" and " $\delta$ -MnO<sub>2</sub>" after the synthetic phases whose d-spacings were most closely matched by the phases in nodules. Later workers investigating the mineralogy of these deposits identified the phases they observed by comparing their X-Ray powder photographs with those of naturally occurring manganese minerals. Thus Straczek et al (1960), Hewitt et al (1963), Manheim (1965), and Grill et al (1968) identified the minerals present as todorokite (Yoshimura, 1934) and birnessite (Jones & Milne, 1956).

This terminology was adopted by many subsequent workers.

A further terminology was set up by Giovanoli et al (1970 a,b, 1971) who compared the manganese phases in nodules with various synthetic phases which they had prepared and analysed. Thus they termed the manganese phase giving lines close to those of todorokite, sodium manganese (II,III) manganate (IV) hydrate, and the manganese phase which gave lines close to those of  $\delta$ -MnO<sub>2</sub> they termed manganese (III) manganate (IV). This terminology is rather complex and has not found general acceptance in the subsequent literature.

Arrhenius (1963) and Burns and Fuerstenau (1966) have pointed out that the terms "10Å manganite" and "7Å manganite" are not ideal since they may lead to confusion with the mineral manganite ( $\chi$ -MnOOH), which has not yet been reported as occurring in manganese nodules and which is structurally different to 7Å manganite and 10Å manganite. Since Frondel (1953) and Straczek et al (1960) have shown that the mineral todorokite is quite a widely occurring terrestrial manganese mineral, and since their published X-Ray data for this mineral closely resembles that obtained from many ferromanganese nodules, the term todorokite has been accepted by many authors (Grill et al, 1968; Cronan and Tooms, 1969; Price and Calvert, 1970; Burns et al, 1974; Meylan, 1975) to refer to that phase in ferromanganese oxides which gives strong reflections at 9.5Å - 9.8Å and 4.7Å - 4.9Å. However, Giovanoli et al (1971), suggested from electron diffraction measurements on synthetic phases, that todorokite is actually a mixture of a mineral which they termed "primary busserite", partly dehydrated to birnessite and partly reduced to manganite ( $\chi$ -MnOOH). They suggest that the  $\chi$ -MnOOH crystals are so small as to be undetectable by X-Ray diffraction analysis.

Buserite was accepted as a new mineral in 1970 by the I.M.A. Commission on New Minerals. Since many analyses of todorokite have been presented in the literature which show no signs of even the strongest lines of birnessite and manganite, several workers believe that much stronger evidence is required before todorokite is discredited as a mineral (Margolis and Burns, 1975). No evidence to support the theory of Giovanoli et al was found in this study and thus in view of its preference in the literature, the term todorokite is used throughout this thesis to refer to that mineral phase which has strong peaks at  $9.5\text{\AA} - 9.8\text{\AA}$  and  $4.7\text{\AA} - 4.9\text{\AA}$ .

The other manganese phases originally identified in nodules by Buser and Grutter (1956) were " $7\text{\AA}$  manganite" and " $\delta\text{-MnO}_2$ ". These phases have also been the subject of much confusion. It is now widely accepted however, that the " $7\text{\AA}$  manganite" of some authors (Buser and Grutter, 1956; Glasby 1970, 1972; Price and Calvert, 1970) is identical with the "birnessite" of others (Cronan and Tooms, 1969; Manheim, 1965; McKenzie, 1971; Moore and Vogt, 1976). Again, in view of the structural differences between this phase and the mineral manganite the name birnessite is preferred for that phase in ferromanganese oxides which gives peaks at  $7.0\text{\AA} - 7.2\text{\AA}$  and  $3.5\text{\AA}$  to  $3.6\text{\AA}$ .

The original birnessite investigated by Jones and Milne (1956), apart from having intense lines at  $7\text{\AA}$  and  $3.6\text{\AA}$  also showed two weaker lines at  $2.44\text{\AA}$  and  $1.41\text{\AA}$ . Thus, comparing their diffraction data with that of " $\delta\text{-MnO}_2$ " (McMurdie and Golovato, 1948) and "manganous-manganite" (Cole et al, 1947) Jones and Milne reached the conclusion that birnessite was simply a naturally occurring  $\delta\text{-MnO}_2$  with an O:Mn ratio of 1.90:1. Buser et al (1954) suggested that the  $\delta\text{-MnO}_2$ 's reported in the literature as giving

only two lines (at 2.44Å and 1.42Å) were simply more oxidised forms of the four-line form (i.e. "birnessite" of Jones and Milne(1956), "manganous-manganite" of Cole et al (1947)). Feitknecht and Marti (1945) gave a formula for manganous-manganite as approximately  $4\text{MnO}_2 \cdot \text{Mn}(\text{OH})_2 \cdot 2\text{H}_2\text{O}$  and interpreted them as double-layer compounds consisting of sheets of formula  $\text{Mn}(\text{OH})_2 \cdot 2\text{H}_2\text{O}$  interspersed with layers of  $4\text{MnO}_2$ , approximately 7Å apart giving basal reflections at about 7.0Å (001) and 3.5Å (002). The most oxidised forms of manganous-manganite were considered to be disordered from this idealised sandwich structure, as more and more  $\text{Mn}^{2+}$  lattice sites become filled by  $\text{Mn}^{3+}$  or  $\text{Mn}^{4+}$  ions. The progressive replacement destroys the  $\text{Mn}(\text{OH})_2$  sheets, the basal reflections become very weak or disappear and only two broad lines at about 2.4Å and 1.42Å are obtained. Buser et al (1954) therefore suggested retaining the terms  $\delta\text{-MnO}_2$  and manganous-manganite and using them to describe manganese oxides with O:Mn ratios greater or less than 1.90 respectively. However Gleener et al (1961) synthesised manganese oxides with O:Mn ratios up to 1.99 which gave X-Ray patterns showing the basal reflections at about 7.2Å and 3.6Å. This led Bricker (1965) to suggest that particle size rather than degree of oxidation influences the X-Ray powder pattern of these manganese oxides, the basal reflections being absent in very small crystallites. More recent work suggests that this may not be the case, at least for marine manganese oxides. Brown (1971) and Burns et al (1974) took samples which showed only two diffuse lines at 2.4Å and 1.42Å and immersed them in sea-water at high pressure and room temperature. Partial re-crystallisation was found to have taken place and the samples showed additional peaks at 9.6Å and 4.8Å, but no signs of reflections at 7.2Å and 3.6Å. Samples already showing reflections at 7.2Å and 3.6Å showed no changes when subjected to similar pressure and temperature conditions. However Brooke (1968) carrying out ageing studies by heating samples found that with increasing temperature some nodules show a complete transition from a 10Å form to a 7Å form

to  $\delta\text{-MnO}_2$  whilst other samples showed no change. Similar findings were also observed by Cronan (1967).

Clearly then, the interrelationships between the synthetic and naturally occurring minerals "birnessite", " $\delta\text{-MnO}_2$ " and manganous-manganite are still imperfectly understood and are made all the more complicated by their inherently non-stoichiometric nature (Giovanoli et al, 1973).

In this study many samples were analysed which showed only broad peaks at  $2.44\text{\AA}$  and  $1.42\text{\AA}$  and it is thus proposed to use the term  $\delta\text{-MnO}_2$  to describe this phase. In only comparatively few samples were peaks at  $7.2\text{\AA}$  and  $3.6\text{\AA}$  observed which were definitely assignable to a manganese phase. However where this phase occurs it is regarded as being a distinctly different phase to  $\delta\text{-MnO}_2$ , and therefore, taking into account the work of previous authors, termed birnessite. Thus the three manganese phases recognised in the samples analysed, and their characteristic diffraction lines, are given in Table 1.

d( $\text{\AA}$ )	I	PHASE
9.6 - 9.8 4.6 - 4.8 2.46 2.39	vs s m m	Todorokite
7.0 - 7.2 3.5 - 3.6 2.46 2.33 1.42	vs s m m w	Birnessite
2.40 - 2.44 1.40 - 1.44	v.br.m. v.br.m.	$\delta\text{-MnO}_2$

TABLE 1

Diffraction patterns of the manganese phases recognised in Indian Ocean ferromanganese-oxides.

## IRON PHASES

Less work has been done on the iron phases in marine ferromanganese oxides than on the manganese phases, mainly because the iron appears to be present predominantly as X-Ray amorphous material even when the iron content of the sample is relatively high. However, a knowledge of the physical state of the oxides and oxyhydroxides in ferromanganese oxide deposits is important if the geochemistry of these deposits is to be fully understood. Indeed many authors believe that the iron phases play a vital role in the nucleation and authigenesis of marine ferromanganese oxides (Burns and Brown, 1972; Burns and Burns, 1977).

Some workers suggest that a significant amount of iron is present randomly distributed in the hydroxyl sheets of the manganese phases in ferromanganese oxide deposits (Goldberg and Arrhenius, 1958; Goldberg, 1965) or as unidentified mixed-layer iron-manganese oxide (Glasby, 1972). However, it is generally accepted that the iron which is present as a discrete phase in marine ferromanganese oxides, is present exclusively as ferric oxyhydroxides of general formula  $\text{FeOOH}$  (Burns and Burns, 1977). The most commonly reported of these minerals in marine ferromanganese oxides, is goethite ( $\alpha\text{-FeOOH}$ ) (Arrhenius, 1953; Aumento et al, 1968; Bonatti and Joensuu 1966; Glasby, 1972; Bezrukov and Andrushchenko 1973). Lepidocrocite, maghemite, hematite and akaganeite have also been reported in the literature as occurring in marine ferromanganese oxides, but these all appear to be of very minor importance.

Much of the ferric oxyhydroxide material however is present as an X-Ray amorphous species of small particle size, variously called "Amorphous  $\text{Fe}(\text{OH})_3$ ", "iron  $\square$ oxide hydrate gel", "colloidal ferric species" and "hydrated ferric oxide polymer"



(Burns & Burns, 1977). Mossbauer spectroscopy of marine ferromanganese-oxides from various localities has shown that the mean particle diameter of the iron phases is extremely small, generally less than 200 - 300Å (Herzenberg & Riley, 1969; Johnson & Glasby, 1969; Carpenter & Wakeham, 1973). This is too small by at least one order of magnitude to be amenable to X-Ray diffraction studies.

Thus there are three possible sites for the iron in marine ferromanganese-oxides which is not present as adsorbed ions:-

1. Within the lattices of the manganese phases, substituting for Mn ions.
2. As an unidentified random mixed-layer iron-manganese oxide.
3. As a discrete iron phase:
  - (a) of sufficiently large particle size and sufficiently well-ordered structure as to be identifiable by X-Ray diffraction techniques.
  - (b) of extremely small particle size and/or disordered structure and thus essentially amorphous.

Of these, only those phases of type 3(a) are likely to be amenable to standard X-Ray diffraction study. Of the various iron minerals listed in the literature as being found in marine ferromanganese-oxide deposits, only goethite was identified in the samples analysed in this investigation. In samples where no goethite peaks were observed, the iron phases were regarded as essentially amorphous.

#### (ii) MINERALOGY OF THE FERROMANGANESE PHASES OF INDIAN OCEAN SAMPLES

Almost all the 116 samples analysed chemically during this study were also subjected to mineralogical investigations by X-Ray

diffraction techniques using a Phillips diffractometer. Details of these techniques are given in Appendix 2.

(a) Mineralogy of the Manganese phases

Table 2 gives the total number of samples in which each of the three recognised manganese phases was identified. In some of the samples analysed, lines were observed at  $2.4\text{\AA}$  and  $1.4\text{\AA}$  together with weak lines at  $9.8\text{\AA}$  and  $4.8\text{\AA}$  which at first sight were indicative of the presence of todorokite in small amounts. However, after careful comparison of these lines with the patterns obtained from todorokite-rich samples and a pure terrestrial sample of todorokite from Fiji, it was decided that these powder patterns could only be accounted for by assuming the presence of  $\delta\text{-MnO}_2$  in addition to todorokite. The  $\delta\text{-MnO}_2$  was inferred to be present because the broad peaks at about  $2.4\text{\AA}$  and  $1.4\text{\AA}$  were more intense than could have been produced by the amounts of todorokite present.

Amongst those samples in which todorokite was particularly abundant, 15 samples also showed a broad weak band at about  $7.2\text{\AA}$ . In an attempt to establish whether this was due to poorly crystalline birnessite or not, one of these samples was heated to various temperatures and re-examined after each heating. The results of this experiment are given in Table 3.

As can be seen from Table 3, as the temperature was raised the height of the  $7\text{\AA}$  peak increased, whilst that of the  $10\text{\AA}$  peak decreased and collapsed. Above  $120^\circ\text{C}$  the  $7\text{\AA}$  peak also collapsed. This behaviour is in agreement with that observed for birnessite by Jones and Milne (1956) and with that observed for Pacific Ocean samples containing both todorokite and birnessite (Cronan, 1967). No noticeable changes were observed when samples containing  $\delta\text{-MnO}_2$  only were heated through the same temperature range.

TABLE 2 Frequency of occurrence of manganese minerals in Indian Ocean ferromanganese oxides.

Manganese phase(s)	Number of samples	Total for each phase
Todorokite	20	Total number of samples containing todorokite = 45
Todorokite & Birnessite	13	
Birnessite	3	Total number containing birnessite = 16
$\delta$ -MnO <sub>2</sub>	27	Total number containing $\delta$ -MnO <sub>2</sub> = 39
Todorokite & $\delta$ -MnO <sub>2</sub>	12	
Amorphous	20	

TABLE 3 Results of heating experiments conducted on sample 91GBX

Temperature (°C)	Height of 9.6Å Peak (in scale divisions)	Height of 7.2Å Peak (in scale divisions)
20°	26	8v.br.
60°	14	13br.
90°	8br.	16
120°	8v.br.	18
170°	0	5v.br.

The powder patterns of typical well-crystalline samples analysed are given in Table 4 together with the powder patterns of todorokite, birnessite and  $\delta$ -MnO<sub>2</sub>.

(b) Mineralogy of the Iron phases

As already discussed, goethite was the only iron mineral identified in the samples analysed, and in all it was identified in 20 samples. The diffraction patterns of two such samples are given in Table 5, together with the diffraction data for goethite taken from the literature. Only in a very few samples did the goethite appear well-crystalline. In sample AB369F, the goethite was particularly well-crystalline and 8 peaks were identifiable. This sample contained 40% Fe, however the degree of crystallinity of the goethite appeared to be a more important factor than the amounts which may have been present, thus sample D000110PG which contained only 12% Fe showed 6 clearly identifiable peaks. In most of the other samples in which goethite was recognised, only a broad peak at 4.18Å was clearly visible although sometimes small peaks at 2.69Å and 2.45Å were observed.

Many samples, even though they contained up to 20% iron, did not exhibit any lines attributable to a discrete iron phase and the iron phase in these samples was therefore regarded as amorphous.

(iii) OTHER MINERALS

Ferromanganese nodules often contain minerals, other than the authigenic iron and manganese phases, of both detrital and authigenic origins. Those which have been identified include pyroxenes, amphiboles, feldspars, rutile, sphens, anatase, barite, apatite,  $\alpha$ -quartz, various clay minerals, carbonates and zeolites such as

TABLE 4 Powder patterns of selected ferromanganese oxide samples. (Columns 1 - 5)

1. AB375 (b)		2. ANTP117D		3. SH1317D		4. 95GBX	
d(Å)	I	d(Å)	I	d(Å)	I	d(Å)	I
9.67	100					9.65	100
		7.25	100			7.25	30br.
4.80	55					4.87	60
		3.65	70			3.67	20
3.22	10br.						
2.45	15br.	2.46	55br.	2.43	100br.	2.45	34br.
2.36	15						
		2.33	35br.			2.32	15br.
2.22	15br.					2.33	15
		2.05	15br.			2.07	10
1.98	10						
1.42	15br.	1.42	40v.br	1.42	60v.br	1.42	30br.

(Continued overleaf.....)

TABLE 4 Powder patterns of todorokite, birnessite and  $\delta$ -MnO<sub>2</sub>. (Columns 6 - 8)

5. 23GBD (a)		6. Todorokite		7. Birnessite		8. $\delta$ -MnO <sub>2</sub>	
d(Å)	I	d(Å)	I	d(Å)	I	d(Å)	I
9.60	100	9.68	100				
		7.15	2br.	7.21	100		
4.80	90	4.80	80				
		4.45	5br.				
				3.61	100		
		3.22	15				
2.45	90br.	2.46	20	2.46	100	2.43	100br.
2.39	30	2.39	40				
		2.34	15	(2.33	100)		
		2.22	20				
		2.15	5br.				
				(2.04	80)		
		1.98	20				
		1.92	5				
				(1.802	10)		
		1.75	10				
				(1.723	80)		
		1.54	5				
				(1.45	20)		
1.42	40v.br.	1.42	30	1.42	60	1.41	60v.br.

TABLE 5 Powder patterns of selected ferromanganese oxide samples containing goethite.

1. AB369F		2. DOD0110PG		3. Goethite	
d(Å)	I	d(Å)	I	d(Å)	I
4.96	20			4.98	10
4.18	100	4.18	100	4.18	100
				3.38	10
2.70	80	2.66	20	2.69	30
				2.58	8
				2.52	4
2.51	50	2.47	60	2.49	16
2.44	90	2.44	70	2.452	25
2.25	45	2.17	30	2.192	20
1.72	30	1.71	40	1.721	20

phillipsite and clinoptilolite. Whilst most of these are of detrital origin, minerals such as apatite, calcite and the zeolites are regarded as authigenic phases.

Quartz was almost ubiquitous in the samples analysed, the only samples not showing the major  $\alpha$ -quartz peak at  $3.34\text{\AA}$  being a few thin encrustations. Rex and Goldberg (1958) regard a significant amount of quartz in marine sediments to be detrital in origin. Another important source, especially for samples underlain by siliceous sediments might be regarded as biogenic opal. However Calvert (1974) has shown that biogenic opal tends to re-crystallise to cristobalite rather than to quartz, and therefore, the quartz in ferromanganese-oxides is likely to be predominantly detrital in origin.

The cores of several samples were analysed and found to contain abundant plagioclase feldspar of oligoclase to andesine composition. This indicated that the core material was of volcanic origin. In nodules and crusts which had accreted round compacted sediment the commonest minerals identified were montmorillonite (34 samples) and phillipsite (24 samples). Many samples also showed a very broad weak band between about  $3\text{\AA}$  and  $4\text{\AA}$ , this is a characteristic band produced by palagonitic glasses and provides further indication of the volcanic origin of most of the material.

The clay minerals, especially montmorillonite were often identified in the ferromanganese-rich part of nodule samples. This is probably due to their adhering to the nodule surface and being incorporated in the nodule as it continues to grow, or being remnants of a replacement process. In addition to montmorillonite, illite was identified in 10 samples, and kaolinite in 3 samples.

Calcite was identified in 8 samples, all of which were



thin deposits on limestone or coral from depths of less than 2500 metres. One sample from a sea-mount in the Somali Basin (SH1318D) was found to contain carbonate-fluorapatite.

#### (iv) DISCUSSION

The regional distribution of the phases todorokite, birnessite,  $\delta$ -MnO<sub>2</sub> and goethite in the Indian Ocean is shown in figures 12 to 16. As can be seen from figure 12, todorokite occurs in samples from all the basins from which material was obtained and also in samples from the continental margin off southern Africa. The typical areas in which samples containing this mineral are found are therefore generally similar to those observed in the Pacific and Atlantic Oceans (Cronan, 1969, 1975). However, in general, todorokite appears to be more widespread in Indian Ocean ferromanganese-oxides than has previously been reported (Cronan 1967; Glasby, 1970; Bezrukov & Andrushchenko, 1973) although the conclusions of Cronan (1967) and Glasby (1970) would have been influenced by the limited nature of the sample population used. Bezrukov and Andrushchenko (1972) reported that todorokite was subordinate in Indian Ocean ferromanganese nodules to psilomelane and a poorly-crystalline form of manganese dioxide which they termed vernadite. However, detailed scrutiny of their data reveals that what they regard as psilomelane in nodules, is a mineral phase which displays a powder pattern much closer to  $\delta$ -MnO<sub>2</sub> than to psilomelane. The principal differences between the findings of Bezrukov and Andrushchenko (op. cit.) and other workers may therefore be due to misinterpretation and confusion of terminology rather than to actual differences in the phases found.

Todorokite has a lower O:Mn ratio than either birnessite or  $\delta$ -MnO<sub>2</sub> and might therefore be expected to form preferentially in

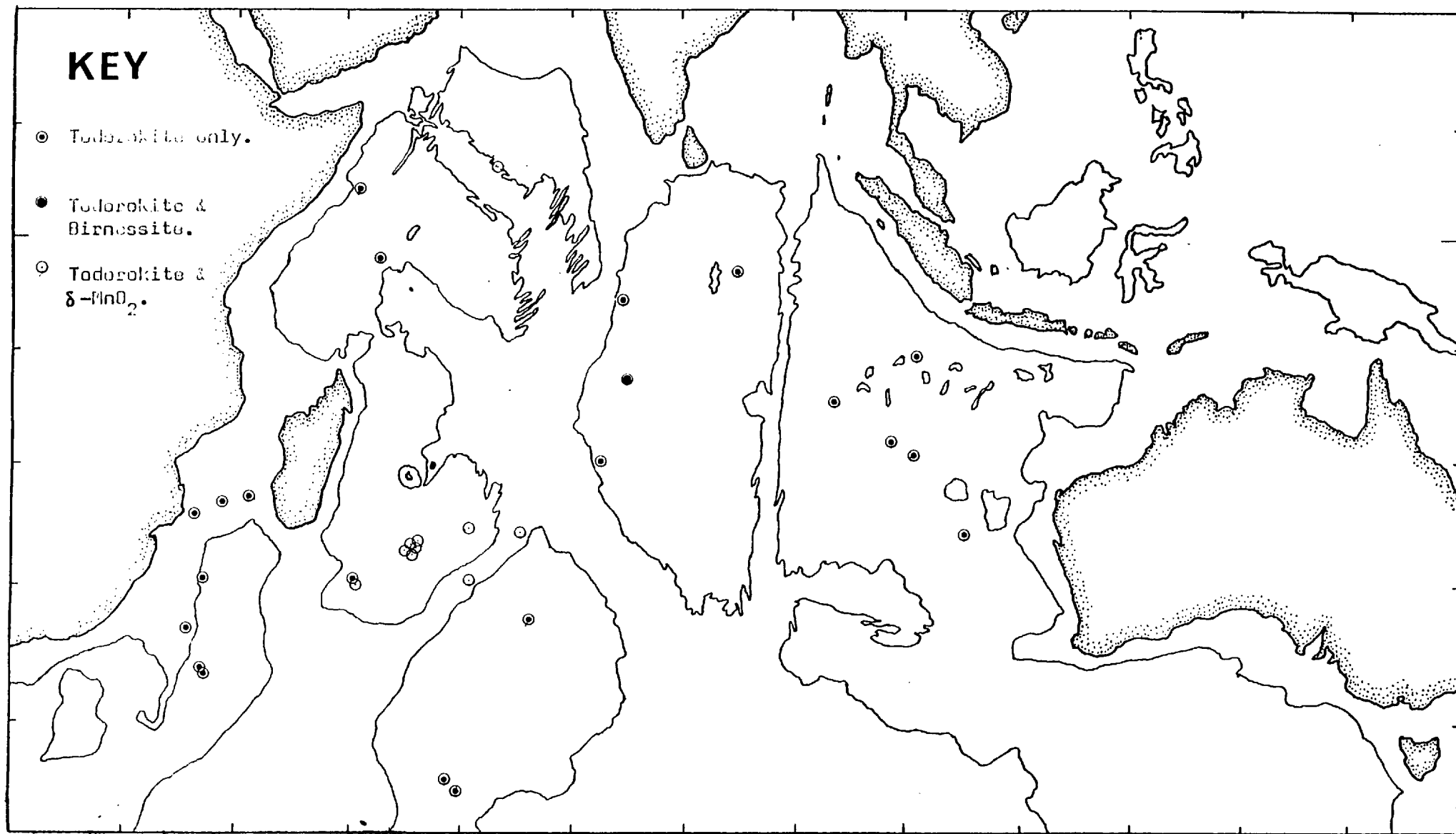


FIGURE 12 Distribution of todorokite in Indian Ocean ferromanganese-oxide samples.

less well-oxygenated environments. According to Baas Becking et al (1960) sediments in continental margin areas have generally lower Eh values than those from the open ocean. This would explain the occurrence of todorokite in continental margin samples off southern Africa. Cronan and Tooms (1969) and Price and Calvert (1970) also reported todorokite as occurring in continental margin samples in the Pacific Ocean. These findings contradict the theory of Barnes (1967) that todorokite tends to develop in deeper water areas, and  $\delta\text{-MnO}_2$  in shallow areas. This is in response to variation in pressure and temperature conditions with depth, todorokite development being preferred in greater water depths. A further argument against the pressure dependence of these minerals is the wide, overlapping range of depths over which each mineral was found (see Table 6). However, todorokite, on average, does occur in samples from greater depths than  $\delta\text{-MnO}_2$ . Some other factor must therefore be operating which varies in a general way with depth but which is not exclusively depth-dependent.

Apart from an isolated continental margin sample, the most todorokite-rich samples occurred in the Central Indian Basin. According to Wyrcki (1971), dissolved oxygen levels in the bottom waters of this basin are lower than those in any other Indian Ocean Basin. Dissolved oxygen levels in the bottom waters of the Wharton and Somali Basins are also comparatively low and these basins also yielded nodules containing fairly abundant todorokite. The dissolved oxygen content of bottom waters is affected by the presence of strong bottom currents, the lack of such currents in the Wharton, Somali and Central Indian Basins accounting at least in part for the lower dissolved oxygen levels occurring there (see Section 2). Strong bottom currents are known to occur at

TABLE 6 Average depth and depth ranges of various authigenic phases in Indian Ocean ferromanganese oxides.

PHASE	AVERAGE DEPTH OF OCCURRENCES (m.)	DEPTH RANGE (m.)
Todorokite	4520	1265 - 5991
Birnessite	4950	4570 - 5730
$\delta$ -MnO <sub>2</sub>	3500	1200 - 5209
Amorphous	4050	860 - 4940
Gothite	3130	1720 - 5410

least in some parts of the Moçambique and Crozet Basins and Wyrteki (1971) has shown that comparatively high levels of dissolved oxygen are found in the bottom and near bottom waters of these basins. However, todorokite was also identified in some samples from these basins, indicating that bottom water conditions are not the only factors affecting nodule mineralogy.

Calvert and Price (1977) suggested that todorokite tended to develop in nodules, in deep-water areas, wherever Mn was being supplied in a reduced form to the growing nodules, by diagenetic remobilisation from the underlying sediment. The comparatively rapid sedimentation occurring in the Moçambique Channel may favour remobilisation of Mn if the sediment has an appreciable content of organic material, (Price & Calvert, 1970) but insufficient knowledge of this and the bottom environment in this and the Crozet Basin prevents an accurate assessment of whether this process is actually occurring.

In summary, the following conditions generally, but not exclusively favour the development of todorokite:

1. Comparatively low dissolved oxygen levels in the bottom waters.
2. A supply of reduced Mn, possibly from the diagenetic remobilisation of this element in underlying sediment.

Birnessite was identified in 16 samples. In 3 of these, it was the only Mn mineral, the remaining 13 samples containing birnessite in subordinate amounts to todorokite. The distribution of these samples is shown in figures 13. The samples containing only birnessite (samples ANTP114D and ANTP117D) were from stations occupied in a fracture zone on the south-west Indian

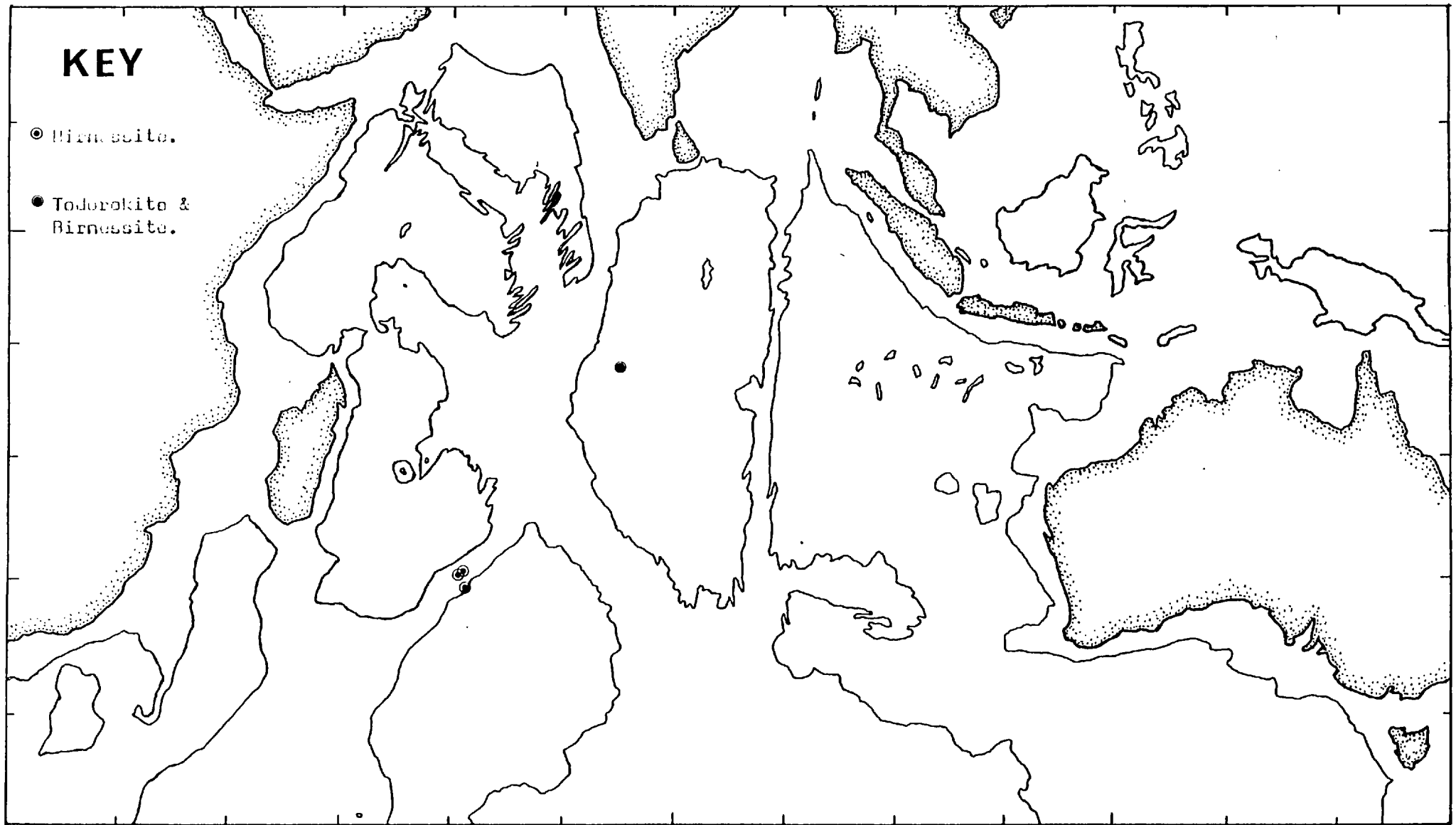


FIGURE 13 Distribution of Birnessite in Indian Ocean ferromanganese-oxide samples.

Ridge, whilst all the samples in which birnessite and todorokite occurred together were from the Central Indian Basin.

According to Buser and Grutter (1953) 7Å manganite (i.e. birnessite in the terminology adopted in this thesis) has a higher O:Mn ratio than todorokite, and might therefore be expected to occur in more highly oxygenated environments. However, Glemser et al (1961) found that birnessite and  $\delta$ -MnO<sub>2</sub> exhibited a wide range of O:Mn ratios which makes the relationship between birnessite and todorokite on the one hand, and birnessite and  $\delta$ -MnO<sub>2</sub> on the other, rather ill-defined if considered solely on these grounds.

The occurrence of birnessite in the todorokite-rich Central Indian Basin nodules is difficult to explain if indeed this mineral does develop more favourably in particularly well-oxygenated environments, since as has already been discussed, bottom conditions in this basin are not thought to be highly oxygenated compared to other areas of the ocean floor. However, the birnessite in all the Central Indian Basin samples was poorly crystalline, producing wide bands rather than peaks in the diffraction pattern, and this may indicate that conditions are not particularly favourable for the development of this mineral. The birnessite in the South-West Indian Ridge samples was by contrast, well-crystalline. Unfortunately, little is known about the bottom environment from which these samples were recovered. It is thus not possible to compare conditions in the two areas with any accuracy. However the fracture-zone samples were all encrustations, and thus indicating that they came from a rock substrate rather than a sediment covered substrate. The fracture-zone samples may therefore have accumulated under more well-oxygenated conditions than those

from the Central Indian Basin.

Whilst all this evidence is very tentative it does suggest that the development of birnessite in both groups of samples may not have occurred solely in response to a particular combination of environmental conditions. Further weight is added to this theory by the experimental work of Brooke (1968) who suggests that birnessite may simply be an ageing product of todorokite over geologically significant periods of time. This would infer that Central Indian Basin nodules containing birnessite are likely to be older than nodules from other localities in the Indian Ocean. No age-dating evidence is available however, and therefore no definite conclusions can be drawn. No age-data is available for the fracture-zone samples either, and although they occurred fairly near the spreading axis of the south-west Indian Ridge, the very slow, erratic spreading history of this ridge (see Section 1) prevents any calculation of a likely maximum age for the encrustations.

Brooke (1968) and Brown (1971) suggest that sample storage under unfavourable conditions, may promote ageing by enabling relatively rapid dehydration and oxidation to occur. However the Central Indian Basin samples were amongst the newest analysed, and had been stored in sealed containers in contact with seawater. Other samples containing todorokite, which had been collected several years previously and stored unprotected in air, showed no trace of birnessite. Moreover, as an experiment, several samples were crushed for analysis under liquid nitrogen as suggested by Brown (1972) and it appears from this that no significant mineralogical changes due to the normal crushing operation have occurred in the samples analysed.

The problem of the relationship between todorokite and



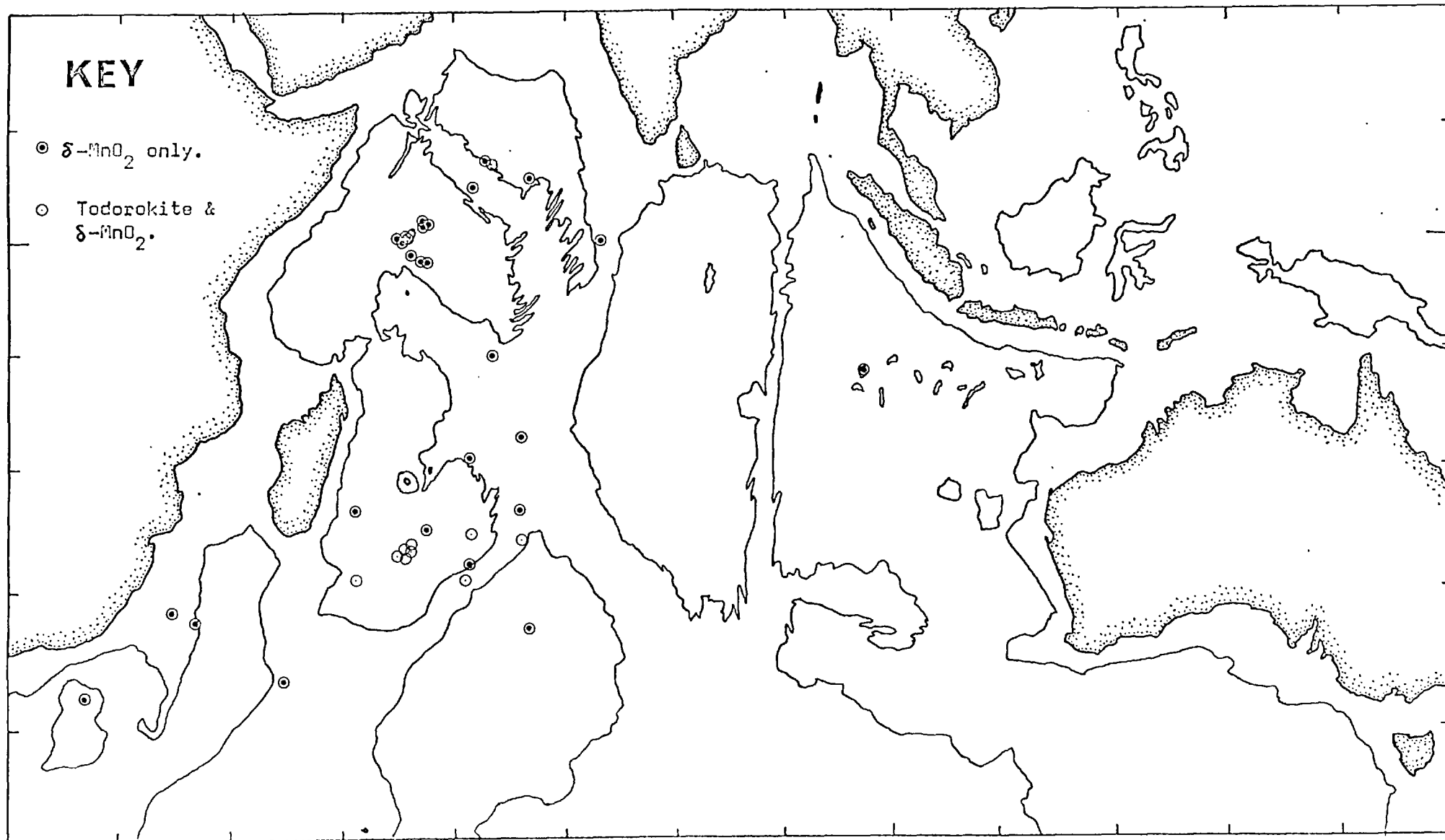


FIGURE 1. Distribution of  $\delta$ -MnO<sub>2</sub> in Indian Ocean carbonate-oxide samples.

birnessite therefore remains largely unsolved.

As can be seen from figure 14,  $\delta\text{-MnO}_2$  was found mainly in samples from elevated areas of the Indian Ocean, in particular from the mid-ocean ridge and isolated sea-mounts. Because of the elevated and rugged nature of their topography these areas tend to be amongst the most highly oxidising in the ocean (Mero, 1955). According to Buser and Grutter (1956)  $\delta\text{-MnO}_2$  is the most highly oxidised of the various manganese phases found in nodules, and the types of environment in which it occurs in the Indian Ocean tend to confirm this. The occurrence of  $\delta\text{-MnO}_2$  in elevated areas, particularly the upper parts of sea-mounts, agrees with the findings of Barnes (1957), Cronan (1957, 1975) and Cronan and Tooms (1959) in samples from the Pacific, Atlantic and Indian Oceans.

Uncharacteristically, quite a few samples were recovered from the floor of the Madagascar Basin, at depths of around 5000 metres which contained  $\delta\text{-MnO}_2$  in addition to small amounts of todorokite. Strong bottom currents are a marked feature of this basin (see Section 2) producing widespread ripple marking (Ewing et al, 1958) and Wyrski (1971) has shown that the dissolved oxygen content of the deep water in this basin is particularly high. The strong bottom currents are caused by Antarctic Bottom Water which flows north-westward out of the Crozet Basin, via passages in the south-west branch of the mid-Indian Ocean Ridge. Whilst data is scarce it seems that this water mass is at least as well-oxygenated in the Madagascar Basin as it is in the Crozet Basin, perhaps because of its passage through the ridge where it may become mixed with more highly-oxygenated water. The presence of a strong flow of well-oxygenated bottom water may therefore be the cause of the development of  $\delta\text{-MnO}_2$  in the nodules recovered

from this basin.

The identification of todorokite also in the samples suggests either that conditions favourable for  $\delta$ - $\text{MnO}_2$  growth occur intermittently and that todorokite develops during less favourable periods, or that under certain conditions, both these minerals can develop together. The first theory might be explained in terms of a mineralogical response to repeated **burial** and exhuming of the growing nodules, or by intermittent pulses of Antarctic Bottom Water. However, an investigation of whether micro-layering of minerals occurred in the samples was beyond the capabilities of the analytical methods employed. The presence of intimate mixtures of different manganese minerals within single nodules has been demonstrated by Bezrukov and Andrushchenko (1972) and von Heimendahl et al (1976). According to all these authors, the minerals tended to be randomly intermixed rather than occurring in discrete layers.

Barnes (1967), Cronan and Tooms (1959) and Skornyakova et al (1975) analysed many samples from the Pacific Ocean which contained both todorokite and  $\delta$ - $\text{MnO}_2$  or both todorokite and birnessite, but did not investigate whether these minerals developed together or in separate cycles. The exact nature of the relationship between different manganese phases within the same nodules and in particular that between  $\delta$ - $\text{MnO}_2$  and todorokite in Madagascar Basin samples, must therefore remain in doubt in the absence of detailed microscopic studies.

Samples in which no manganese phase could be identified occurred mainly in the southern and western parts of the Indian Ocean (see figure 15). These came from several different basins and from the mid-ocean ridge, sea-mounts and plateaux which might safely be assumed to display a very wide range of bottom

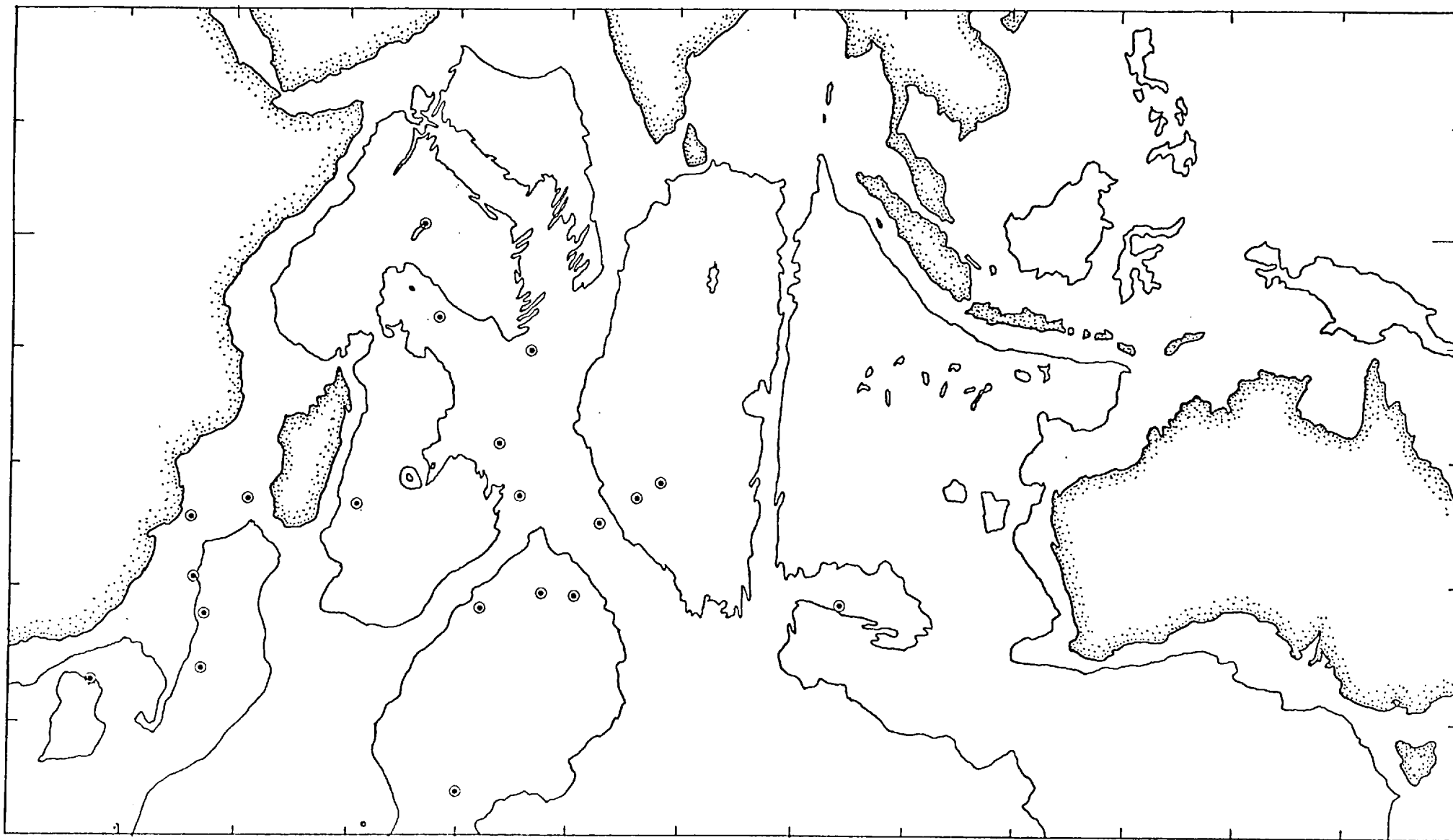


FIGURE 18. Distribution of MnO<sub>2</sub> and manganese-oxide samples containing no identifiable manganese phase.

environments. No single type of environment can therefore be suggested as favouring the development of amorphous deposits. Amorphous samples are characterised by low Mn contents (see Section 5), thus the principal factor determining whether or not a sample displays a distinct manganese phase may simply be the amount of Mn present. This is because the weakly crystalline nature of much of the material in ferromanganese oxide deposits produces a large amount of fluorescent background radiation. A comparatively large amount of a poorly crystalline phase may therefore need to be present before it can be identified above the background noise. As a test, a sample containing no recognisable manganese phase and high background fluorescence was "spiked" with increasing amounts of todorokite. It was found that a mixture of 10% todorokite to 90% sample was the lowest concentration of todorokite at which the  $9.6\text{\AA}$  and  $4.8\text{\AA}$  peaks became clearly visible. Thus samples labelled as amorphous may in fact contain a crystalline manganese phase but in amounts too small to be seen against the background fluorescence. Unfortunately, no method exists of separating the crystalline phases of samples from the amorphous ones. The distribution of amorphous samples in the Indian Ocean therefore probably does not reflect any mineralogical trend but rather a compositional one.

With only two exceptions, all the 20 samples in which goethite was identified came from the mid-ocean ridge, sea-mounts or areas very close to the continents, (see figure 16). As will be discussed later, these are environments in which increased amounts of iron are available for incorporation into nodules and encrustations. Thus the average concentration of iron in samples in which goethite was identified was almost 22% compared with an Indian Ocean average of 15%, and in 3 samples showing many peaks attributable to goethite, the iron content was over 30%. Therefore it may be that goethite was

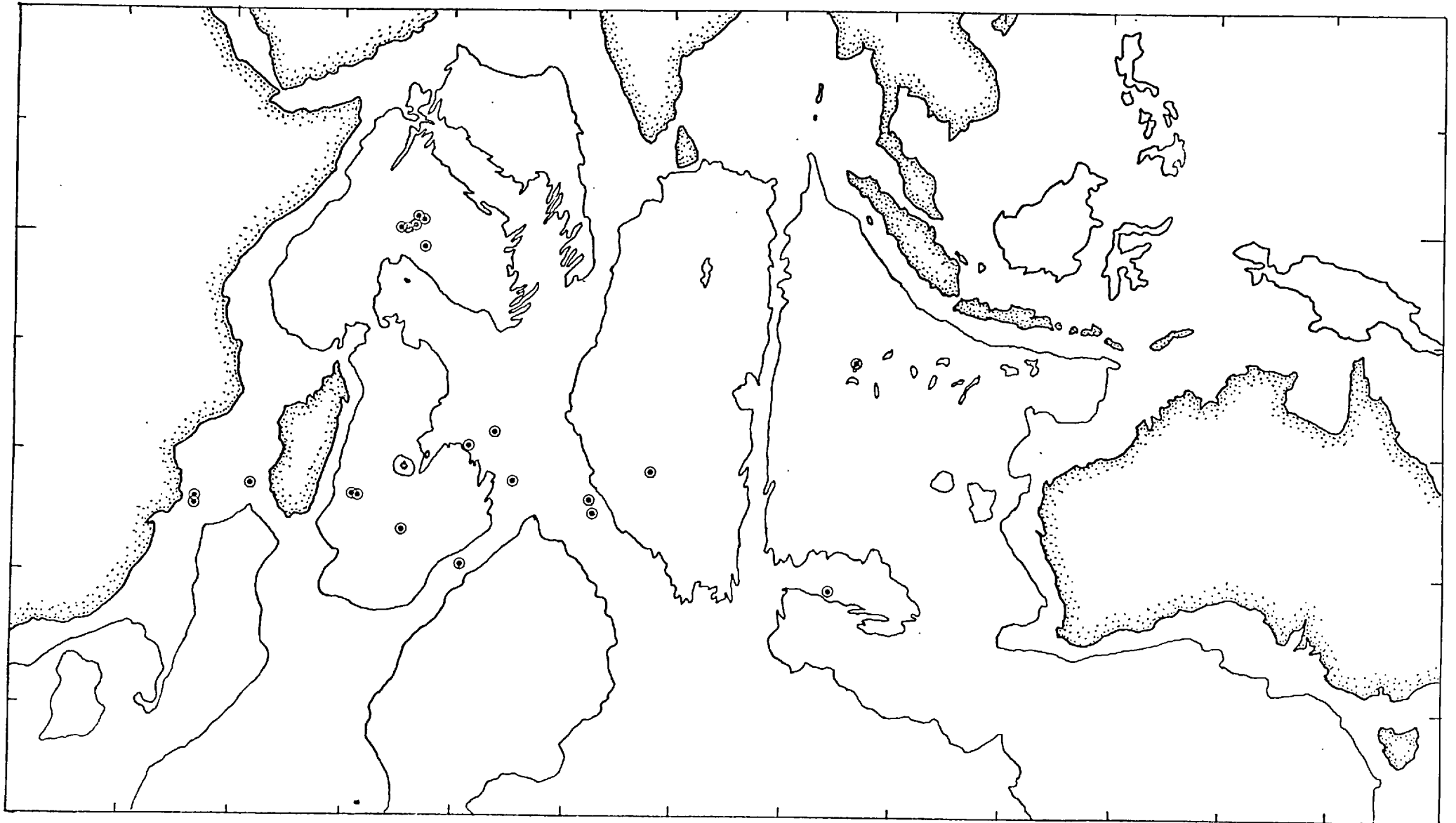


FIGURE 18 Distribution of goethite in Indian Ocean ferromanganese-oxide samples.

present in many of the samples analysed but not in sufficient amounts for its major peaks to become visible above the background noise. This might be especially true where the goethite was poorly crystalline or of small particle size. It must also be noted however, that several samples containing 20% Fe or more, showed no peaks assignable to goethite. Whilst some poorly or finely crystalline goethite may occur in such samples, they do indicate the likelihood that the high Fe content of a sample need not necessarily infer that goethite is present.

#### (v) CONCLUSIONS

Of the three manganese phases recognised in this investigation, todorokite and  $\delta\text{-MnO}_2$  appear to be fairly equally distributed in Indian Ocean ferromanganese-oxide concretions. However they tend to occur preferentially in different environments. Todorokite occurs mainly in samples from comparatively poorly oxygenated areas and was thus observed in continental margin samples and in nodules from most major basins. Nodules from the Central Indian Basin contained the most well-crystalline todorokite of all the samples investigated.  $\delta\text{-MnO}_2$  occurs principally in samples from elevated areas where the bottom environment is thought to be more well-oxygenated, such as the mid-ocean ridge system and the upper parts of sea-mounts. These samples are usually encrustations.

Occurrences of birnessite are rather more limited than the other two minerals. There is insufficient evidence of the relationships between birnessite and todorokite and  $\delta\text{-MnO}_2$  to account satisfactorily for its observed distribution. However the fact that birnessite occurred mainly in deep water samples associated with todorokite agrees with the findings of Skornyakova et al (1975) in Pacific Ocean nodules. The general conclusions reached, concerning the regional distribution of manganese minerals in ferromanganese-oxides from the Indian Ocean, are in agreement

with the behaviour of these minerals in the Pacific and Atlantic Oceans (Barnee, 1967; Cronan and Tooms, 1969; Cronan, 1975; Skornyakova et al, 1975). This indicates that similar environmental controls on mineralogy must be operating in all three major oceans and means that samples from a particular environment in the Indian Ocean are likely to have the same mineralogy as samples from similar environments both elsewhere in the Indian Ocean and in the Pacific and Atlantic Oceans.

From the preceding discussion however, it is obvious that much remains to be explained about the interrelationships between the three manganese minerals found, and the precise conditions favouring their respective growth. Detailed gathering of relevant environmental information has not so far accompanied marine bottom sampling on an ocean-wide basis. Major progress will only be made in our understanding of the factors affecting the regional variation of ferromanganese-oxide mineralogy when the following parameters are met:

- (1) The measurement of Redox conditions at the sediment-water interface.
- (2) The detection of presence and strength of bottom currents.
- (3) The calculation of dissolved oxygen levels in bottom waters.
- (4) The careful transportation and storage of samples prior to analysis.



## S E C T I O N 5

### BULK GEOCHEMISTRY OF FERROMANGANESE - OXIDE DEPOSITS

#### (i) INTRODUCTION

During the course of this study, 116 samples from more than 90 stations throughout the Indian Ocean were analysed for Mn, Fe, Co, Ni, Cu, Zn, Pb, Ca and Al. A limited number of samples from the Madagascar and Central Indian Basins were in addition analysed for Cd, Cr and Ti. The analyses were all carried out by atomic absorption spectrophotometry. Details of the techniques used and the precision and accuracy obtained are given in Appendix 1.

The material obtained was of an extremely varied type, discussed in detail in Section 3, ranging from separated micronodules and small nodule fragments to whole nodules with a variety of core types and sizes and encrustations on a variety of substrates. If analytical results are to be used for the purposes of regional comparison, this variability poses considerable problems when selecting material for analysis. For this reason, whenever a distinct core was encountered in nodules or encrustations it was removed prior to analysis. By this method it was hoped to reduce compositional variations which might occur simply because of variations in the amount of diluting aluminosilicate material present.

Some samples contained a highly-altered clay-rich core which was indurated and replaced to varying degrees by authigenic ferromanganese-oxides. In some such samples there was no distinct break between the core and the authigenic oxide layers (for example, see Plate 17), and thus no core could be removed and the whole sample had to be crushed for analysis. For this reason as well as considering regional trends in terms of bulk analyses, compositional variations were also investigated using three-component variation diagrams. When plotting samples on these diagrams the elements Mn, Fe, Co, Ni, Cu, Zn and Pb were summed to 100%, thus partly removing the diluting effects of the non-ferromanganese phases.

#### (ii) LOCAL VARIATIONS IN SAMPLE COMPOSITION

Variations in sample composition, both within a single sample and between separate samples from the same site, have been investigated by several workers (Cronan and Toomey, 1967; Glasby, 1970, 1973; Raab, 1972). Significant variations were observed by these authors even though the analytical precision obtained by the optical spectrographic techniques employed was comparatively low. Raab (1972) found variations of up to 100% in trace metal content within single nodules. Since a fairly high degree of precision was obtained in the analyses carried out in this investigation it was thought worthwhile to re-investigate this phenomenon.

Abundant material was obtained from some sample sites and it was felt important that, apart from taking a representative sample for analysis, some small pieces of material should be analysed separately as a check on the compositional variability of the material from that site. Where material of more than one morphological type was obtained from a single station, a representative portion of each morphological

type was analysed separately to see if compositional differences reflected morphological differences.

(a) Compositional Variations within single samples

In most of the samples analysed, there did not seem to be any major differences in the appearance of the ferromanganese phases from core to outer surface, although banding due to alternate ferromanganese-rich and silicate-rich layers was often seen as discussed in Section 3. However, one particular encrustation from the mid-Indian Ocean Ridge, had an outermost layer which was very different in appearance from the rest of the sample (see Plate 8). This outer layer was therefore analysed separately, as well as being taken as part of a bulk sample for separate analysis. The analytical results are summarised in Table 7.

From the results in Table 7 it can be seen that there is a significant compositional difference between the outermost layer and the encrustation as a whole. The increased Mn and Fe content of the outermost layer can probably be at least partly accounted for by the lower aluminosilicate content of this layer, as indicated by its lower Al Content. This may partly explain the variation in trace metal content, particularly the increase in Ni, Co and Pb in the outer layer. However, this variation may also be partly due to a recent change in the environmental conditions, an increase in Eh for example would promote Co and Pb enrichment (Creerar & Barnes, 1974). Such compositional variation in a single sample enhances the importance of choosing a sufficiently representative sample from any one station for analysis.

(b) Compositional Variations between samples from the same site

Quite often, more than one nodule, crust or fragment is recovered

Sample: ANTP 109D	Mn %	Fe %	Co p.p.m.	Ni p.p.m.	Cu p.p.m.	Zn p.p.m.	Pb p.p.m.	Ca %	Al %
(a) Representative portion	10.5	17.5	2510	920	575	355	970	1.94	3.12
(b) Outer 3 m.m. only	17.1	19.1	3900	1870	605	385	1500	1.85	1.74
Percentage increase in outer layer	67	10	55	105	5	8	55	-5	-44

TABLE 7

Comparison of average composition with composition of outer layer of an encrustation from mid-Indian Ocean Ridge.

from a single sampling operation. In the case of grab or core stations the samples are likely to have been lying in close proximity on the sea-bed and might therefore be expected to be compositionally similar. However, many stations from which material was obtained for the investigation were dredge stations and this material can be expected to have been more widely distributed on the sea-bed. Thus it is likely, particularly in areas of rugged bottom topography, that one dredging operation may recover material from more than one sedimentary environment. This problem was investigated by considering the samples in two groups as follows:

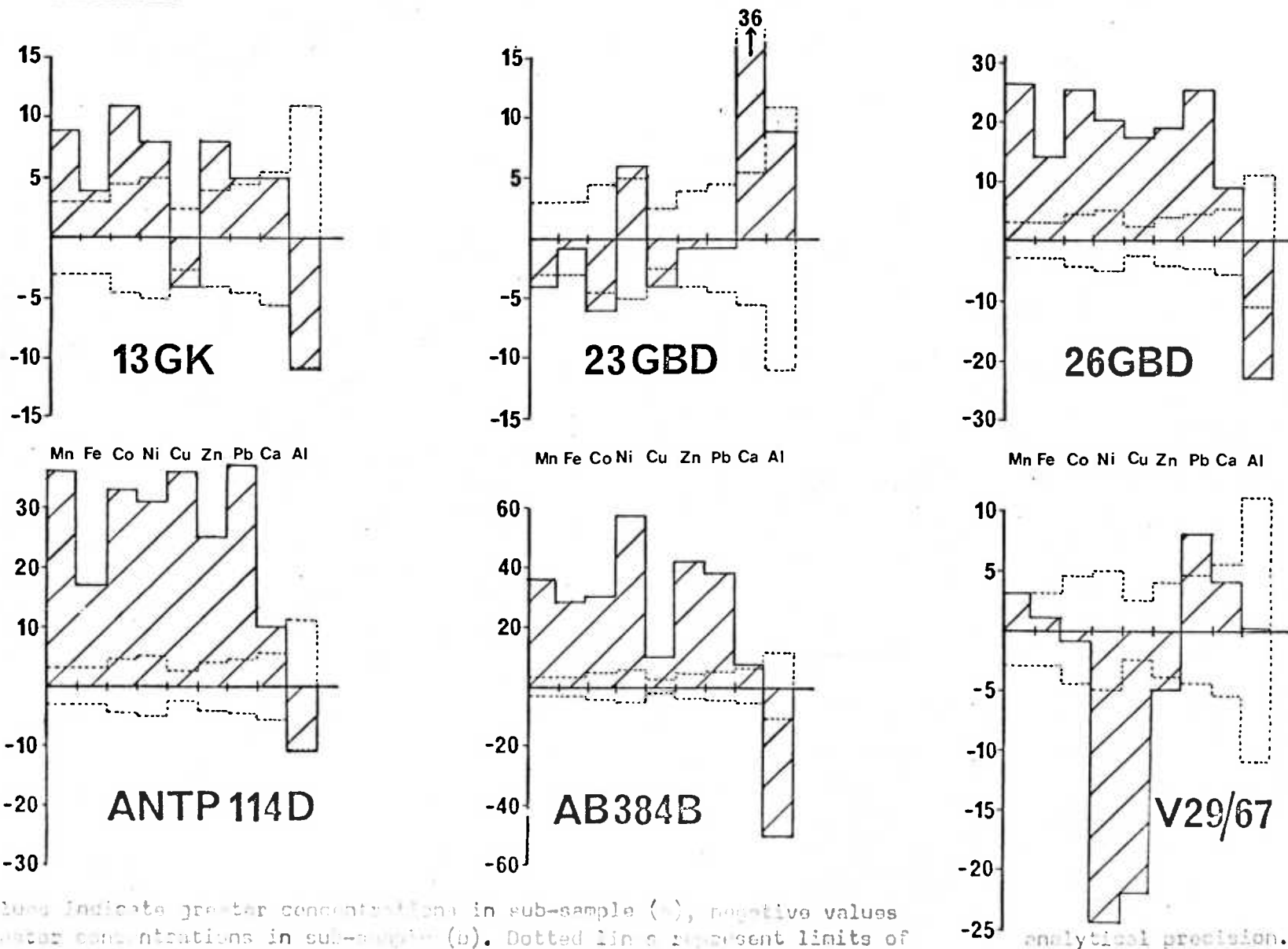
1. Morphologically similar samples from the same site.
2. Morphologically dissimilar samples from the same site.

#### 1. MORPHOLOGICALLY SIMILAR SAMPLES

The variation in bulk composition of morphologically similar samples from six different sites in various localities of the Indian Ocean is summarised in figure 17. The compositional differences between subsamples of stations 13GK and 23GBD are so small as to be near or within the limits of the analytical precision achieved, especially for samples 23GBD(a) and (b). These latter two samples show a large percentage difference in Ca value but the absolute value of Ca in the samples is so small as to make the difference unimportant.

Larger variations in composition between the two subsamples occur at stations 26GED and ANTIPODE 114D. However Mn, Fe and the trace metals show a strong antipathetic relationship with Al which is an indicator of the aluminosilicate content of the samples. The compositional differences might therefore be accounted for simply

FIGURE 17 Variation in chemical composition of morphologically similar samples from the same sample station.



Positive values indicate greater concentrations in sub-sample (a), negative values indicate greater concentrations in sub-sample (b). Dotted lines represent limits of

analytical precision.

by the diluting effect on the authigenic phase produced by a larger amount of aluminosilicate material in one subsample than in the other. A similar explanation would also seem to apply to the variation in composition of samples AB384B (a) and (b) although in this case the enrichment in sample (a) of Ni is rather larger and of Cu rather smaller than that of the other trace metals.

Samples V29/67 (a) and (b) show no significant compositional differences except for Ni and Cu, which are markedly enriched in sample (b). X-Ray diffraction studies of the two samples show sample (a) to contain traces of  $\delta$ -MnO<sub>2</sub> whilst sample (b) contains traces of todorokite. Thus it would seem that though they were recovered at the same core station these two samples may have formed under slightly different environmental conditions. This station was located on the floor of a steep valley in an area of comparatively rugged topography and it is possible that mixing of nodules which have been growing in different environments may have occurred due to transport of material, probably by gravity slumping. This process would tend to bring down nodules from more highly oxygenated conditions on the sides of the valley onto the valley floor where they would become mixed with nodules which had developed in-situ.

#### SUMMARY

Compositional variation between morphologically similar nodules from the same site does occur but often this variation is so small as to be within the limits of the analytical precision of the techniques used. Where the variations observed are outside the limits of precision, they are often due simply to the diluting effects of detrital silicate material which tends to decrease the concentration

of all the authigenic elements by a similar amount. Occasionally morphologically similar samples from the same site show differences in composition which can only be attributable to the separate samples having grown in different sedimentary environments. Some explanation of how these different nodule populations were subsequently mixed must then be looked for. None of the compositional variations observed were very large and therefore it is not likely that any major compositional variations have been missed by selecting only one or two samples for analysis from stations where more material was available.

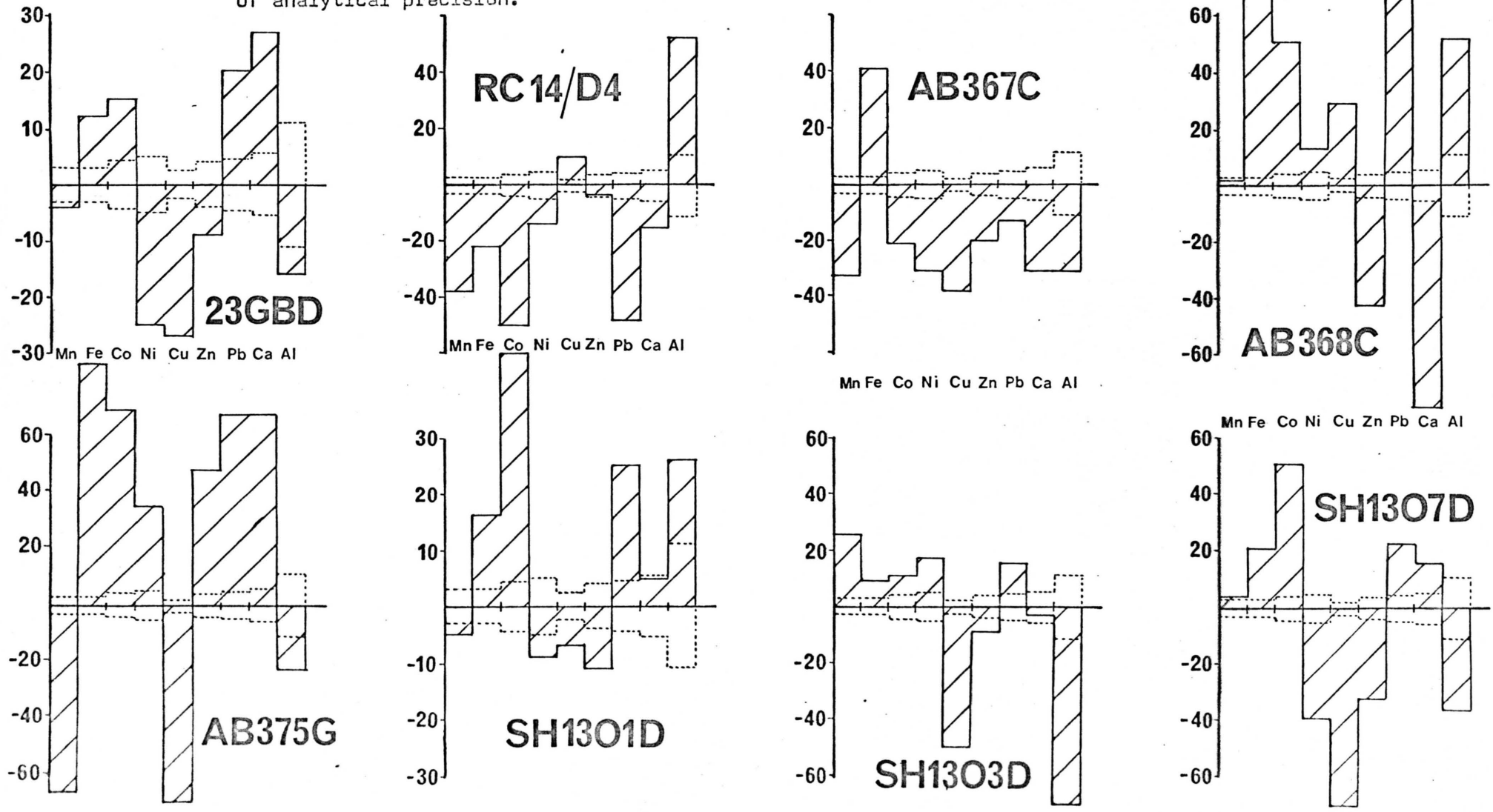
## 2. MORPHOLOGICALLY DISSIMILAR SAMPLES

Morphological differences in ferromanganese-oxide samples appear to reflect different modes and environments of growth (see Section 3) and these differences are likely to be reflected in the chemical composition of the samples.

In this investigation, material obtained from 8 stations in various localities was found to be of more than one morphological type. In order to ascertain whether differing morphology was accompanied by significant compositional differences, a representative portion of each morphological type at each station was analysed separately. The percentage difference in composition of the two subsamples from each station is summarised in figure 18. All the 8 stations investigated showed compositional variations between subsamples which were for the most part much greater than could be accounted for simply by variation within the limits of analytical precision (see figure 18). In contrast to morphologically similar samples, morphologically dissimilar samples show compositional variations which cannot, except in one case, be explained largely in



**FIGURE 18** Variation in chemical composition of morphologically dissimilar samples from the same sample station. Positive values indicate greater concentrations in sub-sample (a), negative values indicate greater concentrations in sub-sample (b). Dotted lines represent limits of analytical precision.



terms of a simple diluting effect produced by different amounts of aluminosilicate material in the sample. The two samples from station RC14/D4 showed variations in Mn and Fe which might be attributable to a simple diluting effect, but the increase in Co and Pb in the encrustation seems rather greater than could be accounted for by this effect alone. The behaviour of Cu indicates that the aluminosilicate phase may contain appreciable amounts of this element. At the other 7 stations however, comparatively large compositional variations occur which do not show a simple dependence on the difference in Al content of the two sub-samples. At stations 23GBD, SH1301D and SH1307D Cu, Ni and Zn values show an antipathetic relationship with Co and Pb. As will be discussed later, this negative correlation is developed markedly on an ocean-wide basis and can be accounted for in terms of different environments of deposition favouring the development of different Mn oxide phases which preferentially incorporate different trace metals (Barnes, 1967). No significant mineralogical differences in the Mn phases were found at these stations however, but it is possible that a minor difference in mineralogy not detectable by the bulk X-Ray diffraction techniques used, is sufficient to cause the comparatively small differences in trace element content observed in these samples.

Mineralogical differences may explain the trace metal behaviour in samples from stations RC14/D4, since the sub-sample which was enriched in Co and Pb was found to contain  $\delta$ -MnO<sub>2</sub>, and samples containing this mineral tend to be enriched in these metals (Barnes, 1967; Cronan, 1972; this study). The Mn phase in the other sample from this station was essentially amorphous.

The morphological differences between sub-samples at station SH1303D were not as marked as those at other stations. The variations in trace metal content which occur between the two samples from this

station do not show the simple antipathetic relationship seen in the material from stations SH1303D and SH1307D. Of particular interest in samples from SH1303D is the marked increase in Cu in the sample containing less Mn and Fe but more Al. This indicates that the aluminosilicate phase may contain appreciable amounts of Cu as was also indicated by the behaviour of these elements in samples from station RC14/D4.

The stations AB375G, AB368C and AB367C were all located in the Mozambique Channel area and show particularly marked morphological and compositional variations which are best discussed individually.

#### STATION AB375G

The two sub-samples from this station are characterised by extreme differences in their Mn and Fe contents. The irregular nodule from this station was extremely rich in Mn, and this coupled with its generally low trace metal content, points to the enrichment of Mn in this sample by diagenetic remobilisation within the underlying sediment (Pachadzhyanov et al, 1963; Lynn & Bonatti, 1965; Presley et al, 1967). The sample is from an area where sedimentation rates are generally high and nodules of similar composition have been found in other continental margin areas undergoing rapid sedimentation (Mero 1965; Price & Calvert, 1970). The other sample from this station was much lower in Mn and higher in Fe and, apart from Cu, higher in trace metals also. This sample, however, was an encrustation and whilst the exact nature of its substrate was not known it is obvious that it cannot have been underlain by sediment and was probably picked up by the dredge from a more elevated area which was sediment-free. Its composition therefore reflects a more normal authigenic precipitation of Mn and Fe oxides and associated trace elements in

contrast to the more rapidly formed diagenetically Mn-enriched nodule from the same dredge haul. No simple explanation can be found to account for the behaviour of Cu in these two samples.

STATION AB368C

Two very different morphological types of ferromanganese-oxide material were recovered from this station, one sub-sample consisting of large nodules and the other of micronodules separated from the underlying sediment. The most noticeable compositional difference between the two sub-samples is the lower Fe, Co and Pb content of the micro-nodules. The difference in the Fe content of the samples can be explained if it is assumed that the nodule accreted predominantly from "normal" seawater whilst the micronodules precipitated from interstitial waters. The latter, because of the lack of mobility of Fe compared to Mn in sediments (Lynn & Bonatti, 1965; Presley et al, 1967) are likely to be depleted in Fe compared to bottom waters and therefore produce a precipitate with a lower Fe content.

In these samples, Co and Pb tend to follow Fe, a correlation which also seems to occur on an ocean-wide basis. This might imply that Co and Pb are bound up in the Fe phase of these samples, especially since there was no observable difference in the mineralogy of the Mn phase of the two sub-samples which might affect trace metal uptake. However, it may simply reflect much lower Co and Pb values in the pore waters from which the micronodules are likely to have accreted.

The high Ca content of the micronodules sample is probably due simply to the inclusion of carbonate material in the material selected for analysis since the micronodules were obtained by simple physical separation from the dried sediment, which was carbonate-rich.

STATION AB367C

This station also produced material of two very different morphologies. The main compositional difference between the two subsamples is the much higher iron content of the cylindrical crusts and their depletion in Mn, Co, Ni, Cu Zn and Pb. As discussed in Section 3, the encrustations appear to have formed very rapidly around iron nails. The Fe content of the nails was over 50% and the high Fe content of the encrustations round them may therefore be due to Fe being supplied to the crusts from the breakdown of the nails themselves. If the trace metals are contained predominantly in the Mn phase then the lower trace metal content of the crusts may simply be a reflection of their lower Mn content. However, low trace metal contents appear to be typical of rapidly accumulated ferromanganese-oxides in general, (Bonatti et al, 1972; Scott et al, 1974), and the lower trace metal content of the crusts may therefore simply be a result of their rapid growth.

SUMMARY

Quite large compositional variations were found to occur in samples of different morphology which were recovered from the same sampling operation. This variation could not generally be explained simply by differences in the amount of aluminosilicate material present; more often the differences appear to be due to the growth of samples in different sedimentary environments.

All the stations from which samples of more than one morphological type were recovered were dredge stations in areas of fairly rugged topography. Environments of deposition are known to vary quite rapidly in such areas and therefore samples of different composition and morphology

might be expected to be recovered in a single dredge haul in these areas. This was found to be the case on Pacific Ocean sea-mounts by Hubred (1970) and in a small area of the Carlsberg Ridge by Glasby (1970). It is important therefore, when selecting material from dredge stations for analysis, to sub-sample any material which displays a variation in morphology since it may show significant compositional differences and therefore give some idea of the variation in environment which occurs along the path travelled by the dredge at that station.

### (iii) MINERALOGICAL INFLUENCE ON COMPOSITION

The average composition of todorokite-rich and  $\delta$ - $\text{MnO}_2$ -rich samples from the Indian Ocean is listed in Table 8 below, together with the average composition of samples containing no identifiable Mn phase. As can be seen from the Table, todorokite-rich samples are markedly enriched in Mn, Ni, Cu and Zn compared to  $\delta$ - $\text{MnO}_2$  samples.  $\delta$ - $\text{MnO}_2$ -rich samples on the other hand contain more Fe, Co and Pb. The enrichment of Cu, Ni and Zn in todorokite-rich nodules has been observed by several previous workers (Barnes, 1967; Cronan & Tooms, 1969; Cronan, 1975b) and these same authors also noted that Co and Pb were enriched in  $\delta$ - $\text{MnO}_2$ -rich samples. The possible reasons for these enrichments will be discussed later.

The enrichment of Fe in  $\delta$ - $\text{MnO}_2$ -rich samples could be explained if volcanism supplied appreciable amounts of Fe to the oceans since  $\delta$ - $\text{MnO}_2$ -rich samples are often found in areas associated with volcanism such as the mid-ocean ridge system and sea-mount areas. The possible reasons for the enrichment of Mn in todorokite-rich samples are not as straightforward and will be discussed in Section 9.

The low Mn content of the samples categorised as amorphous may be the major cause of the fact that no Mn phase could be identified, since

Principal Mn phase	Mn %	Fe %	Co p.p.m.	Ni p.p.m.	Cu p.p.m.	Zn p.p.m.	Pb p.p.m.	Ca p.p.m.	Al p.p.m.	Depth (m.)
Todorokite (37 samples)	20.0	9.5	1300	8440	6890	1030	760	1.66	2.60	4520
$\delta$ -MnO <sub>2</sub> (33 samples)	14.7	19.3	3600	2500	790	540	1420	2.40	1.78	3170
Amorphous (13 samples)	9.9	13.7	1750	2360	1260	480	930	1.40	3.34	4090

TABLE 8

Average composition of samples of different mineralogy.

any crystalline phase which is present is likely to be present in much smaller amounts than in the other samples. The low Mn content may also account for the fact that the trace metal content of these samples is generally low. The reasons for the low Mn content may simply be one of dilution by non-authigenic <sup>silicate</sup> ~~oxide~~ phases since the combined Mn and Fe content of amorphous samples is noticeably lower than that of the other samples and the average Al content is higher than that of the other samples.

#### (iv) INTER-ELEMENT ASSOCIATIONS

There have been many previous attempts to establish inter-element correlations in marine ferromanganese deposits and to try to explain them in terms of chemical, mineralogical and environmental controls on element uptake in these deposits. The results of earlier workers were quite diverse. For example, Goldberg (1954) found positive correlations of iron with Ti, Co and Zr and of manganese with Cu and Ni and tried to explain these in terms of a colloidal "scavenging" hypothesis of manganese and iron oxides. However, Riley & Sinhaseni (1958) found no correlation of Fe with Zr or of Mn with Cu. Cronan (1967, 1969) confirmed the correlation of Mn with Cu and Ni but could find no correlation between Fe and Co. Barnes (1967) and Cronan (1969) also found positive correlations with depth for Ni and Cu and negative correlations with depth for Co, Pb and Ba and tried to explain these in terms of a mineralogical control as influenced by depth.

More recent work (Cronan & Tooms 1969; Rancitalli & Perkins, 1973; Glasby, Toome & Howarth, 1974) has again shown correlations of manganese with Cu, Ni and Zn and of iron with Ti, Co and Zr.

Some element associations were obvious upon simple visual examination of the data presented here. However, in order to clarify



these and investigate less obvious ones a correlation matrix for the data was computed using a programme developed within the Applied Geochemistry Research Group at Imperial College.

The production of a correlation matrix for the 116 samples analysed is made somewhat complicated by the non-normal distribution of elements in manganese nodules and encrustations. In order to compute a reliable correlation co-efficient between two elements, there are two major requirements. The first is that a sufficiently large number of analyses should be used. The 116 samples used in this study provide a sufficiently large number to meet this requirement adequately. The second requirement is that both elements should show similar distribution patterns. Unfortunately a negative skewness is imposed on the distribution patterns of many elements in geological systems because of the constraints applied by the fact that the total element concentration must always sum to 100% (Chayes, 1960). Some elements in ferromanganese-oxides tend towards a normal distribution whilst others tend toward a log-normal distribution. In order to overcome this problem, two correlation matrices were calculated for the data, one using normal data and one using log-transformed data. These matrices are presented in Table 9; arithmetic data appears beneath the diagonal line, log-transformed data above. An examination of both correlation matrices reveals few differences. Most elements are similarly correlated at the 99% confidence level on both. The level at which a correlation co-efficient becomes significantly different from zero at the 95% and 99% confidence levels is given in Table 10.

Both major authigenic elements Mn and Fe, show a marked negative correlation with Al significant at the 99% confidence level, indicating that a negative correlation exists between the authigenic and detrital phases of these deposits. This might be expected in view of Chayes' work on the constraints applied on geological systems due to the fact

	Depth	Mn	Fe	Co	Ni	Cu	Zn	Pb	Ca	Al	Cd	Cr	Ti
Depth		.228	-.298	-.446	.174	.590	.195	-.341	-.621	.602	.360	-.089	-.236
Mn	.199		-.337	.072	.673	.574	.620	.130	-.199	-.338	.754	-.389	-.709
Fe	-.448	-.464		.533	-.551	-.673	-.522	.578	.076	-.200	-.820	.134	.838
Co	-.515	-.082	.270		-.195	-.542	-.267	.888	.192	-.477	-.698	-.184	.746
Ni	.291	.754	-.606	-.234		.781	.895	-.196	-.148	-.147	.849	-.199	-.849
Cu	.422	.721	-.627	-.341	.930		.760	-.491	-.411	.275	.864	-.163	-.851
Zn	.251	.706	-.537	-.274	.929	.874		-.276	-.141	-.142	.866	-.257	-.872
Pb	-.483	-.068	.423	.807	-.353	-.458	-.374		.116	-.438	-.675	-.094	.675
Ca	-.421	-.192	-.067	.071	-.075	-.154	-.061	.055		-.503	-.226	-.042	.404
Al	.504	-.374	-.338	-.438	-.125	.001	-.157	-.518	-.263		-.273	.420	.157
Cd	.227	.621	-.610	-.493	.673	.667	.646	-.518	-.133	-.271		-.139	-.747
Cr	-.081	-.251	.024	-.195	-.161	-.157	-.204	-.112	-.071	.367	-.102		.167
Ti	-.240	-.733	.860	.755	-.814	-.767	-.818	.669	.335	.267	-.554	.003	

TABLE 9

Table of correlation matrices for the total sample data. (116 samples) Arithmetic data beneath diagonal, logarithmic above. No. of samples used to calculate correlation matrices for Cd, Cr & Ti was 27.

Number of samples used to calculate matrix	Confidence Level	
	95%	99%
27	.323	.445
116	.155	.225

TABLE 10      Minimum values of correlation co-efficients  
which are significantly different from zero  
at the 95% and 99% confidence levels.  
(Derived from Fisher & Yates, 1964).

that the constituents must always sum to 100% (Chayes, 1960).

However, the most striking correlations are those between the trace metals Ni, Cu, Zn and Cd and between Co, Pb and Ti. These are equally significant using both arithmetic and log-transformed data sets. Smaller, but still highly significant correlations exist between the major and minor authigenic elements. Thus, Ni, Cu, Zn and Cd correlate strongly with Mn, whilst Co, Pb and Ti correlate strongly with Fe. The correlation between Co and Fe is not as marked however, and there is a marked difference between the correlation co-efficients using normal and log-transformed data indicating that the distribution patterns of these two elements are not similar.

It has been suggested (Glasby, 1970; Glasby, Tooms & Howarth, 1974) that the comparatively low correlations of the trace elements with Mn and Fe indicate that incorporation of the trace elements into nodules is independent of the concentration of Mn and Fe oxide phases present. Electron microprobe studies (Sorem, 1973) have shown bands within nodule samples containing up to several percent of trace metals and thus it would seem that the concentration of Mn and Fe in samples may not be the most important factor in determining the trace element content of samples.

#### Cobalt and Lead

Cobalt and lead correlate strongly positively with each other. They both also correlate strongly positively with Fe whilst showing no significant correlation with Mn. Similar strong positive correlations of Co with Fe have prompted some workers (Burns, 1965; Burns & Fuerstenau, 1966; Barnes, 1967) to suggest that Cobalt, as the  $\text{Co}^{3+}$  ion, is incorporated into nodules within the hydrated iron-oxide phase; by substituting for the  $\text{Fe}^{3+}$  ion. More recent work (Cronan & Tooms, 1968;

Glasby, 1970; Burns & Brown, 1972) has shown that Co is not associated with Fe-rich areas within nodules. In fact Burns & Brown (1972) using electron microprobe techniques found that Co was strongly positively correlated with Mn within single samples and Cronan (1975) has found a positive correlation between Mn and Co in over 150 samples from the Atlantic Ocean. Burns (1976) has shown that  $\text{Co}^{3+}$  in the low-spin state in which it occurs in oxides, is highly unsuited for substitution with high-spin  $\text{Fe}^{3+}$  ions in the  $\text{FeOOH}\cdot\text{H}_2\text{O}$  phase of nodules because of the large difference in their atomic radii (0.53Å for low-spin  $\text{Co}^{3+}$ , 0.65Å for high-spin  $\text{Fe}^{3+}$ ). However, low-spin  $\text{Co}^{3+}$  has an ionic radius very close to that of  $\text{Mn}^{4+}$  (radius 0.54Å) and might thus be able to substitute for  $\text{Mn}^{4+}$  ions in the Mn phases. Burns in fact proposes a favourable thermodynamic scheme whereby  $\text{Co}^{2+}$  ions are adsorbed onto the Mn-oxides near vacancies in the  $(\text{MnO}_6)$  layer and oxidised and incorporated into the lattice by reduction of  $\delta\text{-MnO}_2$ . Thus the high positive correlation of Co with Fe does not seem to infer that Co is incorporated into ferromanganese-oxides within the Fe phase, but that there is a separate factor favouring iron enrichment in environments which also favour Co enrichment.

Much less work has been done on the mechanisms of incorporation of Pb into ferromanganese-oxides. Glasby (1970) found that Pb, like Co was associated with the Mn-rich phases rather than the Fe-rich phases within some nodules. If this is so, then Pb is enriched in samples which are also enriched in Fe, but for different reasons, as was the case with Co.

Goldberg (1965) has suggested that in highly oxygenated marine environments Pb may be oxidised to the tetravalent ion and in view of its close correlation with Co it seems that Pb might be enriched in  $\delta\text{-MnO}_2$ -rich samples by incorporation within the  $\delta\text{-MnO}_2$  lattice. However, the very large ionic radius of the tetravalent Pb ion (0.84Å) compared to  $\text{Mn}^{4+}$

(0.54Å) must preclude the substitution of Pb for  $Mn^{4+}$ . Whilst detailed knowledge of the lattice structure of  $\delta-MnO_2$  is not available it seems unlikely even in the comparatively disordered state in which it occurs in many samples, that this mineral could accommodate the  $Pb^{4+}$  ions within the structure. Much of the Pb in ferromanganese-oxide samples may therefore be present as adsorbed species or perhaps even as a separate insoluble phase such as a hydroxide.

### Nickel and Copper

Nickel and copper correlate very strongly positively with each other and, to a lesser extent, with Mn. Electron microprobe studies (Cronan, 1967; Glasby, 1970; Burne & Brown, 1972) have shown that Ni and Cu are strongly enriched in the Mn-rich areas of nodule samples. Ni and Cu have been shown to be enriched in todorokite-rich nodules (Cronan & Tooms, 1969; Price & Calvert, 1970; Soren & Foster, 1972; this study). According to Goldberg (1965) Ni and Cu are present in sea-water as divalent  $Ni^{2+}$  and  $Cu^{2+}$  and Burne and Fuerstenau (1966) and Cronan & Tooms (1969) have suggested that the enrichment of Cu and Ni in todorokite-rich nodules is due to the ability of these divalent-ions to substitute for the divalent Mn in the todorokite lattice. The ionic radii of  $Ni^{2+}$  and  $Cu^{2+}$  are 0.69Å and 0.72Å respectively. These radii are not particularly close to that of  $Mn^{2+}$  (0.80Å), however they may be close enough to that of  $Mn^{2+}$  to allow substitution under the particular conditions encountered in the environment of growth of the deposit. Fuerstenau et al (1973) using chemical leach techniques showed that much of the Ni and Cu in nodules may not be lattice-held but simply adsorbed onto colloidal-size Mn-oxide particles. These authors also state that this may be the case for Co in samples which are low in Fe. This may avoid several of the problems posed if lattice sites are assumed to be

the major site for the trace metals however it does not explain the observed enrichment of Ni, Cu and Co in samples where the Mn phase appears to be particularly favourable for ionic substitution of the respective trace metals. As already shown, Ni and Cu tend to be enriched in todorokite-rich samples and the positive correlation of these metals with Mn on an ocean-wide basis probably reflects the fact that todorokite-rich samples are also enriched in Mn (see Table 7).

### Zinc

Zinc correlates strongly positively with Ni, Cu and Mn. Positive correlations of Zn and Cu have also been found by previous workers (Cronan, 1975b; Glasby, 1970; Rancitelli & Perkins, 1973). According to Goldberg (1963) Zn occurs in the marine environment as the  $Zn^{2+}$  ion, which has an ionic radius of  $0.74\text{\AA}$ . Like  $Cu^{2+}$  and  $Ni^{2+}$ , this ion is suitable for substitution for  $Mn^{2+}$  in the todorokite lattice and if this is the major method of incorporation of Zn in ferromanganese-oxides it might therefore be expected to follow Ni and Cu closely.

### Cadmium

Only 27 samples were analysed for Cd and the analytical precision obtained was comparatively low (see Appendix 1). These two factors, combined, limit the conclusion which may be drawn about this element's associations with other metals, however Cd does show significant positive correlations with Cu, Ni, Zn and Mn. Like these metals, Cd is probably present in sea-water as the divalent ion. The  $Cd^{2+}$  ion has an ionic radius of  $0.97\text{\AA}$  which would appear too large to enable substitution for divalent Mn and may account for the low concentration of this element in the samples analysed. Virtually no other work has been

published on Cd in marine manganese nodules although Ahrens et al (1967) reported a positive correlation of this metal with Zn in samples from the Cape Basin area off South Africa.

### Calcium

Calcium shows no significant correlations, except with Al, with which it correlates negatively, and Ti, with which it correlates positively. Calcium may be present in the authigenic phase of marine ferromanganese deposits since it is an important minor constituent of todorokite (Strazek et al, 1960) and birnessite (Jones & Milno, 1956). Indeed electron microprobe studies have shown that within some nodules Ca is enriched in the Mn-rich areas (Cronan & Tooms, 1968), however Ca shows no positive correlation with Mn on an ocean-wide basis in this investigation.

Some of the Ca present in the samples may be in the form of authigenic carbonate material, particularly where the total Ca content of the sample is high. Chemical partition studies on some samples have shown that much Ca is acetic acid soluble and may therefore be present as carbonate material (see Section 7). Calcium might thus be expected to be most abundant in samples from shallower depths, above the lysocline and this appears to be borne out by the significant negative correlation of Ca with depth.

### Aluminium

Aluminium shows no very strong correlations with any other element but it does exhibit minor negative correlations with Mn and Fe. This is not unexpected since Al is an effective indicator of the aluminosilicate content of samples and the aluminosilicate content would be expected to



exhibit a strong antipathetic relationship with the authigenic Mn and Fe phases.

Aluminium also exhibits a strong positive correlation with depth. This might also be expected, since nodules growing in sediment-floored basins are likely to incorporate more aluminosilicate material during growth than samples growing on sea-mounts and other elevated areas which are largely sediment-free.

### Titanium

Only 27 samples were analysed for Ti and these samples were all from ocean basin areas. Therefore only limited conclusions can be drawn from the correlation co-efficients obtained. However, Ti does correlate strongly positively with Fe, Co and Pb and strongly negatively with Mn, Ni, Cu and Zn. Goldberg (1954) found a similar correlation of Ti with Fe and attributed it to scavenging of Ti by colloidal iron-oxides. Selective leach procedures carried out on more than 20 samples, however, released only 10 - 30% of the total Ti in the samples whilst 60 - 80% of the total Fe was removed. Thus it seems that a substantial amount of the Ti present in ferromanganese nodules may be contained in phases other than the authigenic oxide phases and that this phase is more abundant in samples enriched in Fe, Co and Pb. These three elements tend to be enriched in samples from elevated areas associated with volcanism and the increased Ti in samples from these areas may therefore be due to the inclusion of volcanic material.

### Chromium

As with Cd and Ti, only 27 samples from a limited range of environments were analysed for Cr. Analytical precision obtained for Cr

was not very high (see Appendix 1) and therefore the co-efficients obtained are not likely to be as reliable as those for the other elements. In fact Cr shows no very significant correlations with other elements except with Al. Chromium is one of the few elements which is depleted in ferromanganese-oxide deposits compared to its average crustal abundance. This is because most Cr enters sea-water as detrital particulate material rather than in solution. Such Cr as there is in solution may well be present as the  $\text{CrO}_4^{2-}$  ion which would not be suitable for incorporation into ferromanganese-oxides. Most of the Cr in the samples is therefore likely to be present in the detrital phases. This theory is borne out by the fact that Cr correlates positively only with Al and by the fact that most of the Cr in nodules subjected to partial chemical attack appeared to be in the resistant phases (see Section 7).

#### Element correlations with depth

Apart from the element correlations with depth already discussed, significant positive correlations of Ni, Cu and Zn with depth occur. These can be attributed to the preferential enrichment of these elements in todorokite-rich nodules discussed earlier, since todorokite-rich nodules tend to be found mainly in the deeper regions of the Indian Ocean. Similarly the negative correlations with depth of Co and Pb are probably due to the fact that these elements are preferentially enriched in  $\delta\text{-MnO}_2$ -rich samples which have been shown to occur predominantly at shallower depths (see Section 4 ). Iron also shows a negative correlation with depth. This is probably due to the fact that sea-mount and mid-ocean ridge samples, which are from comparatively shallow depths, are enriched in iron because of the element's increased availability in this type of environment (see Section 8 ).

(v) AREAL VARIABILITY

The areal variability of ferromanganese-oxide deposits in the Indian Ocean has been the subject of much less study than in the Pacific Ocean. Only two ocean-wide studies have been carried out. Cronan (1967) analysed samples from 25 sites throughout the Indian Ocean and Bezrukov and Andrushchenko (1973) analysed over 50 samples from all the major basins of the Indian Ocean. Detailed studies have been carried out in the north-west Indian Ocean by Glasby (1970) and off South Africa by Ahrens et al (1967). Material from over 90 stations was studied in this investigation and the bulk composition of surface samples from these sites has been plotted on maps of the Indian Ocean together with data from all the previously published reports of Indian Ocean ferromanganese-oxide deposits. A discussion of the regional trends observed is given in Section 8. In addition, the average composition of samples from 11 different physiographic regions of the Indian Ocean has been calculated and is given in Table 11.

Several authors (Mero, 1962, 1965; Price & Calvert, 1970) have used metal ratios such as  $Mn/Ni$  and  $Fe/Co$  to investigate the areal trends in major and minor element composition which occur in oceanic ferromanganese-oxide deposits. However, it was decided that, for the samples analysed in this investigation, a more satisfactory method of displaying compositional trends was by the use of 3-component scatter plots. Such diagrams were used to plot variations of Mn and Fe against Ni, Cu, Zn, Co and Pb. In order to produce meaningful diagrams it was necessary to scale up the values of the trace metals by factors of up to 100. However, the level of analytical precision obtained was such that, even with this scaling up, the variations on the diagram which could be written off as simply due to analytical error were very small. Sample points were plotted on the diagram using a different key symbol for each

TABLE 11

(Parts 1 to 6) - Average compositions and compositional ranges of samples from various physiographic regions of the Indian Ocean.

PART	Average compositions						
	A	1.	2.	3.	4.	5.	6.
Mn %		22.1	12.8	12.6	11.6	15.3	15.1
Fe %		7.6	15.5	16.1	13.0	12.0	11.4
Co p.p.m.		1130	1900	2560	1500	1390	1730
Ni p.p.m.		10300	3390	2280	3150	4810	5570
Cu p.p.m.		9910	1500	1150	1660	2410	3550
Zn p.p.m.		1190	660	490	480	640	710
Pb p.p.m.		650	970	1040	1200	710	870
Ca %		1.33	1.89	1.59	1.30	1.27	1.35
Al %		2.75	3.03	3.27	3.07	2.48	3.64
Cd p.p.m.		20	-	10	-	-	-
Cr p.p.m.		36	-	28	-	-	-
Ti p.p.m.		3240	-	11800	-	-	-
Depth (m.)		5090	4600	5010	5277	4455	5320
Mn/Fe		2.9	0.83	0.78	0.89	1.3	1.3
No. of samples		22	8	15	4	2	5

1. Central Indian Basin
2. Crozet Basin
3. Madagascar Basin
4. Moçambique Basin
5. Somali Basin
6. Wharton Basin

cont/.....

TABLE 11

(Parts 7 to 12) - Average compositions and compositional ranges of samples from various physiographic regions of the Indian Ocean.

<u>PART</u>	<u>A</u>	Average compositions					
		7.	8.	9.	10.	11.	12.
Mn %		16.5	17.5	1.71	13.4	12.5	15.1
Fe %		16.5	14.7	43.9	17.4	19.4	15.2
Co p.p.m.		1200	2640	330	4430	2050	2270
Ni p.p.m.		8000	2850	1330	2750	1190	4510
Cu p.p.m.		2040	940	640	650	880	3010
Zn p.p.m.		1120	560	480	530	510	700
Pb p.p.m.		580	1280	160	1510	925	1010
Ca %		3.09	2.00	0.64	3.91	2.11	2.30
Al %		1.84	1.73	1.21	1.72	2.54	2.44
Cd p.p.m.		-	-	-	-	-	18
Cr p.p.m.		-	-	-	-	-	33
Ti p.p.m.		-	-	-	-	-	6710
Depth (m.)		3120	3180	1720	2240	3920	4040
Mn/Fe		1.0	1.2	0.04	0.77	0.64	1.0
No. of samples		4	7	2	19	19	110

7. Mozambique Channel
8. Southern African Plateaux
9. African Continental Borderland
10. Sea-mounts and aseismic ridges
11. Mid-ocean ridge system
12. Indian Ocean average

TABLE 11

(Parts 1 to 6) - Average compositions and compositional ranges of samples from various physiographic regions of the Indian Ocean.

PART B

Compositional ranges

	1.	2.	3.	4.	5.	6.
Mn %	3.5- 31.0	8.41- 17.1	6.24- 17.1	7.47- 14.6	11.7- 18.9	10.1- 22.2
Fe %	4.22- 15.0	11.5- 17.5	13.6- 19.3	8.66- 16.9	9.15- 14.9	6.45- 15.7
Co p.p.m.	570- 2280	1160- 2210	940- 3900	1040- 1780	1010- 1770	1180- 2290
Ni p.p.m.	750- 15700	1920- 6000	920- 3400	1670- 4920	3460- 6160	2260- 8840
Cu p.p.m.	585- 17700	785- 2340	575- 2040	915- 2280	1730- 3080	920- 6590
Zn p.p.m.	210- 1810	425- 895	355- 600	285- 670	535- 750	450- 1010
Pb p.p.m.	210- 1320	785- 1190	350- 1500	730- 1560	360- 1060	465- 1100
Ca %	0.52- 1.57	1.34- 2.40	1.21- 1.94	1.13- 1.44	0.92- 1.61	1.04- 1.74
Al %	1.83- 7.62	1.70- 3.86	1.63- 5.93	2.50- 4.17	1.68- 3.27	2.41- 6.09
Cd p.p.m.	11-	-	8-	-	-	-
Cr p.p.m.	15-	-	20-	-	-	-
Ti p.p.m.	1480-	-	7180-	-	-	-
Depth (m.)	4435- 5399	4050- 4810	3967- 5209	4960- 5450	4190- 4721	4840- 5991

cont/.....

TABLE 11

(Parts 7 to 12) - Average compositions and compositional ranges of samples from various physiographic regions of the Indian Ocean.

PART B

Compositional ranges.

	7.	8.	9.	10.	11.	12.
Mn %	10.3- 20.3	12.3- 36.5	0.23- 3.20	1.87- 24.7	4.61- 18.1	0.23- 36.5
Fe %	2.35- 33.3	2.46- 19.0	39.9- 47.9	7.94- 30.7	11.9- 24.0	2.35- 47.9
Co p.p.m.	895- 1830	640- 6050	200- 460	820- 14500	375- 3740	200- 14500
Ni p.p.m.	6140- 9090	1200- 7380	755- 1910	875- 4760	1210- 2960	750- 15700
Cu p.p.m.	1360- 2690	450- 2300	550- 725	170- 2580	255- 2960	170- 17700
Zn p.p.m.	845- 1650	250- 835	450- 510	380- 745	220- 645	210- 1810
Pb p.p.m.	225- 915	500- 2180	140- 180	135- 2530	220- 1420	135- 2530
Ca %	1.21- 7.73	0.52- 5.34	0.54- 0.73	1.39- 26.8	1.41- 4.49	0.52- 26.8
Al %	1.25- 2.58	1.47- 2.25	1.10- 1.32	0.34- 5.66	0.44- 6.41	0.34- 7.62
Cd p.p.m.	-	-	-	-	-	8- 28
Cr p.p.m.	-	-	-	-	-	15- 155
Ti p.p.m.	-	-	-	-	-	1480- 13500
Depth (m.)	2995- 3250	1265- 4100	1720	860- 3950	2550- 5730	860- 5991

of the 11 population subsets of samples listed in Table 11.

### Nickel - Fe - Mn

The Mn - Fe - Ni scatter plot is shown in figure 19. Nickel values in samples from the mid-ocean ridge system show a very small spread, the main compositional trend in these samples tending to be toward Fe-enrichment. This trend is not marked however and most samples plot within a comparatively small area of the diagram. By contrast, samples from seamount areas show a wider range of composition. In general they are higher in Ni and lower in Fe than mid-ocean ridge samples but one or two samples do show a pronounced Fe-enrichment.

Samples from the major ocean basins show a very distinct trend of Ni enrichment whilst keeping a fairly constant Mn value. Within the group of ocean-basin samples, those from the Madagascar Basin plot largely in or very near the field of mid-ocean ridge samples whilst those from the Mozambique and Crozet Basins show slightly more Ni-enrichment. This trend of Ni-enrichment is shown to a greater extent by Somali and Wharton Basin samples and by samples from the Mozambique Channel. Central Indian Basin samples show the trend to the most marked degree. In marked contrast, samples from the continental borderland area show extreme iron enrichment.

### Copper - Fe - Mn

Copper has already been shown to follow Ni quite closely and therefore, as might be expected, the variation diagram for copper (figure 20) is quite similar to that for Ni. However there are some small differences. On average, mid-ocean ridge samples contain more Cu than those from seamount areas. This is the reverse of nickel's behaviour and a possible



KEY TO SYMBOLS USED IN FIGURES 19 - 27

Central Indian Basin	▼
Crozet Basin	▼
Madagascar Basin	■
Mocambique Basin	◆
Somali Basin	◇
Wharton Basin	□
Mocambique Channel	■
Southern African Plateaux	⊙
African Continental Borderland	×
Sea-Mounts & aseismic ridges	○
Mid-Ocean ridge system	⊙
Indian Ocean average	*

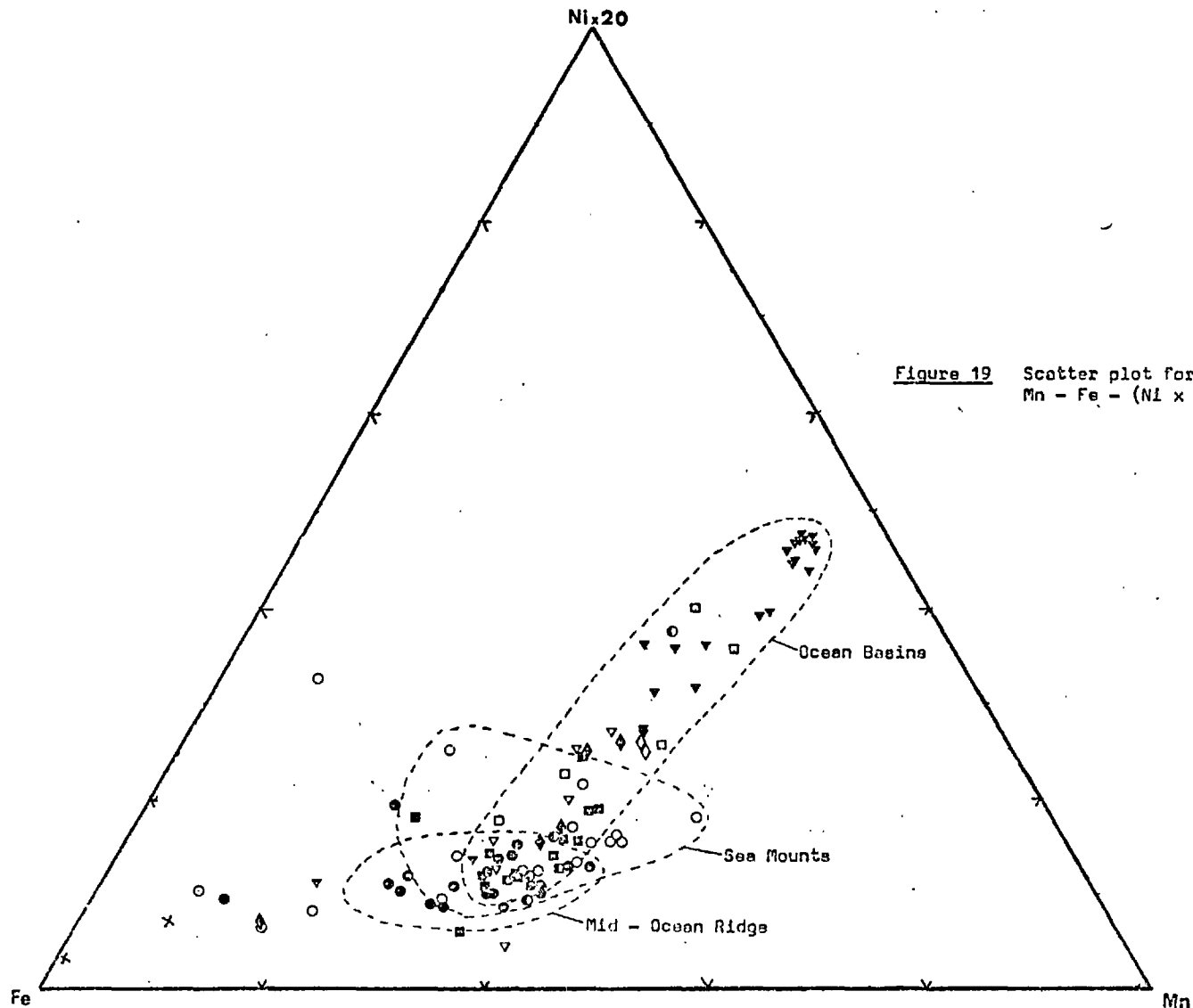


Figure 19 Scatter plot for Mn - Fe - (Ni x 10).

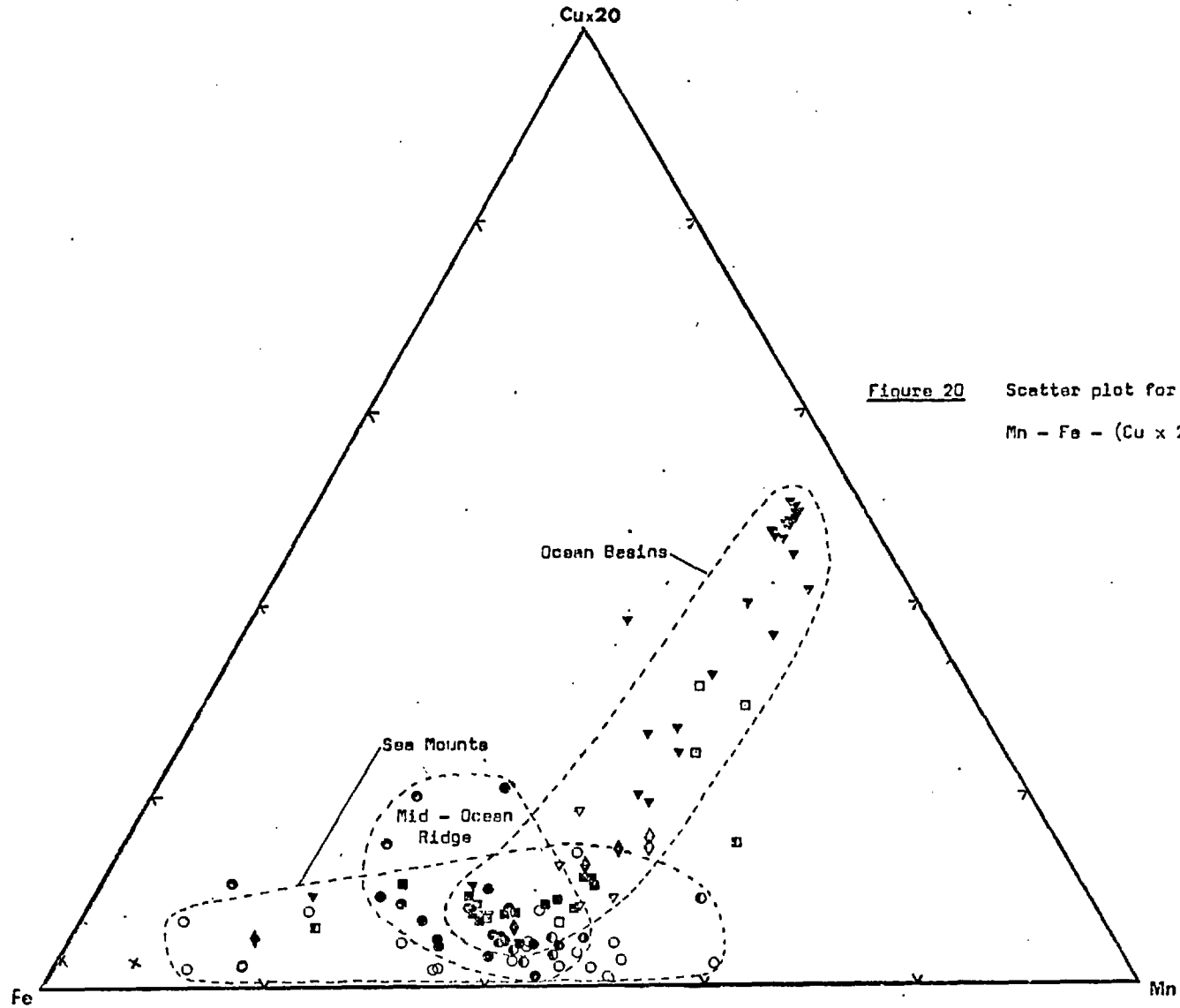
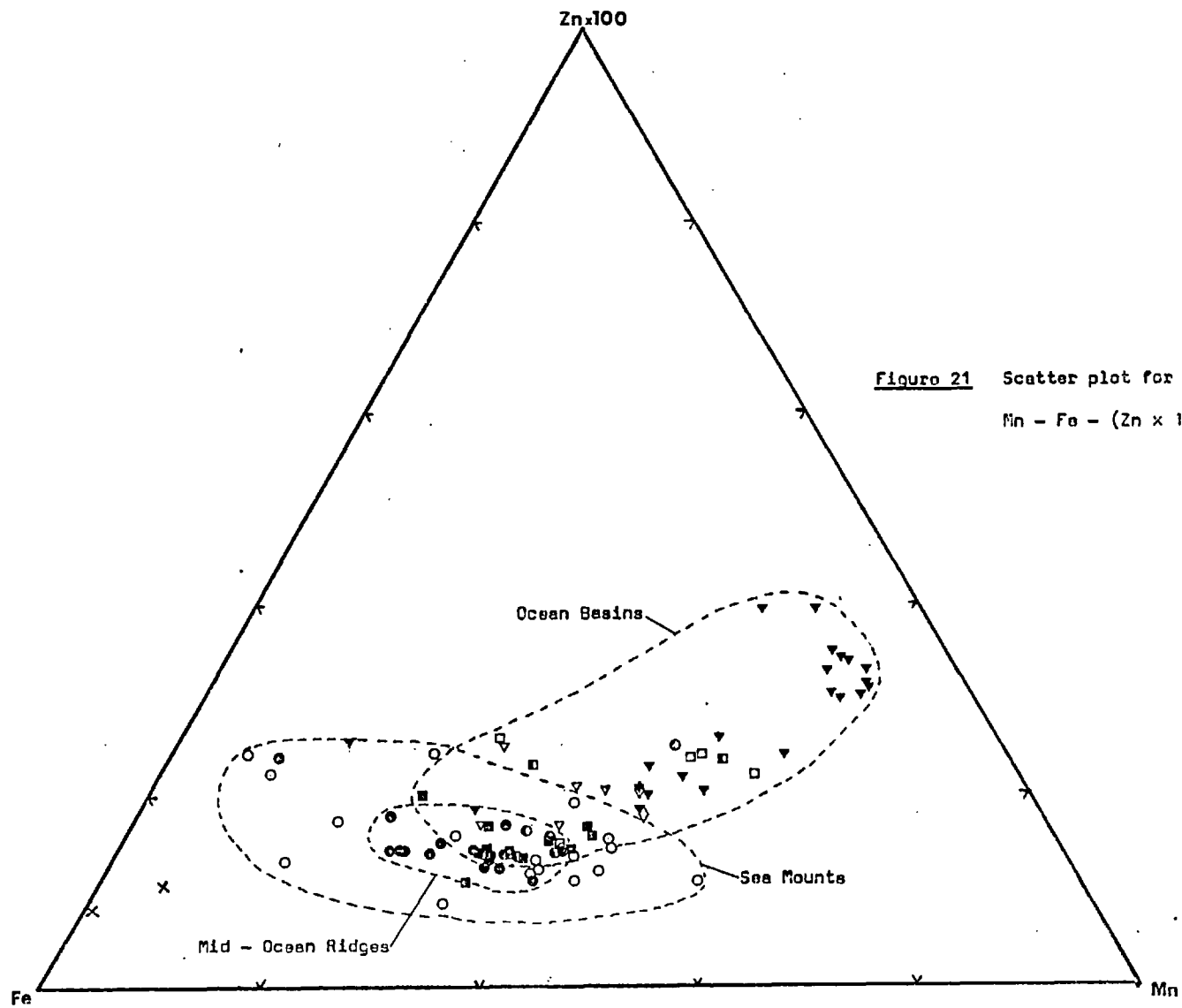


Figure 20 Scatter plot for  
 $Mn - Fe - (Cu \times 20)$ .



**Figure 21** Scatter plot for  
Mn - Fe - (Zn x 100).

reason for this is discussed in Section 9. Also the spread of values of the three major sub-populations is rather greater for Cu than for Ni. Copper behaves very like Ni in ocean-basin samples, showing a marked trend of Cu-enrichment. As is the case with Ni, Central Indian Basin samples show this trend to the greatest extent, whilst those from the Crozet and Madagascar Basins show very little Cu-enrichment and plot largely within the field of mid-ocean ridge samples. Continental borderland samples are very low in Cu and show extreme Fe-enrichment.

#### Zinc - Fe - Mn

Whilst Zn shows some similarities to Ni and Cu it shows a greater spread of values than do Ni and Cu (see figure 21). Ocean Basin samples show a trend of Zn-enrichment but this trend is not as marked as that exhibited by Ni and Cu. Mid-ocean ridge samples are of very uniform composition, being generally low in Zn and exhibiting only a very small trend toward Fe-enrichment. Samples from sea-mount areas show a similar trend but are rather more variable in composition, some of the more Fe-rich samples being comparatively high in Zn. Zinc values in Madagascar Basin samples show more affinity with mid-ocean ridge samples than with other ocean basin samples. This behaviour was also observed for Ni and Cu.

#### Cobalt - Fe - Mn

Cobalt shows very different trends to those shown by Ni, Cu and Zn (see figure 22). Ocean basin samples show a marked trend of Mn-enrichment becoming increasingly depleted in Co and Fe. Once again, Central Indian Basin samples show this trend to the most marked extent and Madagascar Basin samples show the trend to the least extent, showing more affinity

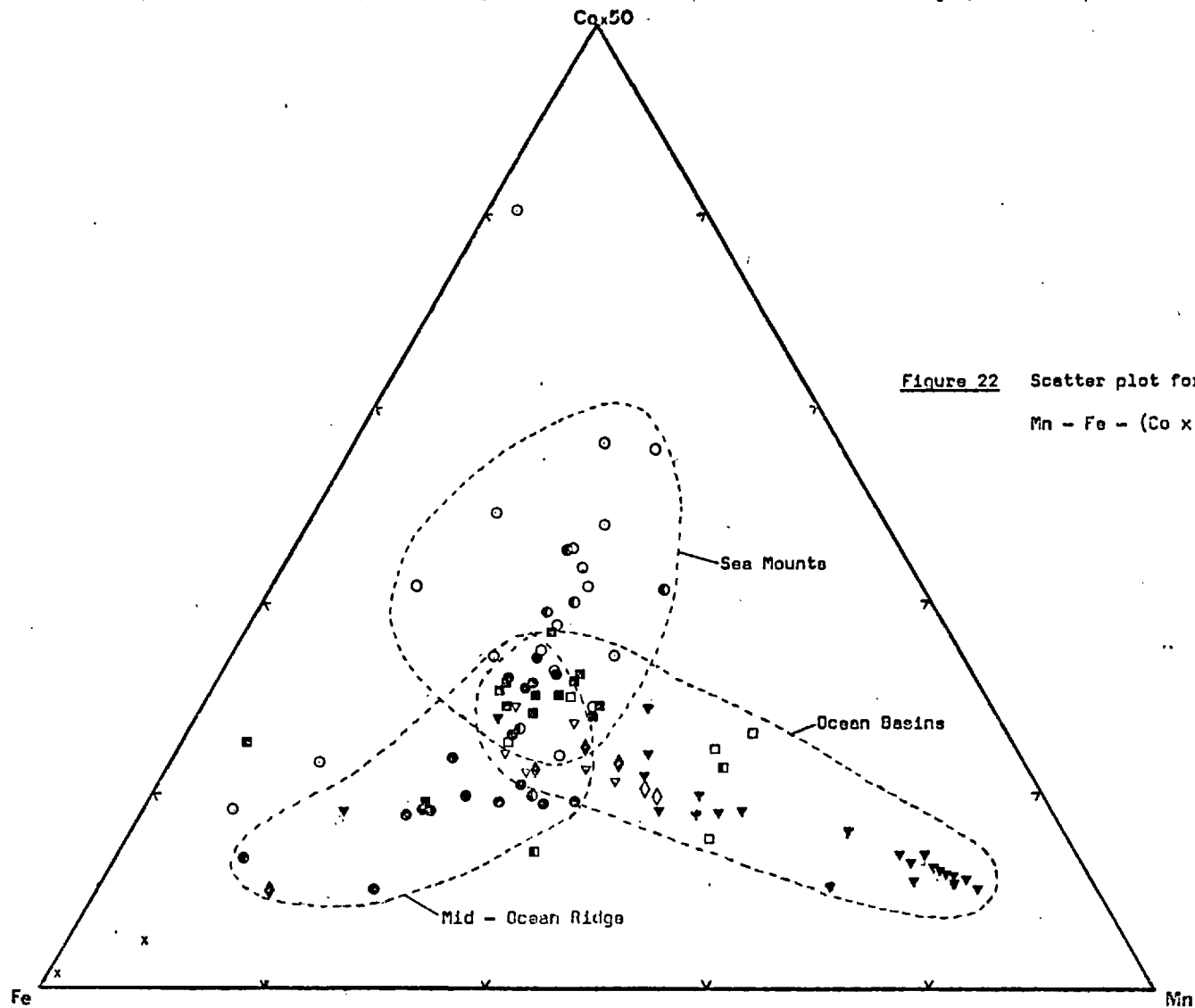
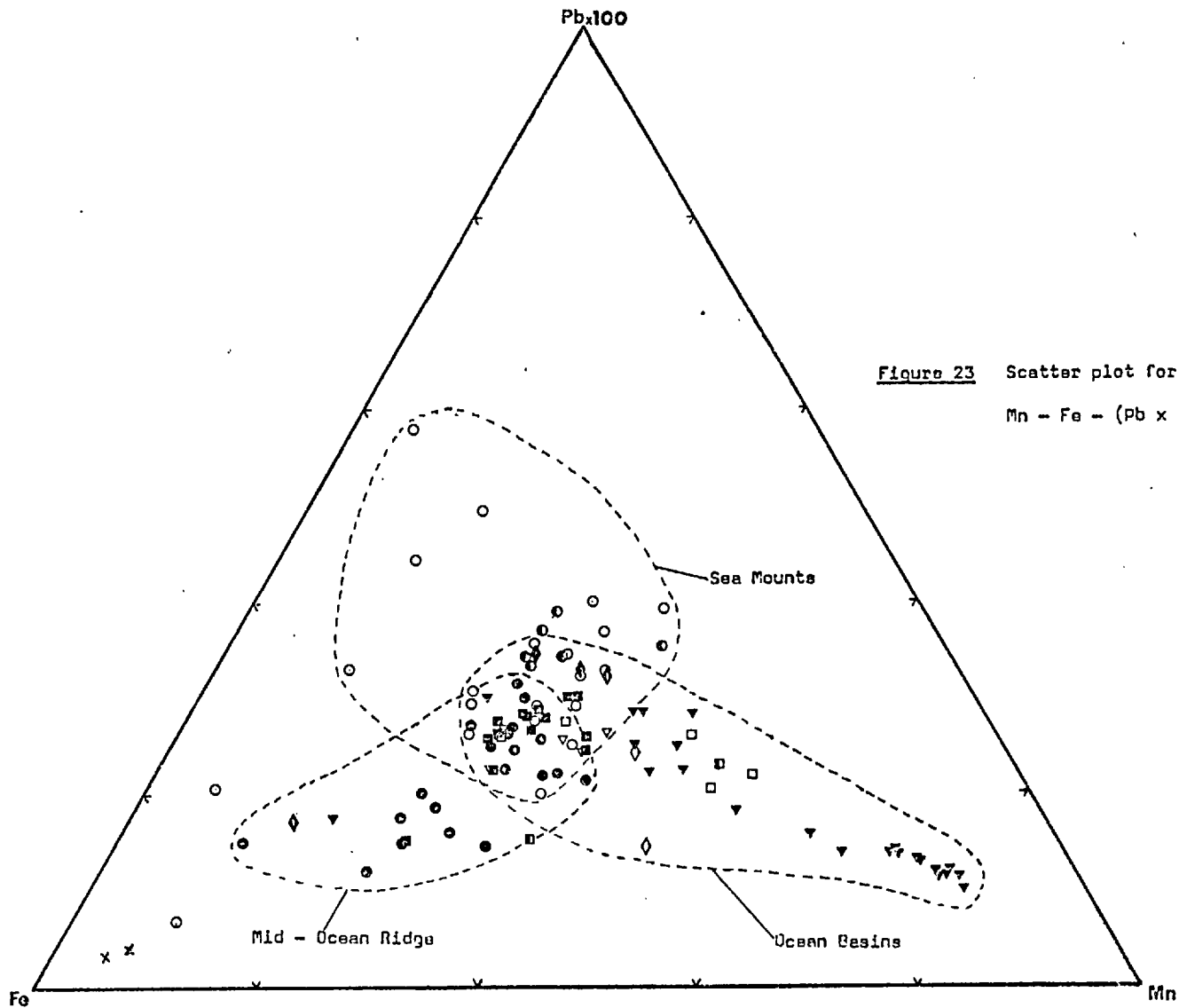


Figure 22 Scatter plot for  
Mn - Fe - (Co x 50).



**Figure 23** Scatter plot for  
Mn - Fe - (Pb x 100).

with mid-ocean ridge samples. Samples from the mid-ocean ridge show a rather wider spread of values for Co than for Ni and Zn and a few of the more Fe-poor samples are comparatively Co-enriched. Nickel, Cu and Zn are similarly depleted in both mid-ocean ridge and sea-mount samples. Co on the other hand shows different trends in these two sub-groups. Cobalt is much more enriched in sea-mount samples than mid-ocean ridge samples, the latter environment favouring Fe-enrichment instead.

#### Lead - Fe - Mn

Lead shows a very similar pattern to that displayed by Co (see figure 23). Again, ocean basin samples show a marked trend of Mn enrichment and are progressively depleted in Pb and Fe. Some overlap of mid-ocean ridge and sea-mount samples occurs but as is the case with Co these two groups of samples exhibit different trends, mid-ocean ridge samples being enriched in Fe whilst sea-mount samples display mainly a Pb enrichment, although showing a rather wide range of compositions.

#### Copper + Nickel - Fe - Mn

Since copper and nickel correlate well together and show similar trends, a further diagram was compiled using the sum of the copper and nickel concentrations as one axis and Mn and Fe concentrations as the second and third. In this way it was hoped to see if further trends became visible. The resulting diagram is given in figure 24. The most noticeable feature of this diagram is the very small degree of variation shown by mid-ocean ridge samples which show a very uniform Cu + Ni content. Sea-mount samples show a greater compositional range with a trend toward Fe-enrichment but still have fairly uniform low Cu + Ni values. Ocean basin samples again show a marked trend of trace metal



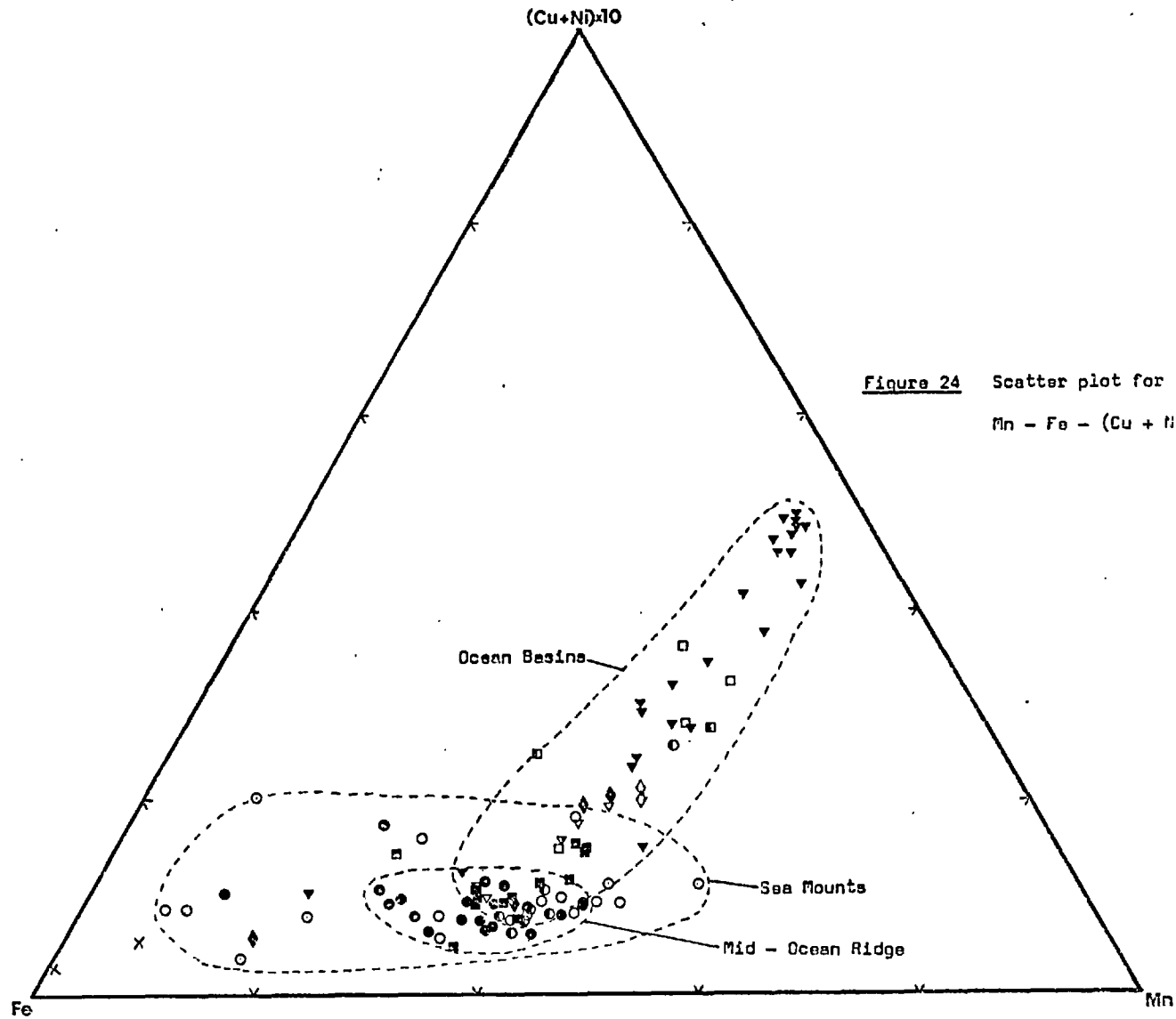


Figure 24 Scatter plot for  
 $Mn - Fe - (Cu + Ni) \times 10.$

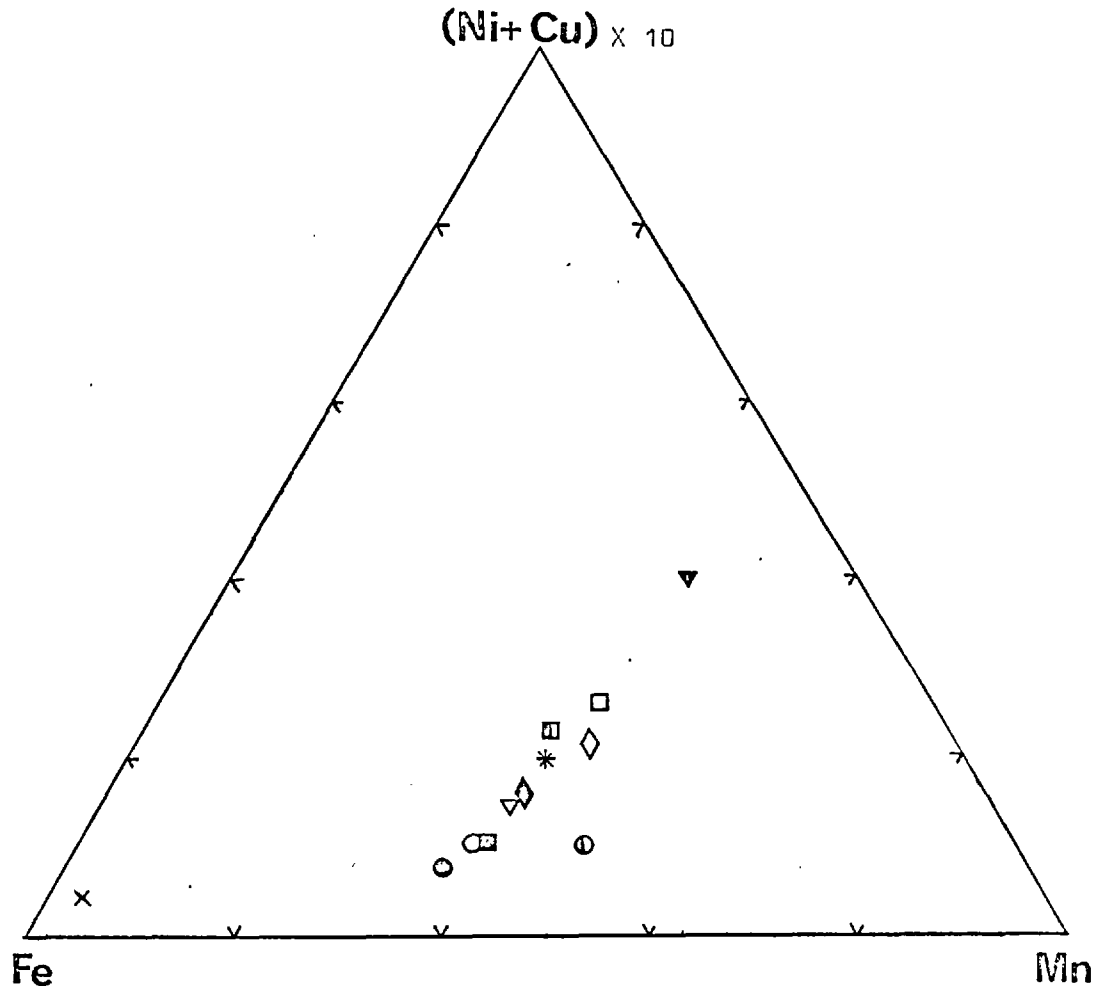


FIGURE 25 Scatter plot of average values of Mn, Fe and (Ni + Cu) for different physiographic regions of the Indian Ocean.

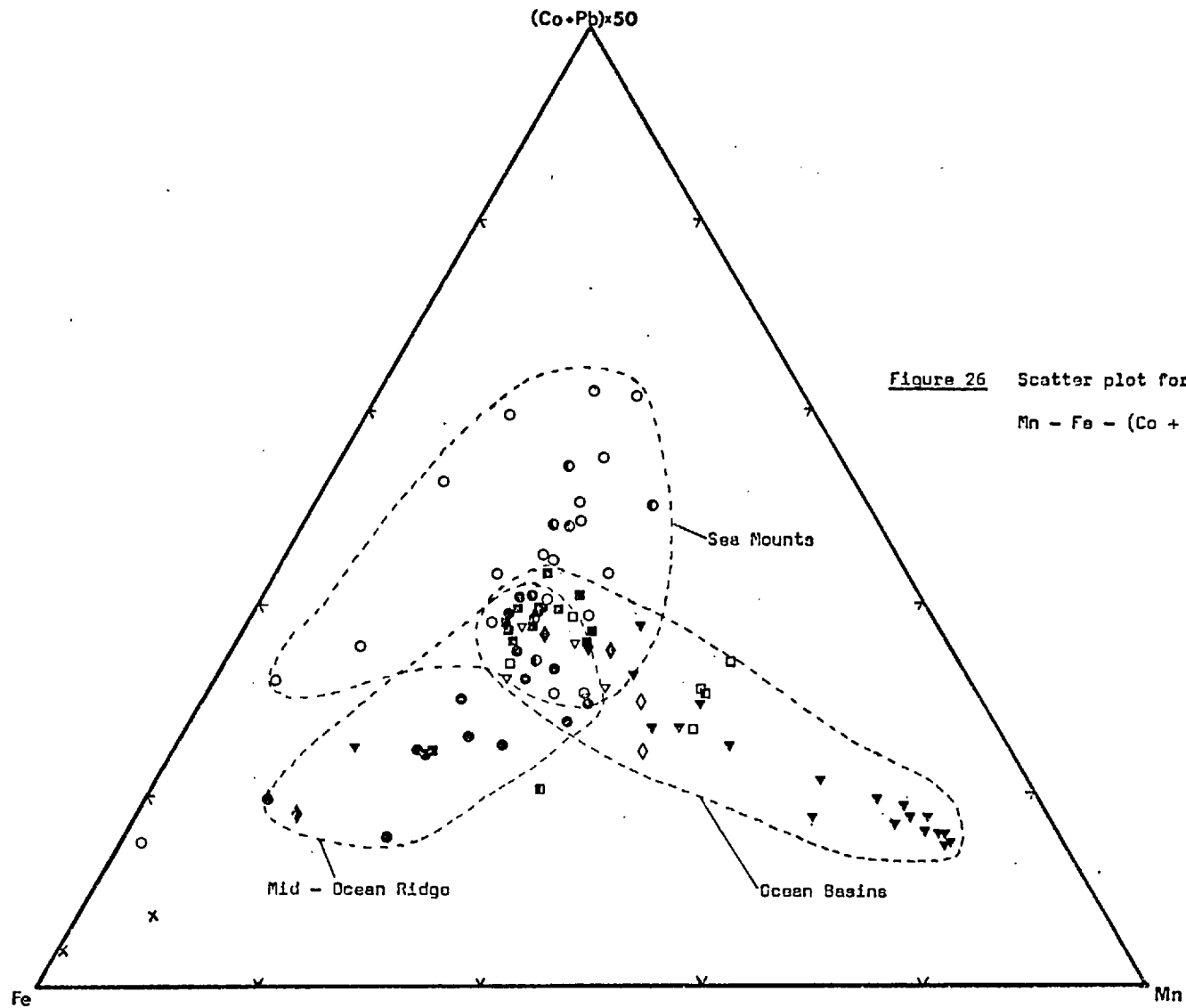


Figure 26 Scatter plot for  
 $Mn - Fe - (Co + Pb) \times 50.$

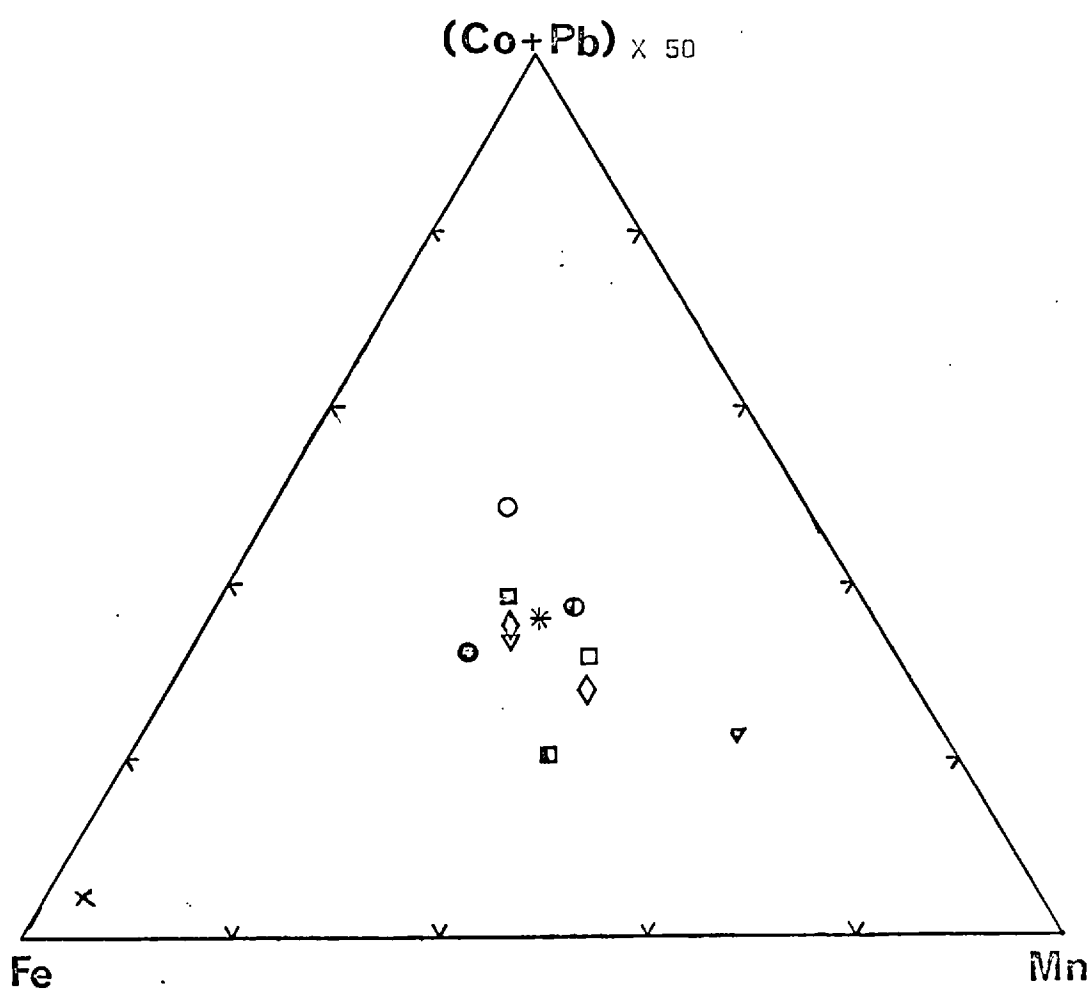


FIGURE 27 Scatter plot of average values of Mn, Fe and (Co + Pb) for different physiographic regions of the Indian Ocean.

enrichment whilst keeping fairly uniform Mn values. Samples from the various basins within this group do not plot completely arbitrarily but show a rough trend of increasing Ni and Cu-enrichment which is shown on the following page.

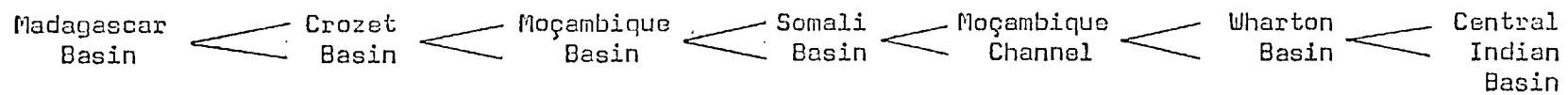
The trend becomes very clear when the average value for each basin, listed in Table 11, are plotted (see figure 25). This diagram also shows the very small range of Mn values observed when the average values from each area are considered. Only 2 groups of samples show appreciably different Mn values, the extremely Fe-rich continental borderland samples and samples from the Southern African Plateaux, which appear to be slightly Mn-enriched.

#### Cobalt + Lead - Fe - Mn

Since Co and Pb correlate well together and show similar trends on their respective scatter plots, a diagram was compiled using Co + Pb as a third axis to see if compositional trends became clearer. However, as can be seen from figure 26, the trends observed are the same as those seen when the two elements were plotted separately. The average values for each physiographic area plotted in figure 27, in contrast to the behaviour of Ni and Cu, do not show any clear trends.

#### (vi) GEOCHEMISTRY OF NORTH-WEST INDIAN OCEAN SAMPLES

In addition to the widely spaced samples which form the basis of the preceding discussion, intensive sampling was carried out in the North-West Indian Ocean, and thus this area is considered separately. Twelve stations were occupied on sea-mounts in the North-East Somali Basin and two were occupied on the Carlsberg Ridge. At some stations, the material recovered was of more than one morphological type and the



Degree of Cu and Ni enrichment in Indian Ocean ferromanganese nodules.

results of separate analysis of this material have already been discussed.

#### Inter Element Associations

A correlation matrix using log-transformed data was computed for the samples analysed in order to investigate element associations in samples specifically from volcanic environments and their possible differences from those observed in samples from the complete range of environments discussed earlier. The results are given in Table 12. Unfortunately, the small sample population available makes the matrix of limited value and in fact very few correlations were found which are significant at the 99% confidence level.

Interestingly, Mn and Fe show no strong correlations with any of the trace elements although Fe correlates strongly negatively with Ca. A strong positive correlation of Cu with Al occurs. This may largely be fortuitous, due to both elements correlating positively with depth, for different reasons. However, it may also infer that where total Cu values are low, as they are in this suite of samples, a significant amount of this total may occur in the aluminosilicate phase rather than, as would normally be expected, in the authigenic oxide phase.

A strong positive correlation between Co and Pb occurs, and these elements also correlate weakly negatively with depth. Calcium, however, correlates strongly negatively with depth. Nickel correlates positively with Co and shows no positive correlation with Cu.

These correlations are in marked contrast to the behaviour of the elements concerned in the total sample population collected ocean-wide. A similar observation was made by Glasby, Tooms & Howarth (1974) who found an extreme non-reproducibility of element associations when they split a large sample population of nodules from the North-West Indian

	Depth	Mn	Fe	Co	Ni	Cu	Zn	Pb	Ca	Al
Mn	.366									
Fe	.517	.407								
Co	-.519	-.130	-.094							
Ni	-.248	.202	-.252	.619						
Cu	.646	.420	.111	-.505	.013					
Zn	.397	.275	.326	-.117	.381	.336				
Pb	-.549	-.063	.174	.839	.459	-.603	.107			
Ca	-.710	-.376	-.811	.070	-.041	-.418	-.577	-.014		
Al	.698	.083	.405	-.585	-.249	.755	.313	-.630	-.641	

Minimum value significant at 95%  
confidence level = 0.412

Minimum value significant at 99%  
confidence level = 0.558

Sample population = 17

TABLE 12

Correlation coefficients using log-transformed data for north-west Indian Ocean samples.



Ocean into 11 small sub-populations. They therefore warned against applying statistical techniques to limited population sub-sets.

### Compositional Variations

On the basis of their locations, the samples obtained from the North-west Indian Ocean can be split into several groups:-

1. Samples from the Carlsberg Ridge.  
samples SH13010(a) and (b), SH13030(a) and (b) - (4 samples)
2. Sea-mount samples from various depth environments.
  - a. less than 1500m. water depth,  
samples SH13150, SH13180, SH13200, SH13250. - (4 samples)
  - b. between 1500m. and 2500m.,  
samples SH13170, SH1317RC, SH13120, SH1322GC - (4 samples)
  - c. greater than 2500m. water depth,  
samples SH13070(a) and (b), SH13230, SH1323GC- (5 samples)  
SH13260.

The compositional variation of these sample groups, plotted against depth, is shown in figure 28. No marked trends in Mn and Fe values occur, although Fe is lower in the shallowest groups of samples compared to those from greater depths. As expected from its negative correlation with depth, Ca shows a marked decrease in deeper water samples, whilst Al increases in deeper water samples. Cobalt, Ni and Pb all show decreases with depth, but for Ni the decrease is very small. Copper, on the other hand, increases with depth whilst Zn shows no trend with depth.

The average composition of Carlsberg Ridge samples was also plotted on the diagram, in order to assess whether metal values in these samples simply reflect trends due to environmental changes

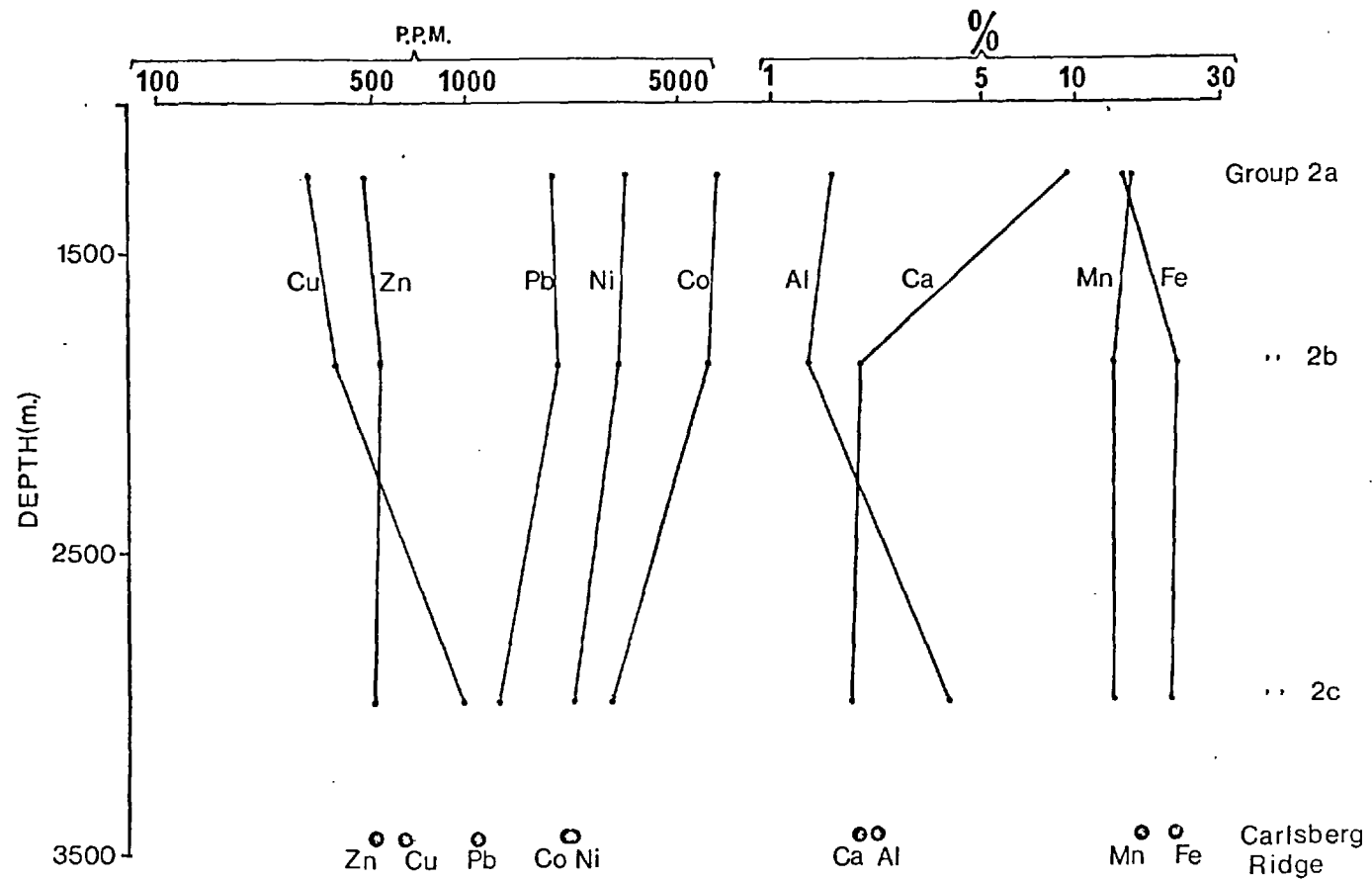


FIGURE 22 Compositional variations with depth in North-West Indian Ocean ferromanganese-oxide deposits.

associated with increase in depth or whether some other factor, such as locally increased metal supply, has been operating. Zinc, Pb, Co, Ni, Fe and Ca all show values in the ridge samples which compliment the trends with depth observed in the sea-mount samples, but Mn, Al and Cu do not. Copper and Aluminium values are lower than expected whilst Mn values are slightly higher.

In view of the variable Mn values normally observed in ridge and sea-mount environments, and the small number of samples analysed, this increase may not be significant, particularly when considered against the lower Al content of the ridge samples indicating the presence of smaller amounts of diluting phases. However, the average Mn content of Carlsberg Ridge samples (16.8%) and their average  $Mn/Fe$  ratio (0.81) are significantly higher than corresponding values for the whole of the mid-ocean ridge (see Table 10) and this may indicate a locally increased supply of Mn.

The behaviour of Cu in Carlsberg Ridge samples is difficult to explain. If its decrease in these samples, compared to the sea-mount trend, were due to a mineralogical control, then a decrease in Ni might also be expected, since these two elements seem to correlate closely in this respect. However, as already observed in the present suite of samples, Cu and Ni do not behave similarly at all. This difference may be due to some local factor influencing the availability of these two elements to a different extent, causing a fractionation of one relative to the other.

Compared to their concentrations in normal sea-water, Cu and Ni are considerably enriched in many marine organisms (Nicholls et al, 1959; Fujita, 1971; Greenslate et al, 1973; Leatherland et al, 1973). However, as some of these authors show, Cu is considerably more enriched in many of these organisms than is Ni. In areas of high biological productivity therefore, the upper part of the water column may exhibit rather lower

$Cu/Ni$  ratios than sea-water in areas of lower productivity, the balance only being redressed in such areas at depths below the lysocline when substantial dissolution of the dead organisms begins to occur. No detailed studies of biological productivity have been carried out in the small areas of the North-West Indian Ocean being considered, although as can be seen from figure 7, some variations are known to occur. This mechanism cannot therefore be advanced as causing the observed variations in Cu content of the samples from the ridge compared with those from sea-mounts. However, this mechanism does help to explain the marked fractionation of Ni from Cu, observed in shallow water samples from this and other areas in general. As can be seen from figure 28 and Table 10, Cu values in shallow water samples are up to an order of magnitude lower than Ni values in the same samples. By contrast, nodules enriched in Ni and Cu from depths well below the lysocline, contain almost as much Cu as Ni. This has also been shown to be the case by Bezrukov and Andrushchenko (1973) and also occurs in the Pacific Ocean (Cronan, 1972; Horn et al, 1973). Thus marine organisms may take up sufficient Cu to cause its depletion in shallow water samples, compared to Ni, and provide an enhanced supply of Cu below the lysocline when the organisms sink and dissolve upon death.

## S E C T I O N 6

### BULK GEOCHEMISTRY OF SEDIMENTS

#### (i) INTRODUCTION

At many of the sampling stations from which the nodules analysed in this study were recovered, sediment samples were also obtained. In some cases the sediment samples came from a separate coring operation at the same site as that from which nodules had been recovered by a different sampling technique. In many cases however, the sediment was recovered in the same operation as that which produced the nodules and in two cases sediment actually in contact with a nodule was obtained. At some sites only sediment was recovered but since no bottom photographs were taken at most of these stations it is not possible to say whether there were in fact no nodules at that locality or whether the sampling techniques employed simply failed to recover nodules. Most of the samples analysed were surface sediments, but six samples were of sediment associated with buried nodules. The distribution of the 37 stations from which surface sediment was analysed is shown in figure 29. From this diagram it can be seen that, apart from a detailed traverse in the Madagascar Basin and one in the Central Indian Basin, regional coverage of the Indian Ocean is poor.

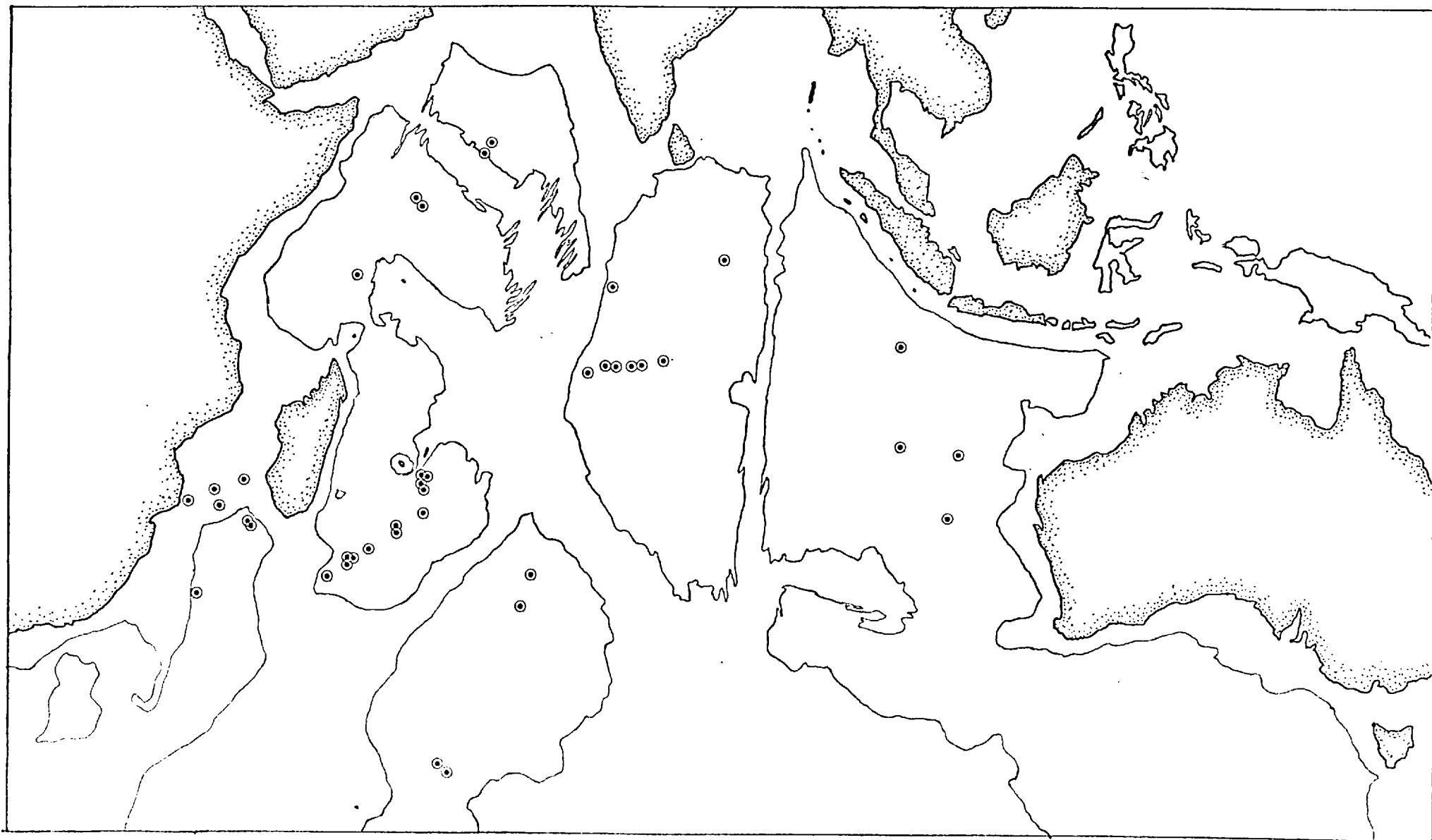


Figure 122 Distribution of sediment sample sites in the Indian Ocean.

The sediment samples were analysed for Mn, Fe, Co, Ni, Cu, Zn, Pb, Ca, Al and in some cases Cd, Cr and Ti also, by atomic absorption spectrophotometry. Details of the analytical procedures adopted are given in Appendix 1. No attempt was made to remove interstitial solids prior to analysis by washing with distilled water since these were regarded as being an integral part of the sediment, as argued by Goldberg and Arrhenius (1959) and Wangersky (1967).

#### (ii) SEDIMENT TYPE

As might be expected in view of their very wide distribution, the sediment samples obtained were very varied in type. Seven samples contained more than 30% calcium carbonate and these were therefore classed as carbonate sediments. A further eleven samples, containing between 10% and 30% calcium carbonate, were regarded as clay-carbonates, whilst the remaining samples were classed as non-carbonate sediments, either of red-clay or siliceous type. These non-carbonate sediments came from greater average depths (5089m.) than carbonate sediments (3918m.), whilst the clay-carbonate sediments, apart from one continental margin sample came from depths intermediate between these two values (4129m.).

The low sampling density precludes a reasonable appraisal of sediment types in the different basins, however some generalisations can be made. A red-brown pelagic clay was the typical sediment obtained from pelagic areas below the carbonate compensation depth. Samples from the Wharton Basin and parts of the Madagascar Basin were of this type. In the latter basin, several samples were recovered which contained more than 10% carbonate. These were all from depths of less than about 4500m. The two samples from the southern Crozet Basin, whilst coming from depths in excess of 4700m., were also fairly carbonate-rich compared to samples from similar depths in other areas. These samples, however, came from latitudes characterised by a depression of the lysocline and the carbonate

compensation depth (see figure 9) and in fact came from depths above the compensation depth.

Sediments from shallower depths, in both pelagic and marginal areas, were generally rich in carbonate. Samples from the Mozambique Channel, from an average depth of 2870m., averaged over 60% calcium carbonate whilst samples from the Carlsberg Ridge and Somali Basin sea-mounts (average depth 4400m.) averaged 50% carbonate. All these sediments were essentially foraminifera-rich carbonate oozes.

Most samples from the Central Indian Basin were from depths in excess of 5000m. and were thus below the carbonate compensation depth in that region (see figure 9). These samples were siliceous oozes consisting predominantly of diatoms, radiolarians and other siliceous biogenic débris together with smaller, variable amounts of fine clays and, occasionally, micronodules.

### (iii) GEOCHEMISTRY

#### (a) Treatment of data

As already discussed, the amount of carbonate in the sediments analysed varied greatly. Since this can be regarded essentially as a diluting phase in marine sediments, in order to examine geochemical variations of importance in regard to the present study all bulk sediment compositions were re-calculated on a carbonate-free basis using the method of Dymond et al (1976). This method involves the solving of the following equation:

(See following page)



Equation:  $Ca_T = Ca_S S + Ca_N N + Ca_C C - 1.$

where:-  $Ca_T$  = weight % Ca in total sample.  
 $Ca_S$  = " " " in salt fraction (=1.14% for sea-salt).  
 $Ca_N$  = " " " in non-carbonate fraction.  
 $Ca_C$  = " " " in  $CaCO_3$  (=40.04%).  
 $S$  = " fraction of salt in the sample.  
 $N$  = " " of non-carbonate phases.  
 $C$  = " " of  $CaCO_3$  in the sample.

Since by definition the sediment must be composed entirely of salt, carbonate and non-carbonate fractions then,

$$S + N + C = 1 \quad -2.$$

This can be substituted in Equation 1 along with the values for  $Ca_S$  and  $Ca_N$  given above, giving

$$Ca_T = 1.14S + Ca_N - Ca_N S - Ca_N C + 40.04C \quad -3.$$

The amount of Ca in the non-carbonate phase was determined from the selective chemical attack work discussed in Section 7. This gives a value for  $Ca_N$ . The average salt content of the samples was determined by measuring the weight loss after washing with de-ionised water. This gives a value for  $S$ .  $Ca_T$  was measured by atomic absorption spectrophotometry for each of the samples, and the values of  $Ca_N$ ,  $S$ , and  $Ca_T$  substituted in Equation 3 enable  $C$  to be calculated for each sample. Once the weight % of  $CaCO_3$  in the sample had been obtained this value was then used to re-calculate the composition of the sediment on a carbonate-free basis in the normal way. As stated by Dymond et al (1976), the accuracy of this method becomes poorer at lower concentrations of  $CaCO_3$  but at the same time this becomes less important because of the much lower correction factor which needs to be applied to the bulk sediment composition.

(b) Comparison of composition of sediment in contact with nodule and additional sediment from same horizon

At two sampling sites, one in the Crozet Basin, one in the Central Indian Basin, sediment was obtained which was actually adhering to a nodule and in addition a separate sediment sample was obtained from the same horizon. The results of analysis of these sediments are given in Table 13.

As can be seen from Table 13, the sediment in contact with nodule sample 94KH, compared with additional sediment from the same horizon, shows only small differences in composition. For all elements except Co and Pb the differences were within the limits of analytical precision and even Co and Pb showed differences which were little higher than this limit. Thus there appeared to be no significant difference in composition between the two sediment samples.

In contrast to this behaviour, sediment adhering to sample RC11/101 was significantly depleted in Mn, Fe, Co, Ni, Cu, Zn and Pb compared to other surface sediment. In this case the ferromanganese-oxide sample was only a thin coating and was particularly low in Mn and trace metals, moreover this sample was a surface sample whereas the nodule from station 94KH was from 1.5 metres down a core. The fact that the nodule samples are very different in morphology and composition and were not from similar sediment horizons makes comparisons between the two very difficult. However it can be said that the ferromanganese sample from the sediment surface, which might therefore be assumed to have been accreting when recovered, had sediment adhering to it which was appreciably lower in Mn, Fe and trace metal content than surface sediment further removed from the ferromanganese-oxide sample. On the other hand, the nodule sample 94KH, which was buried and therefore may not have been accreting at the time of recovery, had sediment adhering to it which was of similar composition to

SAMPLE	Mn %	Fe %	Co p.p.m.	Ni p.p.m.	Cu p.p.m.	Zn p.p.m.	Pb p.p.m.	Ca %	Al %	Cd p.p.m.	Cr p.p.m.	Ti p.p.m.	CaCO <sub>3</sub> %
RC11/101 - top sediment	.486	4.74	63	110	125	195	92	10.2	4.84	-	-	-	24
RC11/101 - adhering sediment	.337	3.99	55	82	95	120	55	8.97	4.16	-	-	-	21
RC11/101 - Fe - Mn coating	.417	9.82	125	190	170	175	185	1.32	4.06	-	-	-	-
94KH - sediment 145 - 150cm.	.850	2.86	72	287	375	105	55	0.50	4.53	5	80	2210	0
94KH - adhering sediment	.848	2.81	85	282	382	116	65	0.55	4.63	6	90	2420	0
94KH - buried nodule	18.7	6.54	600	7990	8330	775	460	1.33	3.59	17	110	7020	-

TABLE 13 Comparison of composition of sediments associated with ferromanganese-oxide deposits

other sediment within the core from the same depth. The possibility that accreting ferromanganese-oxides may preferentially incorporate trace metals from their immediate surroundings thereby depleting the trace metal content of closely associated sediment cannot be realistically evaluated using only the two samples available. However such a process is indicated by the results obtained and the theory is one which is perhaps worthy of more detailed future study.

(c) Comparison of composition of surface sediment with sediment from depth

At four stations, sediment from depth within a core was obtained, in addition to a surface sediment sample. In three of these cases, the buried sediment was from the same depth as a buried manganese nodule. In the fourth case, the sediment from depth was from a layer which was noticeably different to the surface sediment, was rich in manganese micronodules but contained no macronodules. The compositions of these sediments together with that of associated nodules, where present, are given in Table 14.

At station RC14/49, the sediment from two metres depth was appreciably higher in Mn, Fe, Co, Ni, Cu, Zn, Ca and Al. At station V16/80, no surface sediment was obtained but samples from two different depths 60cm. apart were taken. In this case also, sediment from lower down the core was enriched in Mn, Co, Ni and Cu but Pb, Ca and Al showed no significant change. Exceptionally high Zn values were observed in nodule and sediment samples from this core and these may be due to contamination because samples from this source (Lamont-Doherty Geological Observatory) are known to have been stored in Zn-rich containers. This precludes any examination of the behaviour of Zn in this core. According to the calculations of Bondar and Schultz (1969) the level of Zn present in these samples, if due solely to contamination, infer that up to half of the Fe content of the samples may also be due to contamination. Thus the behaviour

	Mn %	Fe %	Co p.p.m.	Ni p.p.m.	Cu p.p.m.	Zn p.p.m.	Pb p.p.m.	Ca %	Al %	Cd p.p.m.	Cr p.p.m.	Ti p.p.m.	CaCO <sub>3</sub> %
RC14/49 surface sediment	.419	2.49	49	126	189	108	69	0.90	5.98	-	-	-	0
RC14/49 sediment - 200cm.	.452	3.73	66	171	250	275	56	1.42	7.94	-	-	-	5
RC14/49 surface nodule	19.8	11.8	1200	7070	5080	1010	1100	1.56	2.41	-	-	-	-
RC14/49 nodule - 200cm.	17.3	13.1	1620	4120	3200	615	1220	1.32	2.99	-	-	-	-
V16/80 sediment - 70cm.	.525	10.2	102	127	270	6370	82	1.20	6.56	-	-	-	5
V16/80 sediment - 130cm.	.796	8.51	125	204	320	6080	85	1.10	6.30	-	-	-	5
V16/80 nodule - 70cm.	12.9	20.5	2500	1780	1330	10400	1220	1.07	2.61	-	-	-	-
V16/80 nodule - 130cm.	12.4	19.4	2640	1610	1370	9270	1210	1.35	2.34	-	-	-	-
84GK sediment 0 - 8cm.	1.96	3.92	109	1200	1050	240	71	4.14	3.18	8	98	2420	8
84GK sediment 8 - 10cm.	5.93	5.02	189	3830	3180	545	102	3.1	6.46	4	21	2120	5
94KH surface sediment	.838	2.70	75	245	450	200	85	0.62	4.26	6	70	1760	0
94KH sediment - 145cm.	.850	2.86	72	287	375	105	55	0.50	4.53	5	80	2210	0

TABLE 14 Composition of sediments from different horizons at the same sample site

of Fe in this core cannot be examined either.

The variation in composition of sediment from cores RC14/49 and V16/80 is especially interesting when compared with the composition of nodules associated with these sediments. At station RC14/49 the nodule from 2m. depth is depleted in Ni, Cu, Zn and to a lesser extent Mn, compared with the surface nodule. This trend is the opposite of that observed in the sediment samples from the same horizons, but the Co content of the buried nodules is higher than that of the surface nodule and this trend is the same as that observed in the associated sediments. No marked trends occur in the samples from station V16/80 but Mn, Co and Cu do show a small increase in sediment from greater depth whilst showing no significant change in the nodules.

At station RC14/49, the lower Mn, Ni, Cu and Zn content of the buried nodule compared with the surface nodule may be due to a release of these elements by partial dissolution of the Mn phase in comparatively reducing conditions. However, a more feasible explanation for the chemical differences is simply that the buried nodule accreted at the sediment-water interface under different environmental conditions to those under which the present surface nodule has accreted, or may even have accreted within the sediment. The higher Mn, Fe, Co, Ni, Cu and Zn content of the buried sediment may be due to the presence of larger amounts of trace-metal-rich clays, as suggested by the higher Al content, compared with the surface sediment. This is likely to have been caused by a change in sedimentary conditions and thus this explanation ties in with that suggested to explain the differences in the composition of the nodules from the two horizons.

If this theory is applied to samples from station V16/80 it would seem that environmental conditions affecting nodule composition were essentially the same when both nodules were accreting. The differences in sediment composition infer some differences in conditions but the Al content of both samples is similar, and the clay content of both samples is

therefore likely to be similar. The higher Mn, Co, Ni and Cu content of the deeper sediment may be due to the presence of micronodules in slightly larger amounts than in the upper sediments.

Since no nodules were recovered from stations 84GK and 94KH only a simple comparison of buried and surface sediment could be carried out at these sites. At station 84GK there was a thin layer of sediment 8 to 10cm. from the top of the core which was of noticeably darker colour than that above and which was therefore analysed separately. Sediment from this layer contained about 3 times as much Mn, Ni and Cu as surface sediment whilst being particularly depleted in Cr. Microscopic examination of the buried sediment layer showed the presence of much more abundant micronodules than in the surface sediment, and this would account for the higher Mn, Ni and Cu content and perhaps the lower Cr content also by dilution. However, the lower Cr content of the buried layer may be a result of a lower volcanic contribution to this sediment since Goldberg and Arrhenius (1958) and El Wakeel and Riley (1961) have found that in pelagic sediments Cr is often enriched in volcanically derived material and Kennett and Thunell (1975) have shown that volcanism has increased globally in the Quaternary Period.

The two sediment samples from station 94KH do not show marked compositional differences and are essentially similar in Mn, Fe, Co, Ni, Cu, Ca, Al, Cd, Cr and Ti content. The buried sample does exhibit lower Zn and Pb values however. It is apparent from the shipboard log taken at station 94KH that some mixing of surface and sub-surface sediment occurred when the sample was being taken. If surface sediment did become mixed in this way its composition may have been significantly altered and this precludes any worthwhile comparison of the two samples from this station.

An insufficient number of samples of the same type were available to investigate thoroughly the relationships between surface and buried nodules and accompanying sediment, however such a study might be worthy of future

investigation.

(d) Inter-Element associations

The problem of investigating correlations between variables in closed systems and where not all variables show the same statistical distribution was discussed in Section 5(iii). A further constraint on the usefulness of correlation coefficients is sample population; small numbers of samples are particularly prone to producing anomalous correlations because of sampling bias. Bearing these considerations in mind, correlation coefficients using both normal and log-transformed data were calculated using the method described in Section 5 and only those correlations which were significant at the 99% confidence level were regarded as meaningful. The correlation matrices are given in Table 15.

At the 99% confidence level most significant correlations are very similar, using both normal and log-transformed data. As might be expected, in view of their concentration in manganese micronodules Co, Ni, Cu and Zn correlate strongly positively with Mn, the correlation being particularly strong for Ni and Cu. No other element shows significant correlation with Mn. Even Fe does not correlate significantly with Mn. This is in contrast with the findings of Bender and Schultz (1969) who showed that sediments along a traverse in the southern Indian Ocean which were highest in Mn were also highest in Fe. In this study Fe was found to correlate strongly positively only with Al and Ti. This probably reflects the presence of abundant Fe in volcanically-derived material (Ti-rich) and Fe-bearing clay minerals (Al-rich). Cadmium and chromium show weak positive correlations with Fe using log-transformed data, but not using normal data, this indicates a substantial difference in the statistical distribution of these elements about their mean values. The positive correlation agrees with the fact that these elements, more particularly Cr, tend to be enriched in basaltic and



	Depth	Mn	Fe	Co	Ni	Cu	Zn	Pb	Ca	Al	Cd	Cr	Ti
Depth		.311	-.023	-.179	-.020	.336	.089	-.402	-.516	-.093	-.540	-.079	-.277
Mn	.024		.214	.579	.831	.903	.510	.151	-.332	-.125	-.330	-.088	-.145
Fe	-.013	.057		.378	.149	.132	.316	.045	-.256	.697	.483	.511	.607
Co	-.334	.583	.154		.708	.537	.450	.735	.267	.078	.133	.293	.178
Ni	-.037	.973	.036	.538		.821	.565	.408	-.006	-.131	-.193	-.042	-.145
Cu	.126	.917	.046	.341	.953		.474	.156	-.250	-.185	-.310	-.131	-.285
Zn	.073	.540	.189	.427	.558	.497		.452	.034	.123	.325	.221	.086
Pb	-.490	.251	-.115	.843	.255	.053	.322		.345	-.011	.578	.296	.127
Ca	-.666	-.065	-.082	.531	.004	-.160	.103	.413		-.159	.449	.280	-.100
Al	-.088	-.182	.642	-.071	-.151	-.140	.040	-.136	.020		.499	.176	.708
Cd	-.483	-.165	.375	.219	-.115	-.150	.336	.642	.509	.516		.575	.449
Cr	-.059	.042	.271	.224	.091	.050	.347	.296	.171	-.074	-.049		.147
Ti	-.319	-.287	.689	.067	-.253	-.300	-.072	.008	.263	.660	.383	-.028	

N O R M A L

TABLE 15 Correlation coefficients in Indian Ocean sediments (Correlation significant at 99% confidence level are boxed). Number of samples used to correlate matrix = 51 (28 for Cd, Cr & Ti)

L  
O  
G  
T  
R  
A  
N  
S  
F  
O  
R  
M  
E  
D

detrital material. Aluminium shows no correlations, other than with Cd and Ti, which are significant at the 99% confidence level for both data sets. The correlation of Al with Ti reflects the presence of comparatively large amounts of these elements in detrital phases in sediments (Horowitz, 1974) whilst that of Cd with Al suggests that Cd in sediments may be present predominantly in detrital, aluminosilicate phases.

As might be expected in view of the increasing solubility of calcium carbonate with depth in the oceans, Ca correlates strongly negatively with depth. The only other significant correlations of Ca are small positive correlations with Pb and Cd. These elements both suffer from very strong interference effects from Ca when determined by atomic absorption spectrophotometry, thus in carbonate-rich sediments, spuriously high values of these metals are obtained. A correction procedure for this effect was used and is described in Appendix 1, however at the low levels at which Cd and Pb occur in the samples, inaccuracies in this correction cannot be ruled out.

Several workers, (Nicholls et al, 1959; Fujita, 1971; Leatherland et al, 1973) have shown that many carbonate organisms have the ability to concentrate various heavy metals, including Cd and Pb, whilst Turekian and Imbrie (1966), Aston et al (1972) and Horowitz (1974) state that significant amounts of Pb and Cd are actually incorporated in the carbonate lattice of some marine organisms in the Atlantic Ocean. More recently, Horder (pers. comm.) has found high Cd and Pb values in the carbonate phase of Indian Ocean sediments. There is thus substantial evidence to show that Cd and Pb are enriched in calcium carbonate-rich sediments, perhaps because of the ability of these heavy metals with large ionic radii to substitute for the similarly-sized  $\text{Ca}^{2+}$  ion in the carbonate lattice.

The trace metals Co, Ni, Cu, Zn and Pb all show some degree of positive correlation with each other, in contrast to their behaviour in nodules.

However as in nodules, particularly strong positive correlations exist between Ni and Cu and between Co and Pb. These correlations may be explained by the elements Cu, Ni, Co and Pb being associated together primarily in an authigenic Mn phase. By contrast, the association between Cd, Cr and Ti may be due to their being associated with an Al-rich detrital phase. Lead appears to show some association with calcium carbonate, although its strong positive correlation with Co suggests that it may also be incorporated to some extent in the authigenic Mn phase.

Correlation coefficients can only provide a general guide to element behaviour in marine sediments. In order to investigate more fully the ways in which the major and trace elements are incorporated into sediments, many of the samples were subjected to selective chemical attacks, a full account of the results of this procedure is given in Section 7.

(e) Regional geochemistry of surface sediments

Of the 50 sediment samples analysed, 37 were surface sediment samples from different sites throughout the Indian Ocean. The distribution of these sites however, is not uniform (see figure 29), a larger percentage of stations being in the western Indian Ocean than in the east. Because of this it was not possible to make a detailed assessment of inter-basin variations in surface sediment compositions. However, from the data plotted in figures 30 to 38 and summarised in Table 16 it is possible to draw some general conclusions.

From figures 30 and 31 it can be seen that Mn is highest in eastern areas of the Indian Ocean (i.e. east of the active ridge system) although some high Mn values occur in the Madagascar Basin. By contrast, Fe is higher in sediments from the south-western part of the ocean. The highest average Mn values occur in the Central Indian Basin where Fe is at its lowest. Iron is highest in the Crozet and Madagascar Basins where Mn is only intermediate

TABLE 16. Average composition of surface sediments from different physiographic regions of the Indian Ocean

	1.	2.	3.	4.	5.	6.	7.	8.	9.
Mn p.p.m.	8080	2350	5360	1610	1060	6530	4460	7170	1160
Fe %	3.11	6.69	6.76	4.43	4.50	3.80	6.22	3.30	4.45
Co p.p.m.	87	75	115	46	39	90	110	80	55
Ni p.p.m.	365	105	230	125	150	260	210	310	130
Cu p.p.m.	390	170	205	130	100	255	210	330	95
Zn p.p.m.	170	175	170	175	145	135	175	160	125
Pb p.p.m.	65	100	85	55	105	80	95	70	75
CaCo <sub>3</sub> %	5	28	15	9	65	1	20	6	35
Al %	4.50	4.95	6.55	7.45	3.55	6.40	7.60	5.10	7.80
Cd p.p.m.	5	-	8	-	-	-	-	-	-
Cr p.p.m.	60	-	155	-	-	-	-	-	-
Ti p.p.m.	2870	-	6140	-	-	-	-	-	-
Water depth (m.)	5034	4775	4864	4453	2825	5368	4780	5125	3375
No. of samples	8	3	13	3	3	3	22	11	5

1. Central Indian Basin  
 2. Crozet Basin  
 3. Madagascar Basin  
 4. Moçambique Basin  
 5. Moçambique Channel

6. Wharton Basin  
 7. Western Indian Ocean  
 8. Eastern Indian Ocean  
 9. Marginal Ocean Areas

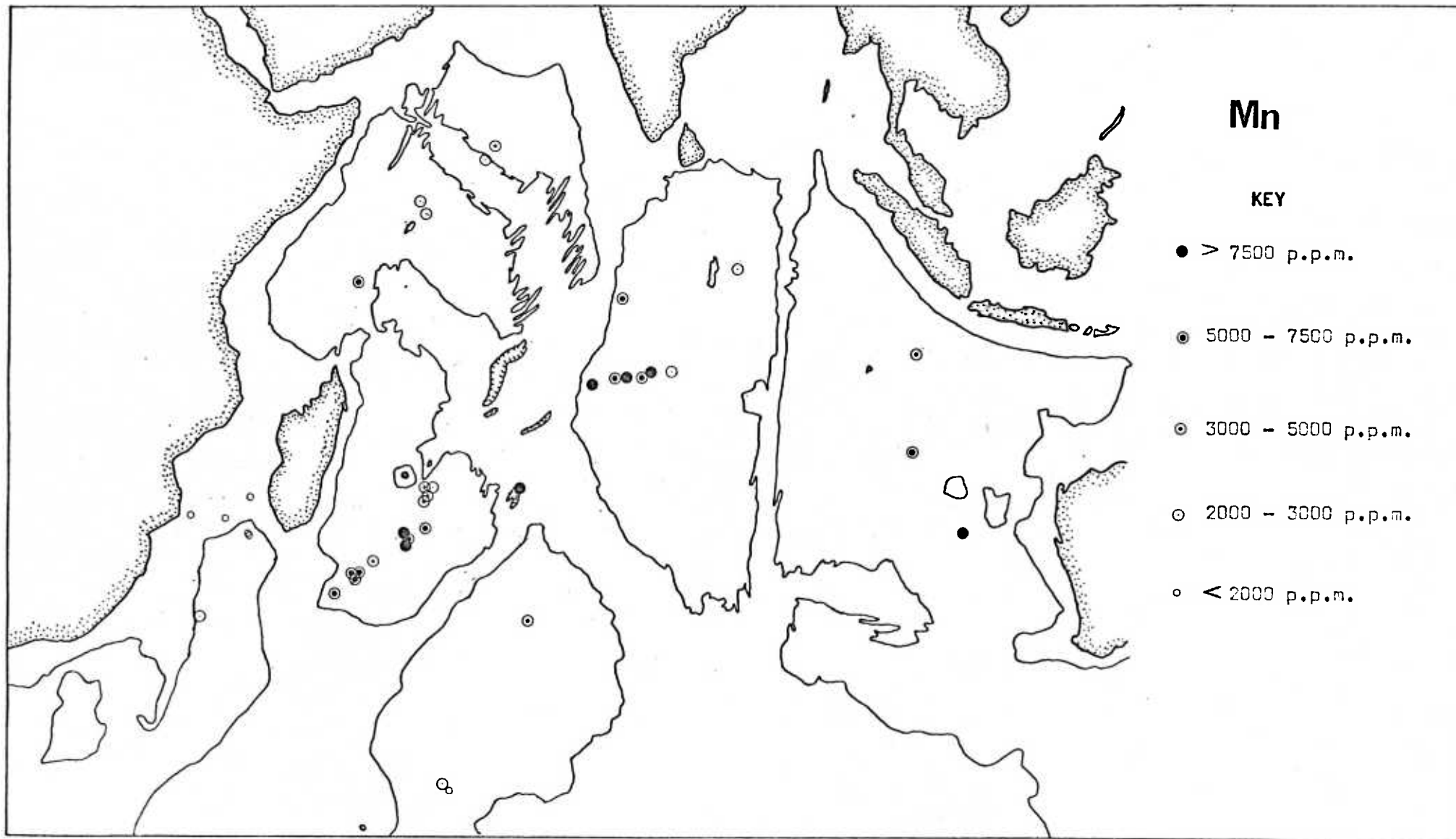


FIGURE 30 Regional variation of Mn in Indian Ocean sediments.

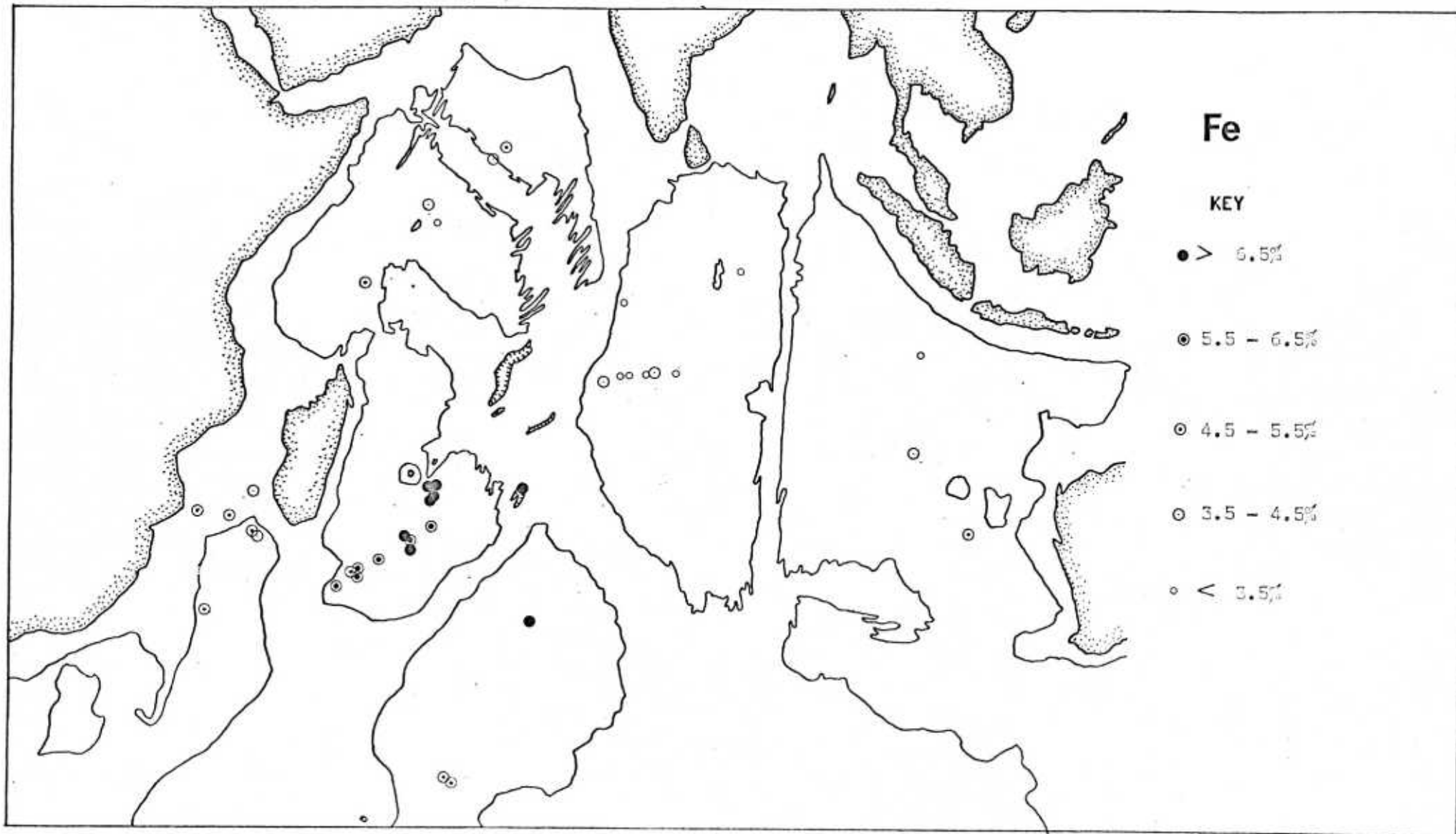


FIGURE 71 Regional variation of Fe in Indian Ocean sediments.

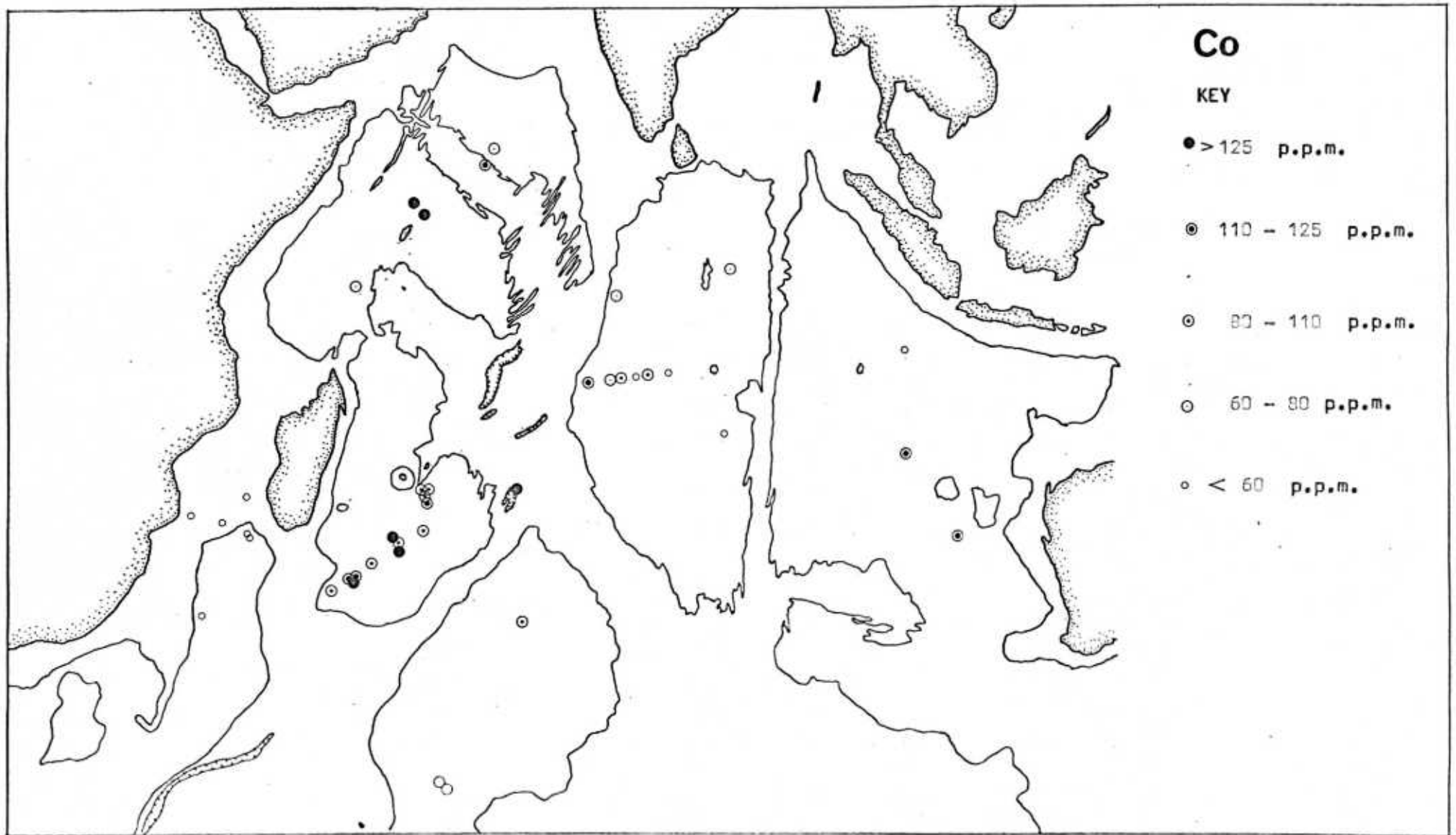


FIGURE 20 Regional variation of Co in Indian Ocean sediments.

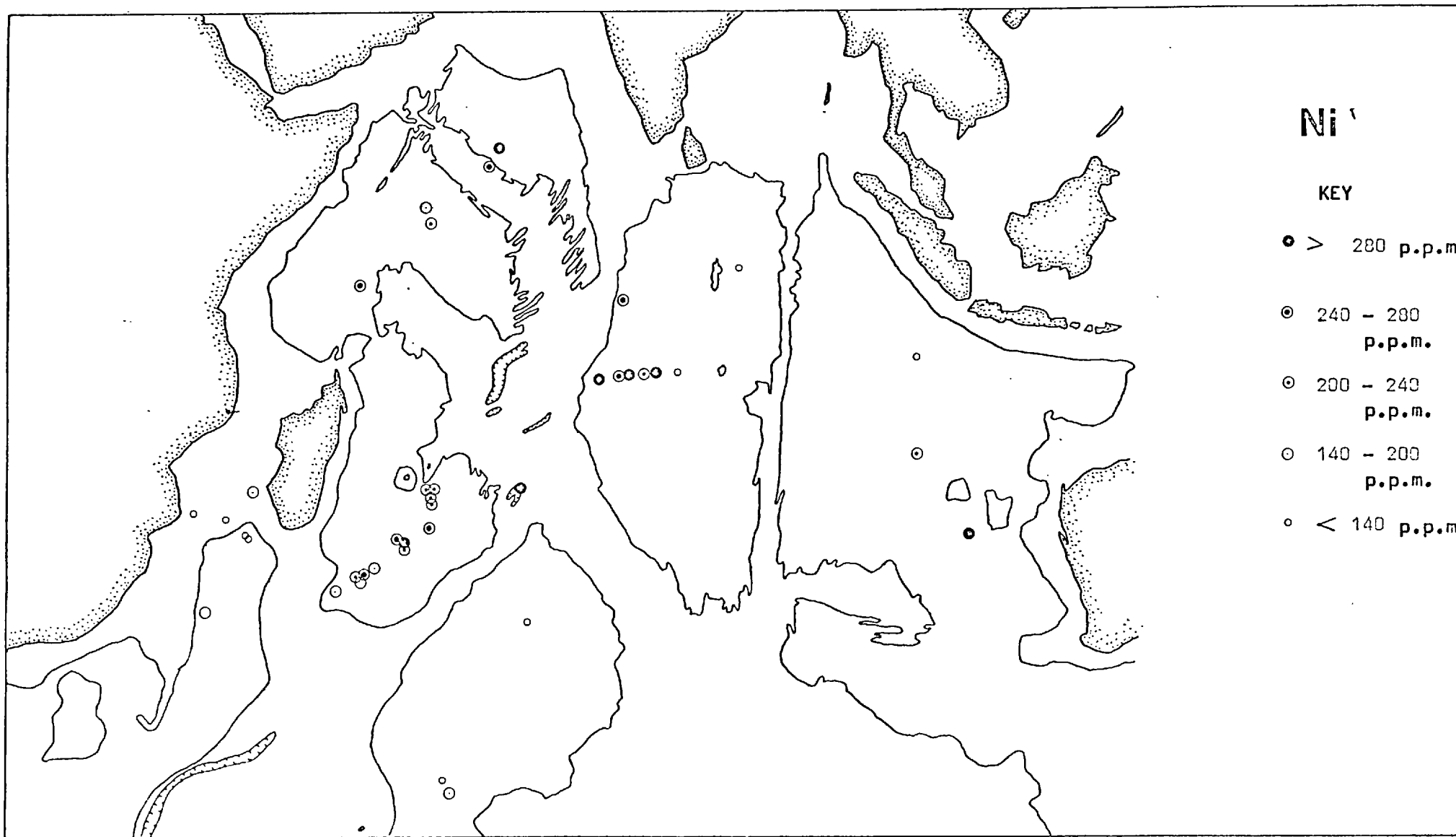


FIGURE 73 Regional variation of Ni in Indian Ocean sediments.



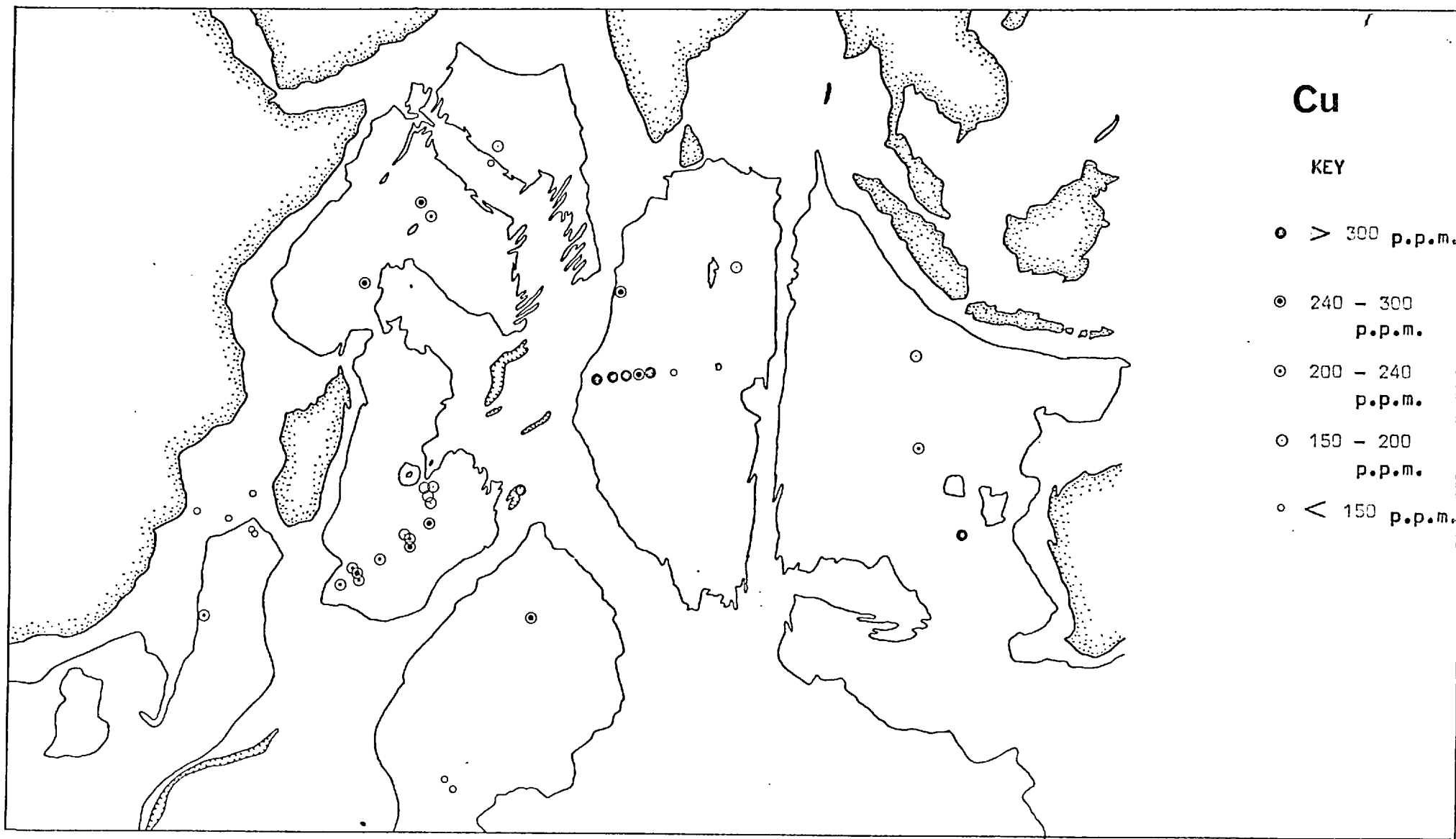


FIGURE 34. Regional variation of Cu in Indian Ocean sediment.

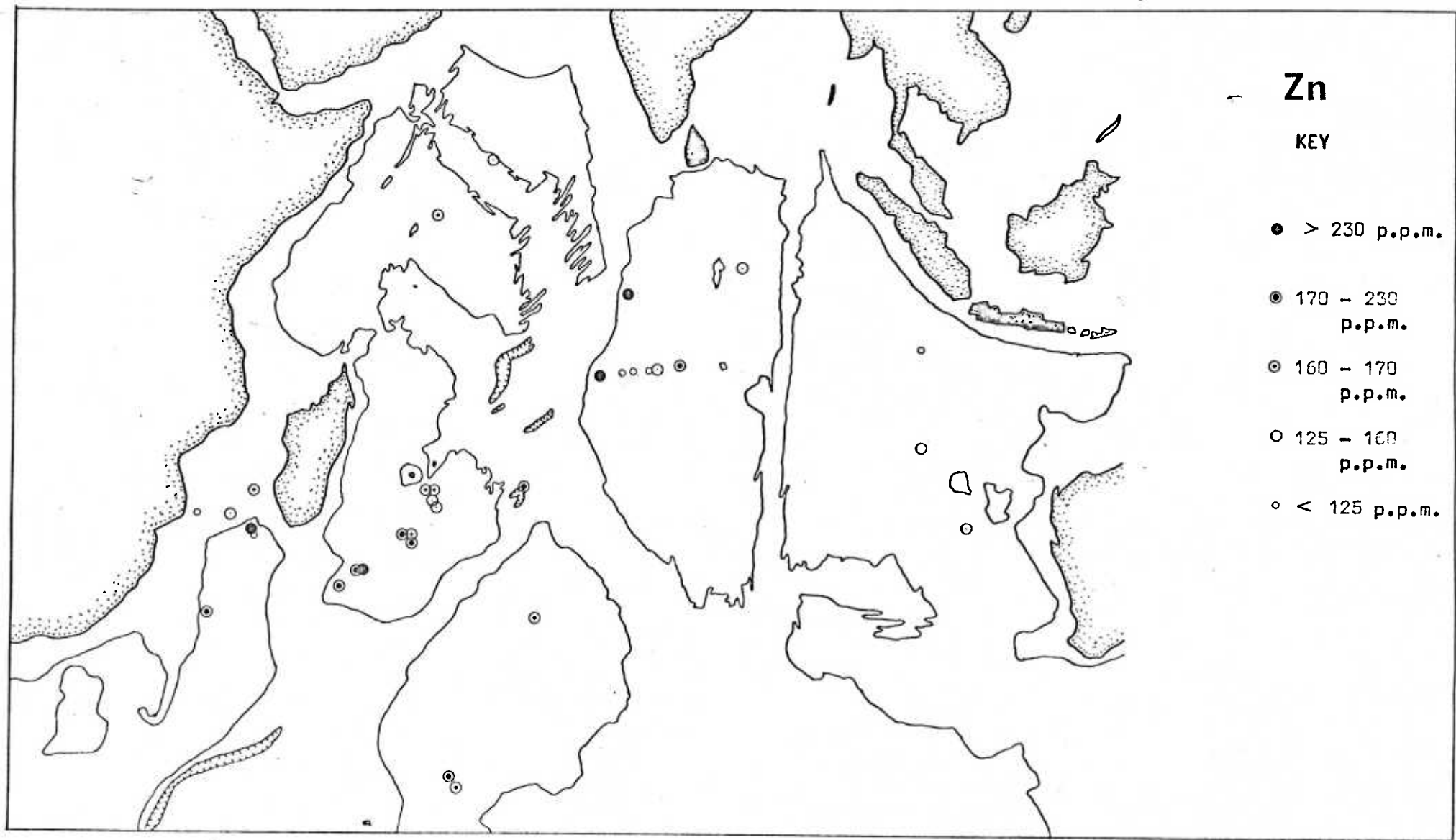


FIGURE 35 Regional variation of Zn in Indian Ocean sediments.

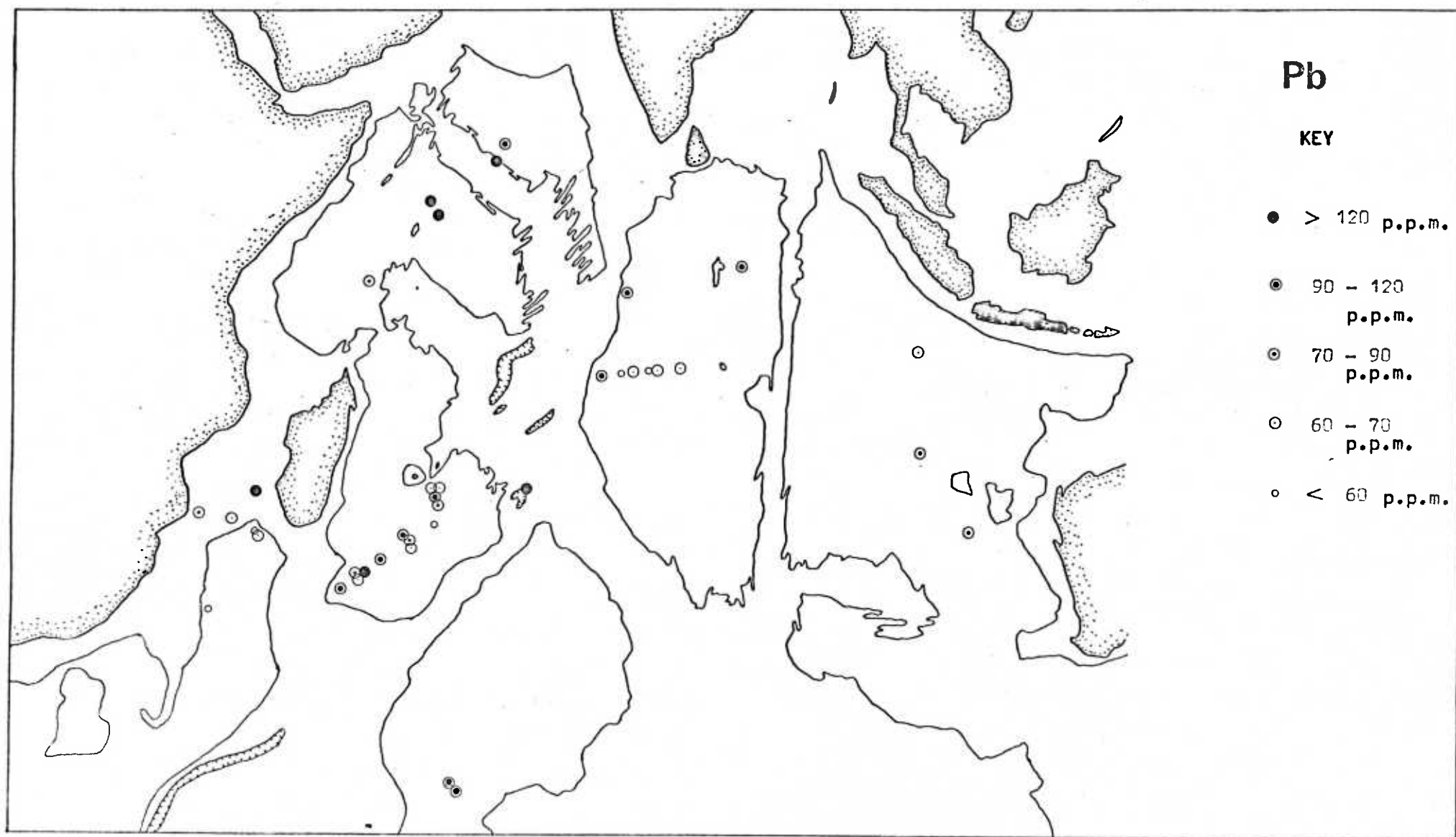


FIGURE 35 Regional variation of Pb in Indian Ocean sediments.

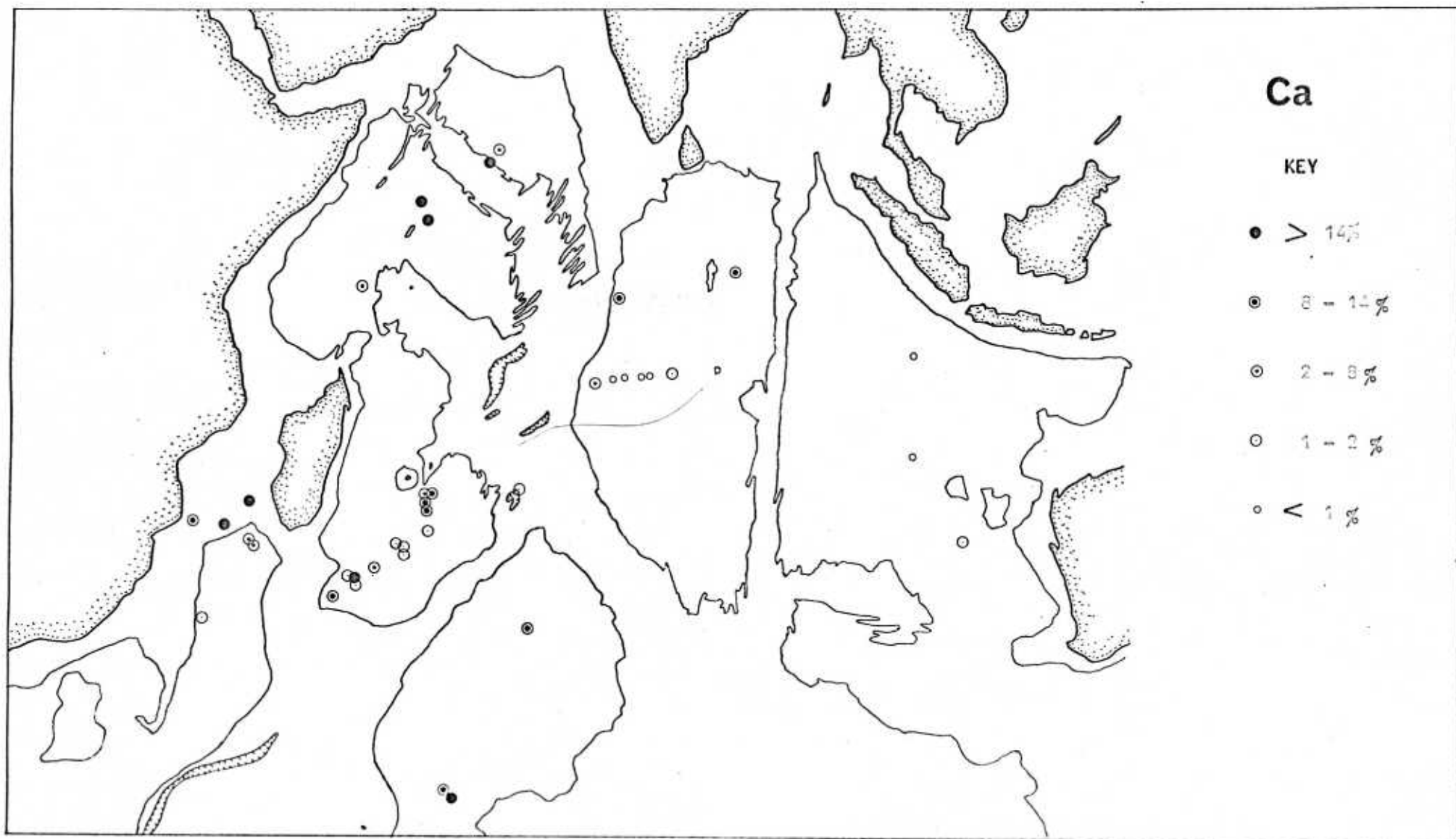
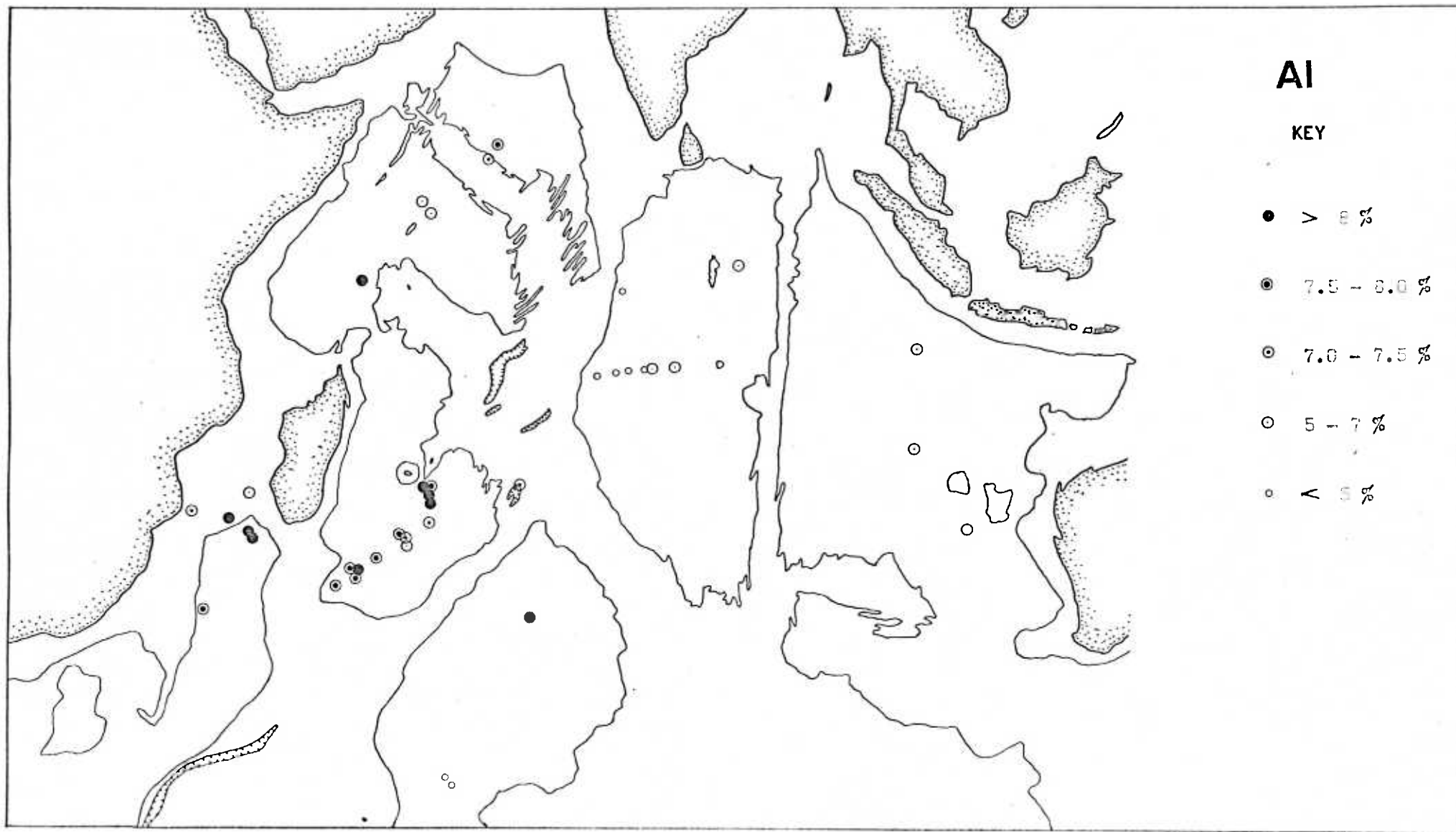


FIGURE 57. Regional variation of Ca in Indian Ocean sediments.



**FIGURE 35** Regional variation of Al in Indian Ocean sediments.

on average. Manganese and iron therefore tend to exhibit some similar trends in surface sediments to those observed in ferromanganese-oxides. In general, the behaviour of Fe observed in the present study agrees well with that observed by Bostrom and Fisher (1971) who found that Fe was highest in the southern and western regions of the Indian Ocean.

The variations in the trace metal content of sediments are much less marked than those observed in nodules. However significant differences do occur between western and eastern regions of the ocean. Nickel and Cu tend to be highest in the eastern Indian Ocean whilst Co, Zn and Pb are highest in the western Indian Ocean. With the exception of Zn, this pattern is very similar to that observed in nodules. Zinc correlates negatively with Co and Pb in nodules but positively with these elements in sediments. No simple geochemical evidence can be put forward to account for this difference in behaviour. The trays used to store some of the sediments analysed in this investigation are known to be potential sources of Zn contamination (Bender & Schultz, 1969). Although samples which were obviously contaminated in this way were not considered in this regional survey, it was not possible to pick out samples which may possess small amounts of contamination. The regional variation observed for Zn and the correlation coefficients of this element with other elements should therefore be disregarded.

Aluminium in sediments provides a good indication of their aluminosilicate (i.e. clay mineral) content. On this basis, western Indian Ocean sediments, on average, contain a greater abundance of clay minerals than those from the eastern Indian Ocean. The carbonate content of western Indian Ocean sediments is much higher, on average, than that of eastern Indian Ocean sediments. Analysis for silica was not carried out, but microscopic examination of the sediments revealed the presence of much greater amounts of siliceous biogenic debris in many eastern Indian Ocean sediments compared with those from the west. Thus the amount and type of

biogenic débris and detrital material supplied to western and eastern Indian Ocean sediments appears to be rather different and accounts for their variability in Ca, Al and Si.

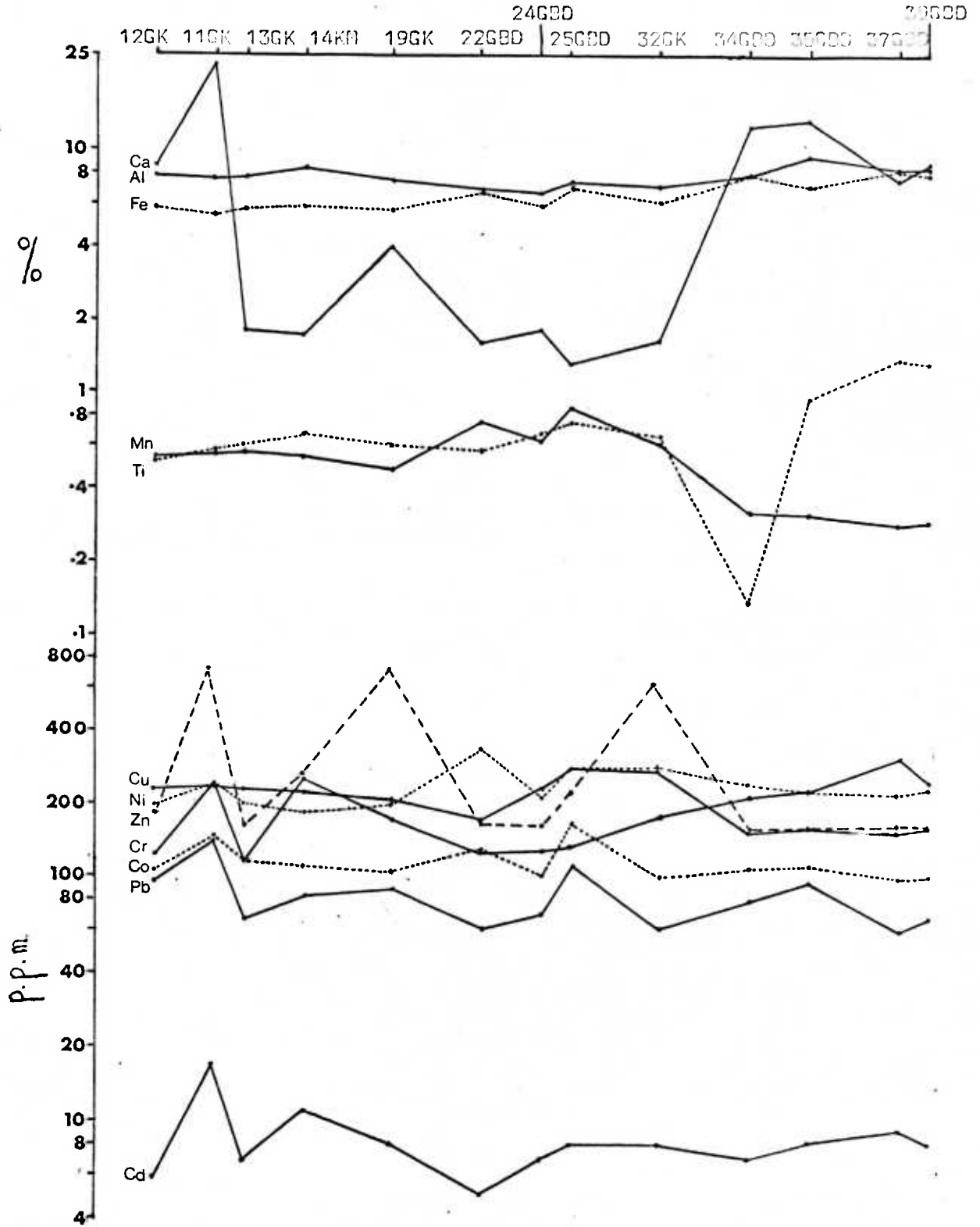
Five sediment samples were obtained from marginal areas of the western Indian Ocean, from the Mozambique Channel area, and these have an average composition which is significantly different from other western Indian Ocean sediments. These marginal sediments are particularly low in Mn and are also lower in Fe than western Indian Ocean sediments although Fe values in these marginal sediments are higher than in sediments from the eastern part of the ocean. Cobalt, nickel, copper and to a lesser extent Pb and Zn are also rather lower in the marginal sediments than in sediments from other parts of the western Indian Ocean. This pattern does not generally agree with that observed in nodules from this region. These marginal sediments are particularly high in carbonate, being mainly from depths well above the carbonate compensation depth, their Al content however is similar to that of other western Indian Ocean sediments.

In the Madagascar and Central Indian Basins more extensive sampling was undertaken along traverses and this enables the geochemical variations in sediment composition across these basins to be examined.

#### Regional compositional variation of Madagascar Basin sediments

The sampling traverse carried out in the Madagascar Basin is shown in figure 49. The variation in the bulk carbonate-free composition of the sediments along the traverse is given in figure 39. Iron shows a gradual but slight increase from the south-west to the northern end of the traverse. By contrast, Mn which is quite high across much of the basin drops off markedly in the north. Calcium is high in the sediments at each end of the traverse but is low in the carbonate-free sediments of the central area. Aluminium shows no marked trend across the basin but Ti, with the exception of sample

**FIGURE 39** Compositional variations in Madagascar Basin surface sediments.





34GBD gradually increases towards the northern end of the traverse. Of the trace metals, Cr shows a marked increase in sediments from the northern part of the basin although it is also fairly high in two sediment samples from the southern part of the traverse. The particularly high Ti and Cr values in sediments from the northern part of the basin provide evidence of appreciable supply of volcanogenic material to the sediments of this area, probably from the Mauritius-Réunion volcanic province to the north.

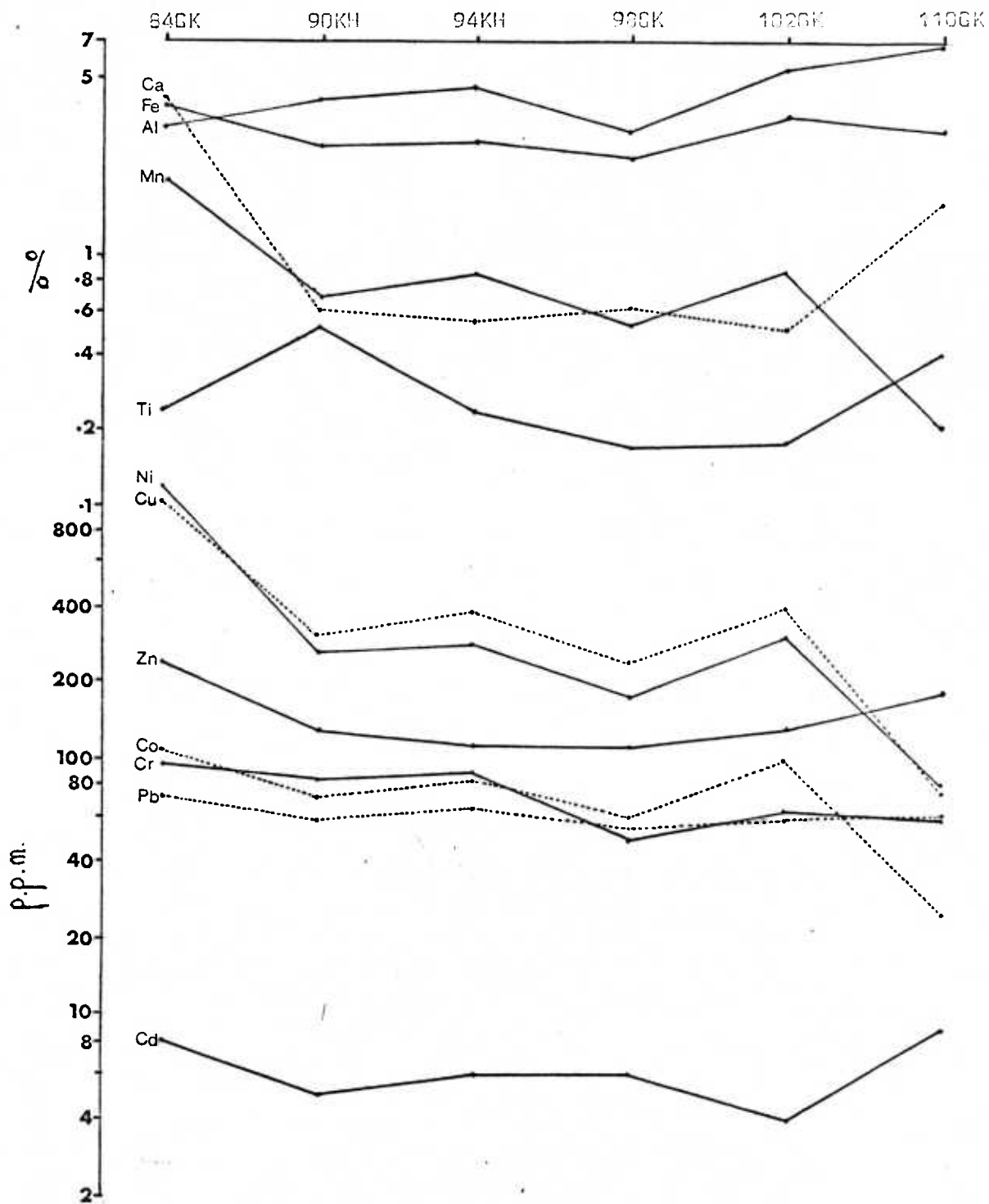
The trace metals Co, Ni, Cu and Pb tend to show little overall variation across the basin. Although Cu is generally slightly lower in the Mn-poor sediments of the northern part of the traverse Co, Ni and Pb show no noticeable fall in concentration. Any trends in the variation of Zn across the basin are obscured by the fact that at least 3 samples showed anomalously high Zn values. Cadmium values in the sediments are generally very low and bearing in mind the low analytical precision obtained at these levels no trends in Cd values across the basin were identified.

#### Regional compositional variations of Central Indian Basin sediments

Six surface sediment samples were collected from the Central Indian Basin along a traverse perpendicular to the Central Indian Ocean ridge system (see figure 50).

Of the major elements, Fe shows little systematic change across the basin although it is highest in the sample from the western end of the traverse (see figure 40). Manganese on the other hand shows a marked decrease from west to east along the traverse. Of the major elements, Al shows a definite increase towards the eastern end of the traverse whilst Ca is low in the central part of the traverse and higher at either end, particularly in the west. Ti and Pb show no definite trend. The trace

**FIGURE 40** Compositional variations in Central Indian Basin surface sediments.



metals Co, Ni and Cu show a fairly marked decrease towards the central part of the basin, which is the eastern end of the traverse. These metals thus exhibit a pattern which closely resembles that of Mn, in contrast to their behaviour in Madagascar Basin sediments. Cr, whilst showing a decrease from west to east does not fall off as markedly as do Co, Ni and Cu. Zinc shows an initial decrease in concentration eastwards but increases again at the eastern end of the traverse. Cadmium shows no distinct pattern of variation across the basin and as in the Madagascar Basin, values are so low as to be near the detection limit.

Little work has been published on the regional compositional variation of Indian Ocean sediments. Cronan (1967) analysed 12 sediment samples from the Indian Ocean but decided that this was an insufficient number to investigate regional variations in composition. Cronan (op. cit.) found no significant variations in Mn and Fe concentration between eastern and western Indian Ocean sediments but did find that Ni and Cu were higher in sediments from the east. Both Cronan (1967) and Bender & Schultz (1969) found that Mn was much lower in sediments from near the continents than from pelagic areas, this agrees well with the data presented here. Furthermore, Bender & Schultz (1969) found higher Mn, Co, Ni and Cu concentrations in eastern Indian Ocean sediments than those from the west. The findings of this study are in general agreement with those of Bender & Schultz although the behaviour of Fe and Co was found to be the reverse of that observed by these authors.

#### (iv) NODULE - SEDIMENT INTERRELATIONSHIPS

Since manganese nodules and their associated sediments are accumulating under similar environmental conditions, some correlation between their chemical compositions might be expected. However, Skornyyakova (1965), Cronan & Tooms (1969) and Price & Calvert (1970) found little

or no correlation between the Mn, Fe and trace metal content of Pacific Ocean manganese nodules and the values of these metals in the associated bulk sediment. Since a study of this type had not previously been undertaken in the Indian Ocean, it was decided to investigate the problem by plotting values of Mn, Fe, Co Ni and Cu in nodules against the concentration of these metals in the associated sediments. The resulting graphs are shown in figures 41 to 45. As can be seen from these graphs, there appears to be no real relationship between the values of Mn, Ni or Cu in bulk sediments and the corresponding value in the associated nodule. There does appear to be a faint correlation for Fe, and more especially for Co but in both cases several samples do not follow the trend at all. Cronan and Tooms (1969) also found some correlation between the Fe contents of nodules and sediments in the Pacific Ocean but they found no similar correlations for Co. The lack of correlation between Mn, Ni and Cu concentrations in nodules and associated sediments has also been noted by previous workers in the Pacific Ocean (Skornyakova, 1965; Cronan and Tooms, 1969; Price and Calvert, 1970). The lack of correlation between the Mn content of nodules and associated sediment is further shown by the large variation in the  $\frac{\text{Mn}_{\text{nodule}}}{\text{Mn}_{\text{sediment}}}$  ratio when this is expressed separately for each of the areas of the Indian Ocean from which samples were obtained (see Table 17). By contrast, the  $\frac{\text{Fe}_{\text{nodule}}}{\text{Fe}_{\text{sediment}}}$  ratio is very constant. This constant ratio is rather different to the behaviour of Fe in the Pacific Ocean where significant variations have been observed, although not as marked as those of Mn (Skornyakova, 1965; Price and Calvert, 1970). A contributing factor to the lack of variation in the  $\frac{\text{Fe}_{\text{nodule}}}{\text{Fe}_{\text{sediment}}}$  ratio in the Indian Ocean, however, may be that the samples investigated were from a more limited range of environments than samples investigated in the Pacific Ocean. The difference in the behaviour of Mn and Fe throughout the Indian Ocean can probably be explained in terms of the greater mobility of Mn compared to Fe in the marine environment (Krauskopf, 1957).

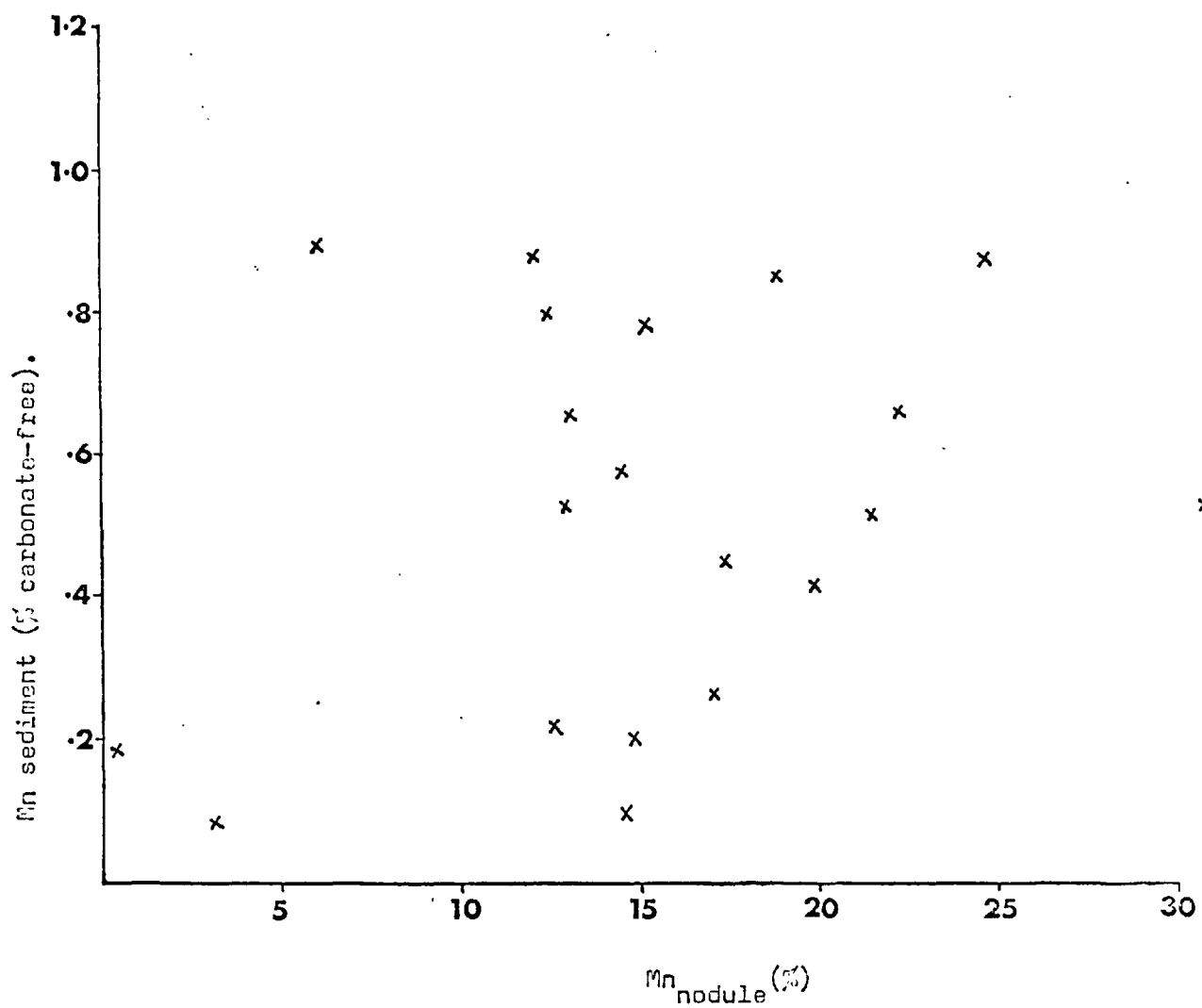


FIGURE 41 Variation of Mn values in nodules and associated bulk sediments.

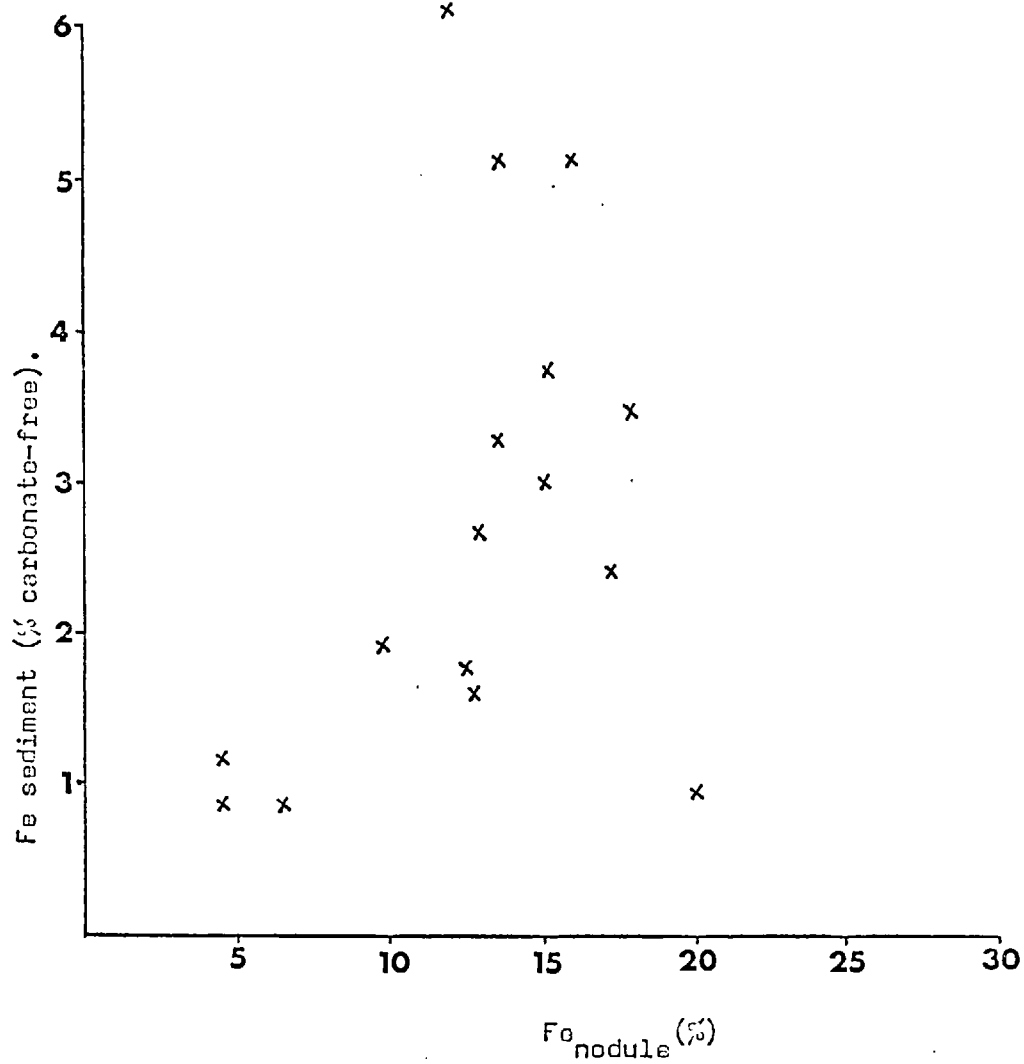


FIGURE 42 Variation of Fe values in nodules and associated bulk sediments.

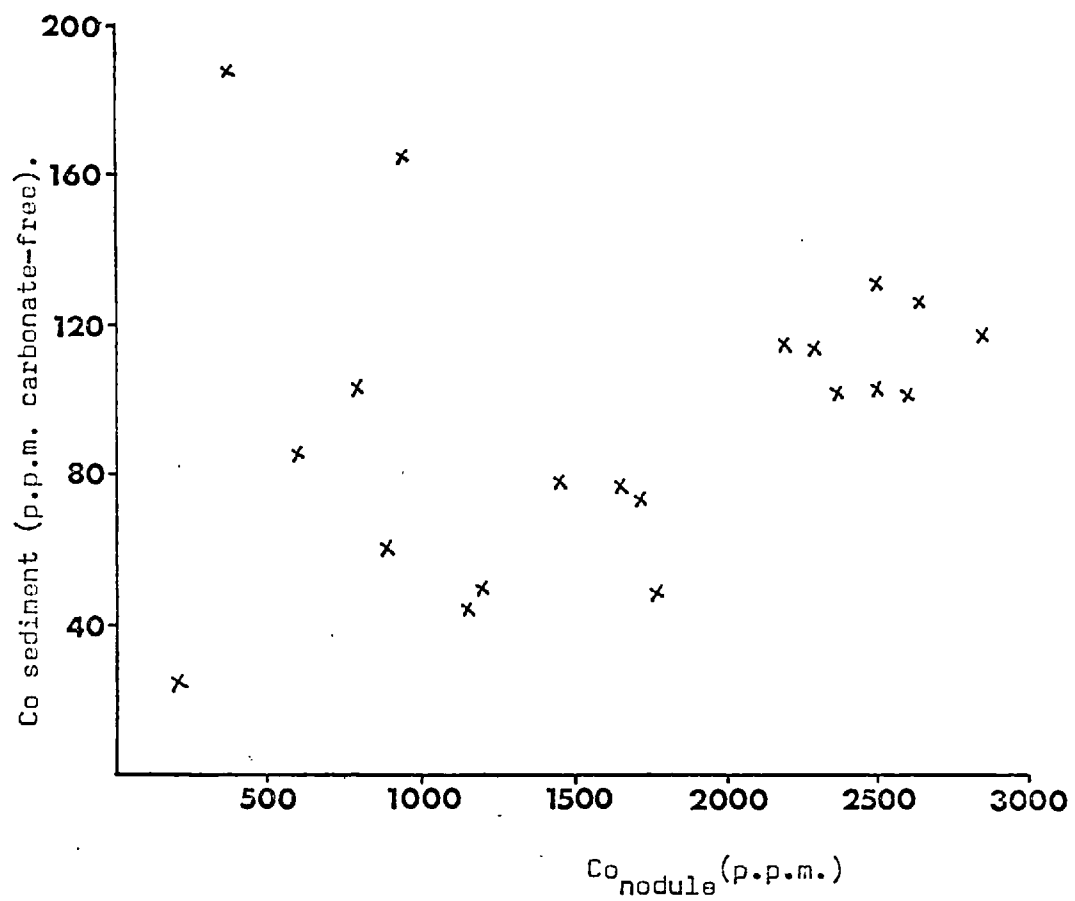


FIGURE 43 Variation of Co values in nodules and associated bulk sediments.

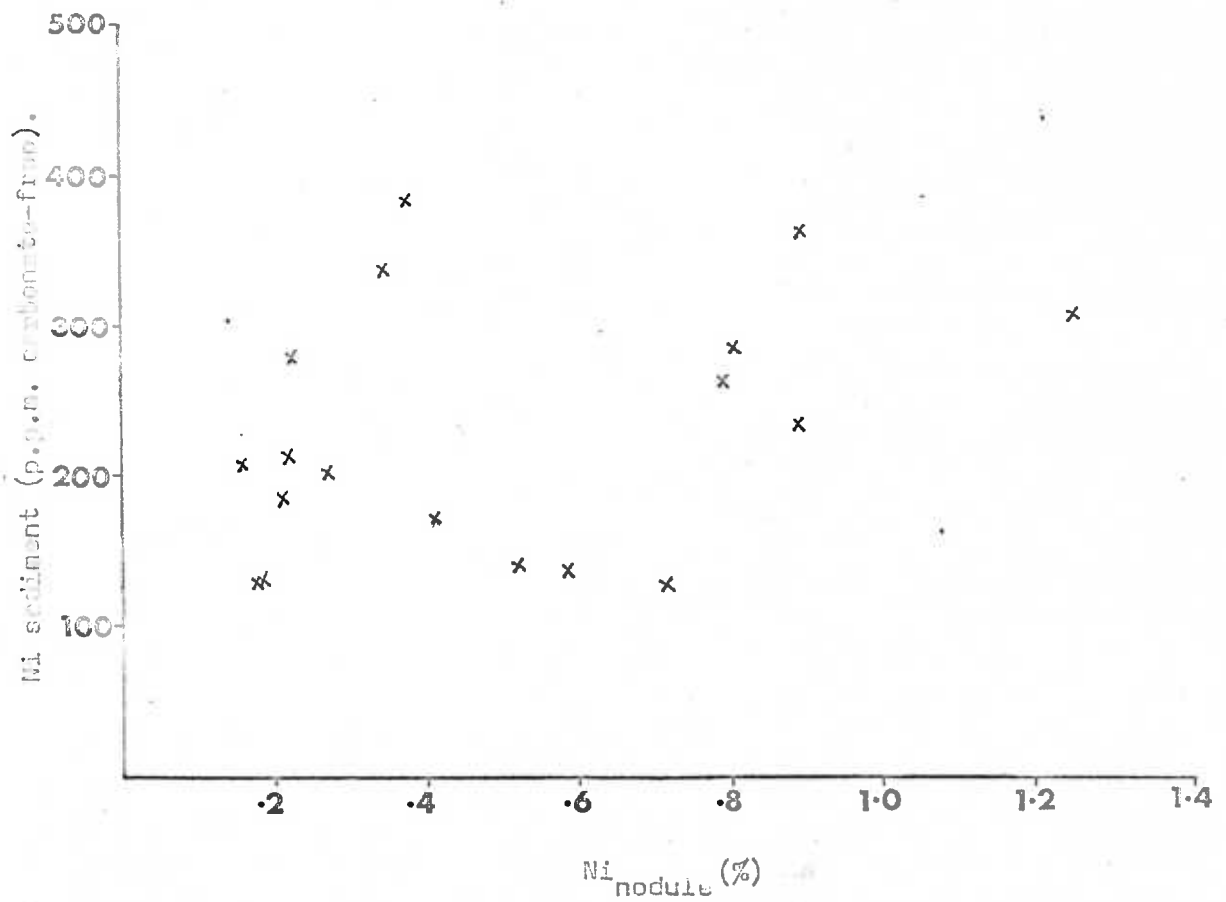


FIGURE 44 Variation of Ni values in nodules and associated bulk sediments.



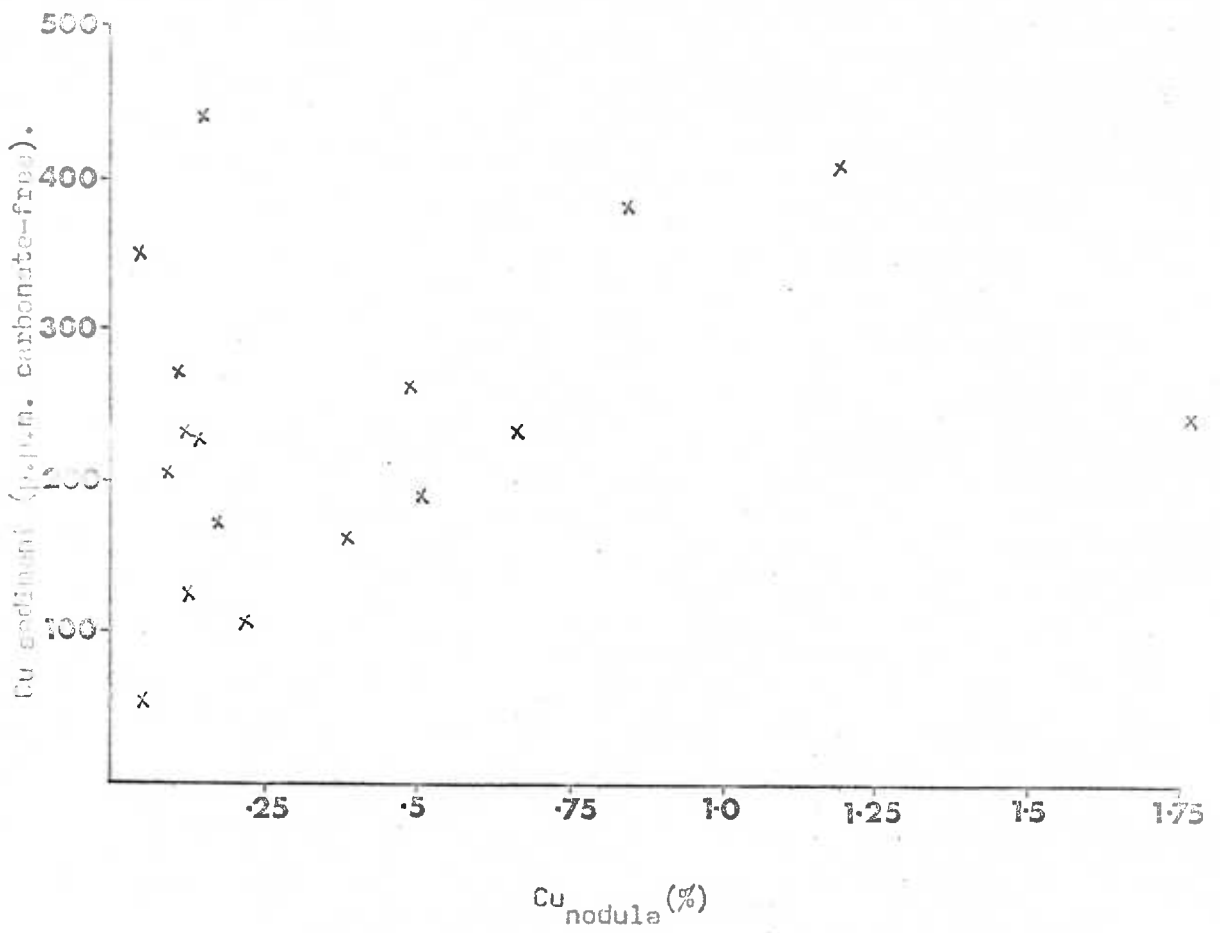


FIGURE 45. Variation of Cu values in nodules and associated bulk sediments.

REGION	<u>Mn nodule</u>	<u>Fe nodule</u>	Average sediment thickness (m.)	Average Mn content of sediment (p.p.m.)	Average Mn content of nodules (%)
	Mn sediment	Fe sediment			
CENTRAL INDIAN BASIN	24	2.9	100	8080	22.1
MADAGASCAR BASIN	24	2.4	150	5360	12.6
WHARTON BASIN	28	3.0	200	6530	15.1
CROZET BASIN	57	2.2	300	2350	12.8
MOCAMBIQUE BASIN	72	2.9	750	1610	11.6
MOCAMBIQUE CHANNEL	122	5.2	1,500	1050	16.5

TABLE 17

Comparison of metal ratios in nodules and sediments and average sediment thicknesses in different physiographic regions of the Indian Ocean.

From Table 17, it can be seen that there is a close correlation between the average thickness of underlying unconsolidated sediment in an area and the average  $Mn_{\text{nodule}}/Mn_{\text{sediment}}$  ratio of that area. However, it can also be seen that sediment thickness correlates negatively with the Mn content of sediments and that areas of thick sedimentary accumulations are not characterised by particularly Mn-rich nodules. It is therefore simply the low Mn content of sediments in areas of rapidly accumulating sediments which causes high  $Mn_{\text{nodule}}/Mn_{\text{sediment}}$  ratios. If much of the Mn in sediments is assumed to be present as authigenically precipitated Mn oxide material and to precipitate out onto the sea-floor at a fairly uniform rate, then an increase in the total sedimentation rate would simply have the effect of diluting this Mn oxide phase and lowering the total Mn content of the sediment. This is in fact found to be the case. Thus the correlation of  $Mn_{\text{nodule}}/Mn_{\text{sediment}}$  ratios with sediment thickness and therefore, indirectly, with sedimentation rates, can be explained without recourse to diagenetic remobilisation of Mn which was suggested by Price and Calvert (1970) as an explanation for Mn enrichment in Pacific Ocean nodules.

Figures 41 to 45 show the co-variance of the elements Mn, Fe, Co, Ni and Cu in nodules and associated sediments. The observation that there is no co-variance at all for Mn, Ni and Cu might be expected in view of the differences in the phases present in the two sample types. Nodules consist essentially of an authigenic-oxide phase containing the majority of the Mn, Fe and most trace metals, and a diluting, predominantly aluminosilicate phase. By contrast, sediments can contain a wide variety of phases of which an authigenic oxide phase is just one. As in nodules, the authigenic oxide phase of sediments is likely to be enriched in Mn, Fe and trace metals but since this phase may be diluted by greatly varying amounts of different phases, the overall bulk composition of the sediments, even expressed on a carbonate-free basis, may not bear much relationship to the bulk composition of associated nodules. Thus total Mn, Fe and trace metal values in sediments

and nodules need show little co-variance even if the compositions of the relative authigenic phases are related to some extent.

In view of the above conclusions the problem then arises of why Fe, and more particularly Co, do show some degree of co-variance. The anomalous behaviour of these elements may arise from the fact that in only a small number of cases were nodule and sediment samples recovered at the same site, therefore the data presented in figures 42 and 43 may represent a biased small sub-population of the total nodule and sediment data. A satisfactory explanation of the behaviour of Co and Fe however cannot be produced on the basis of the limited data available in this investigation and must await further work.

In view of the variation in the relative proportions of different phases present in sediments, a more profitable approach to the problem of nodule-sediment interrelationships might be to consider the composition of a particular fraction of sediments and compare this with the composition of the corresponding fraction in associated nodules. Calvert and Price (1976) examined the composition of the oxide fraction of nodules and the associated sediment in Pacific Ocean samples. However, they established the composition of the oxide fraction of nodules not by direct chemical means but by subtracting from the bulk composition an estimated contribution of each element from the diluting aluminosilicate phase. The composition of the aluminosilicate phase was assumed to be similar to that of the corresponding phase in the associated sediment. Furthermore, these authors plot their data in such a way that a direct comparison cannot be made between the behaviour of an element in the nodule samples and the behaviour of the same element in the associated sediments. Their data as presented, therefore, cannot be compared directly with that obtained in this study and is of limited use in examining any relationships which may exist between nodule and sediment compositions.

A more promising study was conducted by Friedrich (1976). This involved

the physical separation of the Mn-oxide phase of sediments (occurring as micronodules) and a comparison of the chemical composition of this phase with the bulk chemical composition of associated nodules. Interestingly, Friedrich found that in areas where the micronodules were high in Cu and Ni, the Cu and Ni content of associated macronodules was also particularly high. Friedrich's study whilst perhaps providing the best attempt to date to solve the problem of nodule-sediment interrelationships, was a physical method of separating out the authigenic oxide phase of sediments which may not remove all of the ferromanganese-oxide fraction and thus might not present a representative sample. An alternative method of investigating compositional relationships between nodules and sediments would seem to be a detailed examination and comparison of the chemical composition of the various phases present in the two types of sample using purely chemical techniques. Such a study is discussed in the following section.

## SECTION 7

### PARTITION GEOCHEMISTRY

#### (i) INTRODUCTION

Twenty-seven nodule samples and 19 sediment samples from 2 traverses, one in the Madagascar Basin and one in the Central Indian Basin, were analysed by an adaptation of the selective leach techniques developed by Chester and Hughes (1967). In each case the leached fraction was analysed by atomic absorption spectrophotometry for Mn, Fe, Co, Ni, Cu, Zn, Pb, Ca, Al, Cd, Cr and Ti. Details of the procedures employed are given in Appendix 1. Thus, in addition to the bulk chemical composition of the samples, the composition of that fraction of the samples which was soluble in acetic acid, hydroxylamine-hydrochloride and acetic acid, and hydrochloric acid were also obtained. The aim of this procedure was to investigate the partition of the elements examined between the various phases removed by each attack in both nodules and sediments. The phases present in ferromanganese nodules and marine sediments are listed in Table 18. These are likely to be selectively leached from the samples by the chemical attacks employed as follows (Chester & Hughes, 1967, 1969):-

TABLE 18 Material present in pelagic nodules & sediments  
(Adapted from Chester & Hughes, 1967)

1.- Adsorbed components
<ul style="list-style-type: none"> <li>(a) Major elements e.g. Na, Ca, K.</li> <li>(b) Minor elements e.g. Mn, Ni, Cu.</li> <li>(c) Organic material, as organic molecules.</li> </ul>
2.- Organic components (biogenous origin)
<ul style="list-style-type: none"> <li>(a) Carbonates e.g. calcite, aragonite.</li> <li>(b) Phosphates e.g. skeletal apatite.</li> <li>(c) Silicates e.g. opal.</li> <li>(d) Sulphates e.g. celestite.</li> <li>(e) Organic matter e.g. organic molecules.</li> </ul>
3.- Inorganic components
<ul style="list-style-type: none"> <li>(i) Authigenic material           <ul style="list-style-type: none"> <li>(a) Carbonates e.g. calcite, dolomite (uncommon).</li> <li>(b) Phosphates e.g. francolite, phosphorite rock.</li> <li>(c) Silicates &amp; Aluminosilicates e.g. quartz, glauconite, feldspar, zeolites (phillipsite), clay minerals (montmorillonite).</li> <li>(d) Sulphates e.g. barite, celestite, gypsum.</li> <li>(e) Oxides &amp; Oxyhydroxides e.g. todorokite, goethite, mixed iron manganese oxides, amorphous oxides &amp; Hydroxides of Mn &amp; Fe.</li> </ul> </li> <li>(ii) Detrital material           <ul style="list-style-type: none"> <li>(a) Oxides e.g. rutile.</li> <li>(b) Silicates &amp; Aluminosilicates e.g. quartz, clay minerals (illite, kaolinite, montmorillonite), feldspars.</li> </ul> </li> </ul>

### 1. Acetic acid attack-

This attack, employing 25% acetic acid should remove the carbonate minerals (except dolomite), loosely sorbed cations and interstitial seawater evaporates.

### 2. Acid and reducing agent attack-

This attack, using a mixed reagent consisting of 25% acetic acid and 1M hydroxylamine hydrochloride, should remove everything soluble in the acetic acid attack plus the manganese and mixed ferromanganese-oxides and hydroxides which are reducible by hydroxylamine hydrochloride. According to Chester & Hughes (1967) this attack also releases a substantial proportion of the iron oxide phases.

### 3. Hydrochloric acid attack-

This attack, employing 6M hydrochloric acid should remove everything soluble in the previous attacks plus any non-reducible manganese oxyhydroxides, mixed iron-manganese oxyhydroxides, and separate iron oxyhydroxides which are insoluble in the mixed acid and reducing agent attack. This attack will also remove all but the more resistant silicates and aluminosilicates (Cronan, 1976).

In order to minimise analytical error these attacks were performed in turn on separate subsamples of each sample and the leached portion analysed. The amount of each element soluble only in one particular attack was then obtained by subtracting the value for each element released by that attack from the corresponding value obtained in the



previous attack. For example, the amount of Mn soluble in hydrochloric acid but NOT in mixed acid reducing agent or acetic acid equals the concentration of Mn present in the hydrochloric acid leach minus the concentration of Mn present in the mixed acid and reducing agent leach. The amount of metals present in the resistant, HCL-insoluble fraction was obtained by subtracting the concentrations of elements in the hydrochloric acid leach from the bulk composition of the samples. Thus, 4 distinct fractions were recognised in nodules and sediments as follows:-

1. Acetic acid soluble fraction.
2. Acid reducible fraction.
3. HCL - soluble fraction.
4. Acid - insoluble fraction.

In order to discuss the variations observed in the data thus obtained, data on samples from both traverses was considered together, and then a comparison was subsequently carried out of the trends observed in each basin. Finally, the variations of individual elements in nodules and sediments along each traverse is discussed and an attempt made to account for the variations and interrelationships.

#### (ii) ELEMENT PARTITION

In order to investigate the average partition of the elements between the various fractions, the proportion of each element removed by each separate attack was calculated as a percentage of the total amount of that element in the sample. Considering nodule and sediment data separately, the average of these percentages for each element for each separate attack was then calculated, and the standard deviation about the

mean value obtained, using the formula;-

$$\sigma = \sqrt{\frac{\sum_1^n (x_i - \bar{x})^2}{n - 1}}$$

$$\text{where } \bar{x} = \text{mean value} = \frac{\sum_1^n x_i}{n}$$

$\sigma$  = standard deviation

$n$  = number of samples

The results are summarised in figures 46 (a) to (d).

#### (a) AVERAGE PARTITION IN NODULES

From figure 46 it can be seen that essentially all of the Mn in nodules is released in the acid-reducible fraction. Some two-thirds of the total Fe is also removed by this attack, most of the rest of the iron is contained in the HCL-soluble fraction, with less than 10% of the total Fe contained in the acid-insoluble fraction and only trace amounts in the acetic-acid soluble fraction.

Cobalt, Ni, Cu, Zn, Pb, and Cd were all released predominantly in the acid-reducible fraction, however small differences in the partition are noticeable. Of these six elements, Co, Pb and Cd do not appear to be released to any significant amount by acetic acid. The detection limits for Pb and Cd, under the method of determination employed, are comparatively high. The values obtained for these elements therefore tend to be less reliable than those obtained for the other trace elements.

Virtually all the Co present in the samples was released in the acid-reducible fraction and about 90% of the total Pb was released by this attack also. The remaining Pb appears to be partitioned roughly equally

FIGURE 46 (a) & (b) Mean partition values in Indian Ocean nodules and sediments.

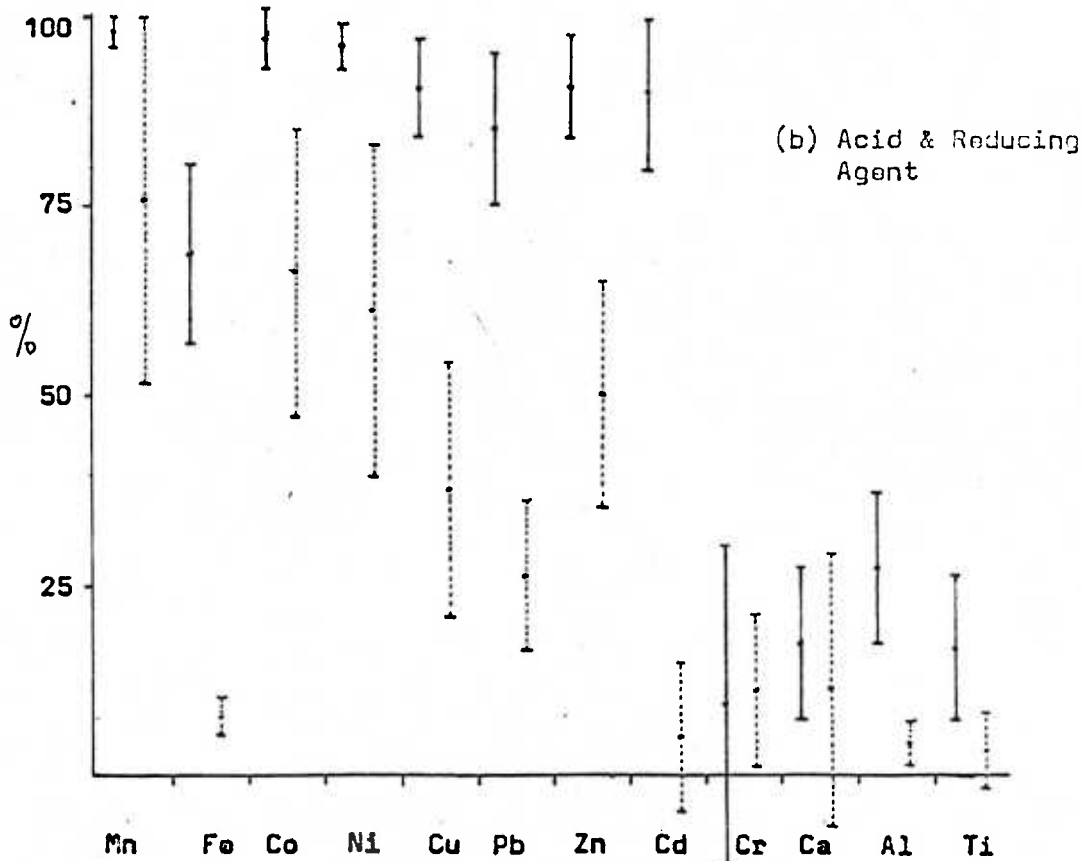
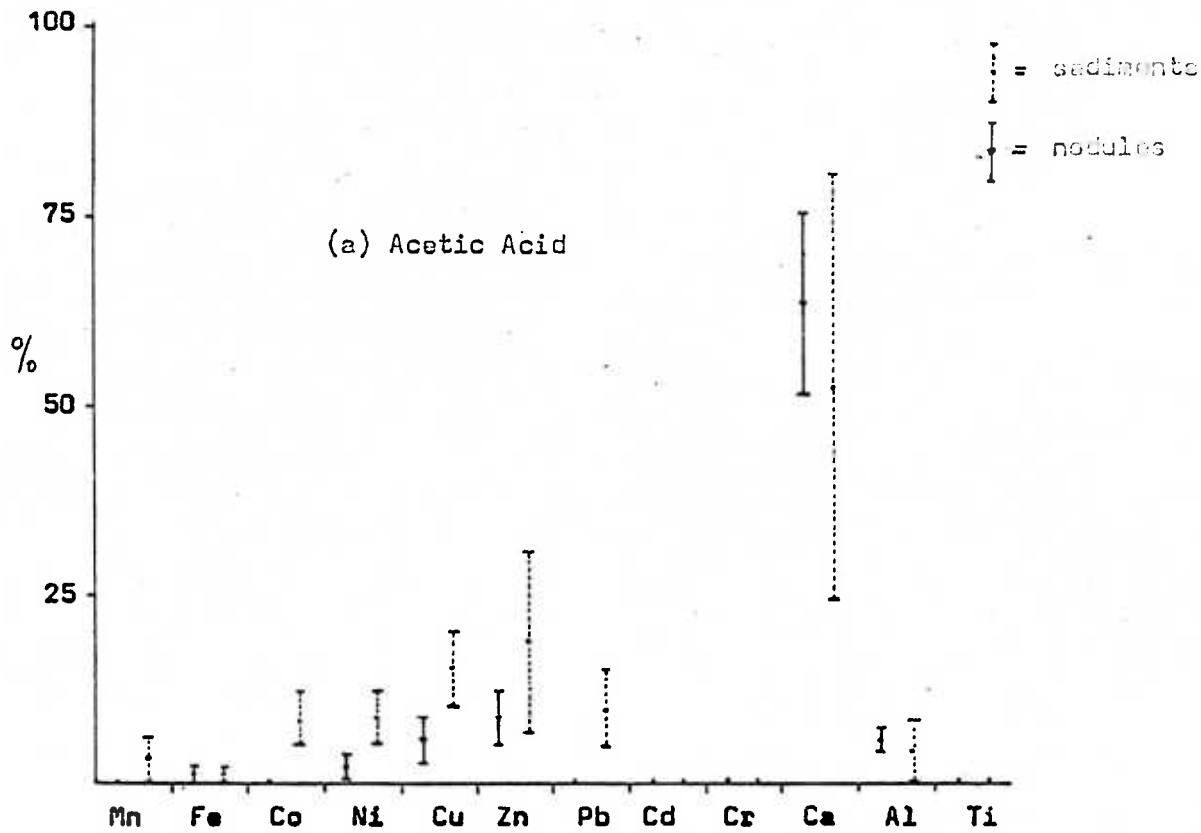
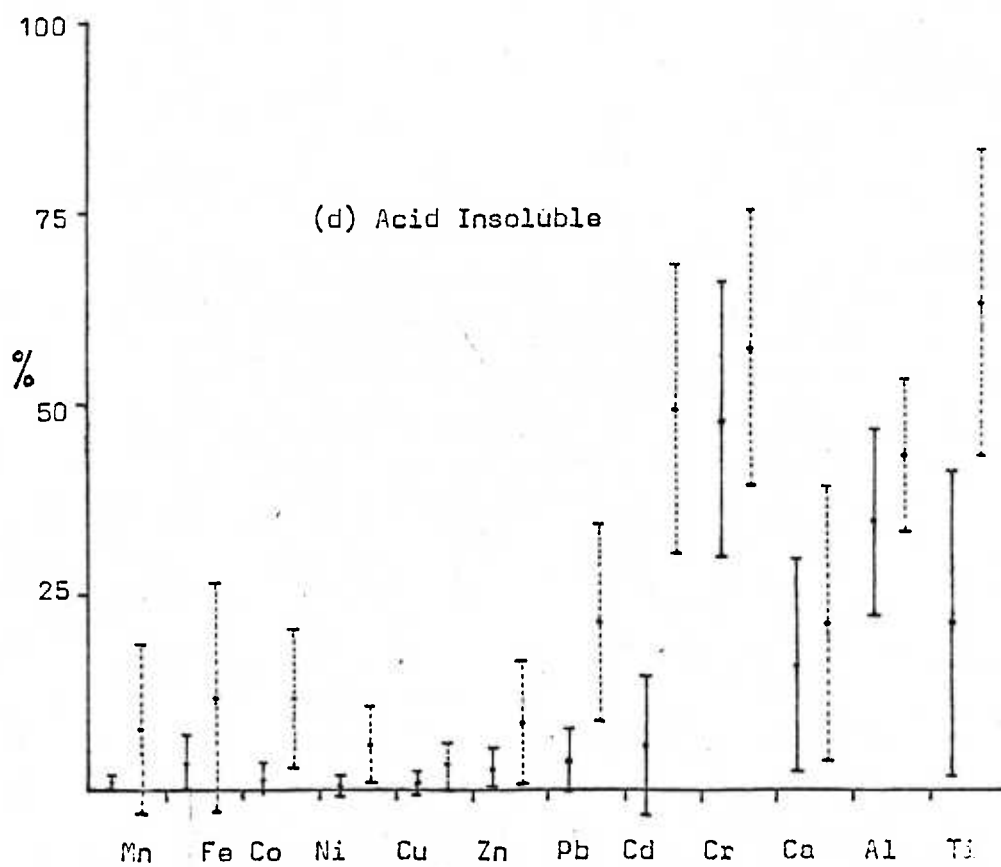
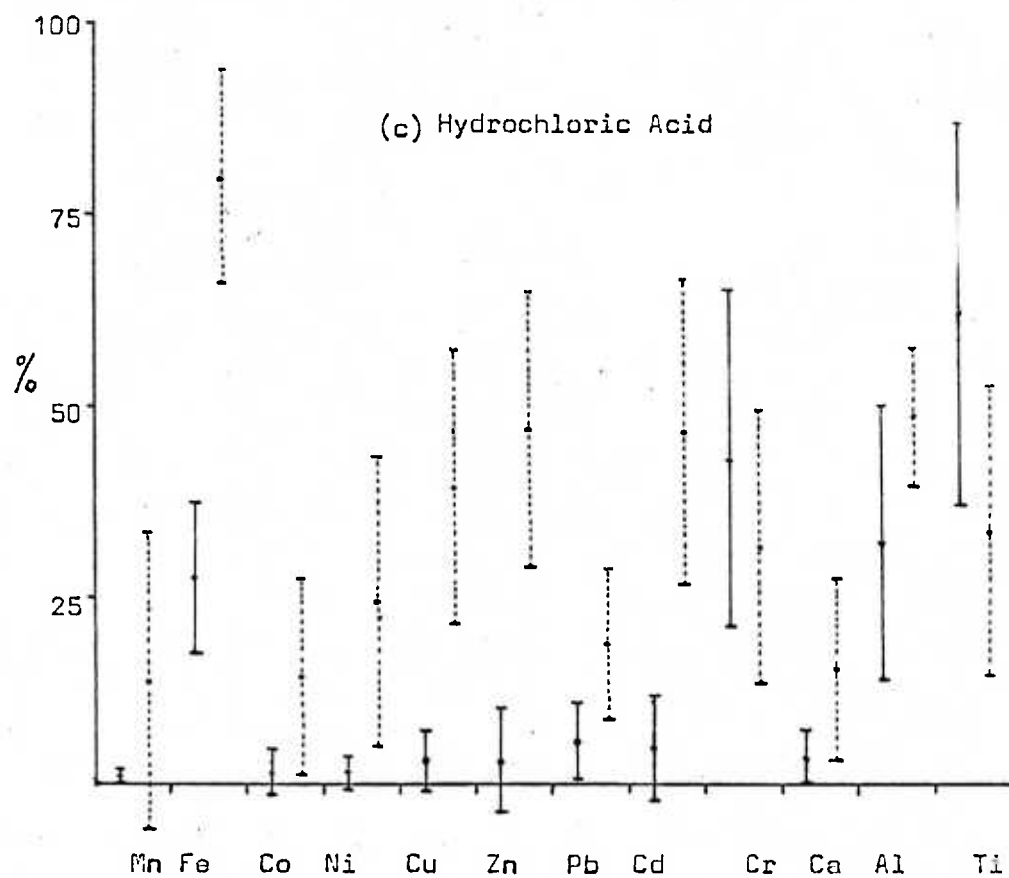


FIGURE 46 (c) & (d) Mean partition values in Indian Ocean nodules and sediments.



between the HCL-soluble and acid-insoluble fractions. Like Pb, about 90% of the total Cd is acid-reducible, however, the low Cd content of most samples combined with the poor precision obtained for this element, precludes an accurate assessment of its partitioning between the other fractions.

Nickel, Cu and Zn are all released in small amounts in the acetic acid-soluble fraction. Some 2% of the total Ni, 5% of the total Cu and 8% of the total Zn occur in the fraction. Differences occur in the amounts of these elements present in the acid-reducible fraction. Over 95% of the total Ni is present in this fraction compared with 90% of the total Cu and 85% of the total Zn. Amounts of all three elements in the acid-resistant fraction were negligible but small amounts of Cu and Zn were contained in the HCL-soluble fraction.

About 10% of the total Cr is present in the acid-reducible fraction but most of the Cr occurs in the HCL-soluble and acid-insoluble fractions roughly equally partitioned between the two. In contrast to Cr, rather more Ti occurs in the acid-reducible fraction and of the remainder, almost three times as much is contained in the HCL-soluble fraction as in the acid-insoluble fraction. None of the Cr or Ti appears to be contained in phases which are soluble in acetic acid.

Almost two-thirds of the total Ca in the nodules was released by the acetic acid attack. The remaining Ca is partitioned almost equally between the acid-reducible and acid-insoluble fractions, with less than 5% of the total Ca being HCL-soluble. The partition of Ca in nodules is therefore markedly different from that of the other metals analysed.

Aluminium too, shows a unique partition pattern. Aluminium is partitioned mainly between the acid-reducible, HCL-soluble and acid-resistant fractions, gradually increasing in amount from the former to the latter. Only trace amounts of Al are soluble in acetic acid.

## (b) AVERAGE PARTITIONS IN SEDIMENTS

The partition of the elements analysed in sediments shows important differences to the trends seen in nodules (see figure 46).

Only 75% of the total Mn occurs in the acid-reducible fraction of sediments, whilst on average rather more than 10% is present in the HCL-soluble fraction and slightly under 10% in the acid-insoluble fraction. A small amount is also released by acetic acid. Most of the Fe in sediments, about 80%, is present in a non-reducible form soluble in HCL, whilst just over 10% is present in the acid-resistant fraction. Less than 10% of the total Fe in sediments is in an acid-reducible form.

The partitioning of the trace elements Co, Ni, Zn, Pb and Cd in sediments is also different from that observed in nodules. Appreciable amounts of all these elements, except Cd, are removed by acetic acid. This acetic acid-soluble portion forms about 10% of the total Co, Ni and Pb but about 20% of the total for Cu and Zn. Over 60% of the total Co and Ni are present in the acid-reducible fraction and about 50% of the total Pb. However, under 40% of the total Cu and only 25% of the total Zn are soluble in this fraction. Very different amounts of Co, Ni, Cu, Zn and Pb are found in the HCL-soluble fraction. Hydrochloric acid-soluble Co and Pb form about 15% of the total of these elements, whilst 25% of the total Ni occurs in this fraction. However, some 40% of the total Cu and 45% of the total Zn are present in this fraction. Only trace amounts of the total Ni and Cu occur in the acid-insoluble fraction, whilst some 10% of the total Zn and Co, and over 20% of the total Pb do so.

The partitioning of Cd in sediments is markedly different to its behaviour in nodules, where it behaves similarly to Co, Ni, Cu, Zn and Pb. In sediments however, Cd shows much closer affinities with Cr and Ti.

No detectable Cd is present in the acetic acid-soluble or acid-reducible fractions, the element being present instead in the HCL-soluble and acid-insoluble fractions, roughly equally partitioned between the two.

Chromium and Ti are both partitioned mainly in the acid-insoluble fraction with the remaining 30 to 40% predominantly in the HCL-soluble fraction, although a small amount of the total Cr occurs in the acid-reducible fraction.

About half the total Ca in sediments is removed by the acetic acid attack whilst almost a quarter occurs in the acid-insoluble fraction. The remaining Ca is roughly equally partitioned between the acid-reducible and HCL-soluble fractions.

Aluminium in sediments is partitioned roughly equally between the HCL-soluble and acid-insoluble fractions, with only trace amounts present in the acetic acid-soluble and acid-reducible fractions.

### (c) RANGE OF PARTITION VALUES

The vertical bars through the mean values in figures 46 (a) to 46 (d) represent the standard deviation about the mean value for each element in each fraction. It is immediately obvious that the standard deviations for almost all the elements in each fraction in sediments are much higher than the corresponding standard deviations in nodules.

In nodules Co, Ni, Cu and especially Mn show very little deviation from the mean values obtained for each attack. This indicates that in the samples analysed there was virtually no variation in the partitioning of these elements, each being very clearly partitioned predominantly in the acid-reducible fraction. Zinc, Cd and Pb show a slightly greater variation in partition, and Zn in particular is partitioned appreciably less in the acid-reducible fraction than, for

example, Co and Ni.

Iron shows appreciable variation in its partition between the acid-reducible and HCL-soluble fractions. In this respect, and in the fact that less than 70% of the total Fe is acid-reducible, Fe differs markedly in its partition to Mn.

The partition of Ca, Al, Cr and Ti in nodules is rather more variable than that of the other elements. The partition of Cr, for example, varies by  $\pm 20\%$  in each fraction and in the acid-reducible fraction this variation is twice as large as the mean partition value itself. Titanium on the other hand shows most variation, compared with the mean, in the acid-insoluble fraction, where the standard deviation is of very nearly the same order as the mean value.

Calcium shows a large variation in partition in the acid-reducible and acid-insoluble fractions, but its variation in the acetic acid-soluble fraction is comparatively small. The variation in the partition of Al is generally rather greater than that shown by the other elements and is particularly large in the HCL-soluble fraction.

With very few exceptions, the partition of the elements in sediments is rather more variable than that shown by nodules. For example Mn shows strikingly more variable partitioning in sediments. The standard deviations about the mean values of Mn in the acid-reducible and HCL-soluble fractions of sediments varies by around  $\pm 20\%$  whereas in nodules the corresponding values are  $\pm 2\%$  or less. By contrast the variation in the partition of Fe is fairly similar in sediments to that in nodules.

The trace elements Co, Ni, Cu, Zn, Pb and Cd show a somewhat less well-defined partition pattern in sediments than in nodules. These elements are present predominantly in the acid-reducible and HCL-soluble fractions but the relative partition of these elements between the two fractions is very variable and trends are not therefore as clear as in



nodules. However, the increased variation in partition of these trace elements in sediments correlates very closely with the increased variability of Mn partition in sediments, compared to nodules.

The partitioning of Ca is quite variable in both sample groups but is especially so in sediments. This variation is particularly noticeable in the acetic acid-soluble fraction where about 50%  $\pm$  30% of the total Ca is present, and in the acid-reducible fraction where about 10% of the total Ca is present but with a standard deviation of almost  $\pm$  20%. The Ca in HCL-soluble and acid-insoluble fractions of both nodules and sediments also displays large standard deviations from the mean values.

Chromium, Al and Ti show a slightly smaller variation in partition values in sediments than in nodules. This is particularly noticeable in the acid-reducible fraction.

#### (d) DISCUSSION

The partition patterns for most elements are rather different in nodules to those in sediments, and in general show a much greater variation in the latter.

Virtually all the Mn in nodules is in the acid-reducible fraction and shows very little variation in partition. This indicates that almost all the Mn in nodules is present as acid-reducible oxides and oxyhydroxides. Just over two-thirds of the total Fe in nodules, on average, is present in the acid-reducible fraction. Almost all the rest of the Fe is soluble in HCL. It would seem, therefore, that the majority of the Fe in nodules is present as either an acid-reducible mixed Fe-Mn oxyhydroxide or as a separate, acid-reducible, hydrated iron oxide phase. In order to investigate this further, synthetic Fe and Mn phases were made, and subjected to the same selective attacks as the samples, (see Appendix 1).

As a result of this investigation it would seem that amorphous or colloidal mixed Fe-Mn oxyhydroxides, and Fe-oxide-hydroxides of the type thought to occur in nodules (Goldberg, 1965; Glasby, 1972; Burns & Burns, 1977) and pelagic sediments (von der Borch & Rex, 1970) are almost completely soluble in the mixed acid and reducing agent used. However, crystalline iron-oxide-hydroxide (goethite) which has also been found in nodules (Glasby, 1972; Bezrukov & Andrushchenko, 1973) and sediments (von der Borch et al, 1971) is only very slightly soluble in this reagent. Neither goethite nor colloidal Fe-Mn oxyhydroxides are extensively attacked by acetic acid, but both are completely dissolved by hot 6M hydrochloric acid. The variability in the relative amounts of acid-reducible and HCL-soluble Fe in nodules can therefore probably be related to the varying ratio of goethite to amorphous iron oxide-hydroxide and mixed Fe-Mn oxyhydroxides present in the samples.

In nodules, virtually all the Co and Ni, 90% of the Cu, Pb and Cd and 85% of the Zn is acid-reducible and therefore occurs within or adsorbed onto, the acid-reducible Mn and Fe-Mn oxyhydroxide minerals. The selective attacks used were not able to determine how these trace metals were partitioned between the Mn and mixed Fe-Mn phases. Small amounts of Ni, Cu and more especially Zn occur in the acetic acid-soluble fraction and in view of the probable absence of carbonates, are probably present as loosely sorbed ions on the Mn and Fe-Mn oxides. Small amounts of all these trace elements, but more especially Pb, occur in the HCL-soluble fraction. The HCL-soluble Co, Ni, Cu, Zn and Pb may be contained in the Fe phases broken down by the HCL attack. However, most of the material removed by the HCL attack consists of aluminosilicate material, especially clays. Small amounts of at least some of the trace metals removed by this attack may therefore be released from clay minerals. The amounts of Mn, Fe, Co, Ni, Cu, Zn and Pb in the acid-insoluble fraction are for the most part at levels which are too low

to be measured accurately by the methods used.

The partition patterns of those elements in nodules which are not incorporated primarily within the Mn and Fe phases is rather more variable than those of the elements so far discussed. About one-sixth of the total Ti occurs in the acid-reducible fraction. Electron microprobe studies on manganese nodules have shown some association of Ti with Fe within nodules (Cronan, 1967; Glasby, 1970). Since much of the Fe in nodules occurs in the acid-reducible fraction, it may be that the fraction of Ti which is released by the acetic acid and reducing agent attack represents that portion of the total Ti in nodules which is associated with these Fe phases. Arrhenius (1963) and Glasby (1970) suggest that Ti can also be present in nodules as rutile or anatase. This is not likely to be soluble in the mixed acid and reducing agent but, depending on particle size, may be partly dissolved by hydrochloric acid (Arrhenius, 1963). Thus the Ti in the HCL-soluble and acid-insoluble fractions of nodules may represent the portion of the total Ti which is present as detrital rutile or authigenic anatase. However, appreciable amounts of the Fe-oxyhydroxide phases are also HCL-soluble and therefore the Ti released by the HCL attack is likely to include a contribution from Ti bound up in the HCL-soluble Fe phases.

The majority of the Al in the deposits is present in the HCL-soluble and acid-insoluble fractions, those being the fractions in which the clay-minerals, zeolites and other aluminosilicates could be expected (Chester & Hughes, 1967, 1969). The small amount of the total Al which is soluble in acetic acid probably represents colloidal Al, perhaps present as a hydroxide, which is either adsorbed on the surface of the ferromanganese phases or occurs as a separate discrete phase. Over a quarter of the total Al is present in the acid-reducible fraction. This Al may be present in an authigenic aluminosilicate

which is easily broken down but it more likely represents Al actually incorporated within or intimately mixed with the acid-reducible ferromanganese phases, as a hydroxide or as  $Al^{3+}$  within the todorokite lattice (Lyle et al, 1977).

Over 90% of the total Cr is present in the HCL-soluble and acid-insoluble fractions. Whilst some of the HCL-soluble Cr may be associated with HCL-soluble Fe phases, previous workers (Cronan, 1967; Glasby, 1970) have found Cr to be strongly correlated with the detrital phases of nodules. The Cr soluble in HCL therefore probably reflects the portion of the total Cr present in HCL-soluble detrital minerals rather than an association of Cr with the HCL-soluble Fe phases.

Almost two-thirds of the total Ca in nodules is soluble in acetic acid. This Ca may therefore be present as carbonate material, adsorbed ion-species, and sea-water evaporates. However, Glasby (1970) has found that nodules growing on high carbonate sediment ( $> 80\% CaCO_3$ ) do not include significant amounts of carbonate material as they grow. The nodules in this study were all recovered from areas near or below the C.C.D. where the carbonate content of the sediments was either very low or nil. It is possible that the cores of some of the nodules contained carbonate material but core material was removed, so far as was possible, prior to analysis. Carbonates are not likely, therefore, to be a major source of acetic acid-soluble Ca in nodules. One alternative is that this Ca represents Ca from sea-salt incorporated when the samples were dried prior to analysis. On the other hand, since Ca ions are very abundant in sea-water and the Mn oxides in nodules are known to be excellent scavengers of cations, it seems likely that at least some of the acetic acid-soluble Ca is present in nodules as adsorbed ion species. Realistically, however, the relative contribution of Ca from each of these various possible sources could only be assessed by carrying out selective attacks designed to liberate each of these

phases separately.

The partition patterns of most elements in sediments are rather different to those observed in nodules, moreover they are generally rather more variable than in nodules. This can be explained in the following way. Ferromanganese nodules consist primarily of two types of component as listed in Table 18:-

- (a) A component consisting of oxides and oxyhydroxides of Mn and Fe together with incorporated trace metals
- (b) A component consisting of silicates and aluminosilicates, comprising a mixture of clay minerals, zeolites, quartz and other silicates such as feldspars

Almost all of the Mn, Fe, Co, Ni, Cu, Zn, Pb and Cd in nodules is incorporated in component (a), and because as much as possible of component (b) was removed physically, prior to analysis, the relative amounts of those components present in nodules is not likely to be a major control on the variation in partition of the elements. By contrast, pelagic sediments are a more complex mixture than nodules of the phases listed in Table 18. The main phases likely to be present are carbonate, phosphate, zeolites (mainly phillipsite), clay minerals, silica (mainly biogenic opal) and oxides and hydroxides of Mn and Fe. Whilst the latter, as micronodules, will tend to be markedly enriched in trace metals with respect to the other phases, the clay minerals are also likely to contain appreciable amounts of these metals. Thus in sediments where clay minerals greatly predominate over ferromanganese micronodules a substantial amount of the total trace element content of the sediment will be contained in the clay mineral fraction.

About three-quarters of the total Mn in sediments appears to occur in micronodules or as oxide coatings on other minerals (i.e. is acid-

reducible) whilst about 20%, on average, is present within silicate material such as clay minerals, and is thus partly soluble in HCL. This agrees well with the findings of Chester & Hughes (1969) on pelagic sediments from the Pacific Ocean.

In contrast to its behaviour in nodules, Fe in sediments is partitioned in almost completely separate phases to Mn, with 80% of the total being in the HCL-soluble fraction, and less than 10% being acid-reducible. The combined amounts of HCL-soluble and acid-insoluble Fe, about 90% of the total Fe, is similar to the partition observed in surface sediment from the Pacific, by Chester & Hughes (1969). However, they ascribe all the non-acid reducible Fe to a lithogenous fraction (i.e. clay minerals). In view of the apparent insolubility of well-crystalline goethite in the acid and reducing agent mixture used, it seems likely that any goethite in the sediments will be dissolved by the HCL attack, even if of authigenic origin. Therefore it is suggested that at least some of the Fe in the HCL-soluble phase of the sediments analysed may be present as goethite. It is likely that this would represent colloidal Fe which was not incorporated by growing micro-nodules and which subsequently aged to goethite (Goldberg & Arrhenius, 1958).

The percentages of the various trace elements in the acid-reducible phase of sediments ranges from over 60% of the total for Co, down to 25% for Zn and probably even less for Cd. These values are likely to represent the percentage of the total of each element associated with micronodules and perhaps ferromanganese-oxide coatings on other minerals in the sediment. A comparatively large percentage of the total amount of some elements, especially Cu and Zn, is present in the acetic acid-soluble fraction. This represents the amounts of these elements present as loosely adsorbed cations, in acetic acid-soluble oxide coatings and, in carbonate bearing-sediments, in the carbonate material itself (Horowitz,

1974; Horder, pers. comm.). Much of the trace element content of the sediments occurs in the HCL-soluble and acid-insoluble fractions, the amounts varying from about 25% for Co to over 50% for Zn and virtually 100% for Cd. From the attacks used it is not possible to elucidate what proportion of these elements is present in clay minerals and what proportion is associated with goethite, since these minerals are all extensively dissolved by HCL. Some amounts of some of these metals, particularly Ni and Cu, are also present in siliceous biogenic debris (Greenslate et al, 1973) and in siliceous sediments this phase is likely to provide another source of HCL-soluble trace metals.

As in nodules Cr and Ti in sediments occur predominantly in the HCL-soluble and acid-insoluble fractions, present in silicates, in the case of Cr, and oxides in the case of Ti. Amounts of acid-reducible Al in sediments are much less than in nodules indicating that a greater percentage of the Al in sediments compared to nodules (over 90%) is present in clays and other aluminosilicates, rather than as a hydroxide phase. Whilst on average, at least half of the total Ca in sediments is soluble in acetic acid, this percentage is very variable. This is due to the presence of variable amounts of carbonate material. Most of the sediments are low in carbonate or essentially carbonate-free. However, one or two samples contain abundant carbonate material. In these samples the large amounts of Ca contained in the carbonate completely swamp the much smaller amounts present in other phases, and in these samples effectively all the Ca appears to be in the acetic acid-soluble fraction. Of the remaining Ca, most appears to be present in acid-insoluble silicate phases although some is also present in the HCL-soluble fraction, probably from Ca-bearing clay minerals.

### (iii) COMPARISON OF PARTITION IN NODULES & SEDIMENTS FROM DIFFERENT BASINS

Comparatively small but nevertheless significant differences occur in the average partition patterns of the elements in nodules and sediments in the two basins investigated. The two basins are floored by, and are currently receiving, very different types of sediment, and are characterised by nodules of markedly different composition and morphology. The average partition data for the samples from each basin were therefore separated and are summarised in figures 47 and 48.

#### (a) ELEMENT PARTITION IN NODULES

The major elements Mn and Fe are partitioned very similarly in nodules from both basins, with virtually all the Mn partitioned in the acid-reducible fraction, along with about 70% of the total Fe. However, the variation in partition of Fe in the Central Indian Basin (C.I.B.) samples is rather less than in the Madagascar Basin samples.

By contrast, the trace metals in nodules do not appear to be partitioned in quite the same way in the two different basins. Rather higher proportions of Zn and Cu appear to be present in the acetic acid-soluble fraction in Madagascar Basin samples than in C.I.B. samples.

In both basins the largest percentage of all the trace metals occurred in the acid-reducible fraction. However, in Madagascar Basin samples significantly lower percentages of Pb, Cu, Cd and especially Zn are present in the fraction compared with C.I.B. samples. Between 7 and 10% of the total Pb and Zn is partitioned in the HCL-soluble fraction in Madagascar Basin samples whereas in C.I.B. samples only trace amounts are present in this fraction. The acid-insoluble fraction of Madagascar Basin samples also contains more Pb and Cd than does the same fraction in C.I.B. samples. However levels of most trace metals in this fraction are



FIGURE 47 (a) & (b) Mean partition values in nodules from the Central Indian and Madagascar Basins.

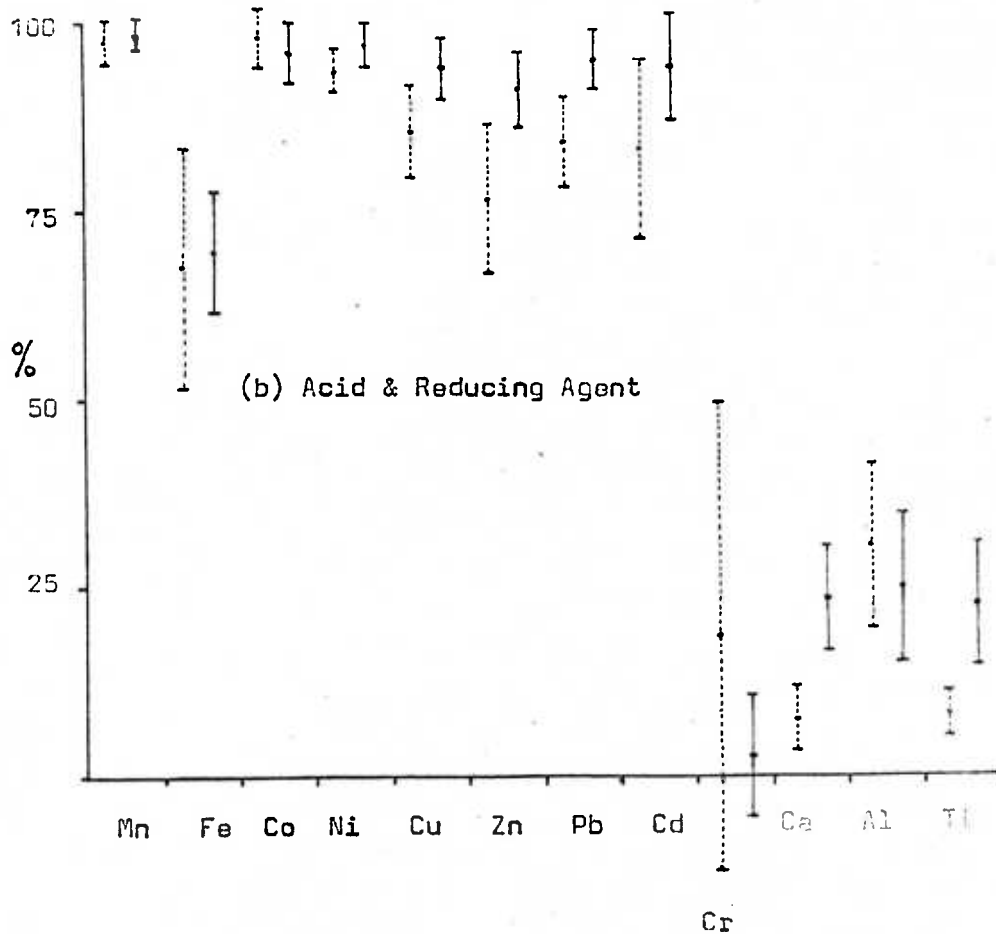
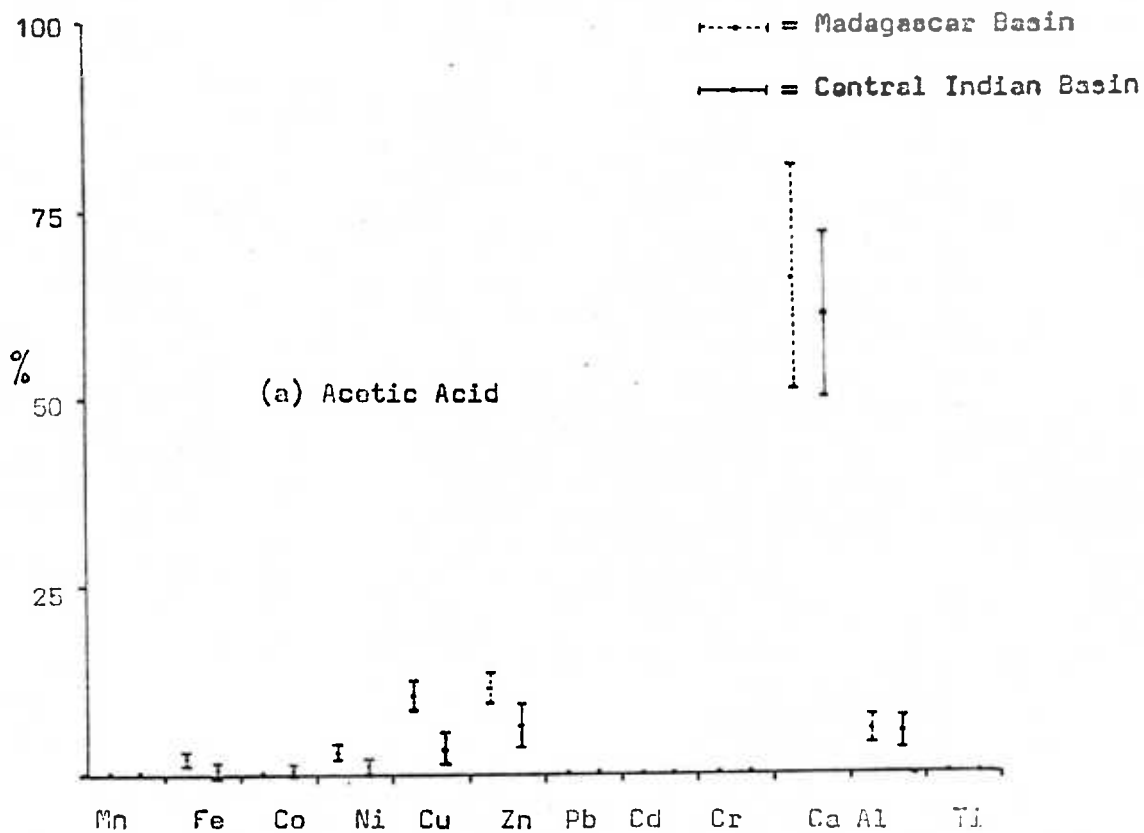
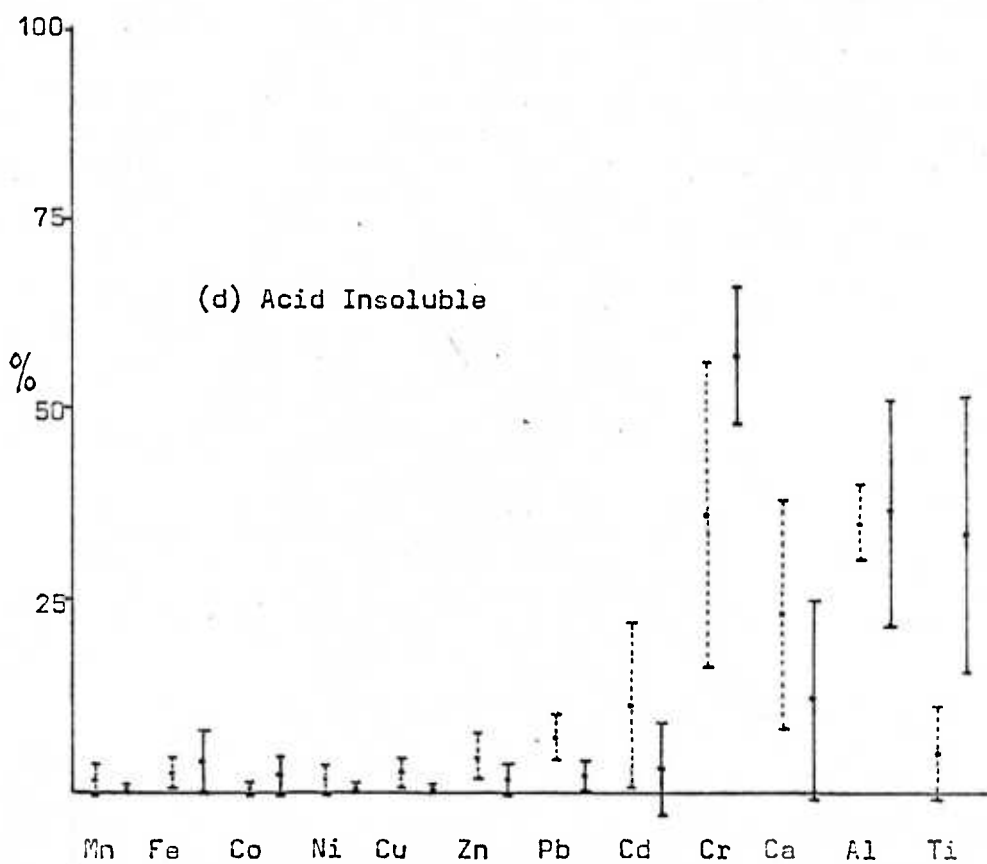
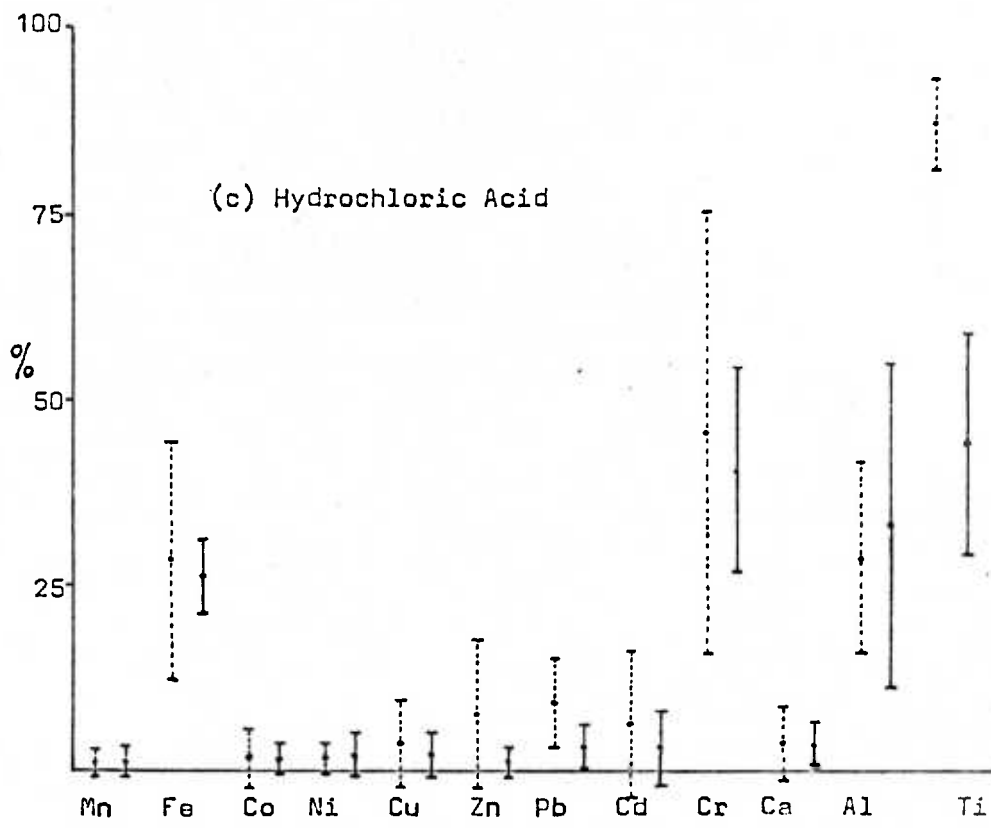


FIGURE 47 (c) & (d) Mean partition values in nodules from Central Indian and Madagascar Basins.



small or zero in most samples in both basins.

The detritally associated elements Cr and Ti also show differences in partition between the two basins. In particular, almost 90% of the Ti in Madagascar Basin samples is HCL-soluble. In C.I.B. samples on the other hand, less than half the total Ti occurs in this fraction, whilst a quarter of the total Ti is in the acid-reducible fraction and the remaining 30% in the acid-insoluble fraction. Chromium in C.I.B. samples is partitioned almost exclusively in the HCL-soluble and acid-insoluble fraction with rather less in the former than in the latter. However, in Madagascar Basin samples almost 20% of the total Cr occurs, on average, in the acid-reducible fraction. As can be seen from figure 47, the partitioning of Cr between the various fractions is very varied, and is particularly so in Madagascar Basin samples.

Aluminium shows a roughly similar partitioning between the various fractions in both basins. The partition patterns of Ca however are rather different in the two basins. Roughly equal proportions of the total Ca are liberated by the acetic acid attack on nodules from both basins. However almost a quarter of the total Ca in C.I.B. nodules is present in the acid-reducible fraction whilst in Madagascar Basin samples acid-reducible Ca accounts for less than 10% of the total, with a correspondingly greater percentage present in the acid-insoluble fraction:

## (b) DISCUSSION

The partition of the major elements Mn and Fe in nodules from both basins shows very few differences, however, the trace metals in general do show some variation in their partition patterns between the two basins.

The mineralogy of the Mn phases in nodules from the two basins is very different (see Section 4), but since all the Mn phases present in the samples analysed appear to be acid-reducible, mineralogical differences

do not appear to have any effect on Mn partition. The mineralogy of the Fe phase is not well known, however, as has already been discussed, the degree of crystallinity of these phases appears to affect the partitioning of the Fe. Well-crystalline goethite is insoluble in the mixed acid and reducing agent used whereas amorphous and colloidal ferric hydroxide and mixed Fe-Mn oxides are more or less completely soluble in this reagent. Thus variation in the ratio of acid-reducible to HCL-soluble Fe should give an indication of the ratio of amorphous FeOOH to crystalline goethite present in the samples. On average, these ratios are very similar in both basins, being 2.4:1 in the Madagascar Basin and 2.7:1 in C.I.B. samples. However, variation of this ratio within each basin was very much larger and ranges from a minimum of 0.33:1 in one sample from the Madagascar Basin to a maximum of 6.8:1 in one Central Indian Basin sample. The sample from the Madagascar Basin showing such a high proportion of HCL-soluble (i.e. non-reducible) Fe, was the only sample from either basin in which goethite was positively identified in the bulk sample.

Whilst mineralogical differences do not affect the Mn partition they do appear to have an effect on the trace element partition. Rather greater percentages of the total Zn, Ni and Cu are acetic acid-soluble in Madagascar Basin samples, than in C.I.B. samples. These metals have ionic radii and charges which makes incorporation into the  $\delta$ -MnO<sub>2</sub> mineral lattice rather unlikely, but which allows fairly easy substitution for divalent Mn in todorokite (see Section 5). These metals are therefore more likely to be present as adsorbed species rather than in lattice sites in  $\delta$ -MnO<sub>2</sub>-rich samples. The increased proportion of Cu, Ni and Zn in the acetic acid-soluble fraction of Madagascar Basin samples is in agreement with this, since  $\delta$ -MnO<sub>2</sub> was the main Mn phase identified in Madagascar Basin nodules, whereas C.I.B. nodules which had a higher percentage of lattice Cu, Ni and Zn were found to be rich in todorokite. Small amounts of Pb, Zn and to a lesser extent Cu, are associated with the HCL-soluble

fraction in Madagascar Basin samples. The amounts of these elements in this fraction are noticeably higher in samples where larger than average amounts of Fe are present as goethite (i.e. are also HCL-soluble). That goethite can contain significant amounts of Cu and Zn but not so Co or Ni, has been demonstrated in nodules by Arrhenius (1963) and in metalliferous sediments by Bignell (1975). The reasons for the enrichment of Pb in this phase are not clear, since its ionic size and radius in the valency state in which it is found in sea-water are unfavourable for its incorporation into goethite by substitution for Fe. It may well be that the HCL-soluble Pb comes at least partly from the breakdown of authigenic phosphates, such as apatite, which are sometimes associated with goethite in nodules (Winterhalter & Sivolla, 1966). This mineral is at least partly soluble in HCL and may contain substantial amounts of heavy metals such as Pb (Arrhenius, 1963; Deer et al, 1966).

The partition of Al in nodules from both basins is similar and consistent with the suggestion that most of this element is released in the HCL-soluble and acid-insoluble fractions by breakdown of clays and more resistant aluminosilicates. Rather substantial amounts are also present probably as a hydroxide or in lattice sites in the Mn phases.

Most of the Ca in the nodules is present in the acetic acid-soluble fraction in both basins, probably mainly as sea-water evaporates and adsorbed ion species. In both basins only trace amounts are associated with the HCL-soluble clay minerals. However there is a large difference in the percentage of acid-reducible Ca between the two basins, less than 10% of the total Ca in Madagascar Basin samples being present in this fraction compared with almost 25% in Central Indian Basin samples. The difference can be accounted for by considering the different nodule mineralogy of samples from the two basins. As already discussed, Madagascar Basin samples contain  $\delta$ -MnO<sub>2</sub> whereas C.I.B. samples are rich in todorokite. As has been pointed out, (Straczek et al, 1960) Ca is an

important minor constituent of the todorokite mineral lattice. This Ca will be released by the acid-reducing agent attack as the Mn minerals are broken down, and probably accounts for the difference in Ca partition observed in the two basins.

The partition patterns of Ti in the two basins are somewhat different. As already discussed, it seems likely that Ti in the acid-reducible fraction is associated with Fe phases and from the average partition data it would appear that Ti shows a very much greater affinity for these Fe phases in C.I.B. nodules than in Madagascar Basin samples (see figure 47) even though total amounts of Fe are lower in the former than in the latter. Another major difference in Ti partition is that a much greater percentage of the total Ti is present in the acid-insoluble fraction rather than in the HCL-soluble fraction in C.I.B. samples compared to Madagascar Basin samples. According to Doer et al (1966) both rutile and anatase are insoluble in HCL. However, when these minerals are of very small particle size and full of impurities such as clay minerals, which is often the case with authigenic  $TiO_2$  (Arrhenius, 1963), it is likely that they will be appreciably soluble in HCL. Thus the different partition of Ti between the HCL-soluble and acid-insoluble fractions in the two basins may reflect the different degrees of crystallinity of  $TiO_2$  in nodules from the two basins.

An accurate assessment of the variation in Cr partition between the basins is precluded by the fact that the inter-basin variations tend to be smaller than the intra-basin variations (see figure 47). The main differences appear, however, to be the presence of more acid-insoluble Cr in C.I.B. nodules compared to Madagascar Basin nodules which by contrast contain rather more acid-reducible Cr. The reasons for these variations are not clear.

FIGURE 48 (a) & (b) Mean partition values in sediments from Central Indian and Madagascar Basins.

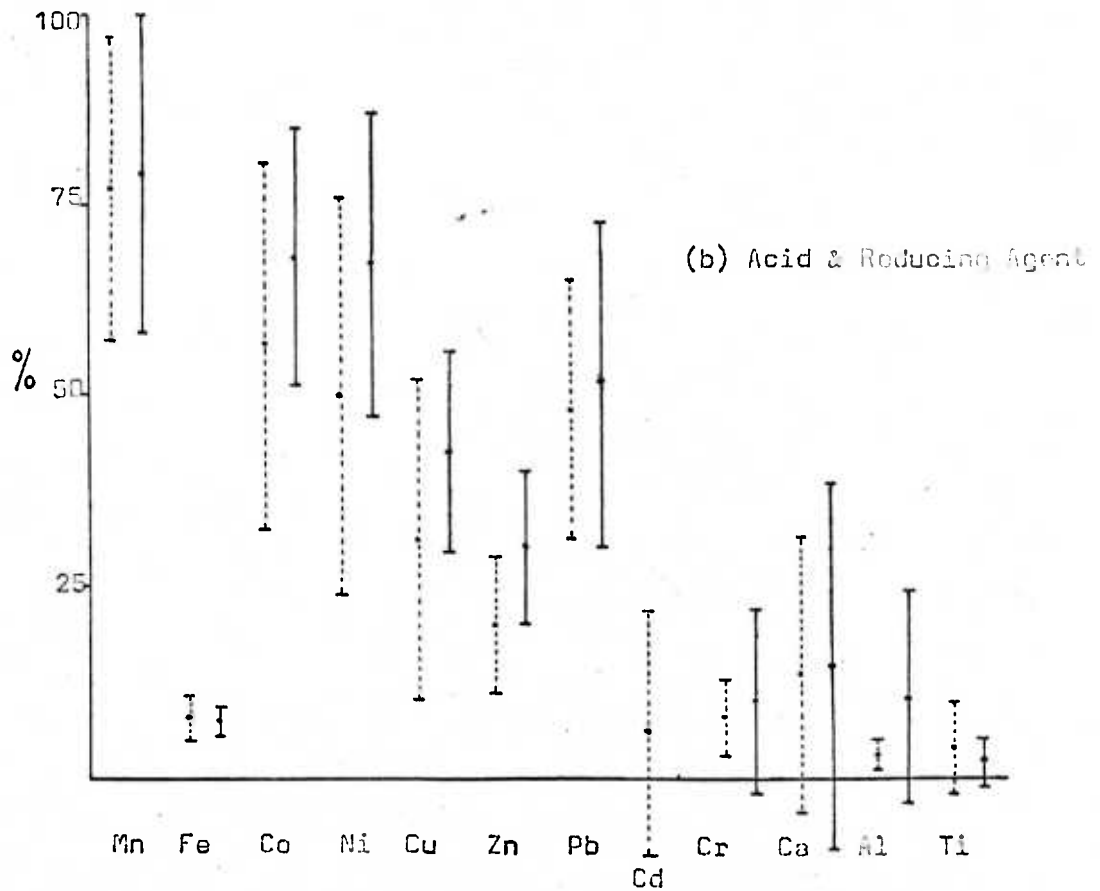
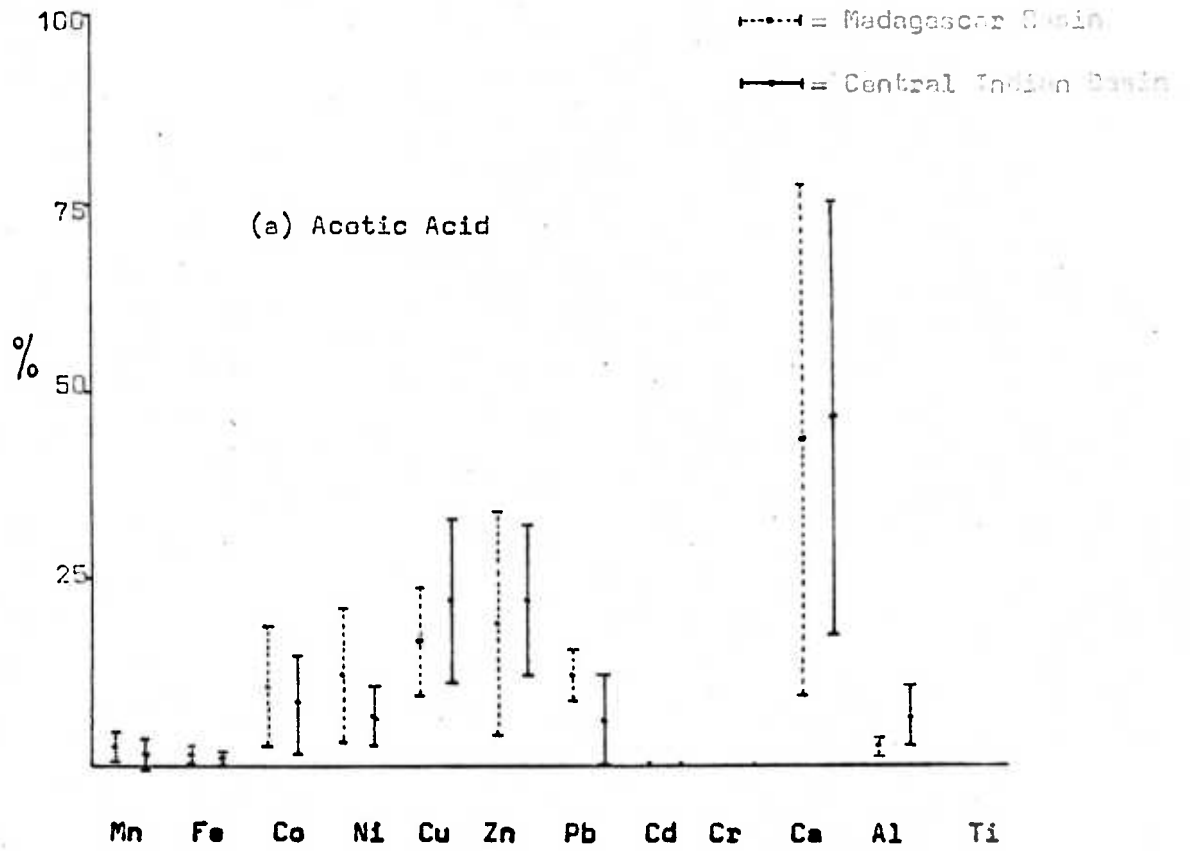
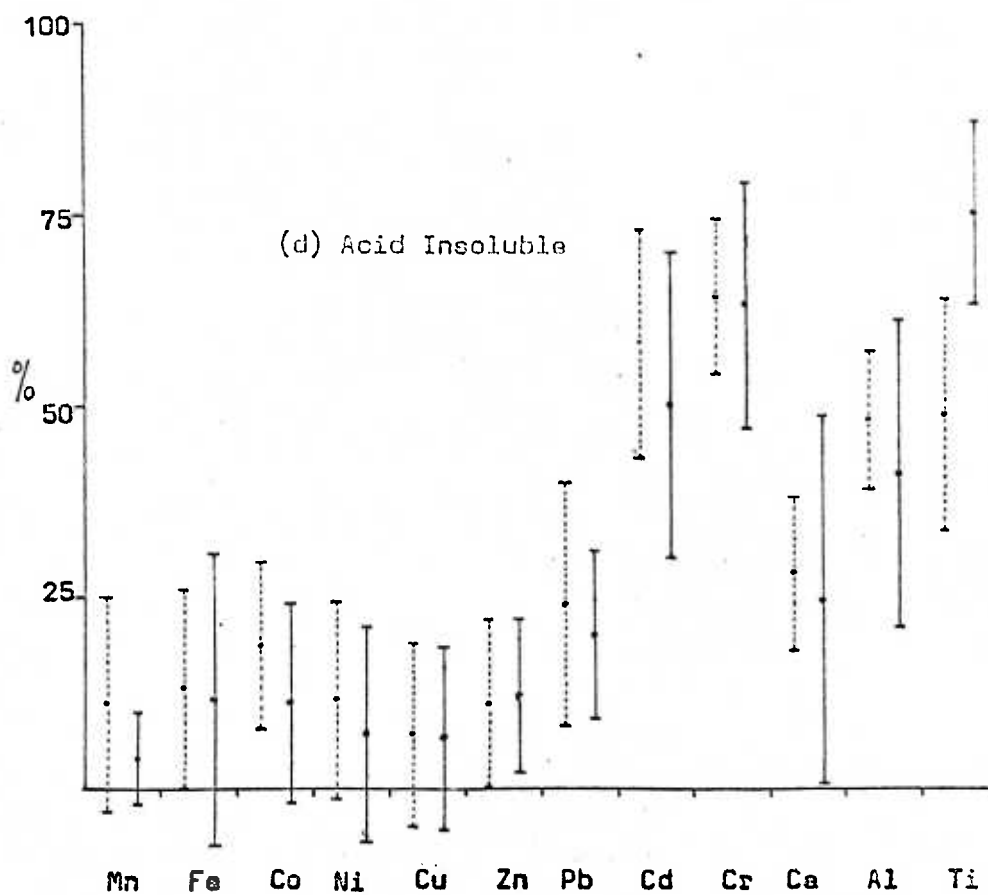
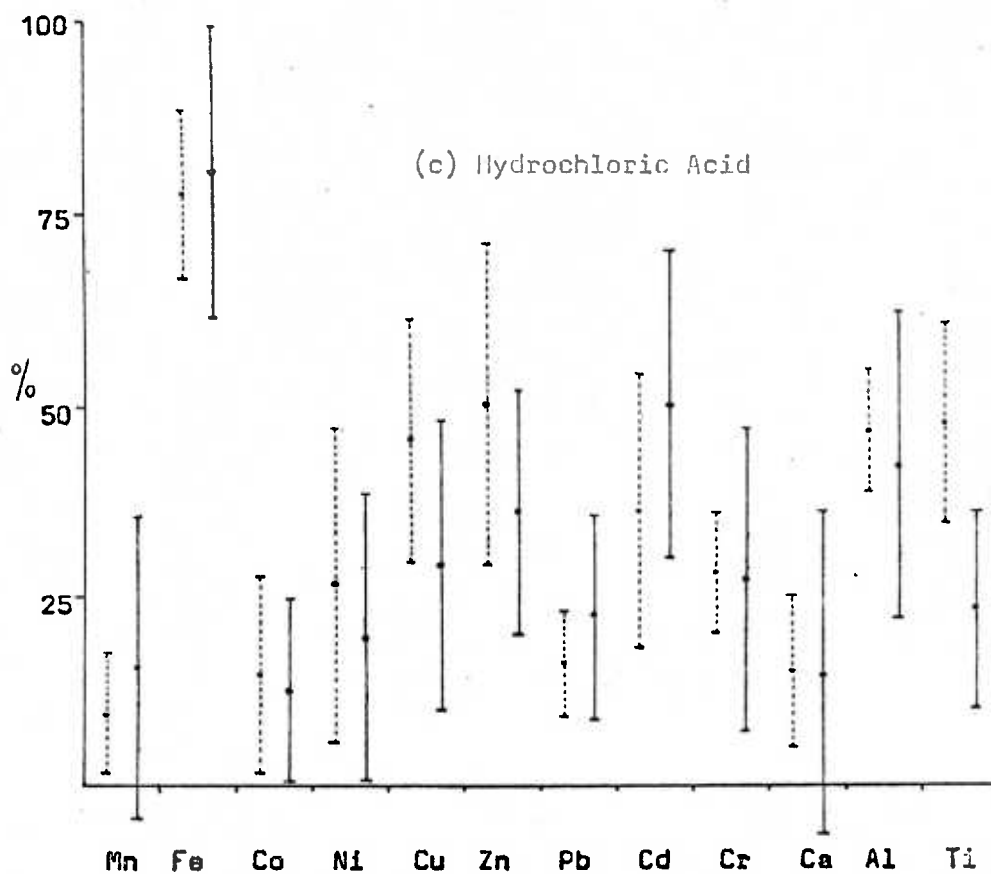


FIGURE 4B (c) & (d) Mean partition values in sediments from Central Indian and Madagascar Basins.





### (c) ELEMENT PARTITION IN SEDIMENTS

The partition of Mn and Fe in sediments is fairly similar in both basins. About three-quarters of the total Mn and about 10% of the total Fe is present as ferromanganese-oxide material, soluble in mixed acid and reducing agent. About 80% of the total Fe in both basins is soluble in HCL and therefore assumed to be present partly as goethite and partly within Fe-bearing clays, such as nontronite, which are HCL-soluble. Slightly more Mn is present, on average, in the HCL-soluble fractions of C.I.B. sediments than in Madagascar Basin samples, although amounts in this fraction are rather variable in the Central Indian Basin.

In general, the partition patterns of all the trace elements are rather more varied in sediments than in nodules. The partition patterns of the trace elements associated with the Fe and Mn phases i.e. Co, Ni, Cu, Zn and Pb are rather different in the two basins. On the whole, a greater proportion of the total Co, Ni, Cu and Zn are acid-reducible in C.I.B. samples than in Madagascar Basin samples, whilst a greater proportion of the Cu and Zn is in the HCL-soluble fraction in Madagascar Basin samples compared to C.I.B. samples. A significantly greater amount of the total Ni and Pb in Madagascar Basin sediments is present in the acetic acid-soluble fraction than is the case with C.I.B. sediments.

Measureable amounts of all the trace elements are present in the acid-insoluble fraction in samples from both basins. However the amounts present in this fraction are rather variable and only Co shows a noticeable difference between the basins. In fact as can be seen from figure 48, the standard deviations from the mean value for all the trace elements in all the fractions are large, and significant differences in partition between the basins are therefore difficult to establish.

Amounts of Cd present in the samples were too low to allow an accurate study of the partition of this element, although in both basins it appears to be present almost exclusively in the HCL-soluble and acid-insoluble fractions.

The partition pattern of Ca is virtually identical in samples from both basins but as can be seen from figure 48 the partition of this element shows large standard deviations in all four fractions examined. On average, just under half the total Ca occurs in the acetic acid-soluble fraction in sediments from both basins, but this percentage is much higher in sediments with abundant carbonate material, and much lower in non-carbonate sediments. This is the reason for the large standard deviations observed. The Ca not released by acetic acid might be expected to be present mainly in aluminosilicate material and thus partitioned mainly in the HCL-soluble and acid-insoluble fractions. In both basins, about 40% of the total Ca is present in these two phases, with almost twice as much, on average, in the acid-resistant fraction as in the HCL-soluble fraction. In both basins an appreciable amount of the total Ca is present in the acid-reducible fraction. The variation in Ca partition within each basin is much larger than the variation observed between basins, and in general, the intra-basin variation in the Central Indian Basin is greater than that in the Madagascar Basin.

Like Ca, Al shows rather greater variation in partition in the Central Indian Basin than in the Madagascar Basin, where in fact the variations in partition are very small. In both basins more than three-quarters of the total Al is present in the HCL-soluble and acid-reducible fractions and in the Madagascar Basin these two fractions contain virtually all the Al.

The partition of Cr is very similar in both basins although, like Ca and Al, Cr shows more variability in its partition patterns in the Central Indian Basin than in the Madagascar Basin. In both basins about 90% of the

total Cr is present in the HCL-soluble and acid-insoluble fractions, with roughly twice as much in the latter, on average, as in the former.

Like Cr, Ti is partitioned almost exclusively in the HCL-soluble and acid-insoluble fractions in both basins, however. Ti shows marked differences in partition between the two basins. In the C.I.B. about three-quarters of the total Ti is in the acid-insoluble fraction and one-quarter in the HCL-soluble fraction whereas in the Madagascar Basin Ti is partitioned almost equally between the two fractions.

#### (d) DISCUSSION

In general, the partition patterns of Mn and Fe are similar in sediments from both basins. However a larger and more variable amount of Mn is present in the HCL-soluble fraction of C.I.B. samples than in Madagascar Basin samples. In Madagascar Basin samples, average amounts of Mn in the HCL-soluble fraction are well below the average value of Mn in pelagic clays from the Indian Ocean (El Wakoel & Riley, 1961). Much of the Mn in this fraction in Madagascar Basin samples may therefore be incorporated in the lattices of the clay minerals present in these sediments. Ten times as much Mn was present in the HCL-soluble fraction of C.I.B. samples as was present in the same fraction of Madagascar Basin samples, although the bulk Mn content of C.I.B. samples is only about twice that of Madagascar Basin samples. Therefore, either the clay mineral fraction of C.I.B. samples is much richer in Mn than the same fraction of Madagascar Basin samples or Mn is being released by the HCL attack from a comparatively Mn-rich mineral phase which is much more abundant in C.I.B. sediments than in Madagascar Basin sediments. Greenslate et al (1973) have shown that siliceous biogenic debris can contain comparatively high amounts of Mn. Siliceous organisms may therefore be a source of the "excess" Mn in the HCL-

soluble fraction of C.I.B. sediments, since siliceous remains are abundant in them.

Greater percentages of the total amounts of Co, Ni, Cu, Zn and Pb are present in the acid-reducible fraction of Central Indian Basin samples than in this fraction in Madagascar Basin samples. This may be due to the fact that amounts of acid-reducible Mn are much higher in C.I.B. sediments than in Madagascar Basin sediments. This Mn is likely to be present as oxides or oxyhydroxides, and these are likely to be enriched in trace metals compared to most or all of the phases present in the sediments. Lead is also higher in the HCL-soluble fraction of C.I.B. samples than in the same fraction of Madagascar Basin samples. This may be due to a higher content of HCL-soluble phosphatic material such as fish débris in Central Indian Basin samples.

The large standard deviations of Co, Ni, Cu, Zn and Pb and the low levels present make a comparison between basins difficult for the acetic acid-soluble fraction of the sediments. However, rather more Cu is present in this fraction in Central Indian Basin samples than in Madagascar Basin samples, whilst for Ni and Pb the reverse is the case. There does not appear to be any clear-cut reason for this, or for the smaller differences observed in the variation of the other trace metals between the basins.

Much of the Ca in sediments which is not present as carbonate occurs in the HCL-soluble and acid-insoluble fractions and this Ca is therefore probably present in clays and phosphatic fish débris (mainly HCL-soluble) and in Ca-bearing silicates such as calcic feldspars (insoluble in HCL). However in both basins some 15% of the total Ca, on average, is acid-reducible. A consideration of the main phases present in pelagic sediments (Table 18) does not indicate any obvious Ca-bearing phase which might be extensively dissolved in this attack but not in acetic acid only. Chester & Hughes (1967) found that dolomite was extensively broken down by mixed acid and reducing agent attack but dolomite is not likely to be present in

surface sediments since it usually develops from calcite only at depth in the sediment column, as part of an ageing process. Cronan (1976) attributes acid-reducible Ca in basal metalliferous sediments from the Pacific Ocean to liberation from phosphatic fish debris. However, according to Arrhenius (1963) and Deer et al (1966) this material is not extensively soluble in acetic acid and hydroxylamine-hydrochloride. An equally likely source for this Ca is from the clay minerals, since Chester & Hughes (1967) have shown that some clays are slightly soluble in acetic acid and hydroxylamine hydrochloride solution.

The partition patterns of Al are similar in the sediments of both basins and are consistent with most of the Al being present in clay-minerals and other aluminosilicates such as zeolites and feldspars. The Al released in the acetic acid-soluble fraction is probably present as a colloidal hydroxide which is soluble in this reagent, whilst the Al in the acid-reducible fraction may also be colloidal species but is more likely to represent Al from the clay minerals, especially illite and montmorillonite which are slightly soluble in mixed acid and reducing agent (Chester & Hughes, 1967).

The partition patterns of Cr are also similar in both basins, Cr being partitioned predominantly in the acid-resistant fraction. In general, Madagascar Basin samples have a larger total Cr content, averaging over 150 p.p.m., whilst average values in the C.I.B. are less than 70 p.p.m. The excess Cr in Madagascar Basin sediments is probably due to the presence of relatively unaltered volcanic material. El Wakeel & Riley (1961) suggest that Cr concentrations of over 100 p.p.m. in sediments are a good indication of the presence of basaltic pyroclasts.

Titanium is partitioned almost exclusively in the HCl-soluble and acid-resistant fractions in sediments from both basins. This points to Ti being present predominantly as a resistant oxide phase. Although, as in nodules, some Ti may be incorporated in the Fe hydroxide phase, this

phase is HCL-soluble and therefore Ti from this source is indistinguishable from HCL-soluble Ti-oxides. The greater percentage of HCL-soluble Ti in Madagascar Basin sediments may be due to larger amounts of Ti associated with Fe-oxides than in the Central Indian Basin, particularly since Fe appears to be more abundant in the former than in the latter. However, the difference in partitioning may be due simply to a difference in particle size and crystallinity of the  $TiO_2$  in the sediments, since well-crystalline anatase and rutile are resistant even to hydrochloric acid.

#### (iv) INDIVIDUAL ELEMENT PARTITION ALONG TRAVERSES

Sampling in the Madagascar and Central Indian Basins was carried out along two traverses (figures 49 & 50). In the Madagascar Basin, the traverse was roughly from south-west to north-east although the last part of the traverse ran almost due north. The traverse across the Central Indian Basin ran almost due west-east. In order to investigate the partitioning of elements in nodules and sediments in more detail, and in particular to investigate trends in partition within each basin, the partition values for each sample along the traverse were plotted separately for each element. Thus figures 51(a) to 62(a) plot the variation in partition in nodules and sediments for each element analysed along the Madagascar Basin traverse. In each case the uppermost graph shows the variation in bulk composition of the samples along the traverse, and beneath this the fractions of the total amount of the element are plotted which were released by each selective attack. Similarly, figures 51(b) to 62(b) plot the same parameters for nodules and sediments along the Central Indian Basin traverse.

FIGURE 49 Sample sites in the Madagascar Basin.

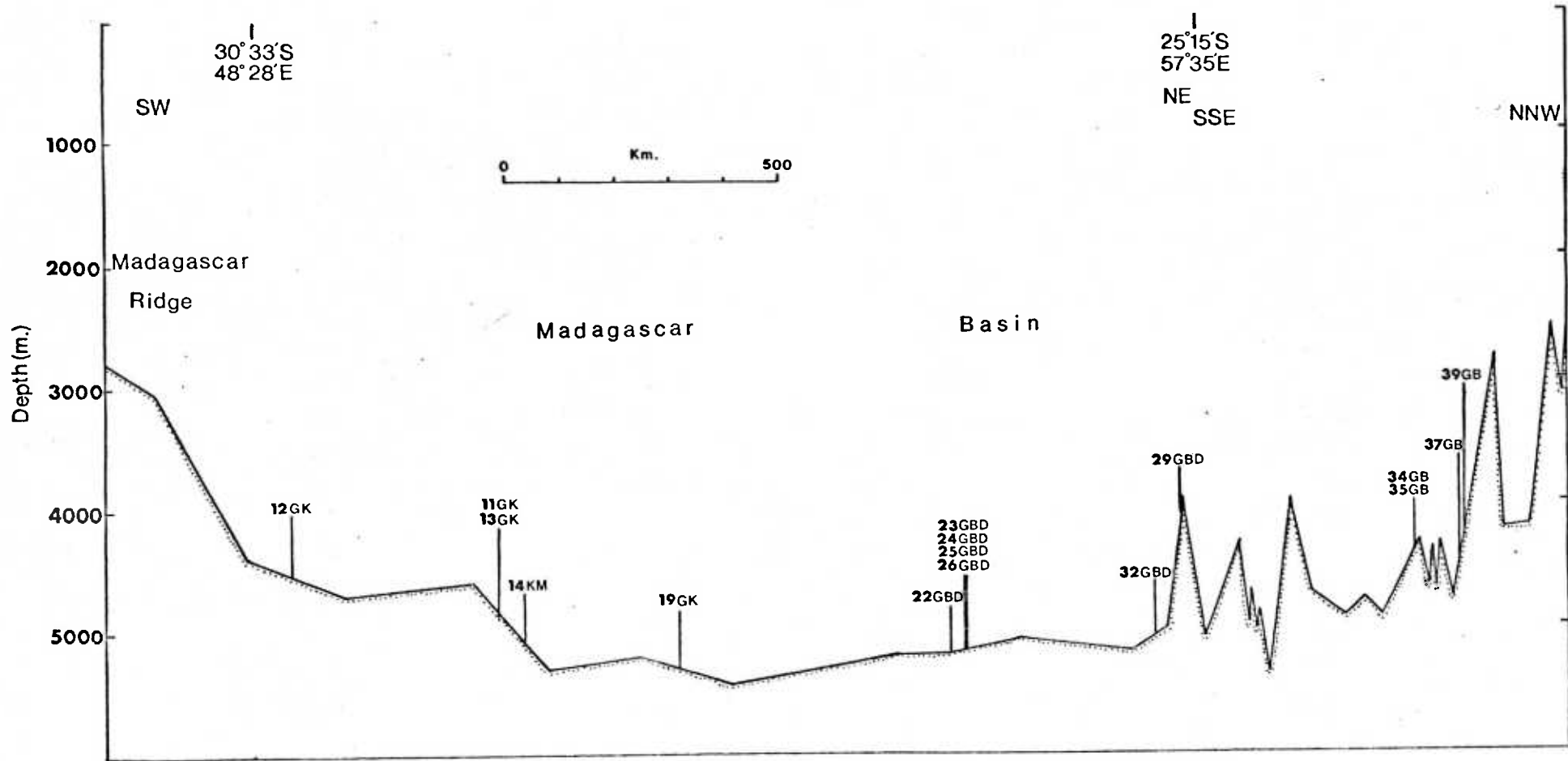
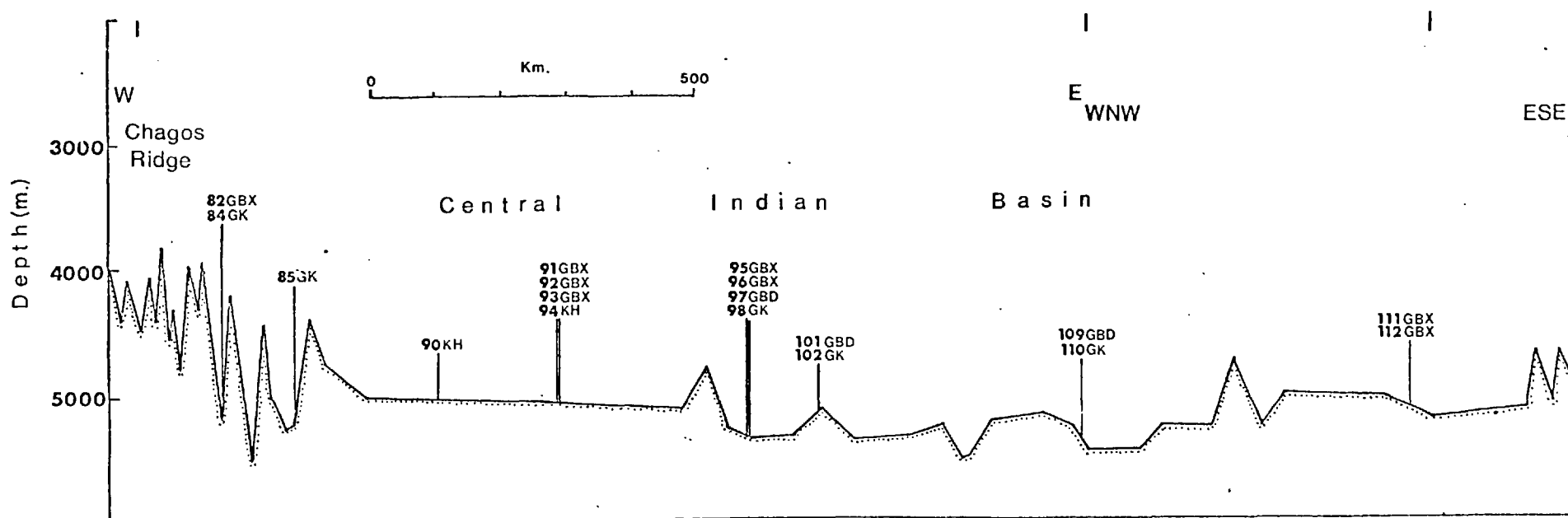


FIGURE 50 Sample sites in the Central Indian Basin.





(a) VARIATION IN NODULE PARTITION ALONG TRAVERSES

Manganese shows very little variation in partition along either traverse, being almost completely contained in the acid-reducible fraction in all the samples. The remaining Mn is mainly in the HCL-soluble fraction but this too shows no trend across the basins. With the exception of one sample, total Mn tends to increase towards the centre of the Central Indian Basin. The length of the nodule traverse in the Madagascar Basin is rather short and therefore of less value in investigating compositional trends across the basin however, it can be seen that Mn is rather lower in samples from the middle of the traverse than in those from the ends.

Total iron shows no well-defined trend across the Madagascar Basin. However in the Central Indian Basin it behaves in the reverse manner to Mn and is lower in nodules in the centre of the traverse. In the acetic acid-soluble fraction, Fe shows an increase in solubility towards the north-east part of the Madagascar Basin. In the Central Indian Basin Fe shows an increase in solubility in this fraction towards the western end of the traverse which correlates well with the greater amounts of Fe present. However the actual amounts present in this fraction in both basins are very small.

The acid-reducible Fe in Madagascar Basin samples shows an overall slight decrease from south-west to north-east. One particular sample (25GBD) shows an extremely marked decrease in acid-reducible iron and a corresponding increase in HCL-soluble Fe. This sample has already been mentioned in sub-Section (iii)(b) as being unique in that it was the only sample from either basin in which goethite was positively identified. Nodules from the central part of the Madagascar Basin show a definite increase in HCL-soluble iron. In the Central Indian Basin there do not appear to be any systematic trends in Fe partitioning across the basin, however in the acid-insoluble fraction Fe does show some increase towards

Figure 51a Mn Partition in Madagascar Basin nodules and sediments.

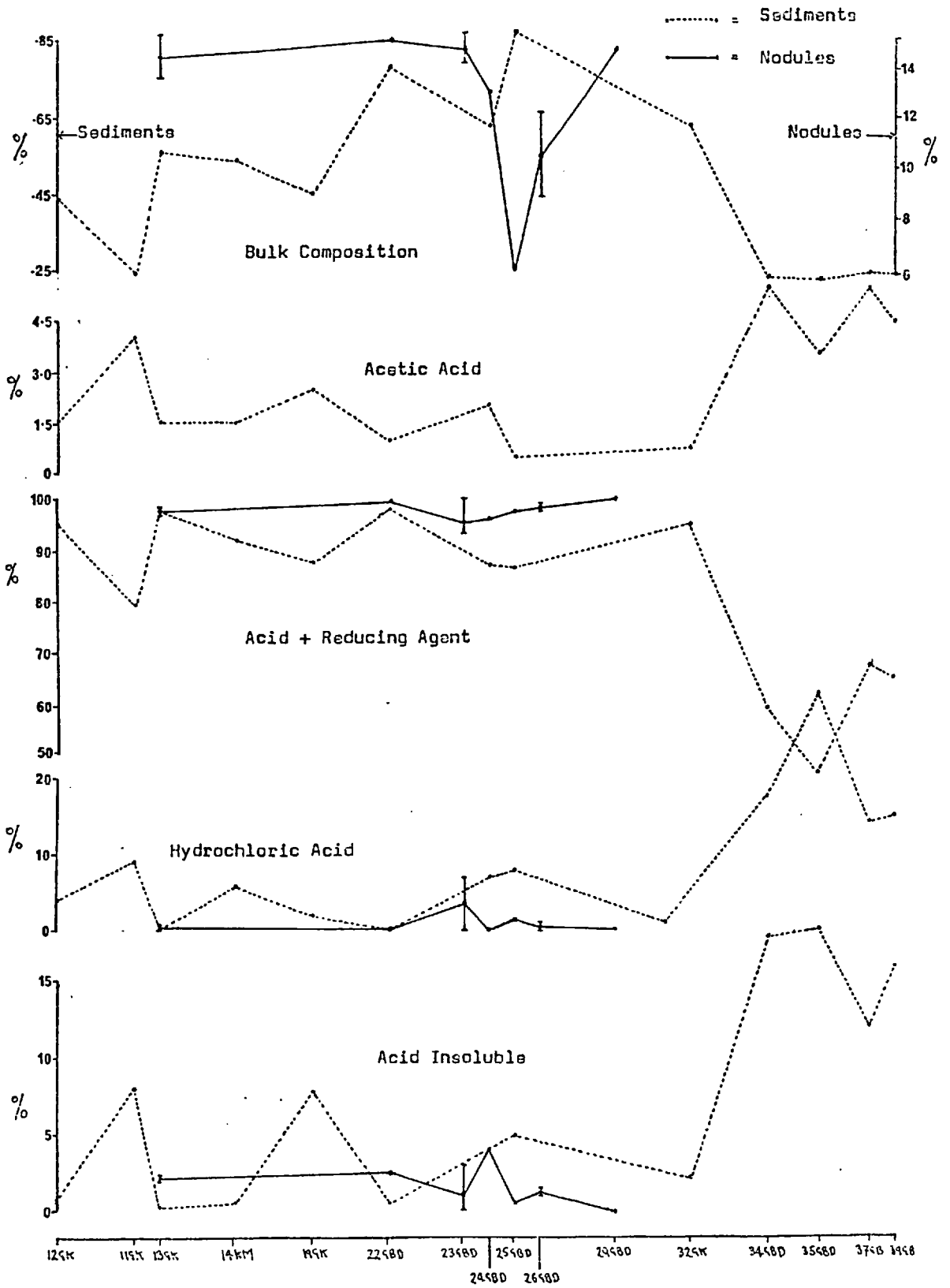


**FIGURE 51b** Mn partition in Central Indian Basin nodules and sediments.

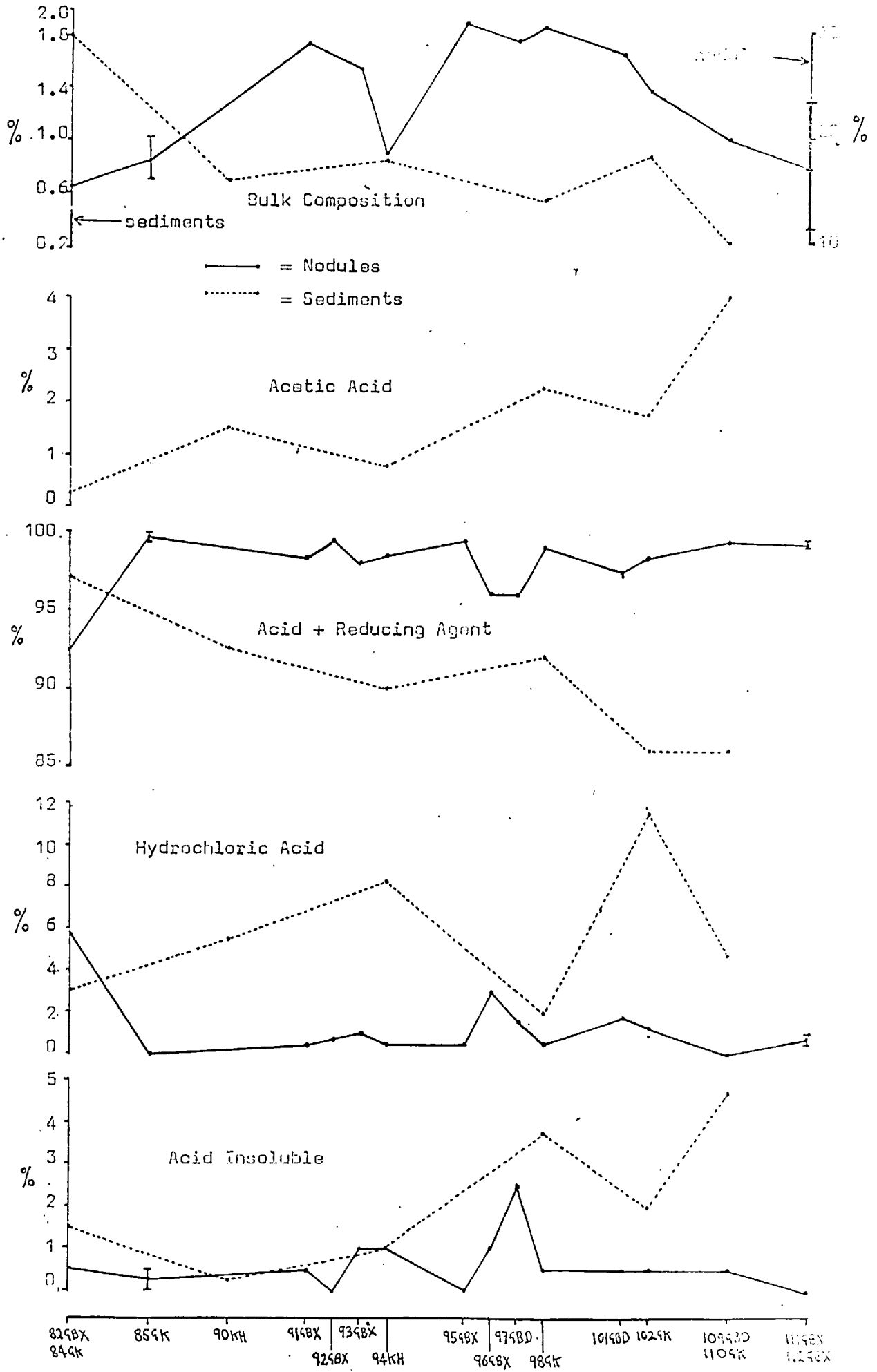
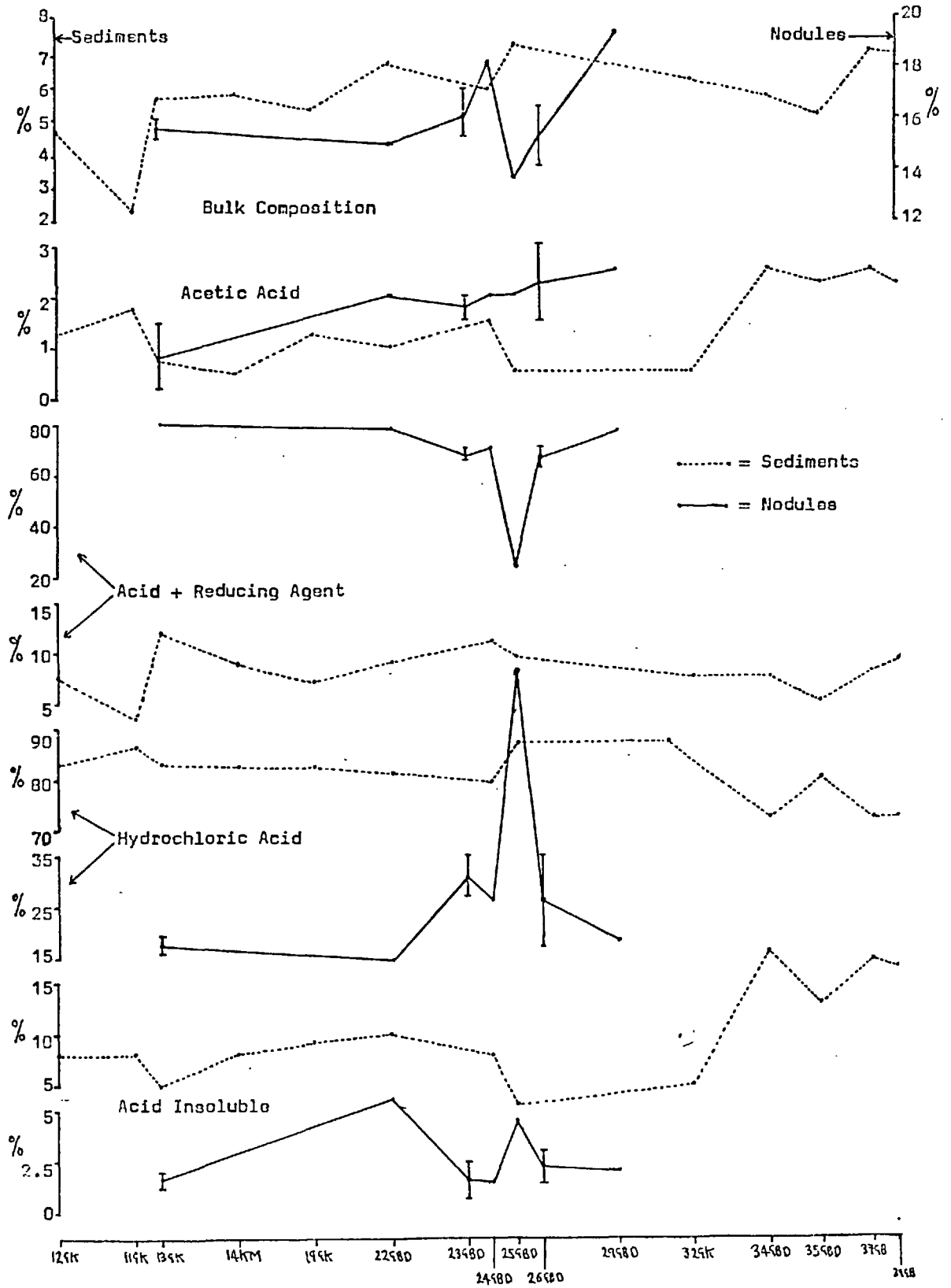


Figure 52a Fe Partition in Madagascar Basin nodules and sediments.



**FIGURE 52b** Fe partition in Central Indian Basin nodules and sediments.

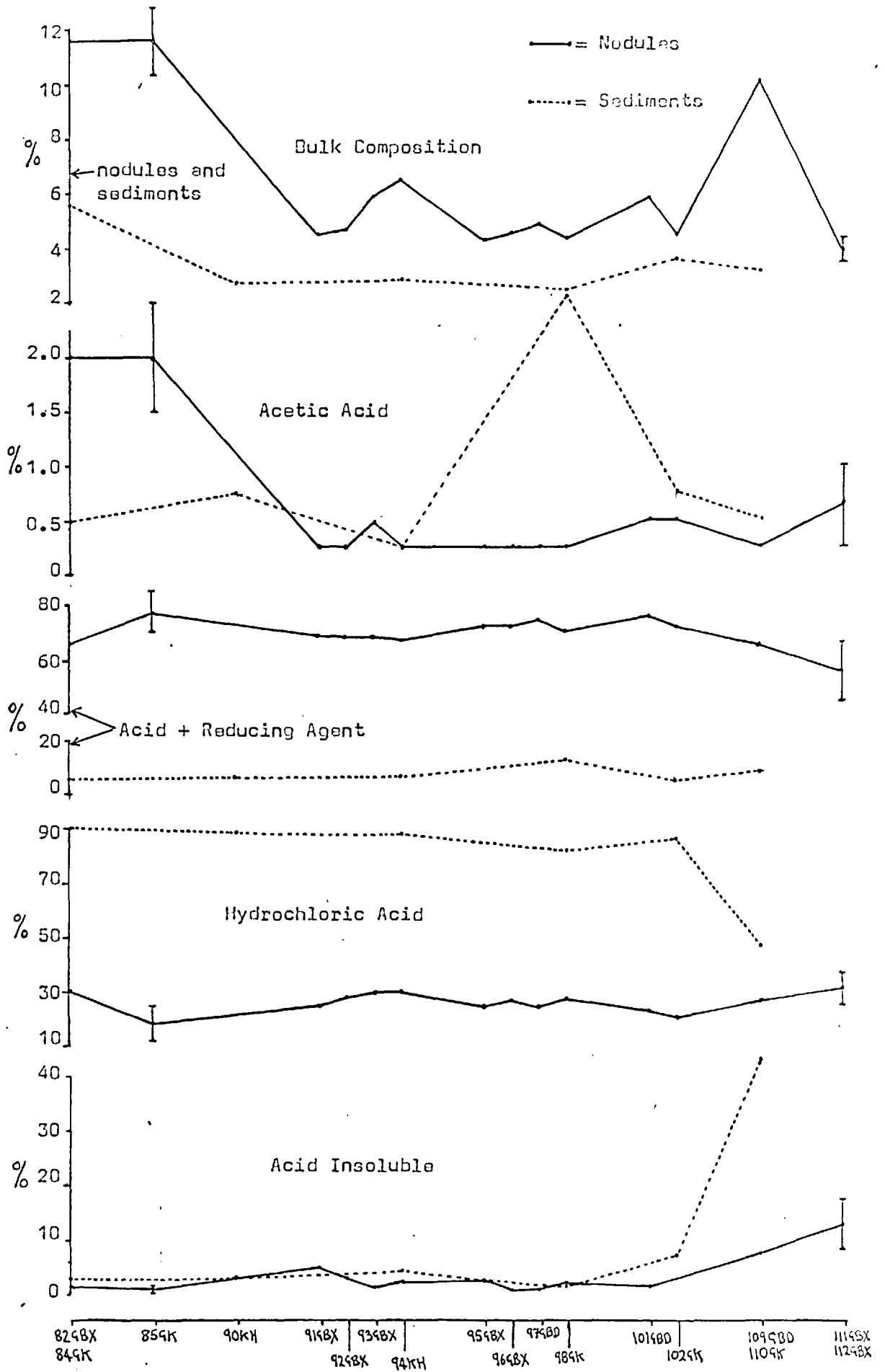


Figure 53a Co Partition in Madagascar Basin nodules and sediments.

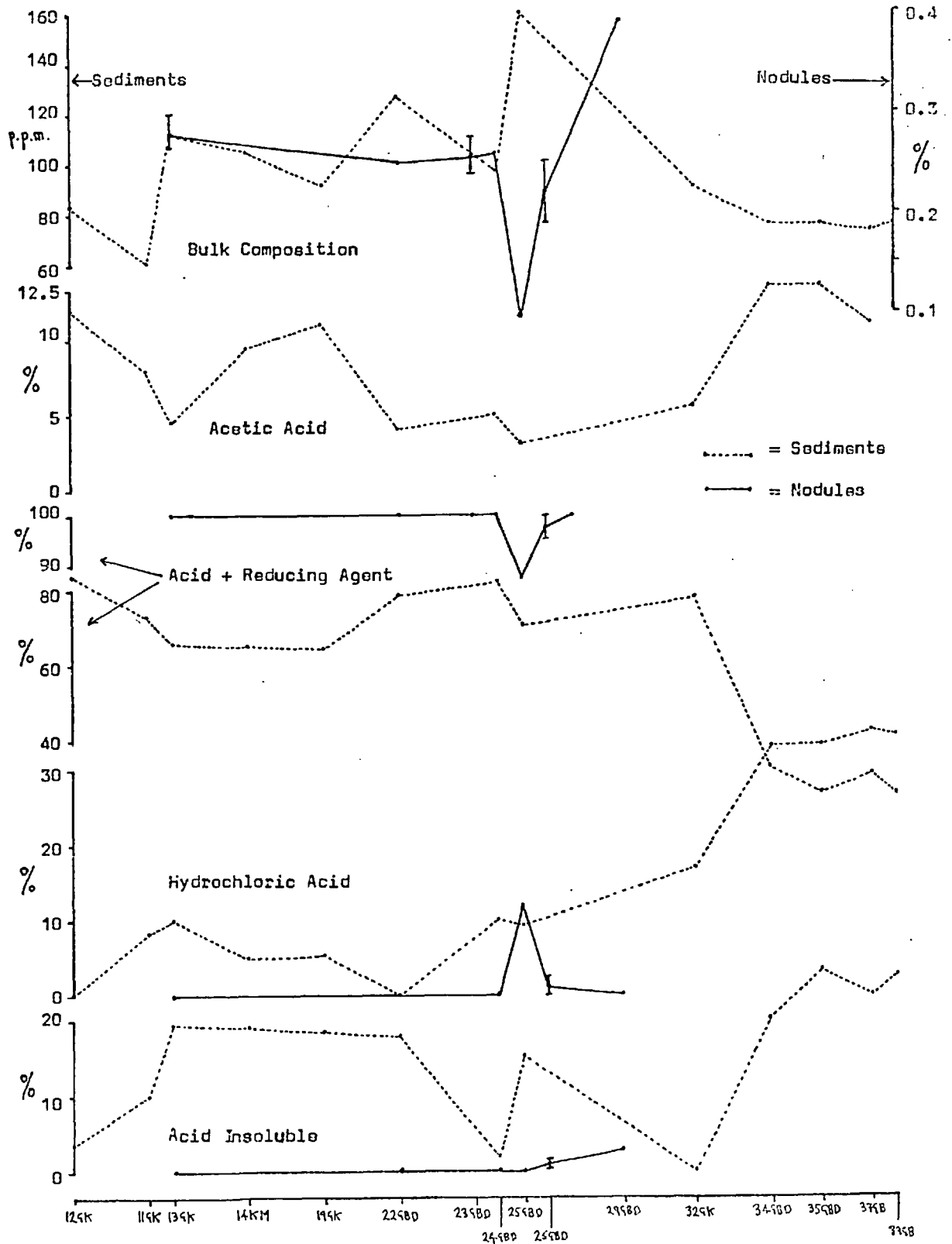


FIGURE 55b Co partition in Central Indian Basin nodules and sediments.

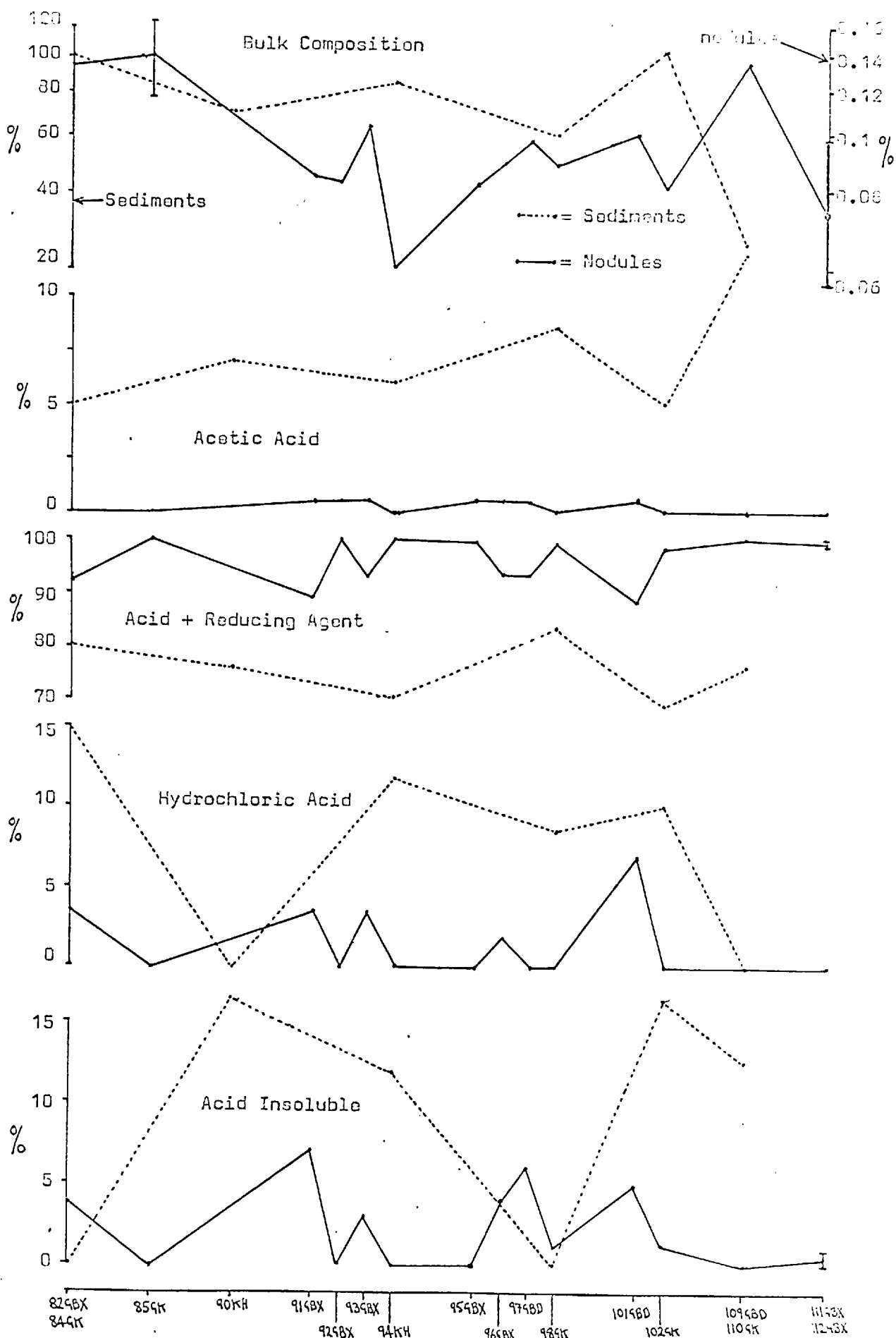


Figure 54a Ni Partition in Madagascar Basin nodules and sediments.

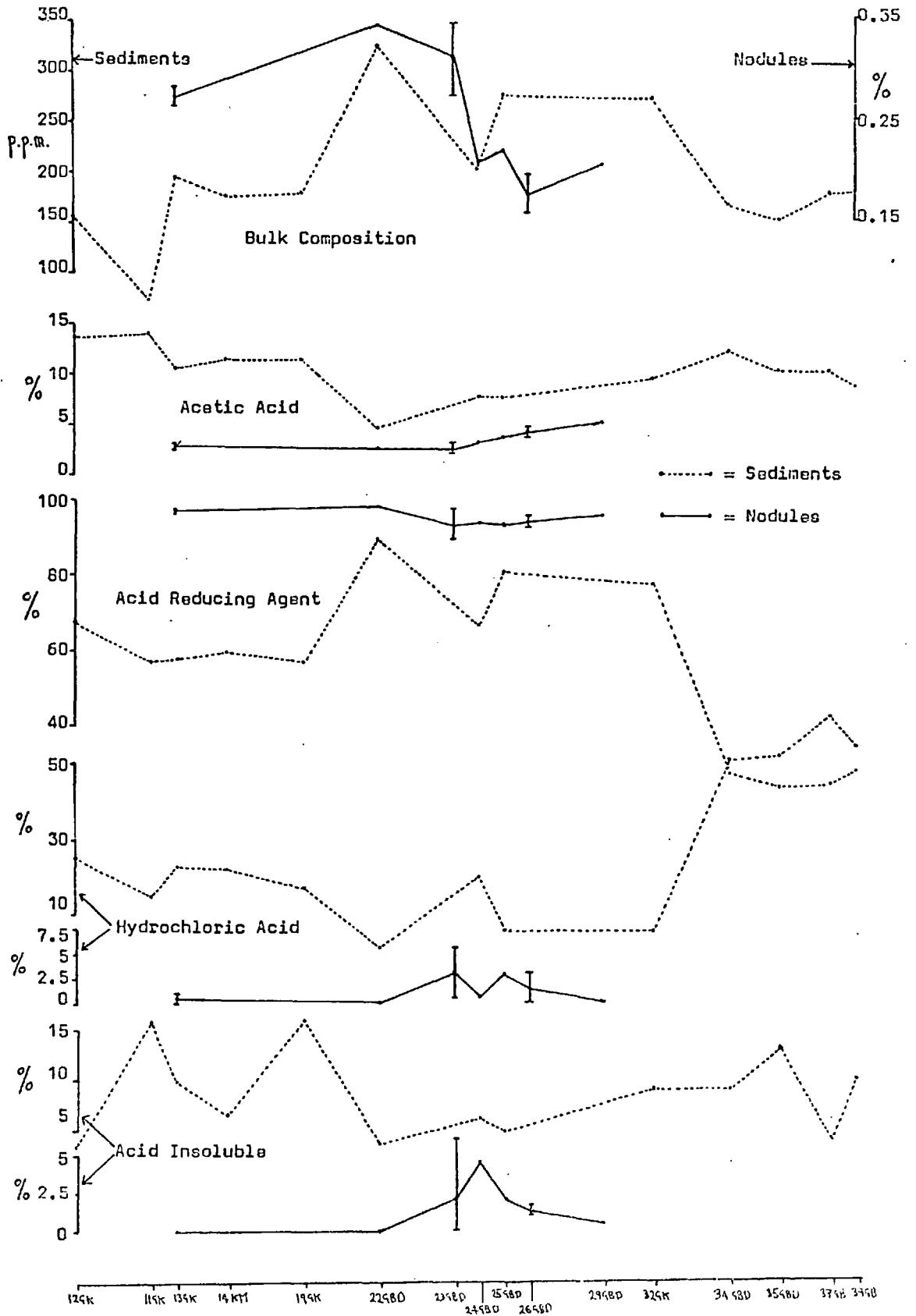




FIGURE 54b Ni partition in Central Indian Basin nodules and sediments.

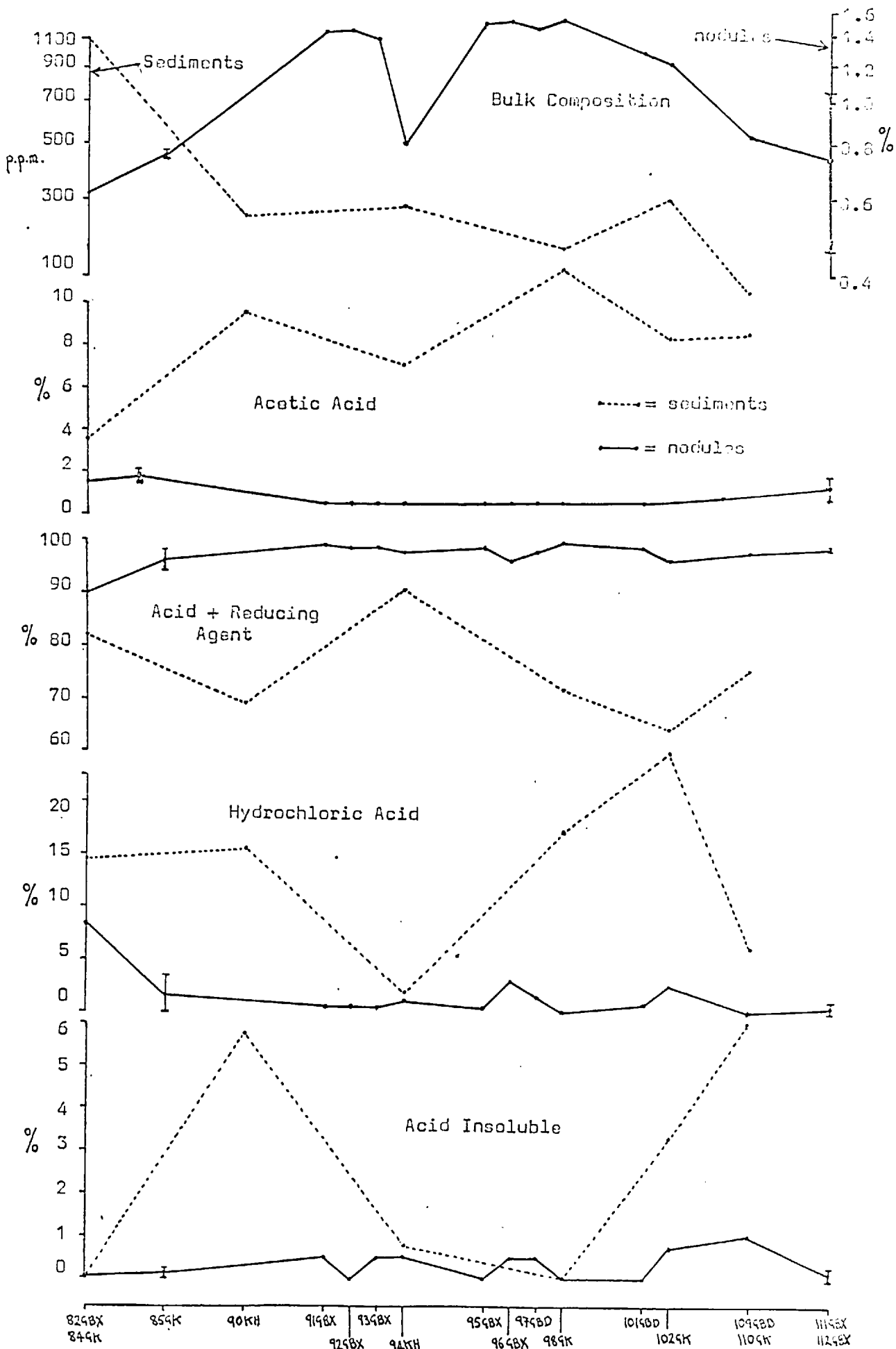


Figure 55a Cu Partition in Madagascar Basin nodules and sediments.

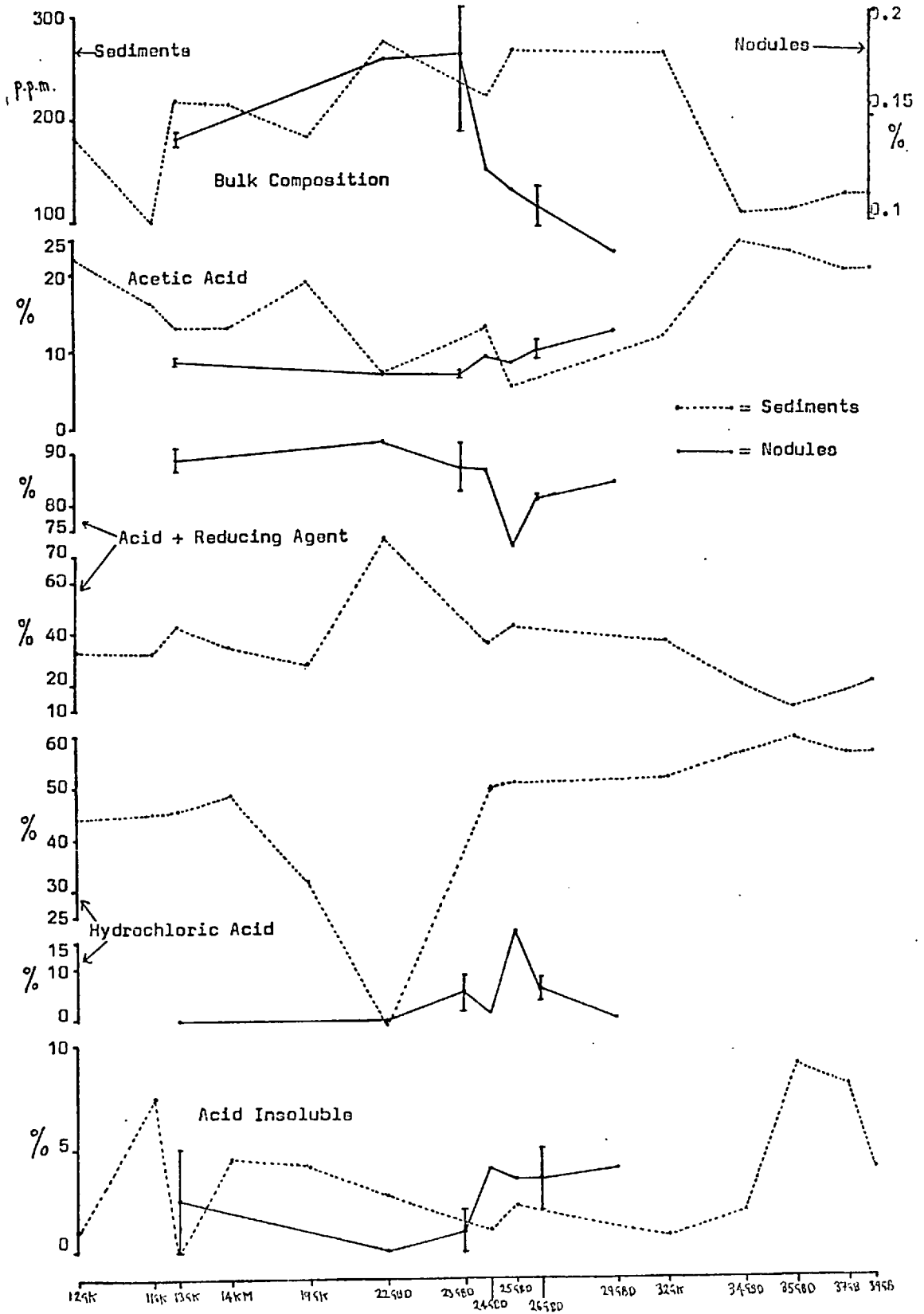


FIGURE 55b Cu partition in Central Indian Basin nodules and sediments.

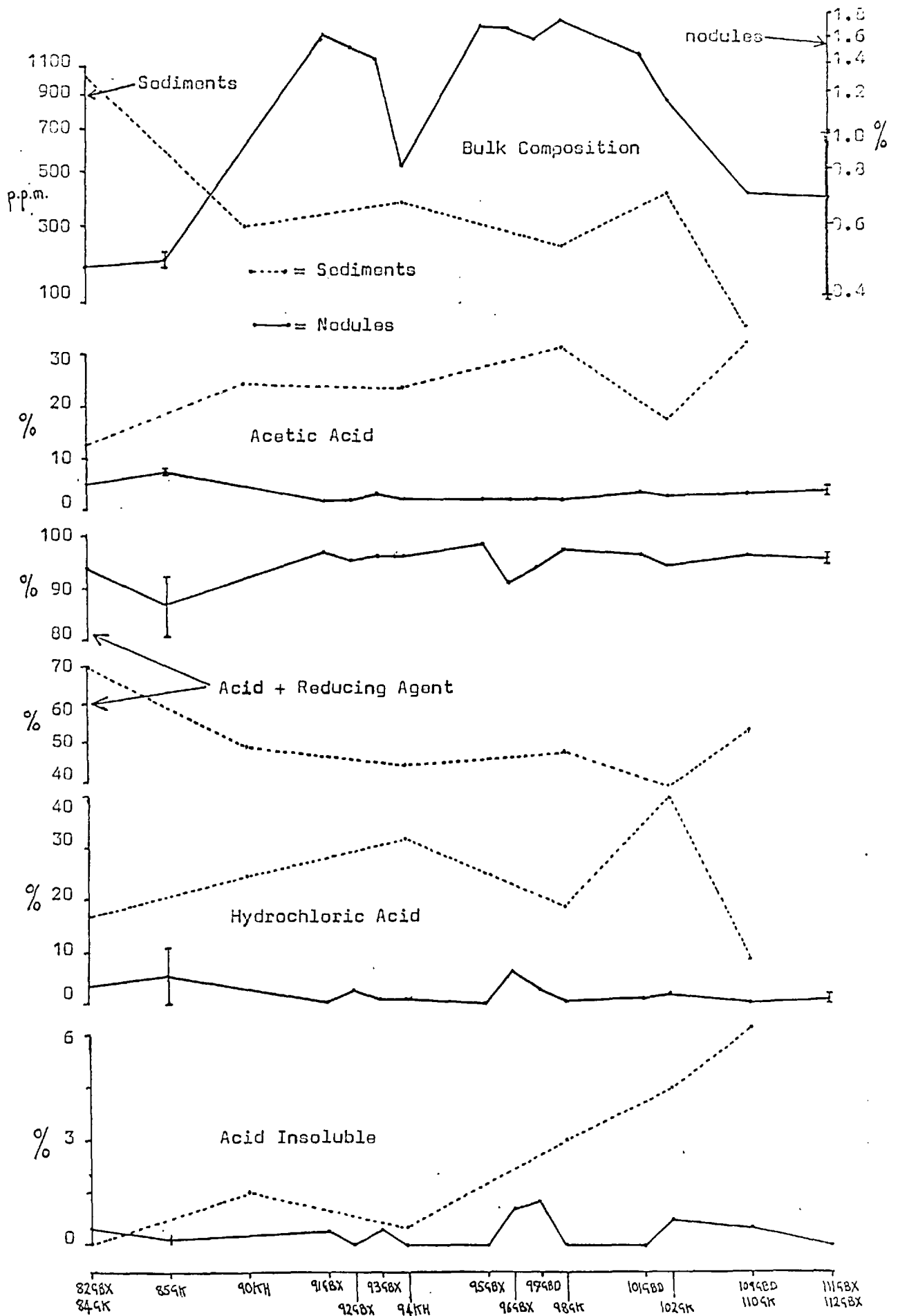
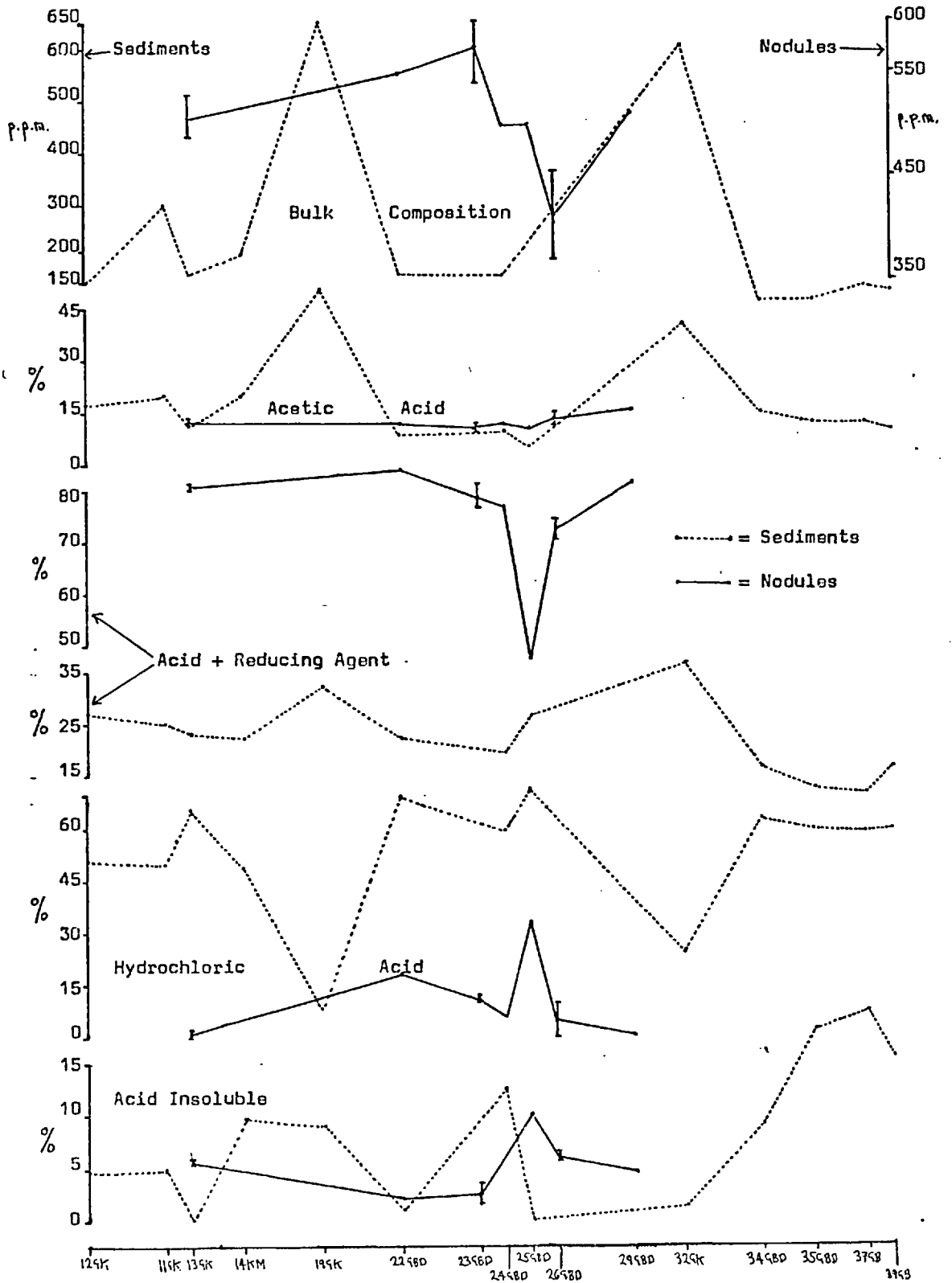


Figure 56a Zn Partition in Madagascar Basin nodules and sediments.



**FIGURE 56b** Zn partition in Central Indian Basin nodules and sediments

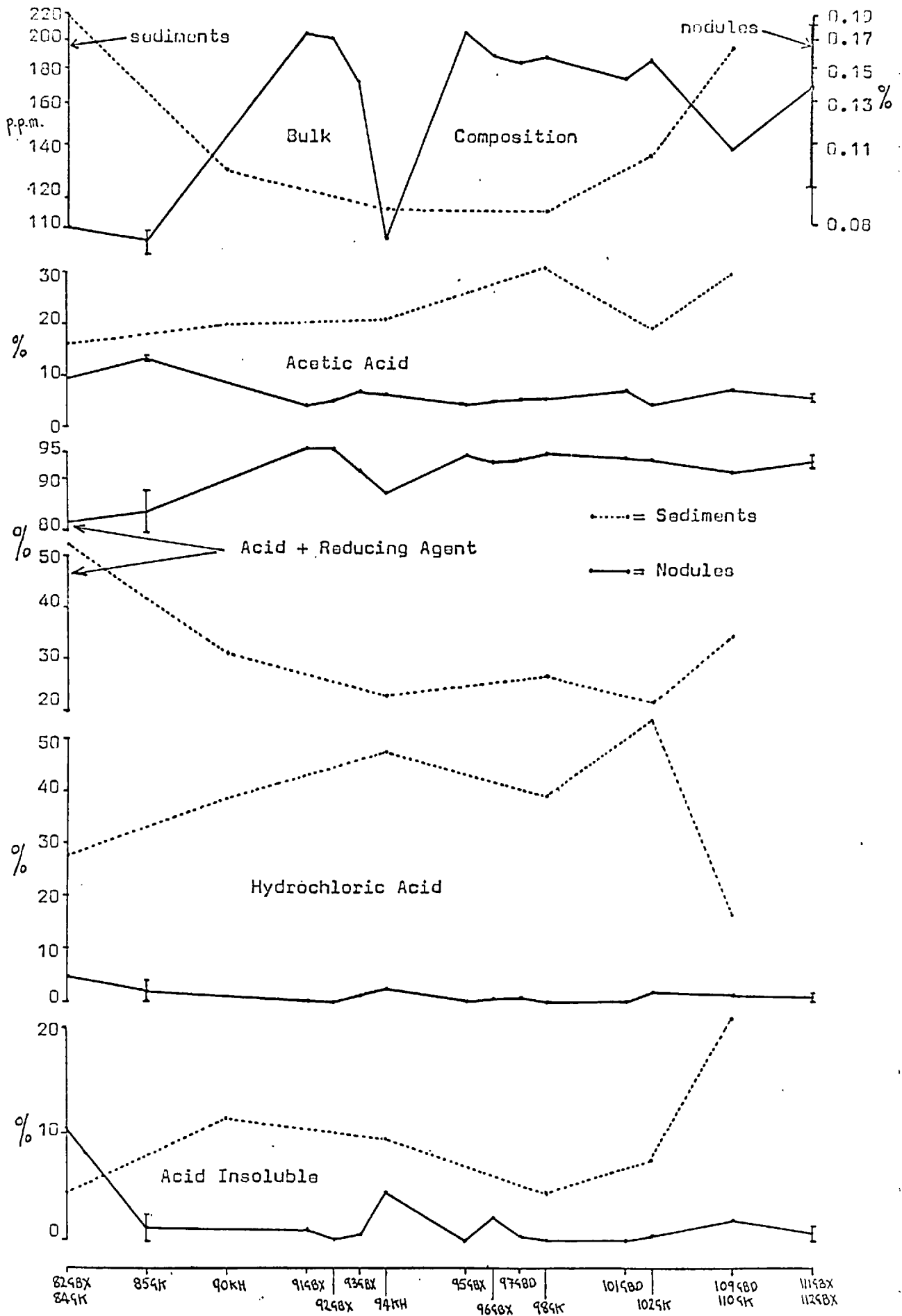


Figure 57a Pb Partition in Madagascar Basin nodules and sediments.

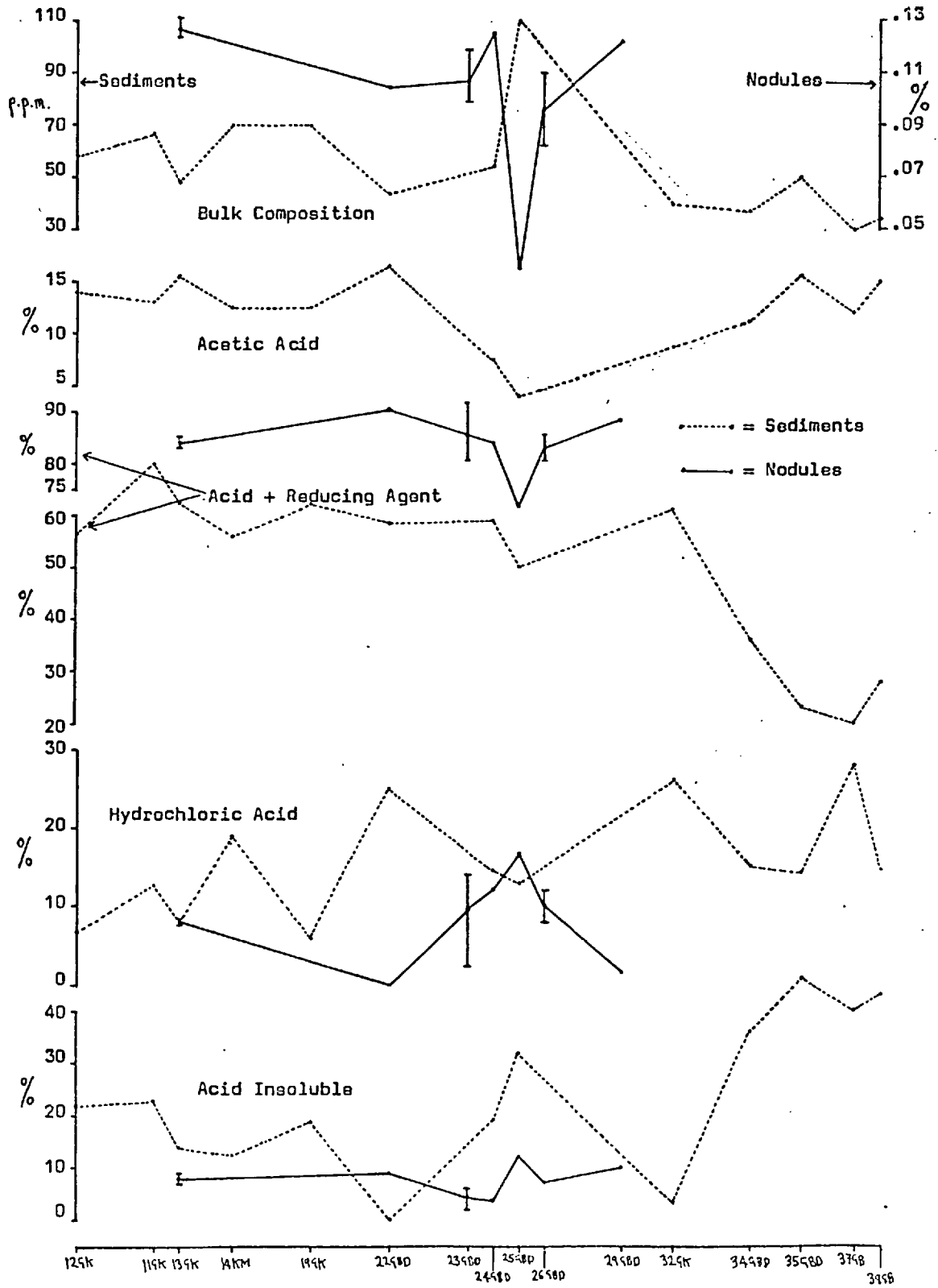


FIGURE 57b Pb partition in Central Indian Basin nodules and sediments.

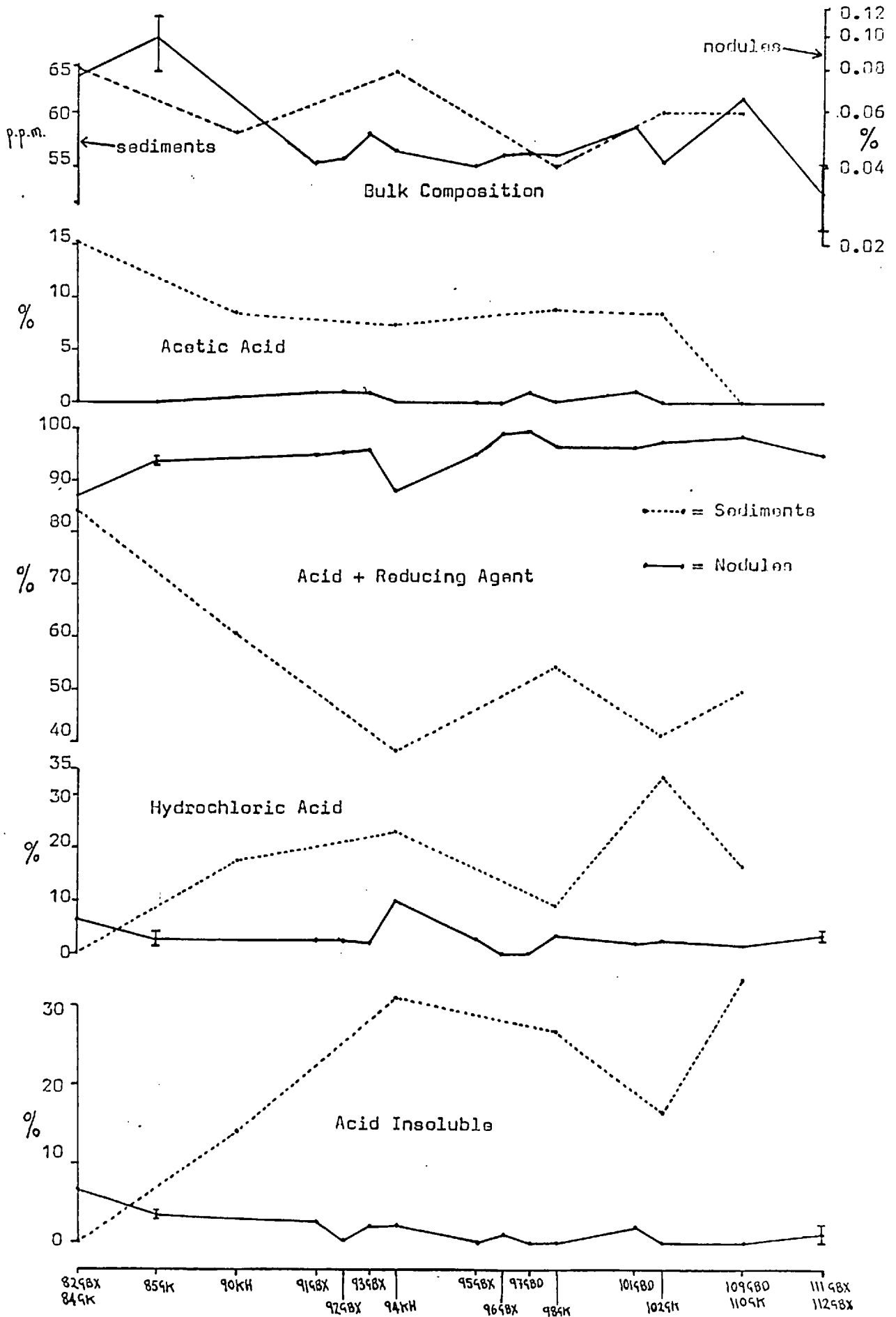
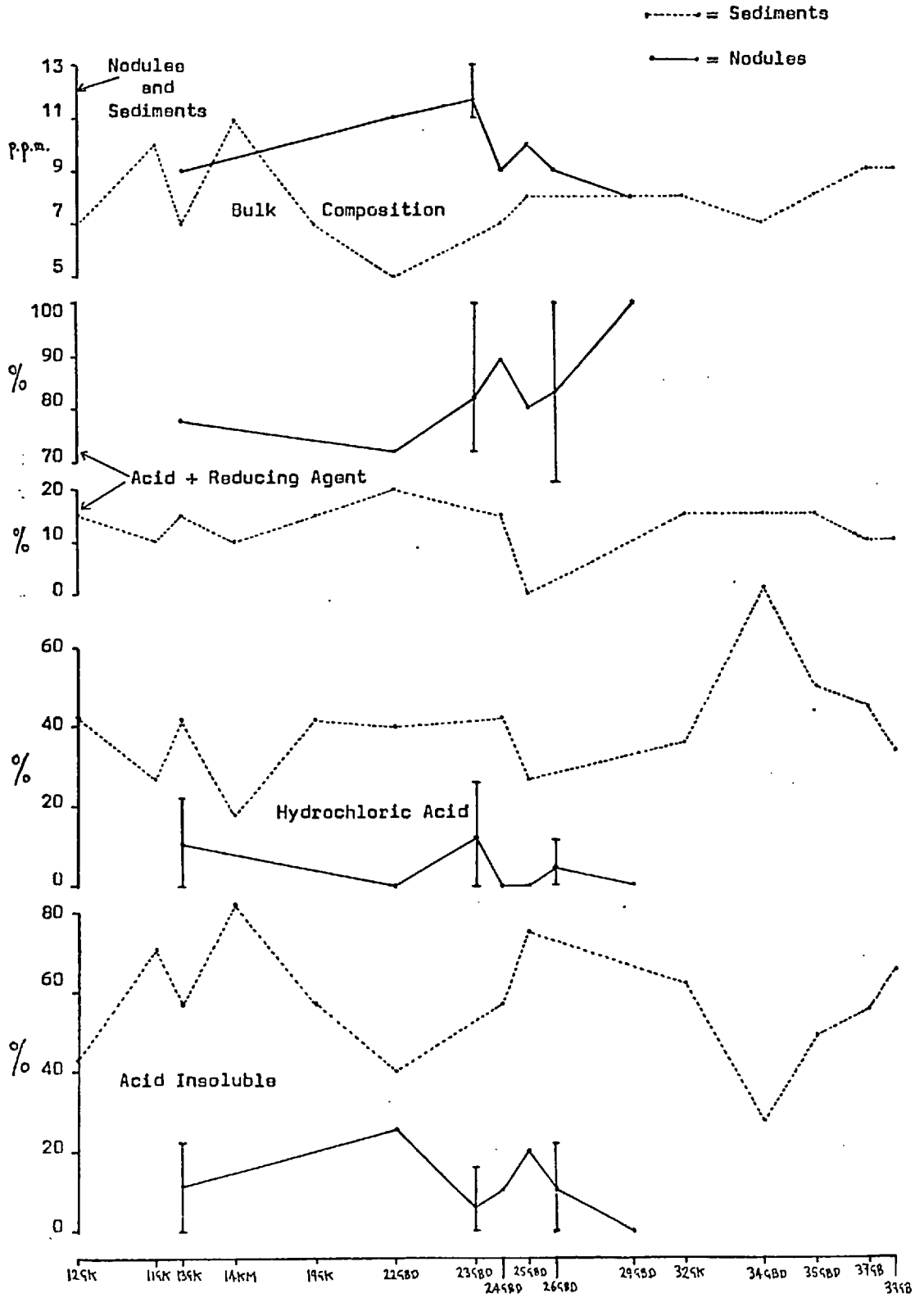


Figure 58a Cd Partition in Madagascar Basin nodules and sediments.





**FIGURE 50b** Cd partition in Central Indian Basin nodules and sediments.

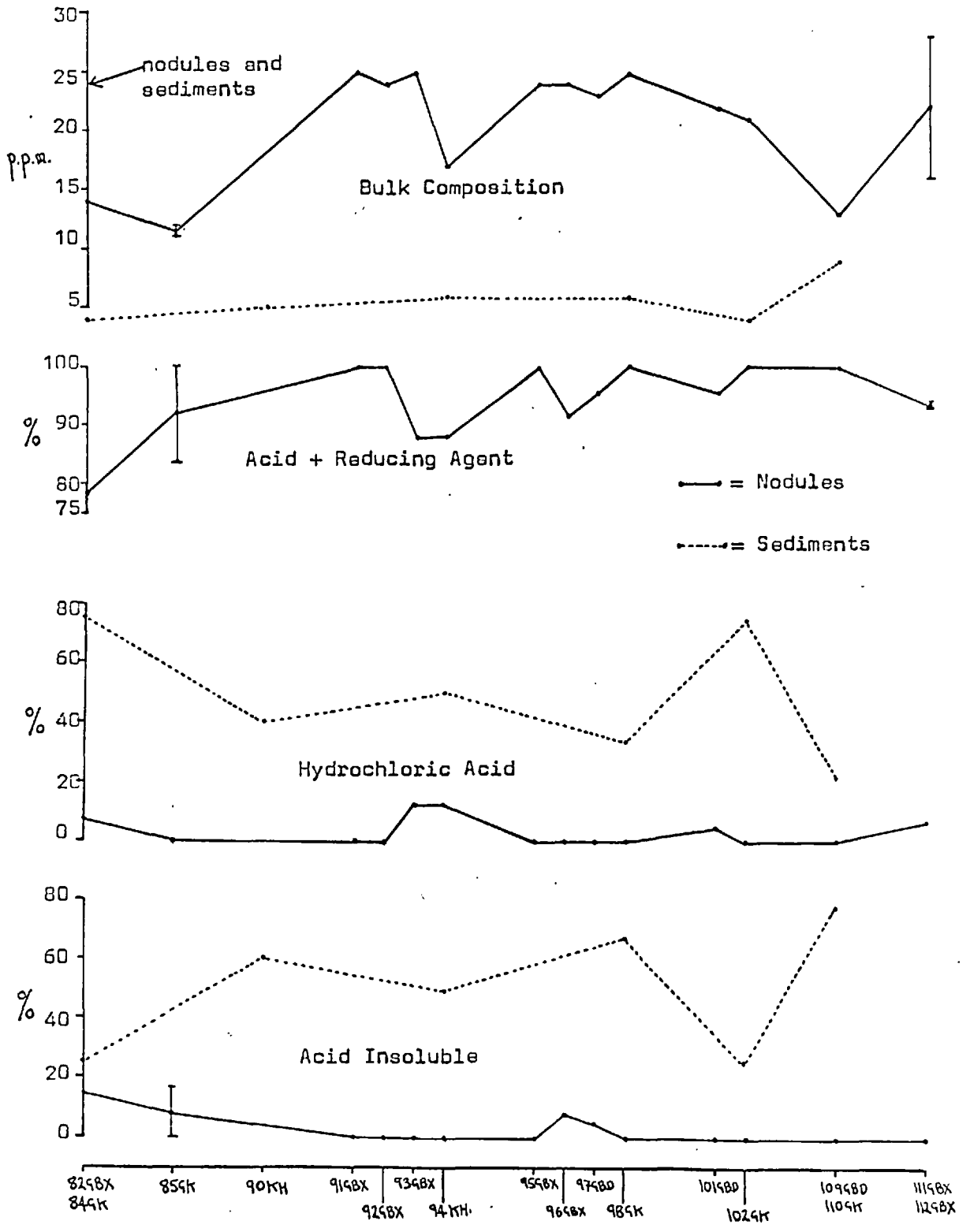
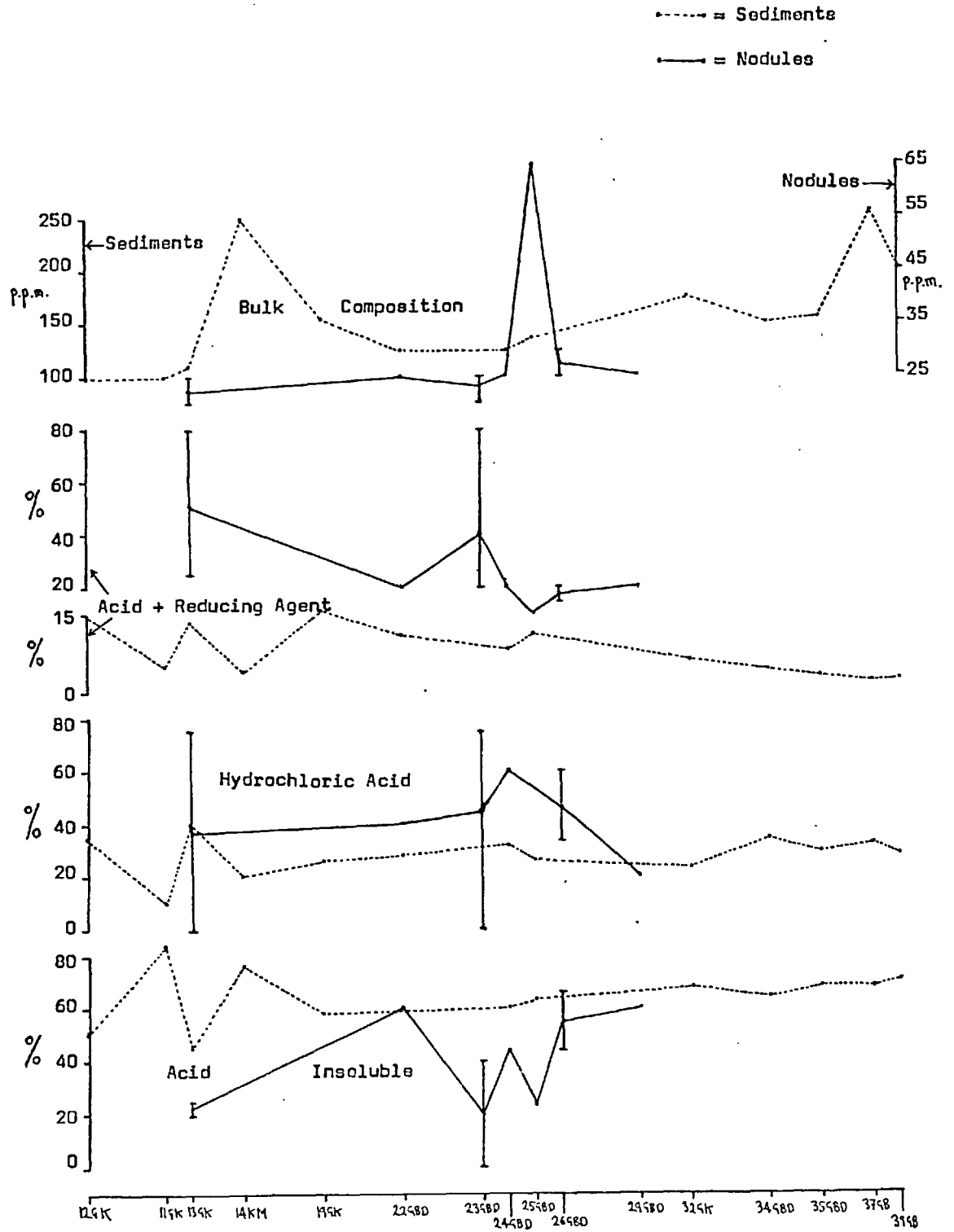


Figure 59a Cr Partition in Madagascar Basin nodules and sediments.



**FIGURE 59b** Cr partition in Central Indian Basin nodules and sediments.

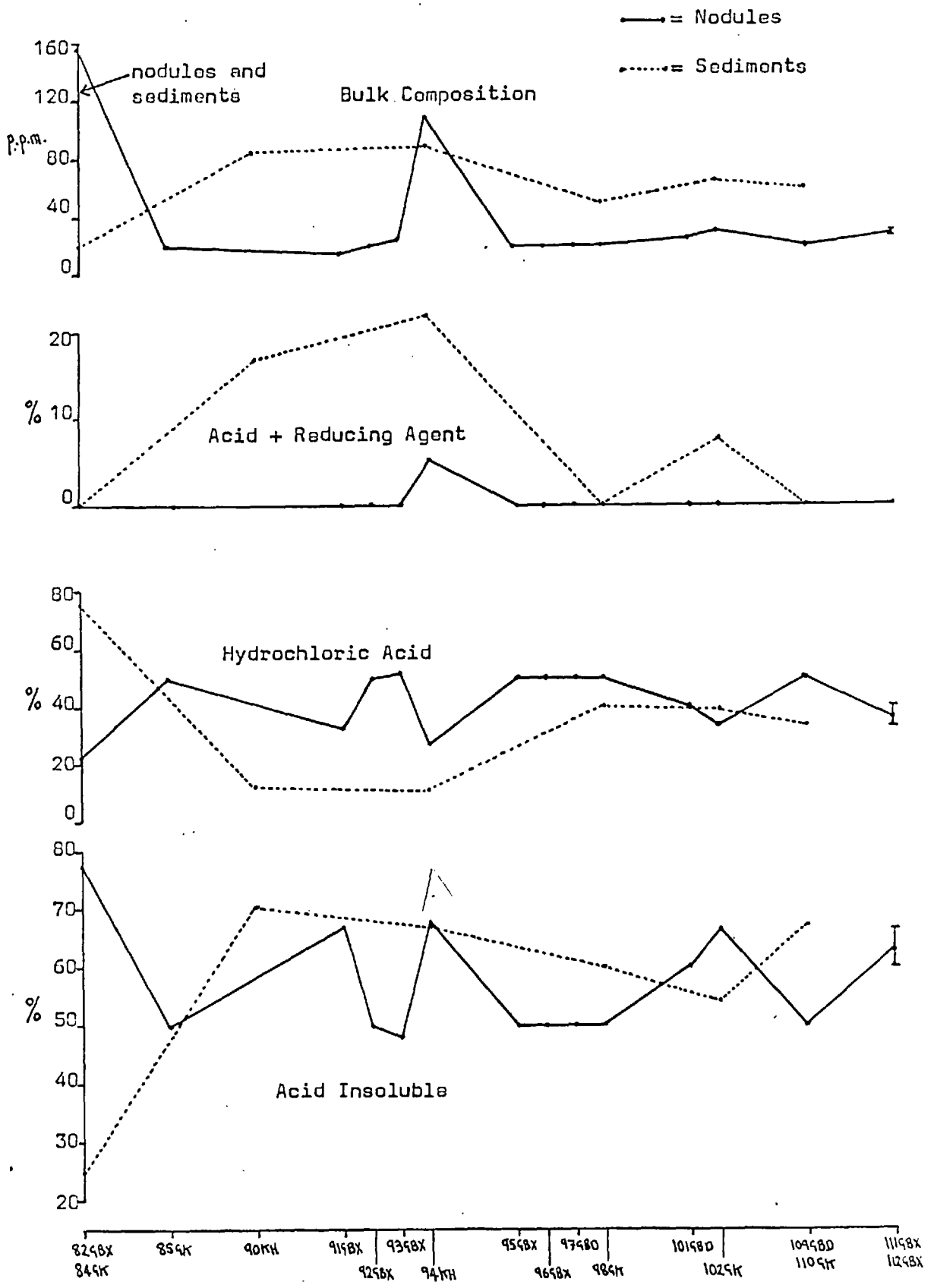


Figure 60a Ca Partition in Madagascar Basin nodules and sediments.

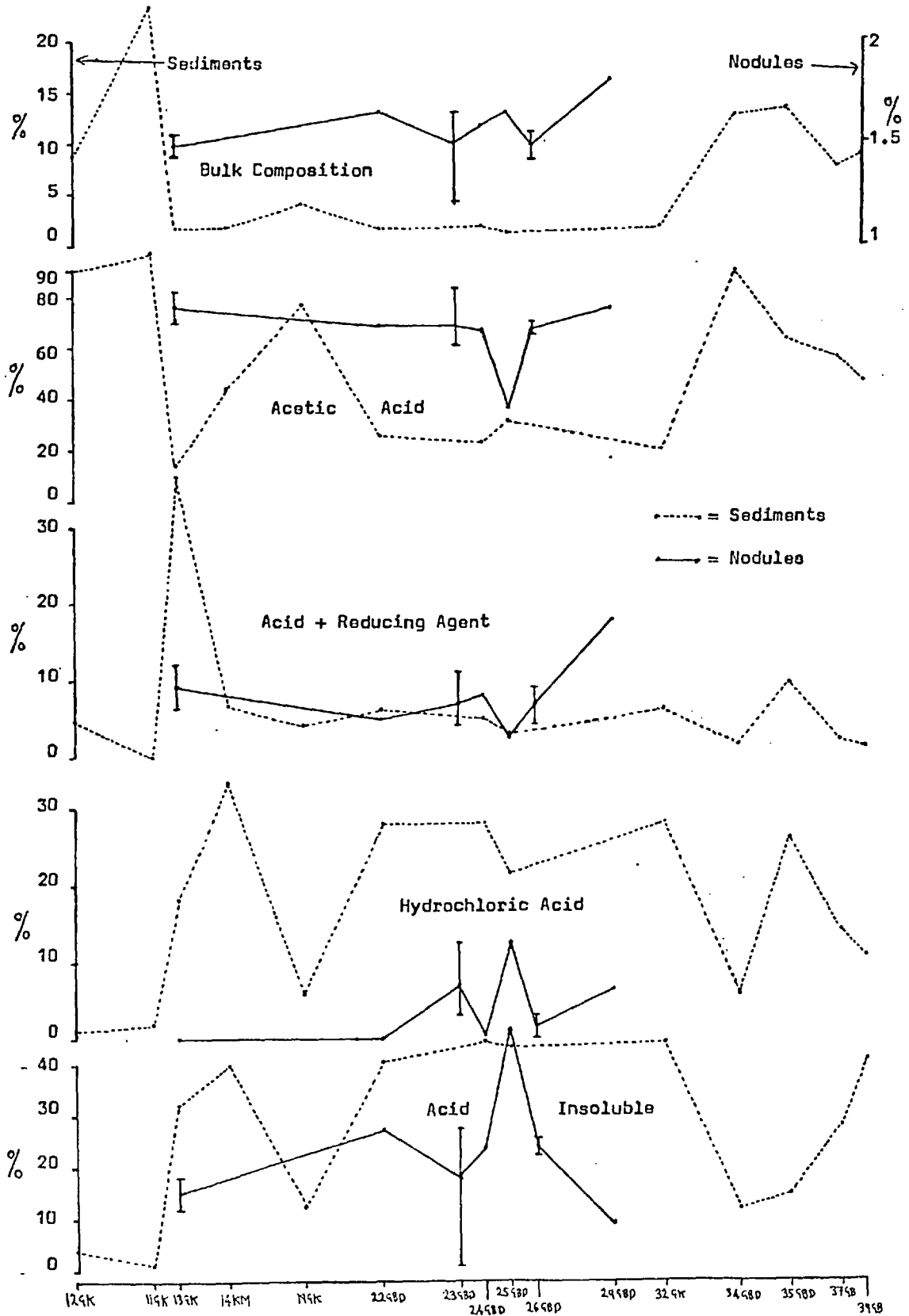


FIGURE 60b Ca partition in Central Indian Basin nodules and sediments.

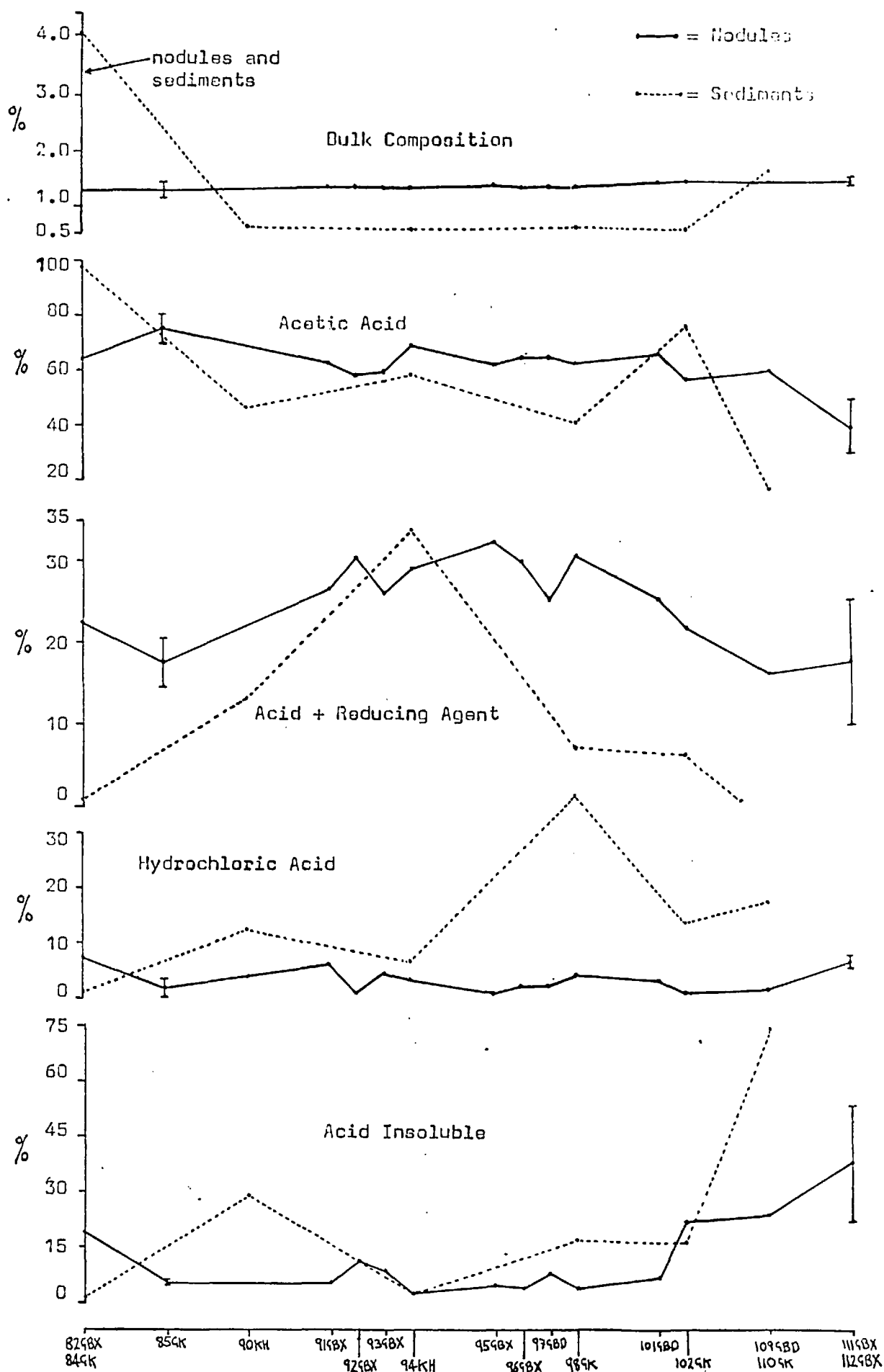


Figure 61a Al Partition in Madagascar Basin nodules and sediments.

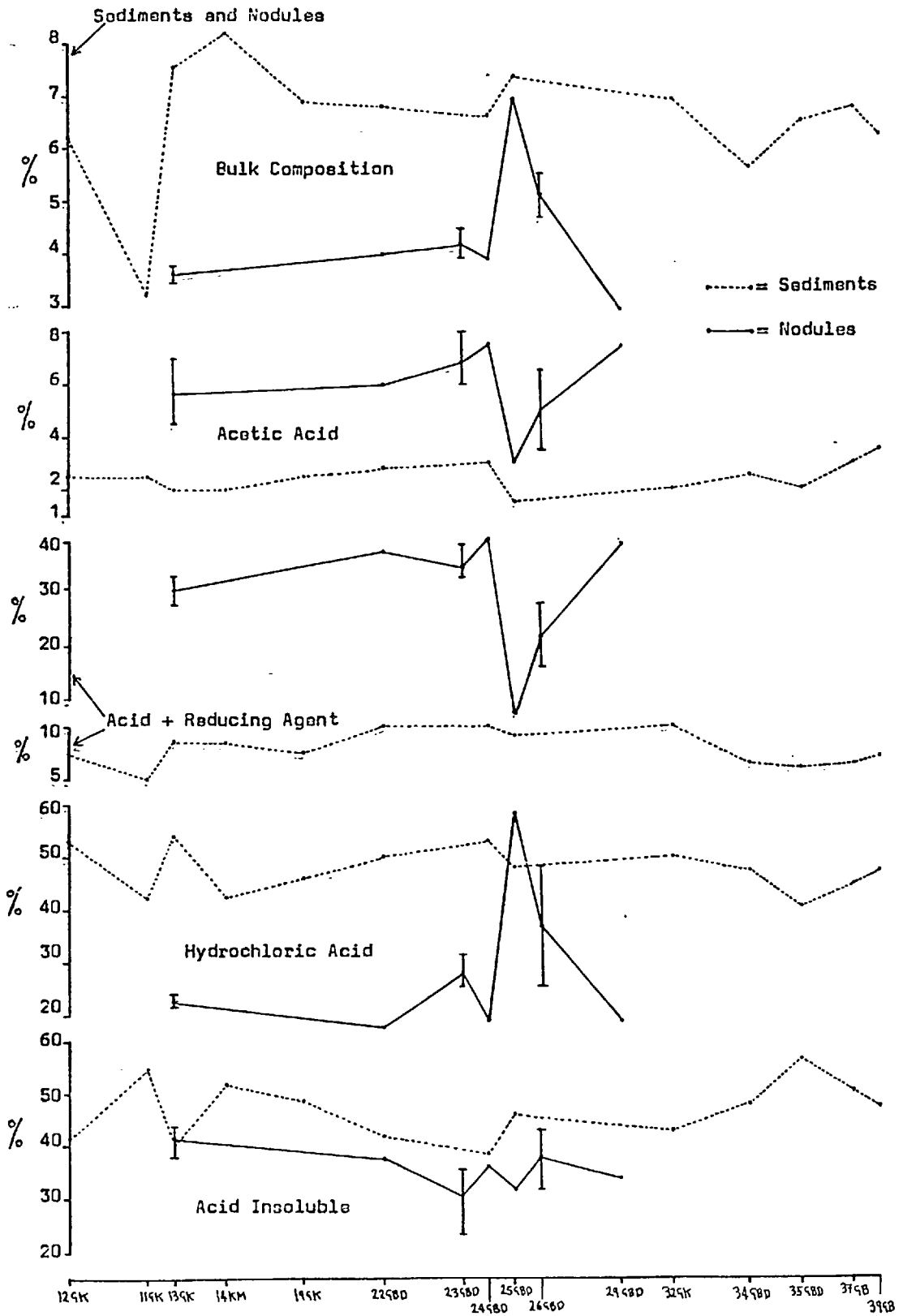


FIGURE 61b Al partition in Central Indian Basin nodules and sediments.

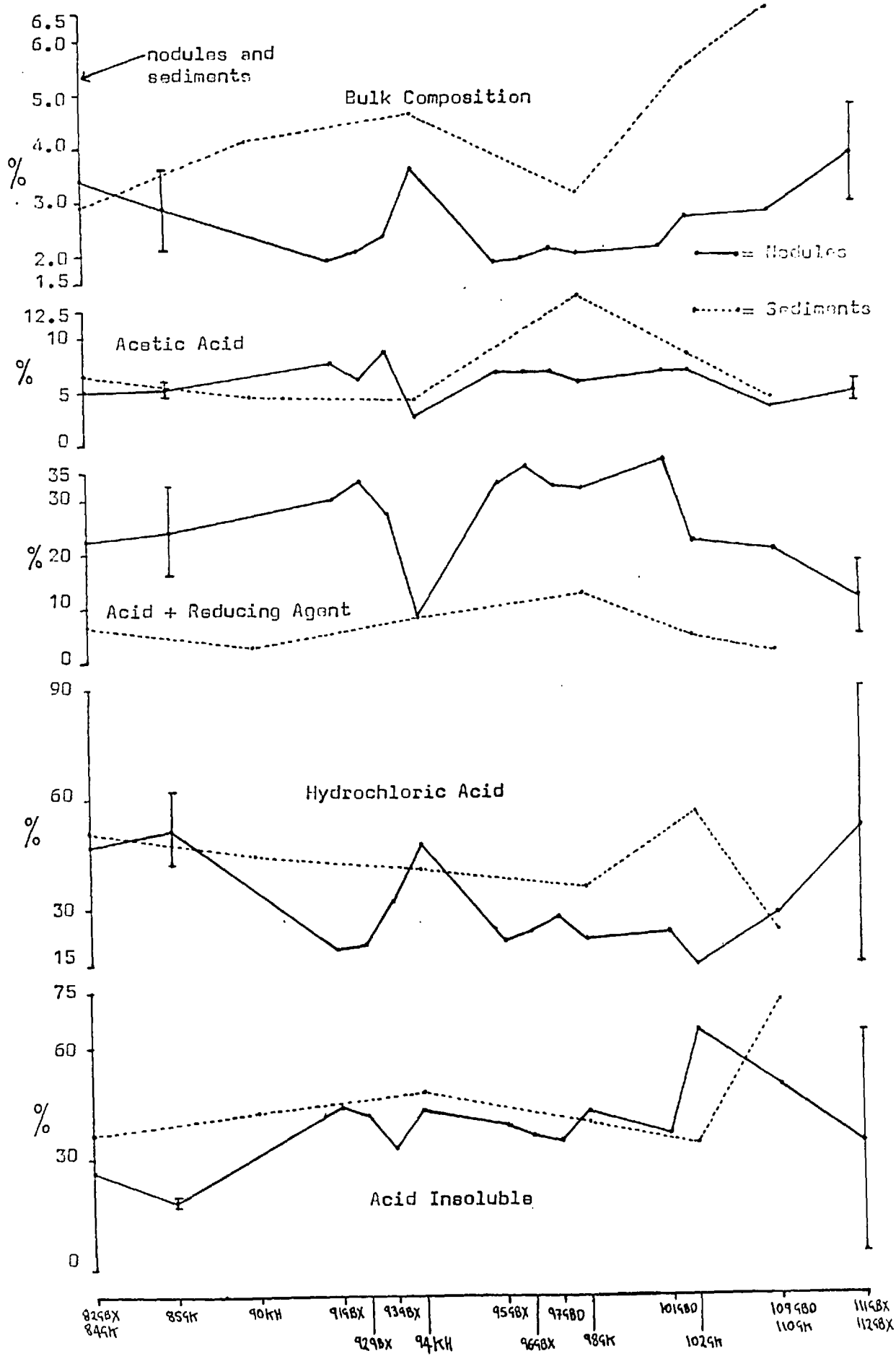
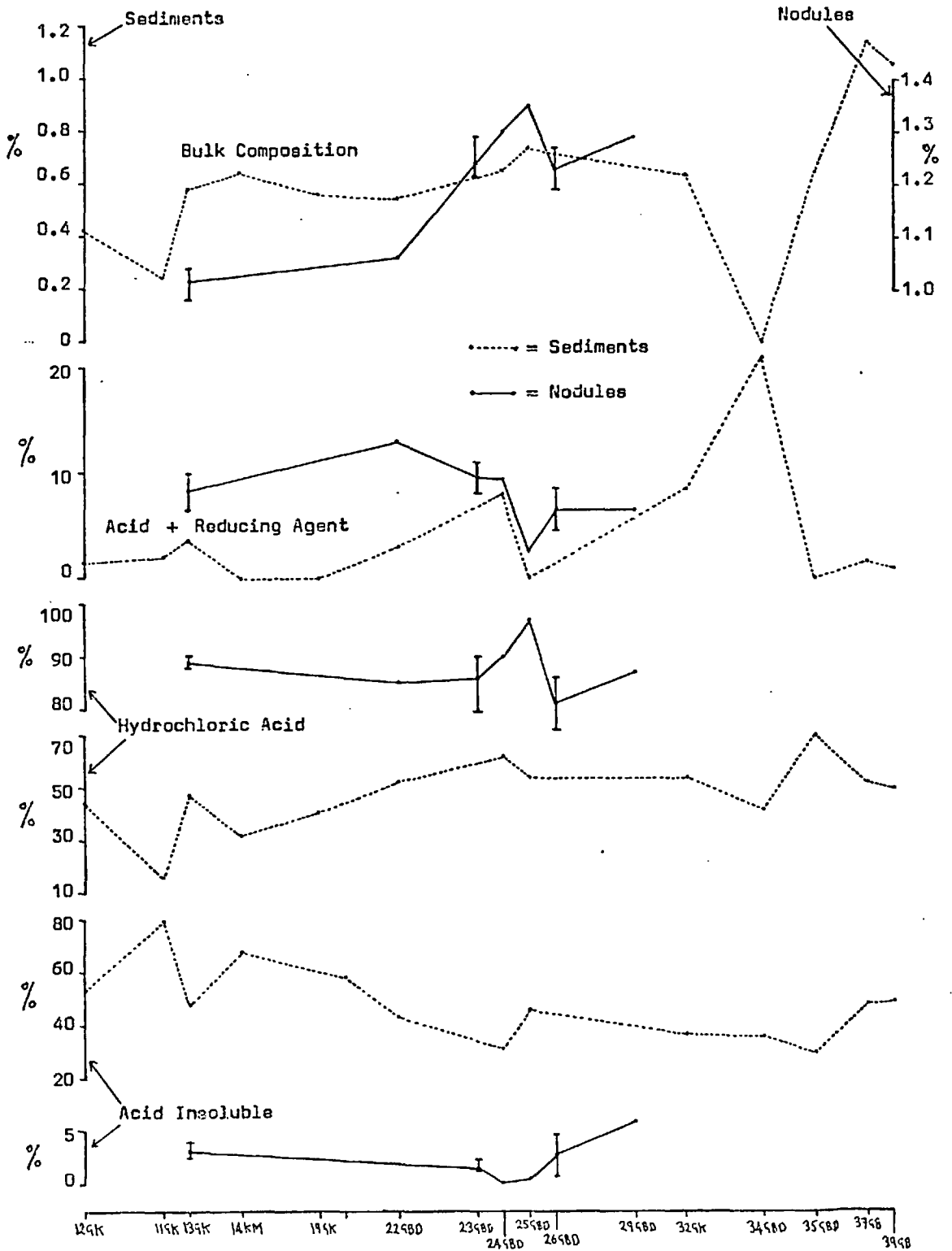
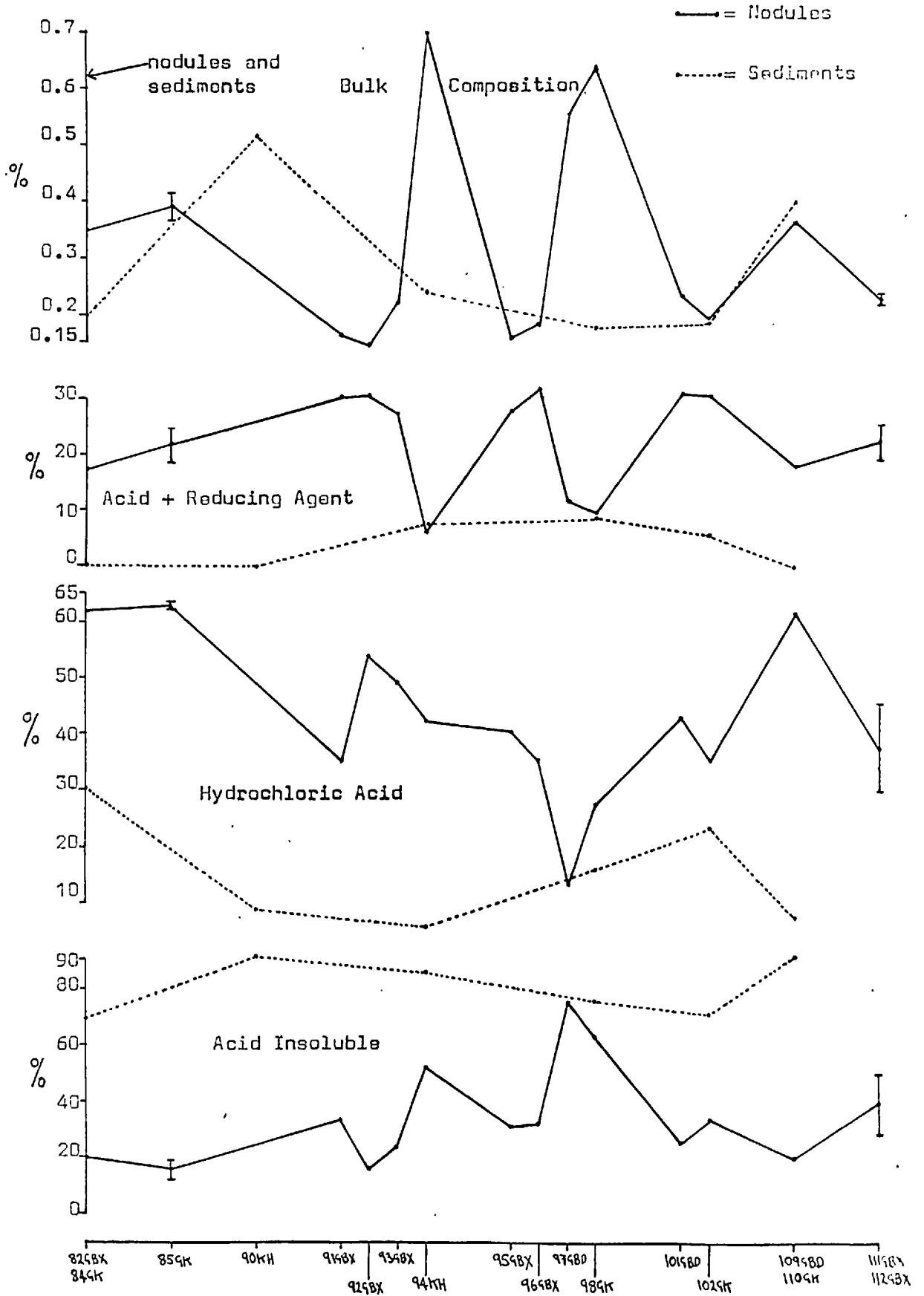


Figure 62a Ti Partition in Madagascar Basin nodules and sediments.





**FIGURE 62b** Ti partition in Central Indian Basin nodules and sediments.



the eastern end of the traverse.

Cobalt shows no recognisable trends in any of the fractions examined in Madagascar or Central Indian Basin samples. Almost all the Co is in the acid-reducible fraction, however a significant amount of Co is present in the HCL-soluble fraction of one sample from the Madagascar Basin. This same sample also contains an exceptionally high percentage of HCL-soluble iron. In both basins, the amounts of Co present in the HCL-soluble and acid-reducible fractions are so small that the variations observed can be accounted for totally in terms of analytical variance.

A slightly lower percentage of the total Ni in nodules is present in the acid-reducible fraction than is the case for cobalt. In the Madagascar Basin, amounts of acetic acid-soluble Ni increase slightly in samples where the total Ni is lower but there are no definite trends in the other three fractions. Again, trends in the HCL-soluble and acid-insoluble fractions fall within the range explainable solely in terms of analytical variance. Nickel shows no marked trends in Central Indian Basin samples either, however there is a slightly lower percentage of acid-reducible Ni in nodules from the western end of the traverse and a corresponding increase in the amounts of Ni in the acetic acid and HCL-soluble fractions.

Copper shows similar, but rather more marked trends to those of Ni. More Cu than Ni is present in the acetic acid-soluble fraction in samples from both basins. As was the case with Co, the Madagascar Basin samples containing goethite contained appreciable amounts of HCL-soluble Cu, but the trends in this fraction generally, and in the acid-insoluble fraction in both basins is explainable totally in terms of analytical variance.

Zinc also shows broadly similar trends to Ni and Cu, and its behaviour in sample 25GBD from the Madagascar Basin, which contained goethite, is similar to that of Co and copper.

Lead also shows a marked enrichment in the HCL-soluble fraction in sample 25GBD from the central part of the Madagascar Basin but levels of Pb in this fraction in other nearby samples are also high. There is a

corresponding decrease in amounts of acid-reducible Pb in these samples, but there is no definite trend in acid-insoluble Pb in this basin. In the Central Indian Basin Pb shows no marked trends in any fraction although there does seem to be a very slight decrease in acid-reducible Pb towards the western end of the traverse.

Any partition patterns of Cd and Cr across the basins are likely to be obscured in most fractions owing to the poor precision obtained for these elements at the low concentrations at which they are present. Only in fractions which contain a high percentage of the total of these elements are reliable trends likely to be observed.

Most of the Cd is present in the acid-reducible fraction of samples from both basins, as is the case with Co, Cu, Ni and Zn. In contrast to these elements however, Cd shows a definite increase in the acid-reducible fraction towards the north-eastern part of the Madagascar Basin traverse. The variations seen in Cd partition in the HCL-soluble and acid-insoluble fractions lie totally within the limits of precision of the method used to determine Cd in those fractions. In the Central Indian Basin Cd shows a similar partition pattern to Ni, Cu, Zn and Pb, being lower in the acid-reducible fraction in samples from the western part of the traverse but showing fairly irregular partition in this fraction over much of the rest of this basin.

The poor precision often obtained for Cr may account for the very large variations in its partition in samples from the Madagascar Basin traverse. Despite the large variation a definite increase in the percentage of acid-insoluble Cr towards the north-east part of the basin is observable and there is some decrease in acid-reducible Cr in the same direction. Chromium does not show any definite trends across the Central Indian Basin in any fraction.

In the Central Indian Basin, Cr appears to be present virtually exclusively in the HCL-soluble and acid-insoluble fractions, whilst in

Madagascar Basin samples at least 20%, and in some cases as much as 30% of the total Cr is acid-reducible.

Calcium does not show any very clear partition patterns in Madagascar Basin nodules, the only noticeable trends being that samples from the central part of the traverse contain a greater percentage of acid-insoluble Ca than those to the south-west and north-east. In the Central Indian Basin Ca shows rather more marked trends in partition. Acetic acid-soluble Ca decreases slightly from west to east across the basin but this trend does not appear to be depth dependent. Nodules from the central part of the traverse show a marked increase in acid-reducible Ca and by contrast amounts of acid-insoluble Ca are low in the centre of the traverse and increase markedly towards the east.

Like Ca, Aluminium shows no obvious trends in partition in Madagascar Basin samples. There does appear to be a very slight general decrease in acid-insoluble Al from south-west to north-east across the basin. Samples from the central part of the traverse show rather variable partition in both fractions. As was the case with Fe and several trace metals, sample 25GBD shows a markedly different partition of Al to most other samples in the basin. In this sample, from the central part of the traverse, there is a much greater percentage of HCl-soluble Al and a much smaller percentage of acid-reducible Al than in other samples from this traverse. The increase in HCl-soluble Al corresponds well with the high total Al in this sample. Aluminium displays much clearer partition patterns in samples from the Central Indian Basin.

There is some increase in acid-insoluble Al in nodules from west to east across this basin although samples at the eastern end of the traverse do show a very wide variation in partition. With the exception of one sample, 94KH, nodules from the central part of the traverse are much lower in HCl-soluble Al than those from the western and eastern parts of the traverse. The trend of HCl-soluble Al closely matches the trends in total Al

in the samples along the traverse. Acid-reducible Al in C.I.B. samples tends to exhibit an inverse trend to that of HCL-soluble Al, being higher in samples from the central part of the basin but again sample 94KH does not follow the general trend, being anomalously low in acid-reducible aluminium.

Titanium does not exhibit any clear trends in partition in the Madagascar Basin. The percentage of acid-reducible Ti tends to decrease towards the north-east but this trend is not marked. No clear trend occurs in the HCL-soluble fraction and levels of Ti in the acid-insoluble fraction are too low for any trend to be identified. In the Central Indian Basin, the partition patterns of Ti along the traverse tend to be obscured by the large variability in Ti partition in samples even from very closely-spaced sites and no clear trends are visible. However samples from the western end of the traverse contain a higher percentage of HCL-soluble Ti than samples from the rest of the traverse.

#### (b) VARIATION IN SEDIMENT PARTITION ALONG THE TRAVERSE

Because of the larger number of samples collected in the Madagascar Basin, trends in element partition in sediments from that basin are more clearly defined than in those from the Central Indian Basin.

In contrast to its behaviour in nodules, Mn shows very clear trends in partition in sediment samples from both basins. In the Madagascar Basin, samples from the north-east part of the traverse contain a larger percentage of acetic-acid soluble Mn than samples from the rest of the traverse. This trend is repeated in the HCL-soluble and acid-insoluble fractions and is the opposite of that occurring in the acid-reducible fraction. In the Central Indian Basin there is a marked decrease in the amount of acid-reducible Mn from west to east across the basin. Correspondingly the percentage of HCL-soluble Mn increases from west to east and there is a

smaller increase in acetic acid-soluble Mn from west to east. Levels of Mn in the acid-insoluble fraction are too low to be meaningfully discussed.

Iron behaves similarly to Mn in the Madagascar Basin, at least in the acetic acid-soluble and acid-insoluble fractions. In both these fractions Fe is enriched in samples from the north-east part of the basin, this enrichment being especially marked in the acid-insoluble fraction. Hydrochloric acid-soluble Fe shows a slight decrease from south-west to north-east across the basin but there does not appear to be any observable trend across the basin in the acid-reducible fraction.

In the Central Indian Basin, Fe shows no trends, but the easternmost sample shows a marked drop in HCL-soluble Fe and an increase in acid-insoluble iron.

Cobalt shows much more clearly-defined trends in the Madagascar Basin than in the Central Indian Basin. In the latter there is a slight increase in acetic acid-soluble Co from west to east but no overall trend is visible in the acid-reducible fraction. The variability in Co partitioning in the HCL-soluble and acid-insoluble fractions, which shows no trends across the C.I.B., is probably due at least partly to analytical variance. In the Madagascar Basin there is a very marked decrease in the percentage of acid-reducible Co in the north-east part of the basin and a corresponding increase in the HCL-soluble Co in these samples. Cobalt levels in the acetic acid-soluble fraction are too low to allow accurate interpretation. Amounts of Co in the acid-insoluble fraction are higher but are very variable and there does not appear to be any significant trend in this fraction across the basin.

Nickel shows some similarities to Co in its partition patterns in both basins. In the Madagascar Basin, Ni is much lower in the acid-reducible fraction and higher in the HCL-soluble fraction in samples from the north-eastern part of the traverse. Nickel does not show any significant trends in the acid-insoluble fraction. In both basins, Ni values in the acetic acid-

soluble fraction are so low that the variations in partition observed lie within the limits of analytical precision and are therefore not significant. In the C.I.B. Ni shows no trends in the acid-reducible fraction or in the HCL-soluble and acid-insoluble fractions, Ni levels in the latter two fractions being very erratically variable.

Copper shows slightly different partition patterns to those of Co and nickel. In the Madagascar Basin, Cu shows a more marked decline in the acetic acid-soluble fraction in the central part of the traverse than do Co and nickel. This decrease is too large to be attributable simply to analytical error. Copper is also lower in the acid-reducible fraction in samples from the north-eastern part of the basin but this decline is not nearly so marked as that displayed by Co and nickel. In the HCL-soluble fraction Cu shows a slight increase from south-west to north-east along the traverse but there is no marked increase towards the north-east as is the case with Co and nickel. Furthermore, the partitioning of Cu in sample 22GBD is markedly anomalous in the acid-reducible and HCL-soluble fractions, this was not the case for Co and Ni in this sample. In the C.I.B., Cu shows an increase in the acid-reducible fraction in the western part of the basin but is fairly constant along the rest of the traverse. The increase in acid-insoluble Cu from west to east across the basin is small enough to be accountable for solely by analytical error. Similarly, Cu values are too low in the acetic acid-soluble fraction for any accurate trend to be assessed. Whilst not as variable as those of Co and Ni, Cu values in the HCL-soluble fraction show no noticeable trends. The total Ni and Cu content of the samples falls very markedly from west to east across the C.I.B. but this does not appear to markedly affect the partitioning of either element in any of the fractions examined.

Zinc shows a very similar partition pattern to Cu in the Central Indian Basin but not in the Madagascar Basin. In the latter basin Zn shows a slight decrease in the acid-reducible fraction in the north-east, but this

trend is not nearly so marked as that observed for Ni and Cu and some samples, particularly sample 32GK, do not follow the trend at all. In the other three fractions, Zn is very variable and shows no definite trends.

Lead shows slightly more well-defined trends in both basins than most of the other trace metals. In the Madagascar Basin, acid-reducible Pb is much lower in samples from the north-east part of the traverse, as is the case with the other trace metals. Amounts of Pb in the HCl-soluble and acid-insoluble fractions are rather variable but there is some enrichment of Pb in the acid-insoluble fraction in samples from the north-eastern extremity of the traverse. In the C.I.B., acid-reducible Pb is fairly constant along the traverse but increases markedly at the western end of the traverse. Conversely, acid-insoluble Pb increases towards the east. Levels of Pb in the acetic acid-soluble phase are too near the detection limit for any significant trend to be observed, and no clear trend occurs in HCl-soluble Pb either.

Levels of Cd in the separate fractions of the sediments were near or below the detection limit, hence no accurate partition patterns could be identified.

Chromium does not show any major trends in partition in either basin. In the Madagascar Basin, acid-reducible Cr does show some decrease towards the north-east but the main feature of Cr partitioning in all three fractions in which it was detected is its increased variability in samples from the south-west part of the basin. In the Central Indian Basin, samples 90KH and 94KH contain a higher percentage of acid-reducible Cr and a much lower percentage of HCl-soluble Cr than other samples along the traverse. The sample from the western end of the traverse, by contrast, displays an anomalously high percentage of HCl-soluble Cr and a very low percentage of acid-insoluble Cr. There are no general trends across the basin however in any of the fractions examined. Calcium is rather variable in its partition especially in the Madagascar Basin. In the acetic acid-soluble fraction



in this basin, Ca is lower in samples from the central part than in those towards the south-west and north-east. In general, high Ca in this phase correlates well with high Ca in the bulk sample which therefore indicates the presence of carbonate material. By contrast, the non-carbonate sediments from the central part of the basin contain a greater percentage of HCL-soluble Ca and acid-insoluble Ca. No obvious trend occurs in the acid-reducible fraction, but one sample, 13GK, contains very much more acid-reducible Ca than any of the other samples. In the Central Indian Basin, acid-reducible Ca is highest in the centre of the traverse. Calcium in the HCL-soluble fraction shows a slight increase from west to east whilst acetic acid-soluble Ca shows a decrease from west to east. The sample from the eastern end of the traverse contains an anomalously high percentage of acid-insoluble calcium.

Aluminium does not exhibit very clear partition trends in either basin. In the Madagascar Basin Al shows no trends in any fraction. In the Central Indian Basin, however, there is a fairly marked decrease in the percentage of HCL-soluble Al from west to east, with the exception of one sample. This is in contrast to a general increase in Al in the bulk sample from west to east. Aluminium shows no definite trends in any of the other fractions.

Titanium also does not show any marked trends in partition across either basin. However, in the Madagascar Basin, acid-insoluble Ti does show a noticeable decrease from south-west to north-east across the traverse. In the HCL-soluble fraction, Ti is fairly constant across much of the basin but is slightly lower than average and more variable in the south-west. In the acid-reducible fraction, Ti is very variable and shows no trends. In the Central Indian Basin, Ti shows no clear trends in partition.

### (c) NODULE - SEDIMENT INTERRELATIONSHIPS

The relationships, if any, between element partition in nodules and sediments are, to say the least, obscure.

The partitioning of the major elements Mn and Fe between the four fractions investigated in nodules, show no relationship at all to the corresponding partition patterns in sediments. This also appears to be the case for the trace elements Co, Ni, Cu, Zn, Pb, Cd, Cr, and Ti.

The partitioning of Ca in nodules and sediments in the Madagascar Basin shows no interrelationship. However in the Central Indian Basin, the acid-reducible fraction of both nodules and sediments is higher in Ca in the central part of the basin and decreases towards the west and east whilst acid-insoluble Ca in both nodules and sediments shows an increase in the east. There is also evidence of some correlation between Al partition in nodules and the corresponding fraction of sediments in the Central Indian Basin but the correlation is rather weak and is seen primarily in the HCl-soluble and acid-insoluble fractions. In the Madagascar Basin, there appears to be no correlation between Al partition in nodules and sediments.

A more accurate assessment of nodule-sediment interrelationships in the various phases is not possible because of the limited number and distribution of nodule samples in the Madagascar Basin and of sediment samples in the Central Indian Basin. In only very few cases were nodules and sediments recovered together from the same site and this requirement must be met at many more sites across the basins for an accurate and detailed study of interrelationships between partition patterns to be carried out.

### (v) DISCUSSION

In general, the major elements in nodules, manganese and iron, show no marked regional trends in partition between the different fractions in either

basin. The trace metals, Co, Ni, Cu, Zn, Pb and Cd are contained predominantly in the acid-reducible manganese and mixed iron-manganese phases. They show no marked regional trends in the acid-reducible fraction, but they do show regional trends in some other fractions.

Arrhenius & Korkisch (1959) and Arrhenius (1963) found that most of the Cu and Ni in 7 Pacific Ocean nodules was contained in the reducible fraction, but that only about 50% of the total Co and 10% of the total Pb was present in this fraction. These authors suggest that the rest is contained in the HCL-soluble fraction which they regard as containing predominantly goethite, with clay minerals being important in some cases. These findings are in marked contrast to the behaviour of Co and Pb in the nodules analysed in this study, even allowing for the fact that the chemical attack employed in this study differed slightly from that used by Arrhenius and Korkisch. The extreme variability of the results of Arrhenius (1963), the low precision obviously obtained for certain elements, and the small numbers of samples analysed all cast some doubt on the general validity of his results. However, where amounts of goethite in nodules are particularly high, greater than average amounts of Co, Ni, Cu, Zn, Pb and Cd may be present in the HCL-soluble fraction. For example, in the Madagascar Basin, Co, Ni, Zn and especially Cu and Pb show some tendency to be enriched in the HCL-soluble fraction of nodules which contain a higher than average percentage of HCL-soluble Fe. This high Fe probably reflects the presence of goethite. This is particularly noticeable in sample 25G8D, in which goethite was in fact positively identified by X-Ray diffraction analysis. Nevertheless, any regional trends of these trace elements in the HCL-soluble fraction produced by regional variation in the goethite content of nodules is likely to be partly obscured by the presence in this fraction of the same metals released from clay minerals, since these are also extensively broken down by hydrochloric acid.

Nodules from the C.I.B. do not show any obvious trends in trace metal

enrichment in the HCL-soluble fraction. Total Fe in these nodules is very low and therefore amounts of goethite must be very small. Within this basin, Ni, Cu, Zn, Pb and Cd tend to be lower in the acid-reducible fraction at the western end of the traverse than elsewhere. There is a corresponding increase in the amounts of Ni, Cu, Zn, Cd and Pb in the more resistant fractions of nodules at the extreme western end of the traverse. This could be due to the proximity of the mid-Indian Ocean Ridge to the west which is likely to be a source of comparatively fresh volcanically derived material and which may have become incorporated in nodules. This material is likely to be fairly resistant to chemical attack and to be relatively enriched in some trace metals.

Trends in element partition in sediments from the C.I.B. are also rather unclear. Manganese shows a marked decrease in the acid-reducible fraction from west to east across the basin and the trace metals Co, Ni, Cu, Zn, Pb and Cd all reflect this trend. However, if the trend in bulk composition is examined it can be seen that the pattern of decreasing acid-reducible Mn closely follows the decrease in total Mn across the basin and that the total amounts of Co, Pb and especially Ni and Cu follow the same trend, although Zn does not. In view of the decrease in total Mn, and since much of the Mn in these sediments is present as acid-reducible manganese-micronodules the trend shown by Mn in the acid-reducible fraction probably represents a decrease towards the east in the micronodule content of the sediments rather than Mn being incorporated increasingly in a non-reducible fraction towards the east. This would also explain the observed trends of Co, Ni, Cu, Zn, Pb and Cd in the acid-reducible fraction since these metals are likely to be enriched in micronodules. Thus it seems that micronodules are more abundant in sediments towards the west of the Central Indian Basin than elsewhere in it.

Manganese behaves slightly differently in Madagascar Basin sediments to its behaviour in the C.I.B. For example, it shows a trend of enrichment

in the more resistant fractions of sediments from the northernmost part of this basin. This part of the basin is in close proximity to the active volcanic centres along the Rodriguez Ridge. Sediments at the northern end of the traverse therefore are likely to be receiving increased quantities of relatively fresh volcanic detritus. This material may be the source of comparatively high levels of Mn in the more resistant fractions of these sediments.

Another feature of the partitioning of Mn in Madagascar Basin sediments is its enrichment in the acetic acid-soluble fraction of samples which are comparatively enriched in total Ca. This Ca is likely to be present mainly as carbonate. Acetic acid-soluble Mn may therefore be present predominantly as very thin oxide coatings on carbonate tests. This would be released when the tests dissolve in the acetic acid attack. Horowitz (1974) found that a substantial amount of the total Mn in some Atlantic Ocean surface sediments was present in this form. Some Mn may however be actually incorporated within the carbonate lattice rather than as an oxide coating.

The partition patterns of the trace metals Co, Ni, Cu, Zn, Pb, Cd, Cr and Ti in the HCl-soluble and acid-resistant fractions of sediments and nodules must reflect in part the mineralogy of these phases. A major component of the more resistant phases of sediments and nodules is likely to be clay minerals. Chester & Hughes (1967) showed that different clay minerals are susceptible to selective chemical attack to different degrees. It is likely that clay particle size also has an effect on the susceptibility of these minerals to chemical attack, although it is not clear to what extent this is an important factor. Since the clay minerals are aluminosilicate-rich the partition patterns of Al are likely to be a good guide to the amount of clay minerals released from the samples by a particular attack. However the partition patterns of Al across both basins do not show any marked trends. Nevertheless, in the Madagascar Basin, one nodule,

sample 25GBD, which contains high total Al has a very high percentage of this element in the HCL-soluble fraction. Iron is also anomalously high in the same fraction in this sample and whilst this is thought to be due mainly to the presence of goethite, it may also indicate the presence of an iron-rich nontronite. Arrhenius (1963) found that Fe-rich nontronite was soluble in HCL and a nodule containing comparatively large amounts of this mineral gave similar partition results to sample 25GBD. The possible presence of appreciable amounts of this mineral in sample 25GBD might partly account for the anomalously high percentage of Co, Ni, Cu, Zn and Pb released in its HCL-soluble fraction.

In conclusion, it seems that in nodules, Mn, Fe and the trace metals may exhibit trends in partition in the more resistant fractions but the amounts present in these fractions are so low compared to those present in the acid-reducible fraction that analytical variance may well mask the trends. In sediments Mn, Fe and the trace metals tend to be partitioned a little more evenly between the various fractions but the total of these elements present are much lower and thus again analytical variance may mask all but the more pronounced trends. The fact that few very pronounced trends were observed indicates that Mn, Fe, Co, Ni, Cu, Zn and Pb tend to be present in roughly the same proportions in the various fractions in most samples from the same general type of environment. However, differences in the mineralogical content of nodules and differences in the sources of sediments are reflected in partitioning of both major and minor elements.

S E C T I O N 5

REGIONAL GEOCHEMISTRY

A brief discussion has been given in Section 5 of the variation in composition of Indian Ocean ferromanganese-oxide deposits using three-component scatter plots. In this section the regional variation of these deposits is examined by means of plotting the data on bathymetric maps of the Indian Ocean. Very few samples were obtained from some parts of the ocean and therefore, in order to provide a more complete picture, the data obtained in this study have been combined with all previously published data on ferromanganese-oxide deposits from the Indian Ocean. The resulting maps, figures 63 to 71, afford the most detailed picture to date of the geochemistry of ferromanganese-oxide deposits in the Indian Ocean. The additional data was taken from Monget et al (1976).

Manganese

The regional variation of Mn is plotted in figure 63. Manganese is highest in nodules from the Central Indian Basin, averaging over 20% and reaching a maximum concentration of more than 30%. East of the Ninety

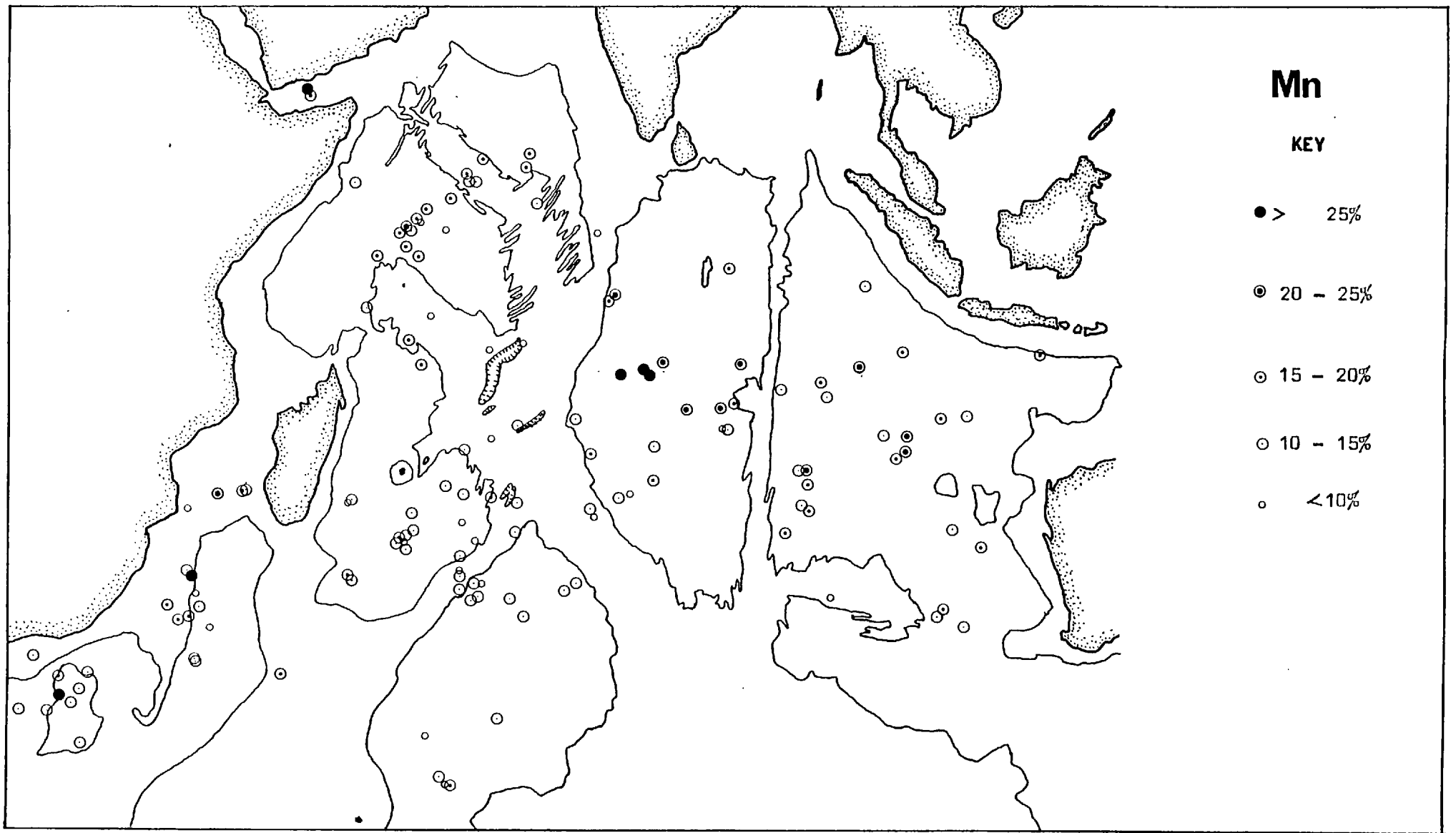


**FIGURE 63** Regional variation of Mn in Indian Ocean ferromanganese-oxide deposits.



East Ridge manganese values are somewhat lower but are still in excess of the Indian Ocean average. By contrast nodules from the basins of the west and south-west Indian Ocean have Mn concentrations which are generally slightly below the Indian Ocean average. The area off the south-eastern coastline of South Africa is characterised by nodules and encrustations of very variable composition and Mn concentrations reach a maximum of 36.5% in one particular nodule sample, however the average Mn content of these samples is only slightly above the Indian Ocean average (see Table 11).

In order of increasing Mn content of samples the Moçambique, Madagascar and Crozet Basins are the lowest, containing only about the same levels of Mn (11 - 13%) on average as mid-ocean ridge samples (see Table 11). Samples from the Arabian, Somali and Wharton Basins contain about the same levels of Mn as the Indian Ocean average of 15% whilst samples from the Moçambique Channel and elevated areas off the South African coast are slightly more enriched again, averaging 16.5 - 17.5% Mn. The maximum enrichment in basin samples occurs in the Central Indian Basin where Mn averages about 22%.

Nodules and encrustations from the mid-ocean ridge system are lower in Mn on average than samples from every other region of the Indian Ocean with the exception of the Moçambique Basin. Encrustations from sea-mounts whilst averaging only about 13.5% Mn are nevertheless richer in Mn than mid-ocean ridge samples and in a few instances, particularly in the Somali Basin, sea-mount samples are comparatively enriched in Mn, containing higher levels than in nodule samples from the surrounding basin itself.

### Iron

The regional variation of Fe tends to be roughly the reverse of

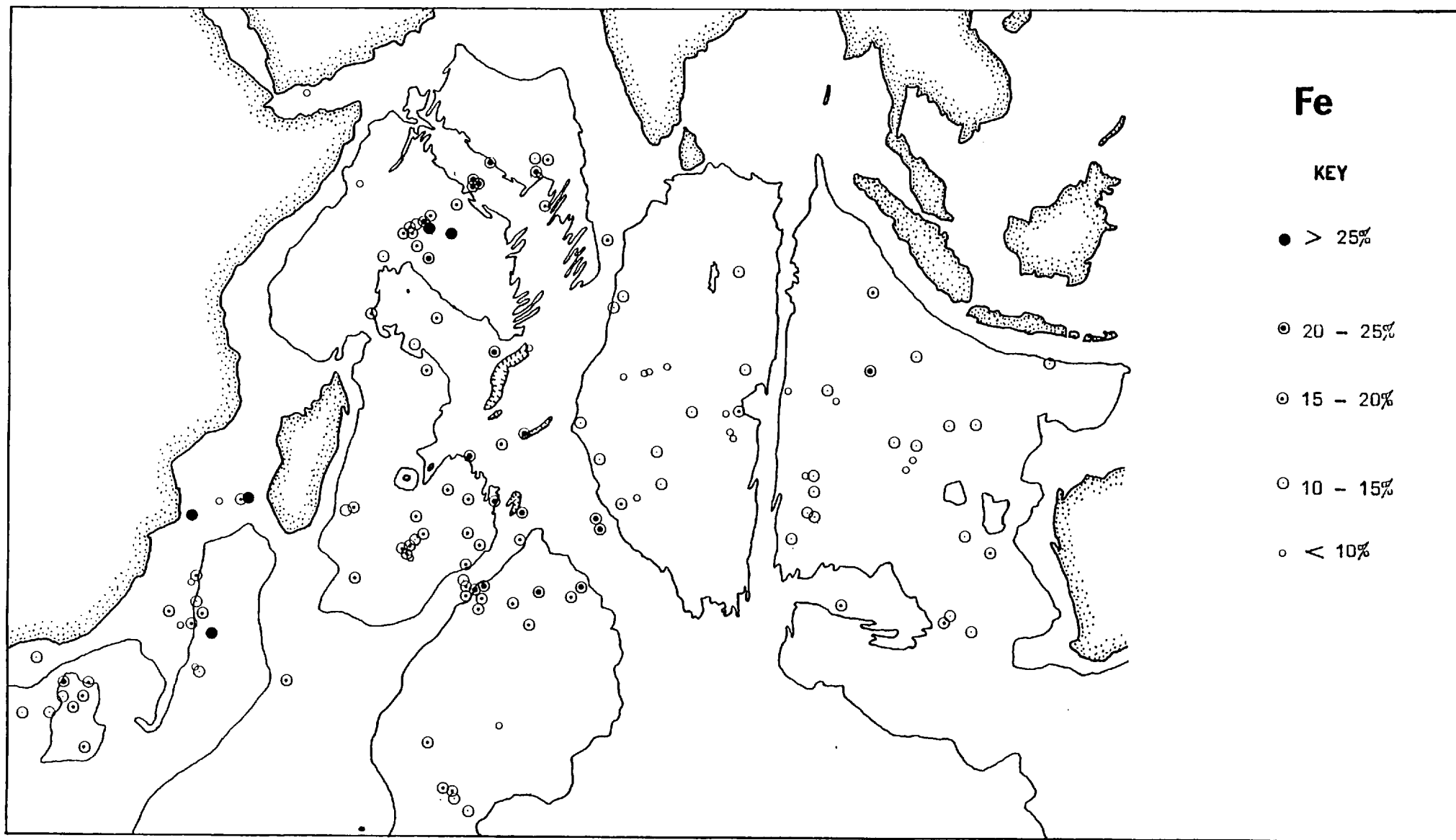


**FIGURE 64** Regional variation of Fe in Indian Ocean ferromanganese oxide deposits.

that exhibited by Mn (see figures 63 and 64). Thus Fe is lowest in Central Indian Basin nodules where it averages well under 10% and is as low as 5% in some samples. Iron values are also well below the Indian Ocean average of 15% in the Wharton Basin, where the average Fe content of samples is slightly over 11%. Iron values are only slightly higher in the Moçambique Basin. In the Crozet Basin and in the plateaux regions off South Africa, average Fe values are very near the Indian Ocean average whilst in the Madagascar Basin and Moçambique Channel average Fe values, at just over 16%, are slightly higher than the average for the whole ocean. Sea-mount samples tend to be higher in Fe than samples from all of the ocean basins, averaging over 17%, but the highest average Fe values found in the Indian Ocean occur in mid-ocean ridge samples which have an average Fe content of just less than 20%.

#### Nickel

Nickel shows many similarities to Mn in its regional variation. The highest Ni values occur in Central Indian Basin samples (see figure 65) where Ni averages almost 1%. High Ni values also occur in samples from much of the Wharton Basin. The southern part of the Arabian Basin is also characterised by samples with high Ni values but the basins of the Western Indian Ocean generally contain samples of only intermediate Ni content. Somali Basin samples average just under 5000p.p.m. Ni, about the same as the Indian Ocean average, however Ni is rather lower in the Crozet, Moçambique and Madagascar Basins, averaging less than 2500p.p.m. in the latter.

As is the case with Mn, the marginal areas of the south-west Indian Ocean are characterised by samples of very variable Ni content. Samples from the Moçambique Channel are enriched in Ni averaging over 7500p.p.m.

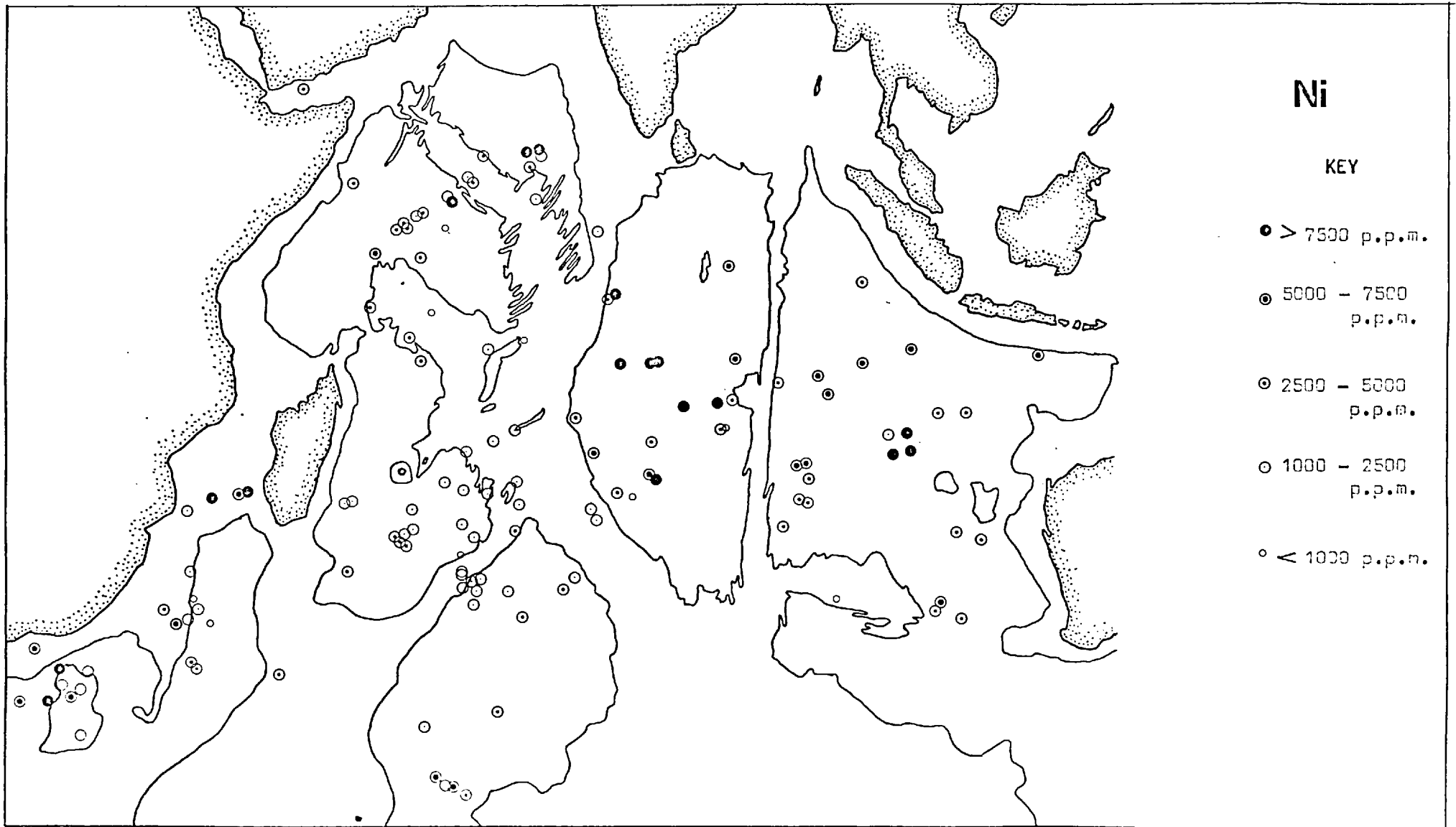


FIGURE 65 Regional variability of Ni in iron-bearing ferrous-oxide deposits.

and samples from the Agulhas Plateau region, whilst displaying a wide range of Ni values, nevertheless also show some overall enrichment in Ni.

By contrast, sea-mount samples are generally low in Ni averaging only about 2700p.p.m., slightly over half the Indian Ocean average. The lowest Ni values in the Indian Ocean generally occur in mid-ocean ridge samples, which average less than 2000p.p.m. Nickel.

### Copper

The regional variation of copper (figure 66) closely follows that of Ni, but Cu shows a greater range of values than does Nickel. Copper is highest in the Central Indian Basin, where it averages about 1%, three times the average Indian Ocean value. Copper is also enriched in the Wharton Basin, particularly in the Central part of the basin, but overall Cu averages less than 5000p.p.m. in this basin. Copper is generally lower than the whole ocean average in all the basins of the west and south-west Indian Ocean ranging from almost 2500p.p.m. in the Somali Basin samples to 1500 to 1700p.p.m. in the Crozet and Mozambique Basins. Like Ni, the lowest values for Cu in basin areas of the Indian Ocean occur in the Madagascar Basin where Cu averages less than 1200p.p.m. Copper shows no marked enrichment in samples from the Mozambique Channel, the plateaux off southern Africa or from the southern Arabian Basin and in these areas therefore, the regional variation of Cu differs from that of Nickel.

Encrustations from sea-mounts and the mid-ocean ridge system are markedly depleted in Cu, averaging less than 1000p.p.m. Copper shows small differences to Nickel in these environments also, being more depleted in sea-mount samples than mid-ocean ridge samples, this is the reverse of the behaviour of Ni in samples from these two types of environment.

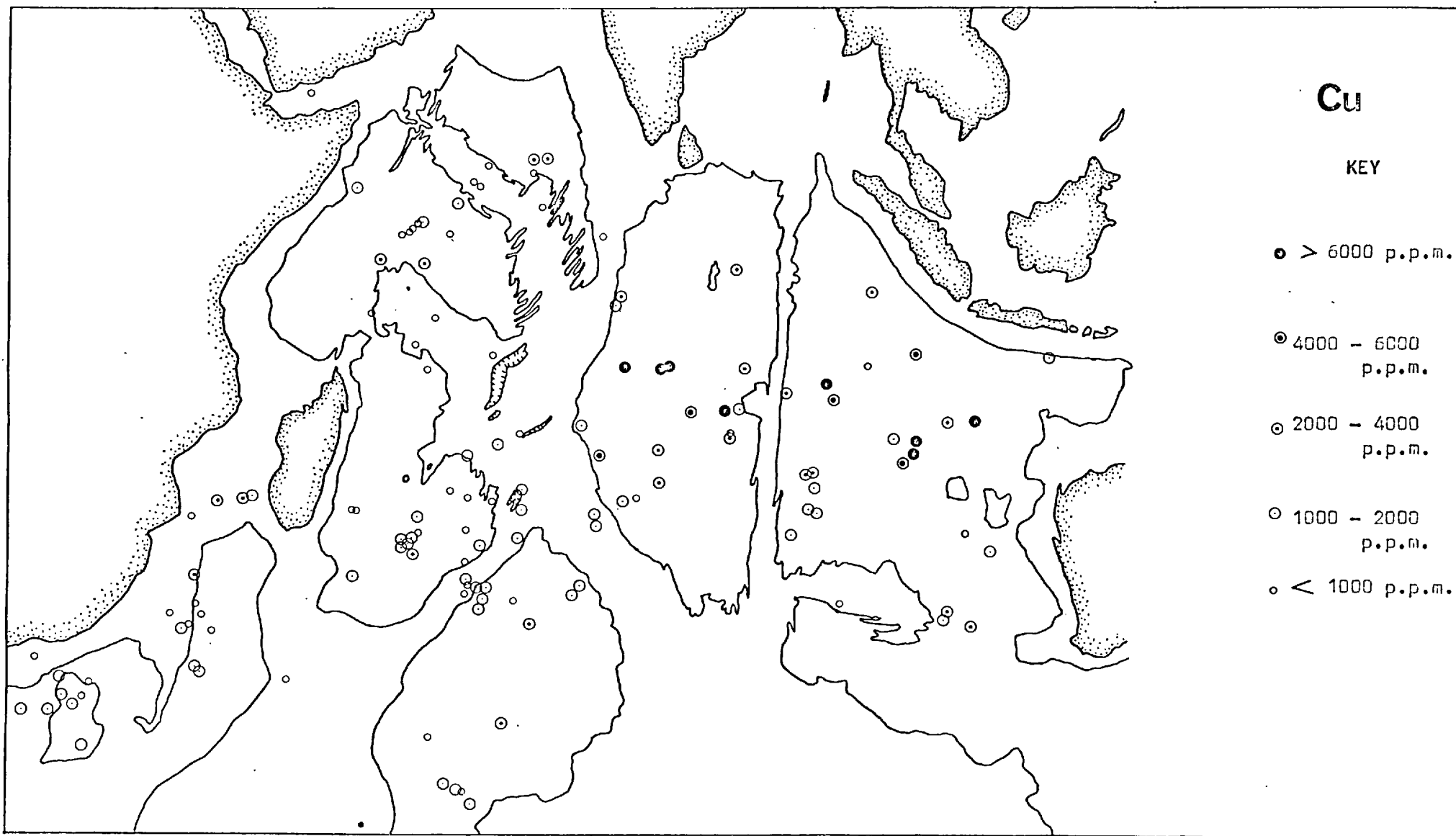


FIGURE 66 Regional variations of Cu in Indian Ocean ferromanganese-oxide deposits.

## Zinc

There is less published data for Zn in Indian Ocean ferromanganese-oxides than for the elements already dealt with and consequently regional trends in Zn values cannot be examined in as much detail as those of the elements so far discussed.

It is obvious from figure 67 that Zn tends to follow Ni and Cu in its regional trends, thus Zn is highest in Central Indian Basin nodules, averaging over 1100p.p.m. Zinc values in the Wharton Basin are only slightly over 700p.p.m., which is the whole ocean average. Zinc values in the Madagascar and Mozambique Basins average less than 500p.p.m. and are thus even lower than Zn values in mid-ocean ridge and sea-mount samples. This is rather different to the behaviour of Ni and Cu in samples from those areas. The Somali and Crozet Basins have Zn values about 650p.p.m. which is only slightly below the Indian Ocean average. By contrast, the Mozambique Channel area is characterised by Zn values well over 1000p.p.m. almost as high as the Central Indian Basin average. A similar enrichment was shown by Ni in samples from this area but Cu did not show similar enrichment. Encrustations from sea-mounts and the mid-ocean ridge system averaged only slightly above 500p.p.m., considerably less than the whole ocean average.

## Cobalt

The regional variation of Co (figure 68) tends to be the reverse of that observed for Ni and Cu. Thus the lowest Co values, averaging only about 1100p.p.m., are found in Central Indian Basin nodules. Cobalt values are also less than 1500p.p.m. in the Mozambique Channel and Basin and in the Somali Basin. In the Wharton and Crozet Basins Co values are above 1700p.p.m. but still well below the Indian Ocean average of over 2200p.p.m.

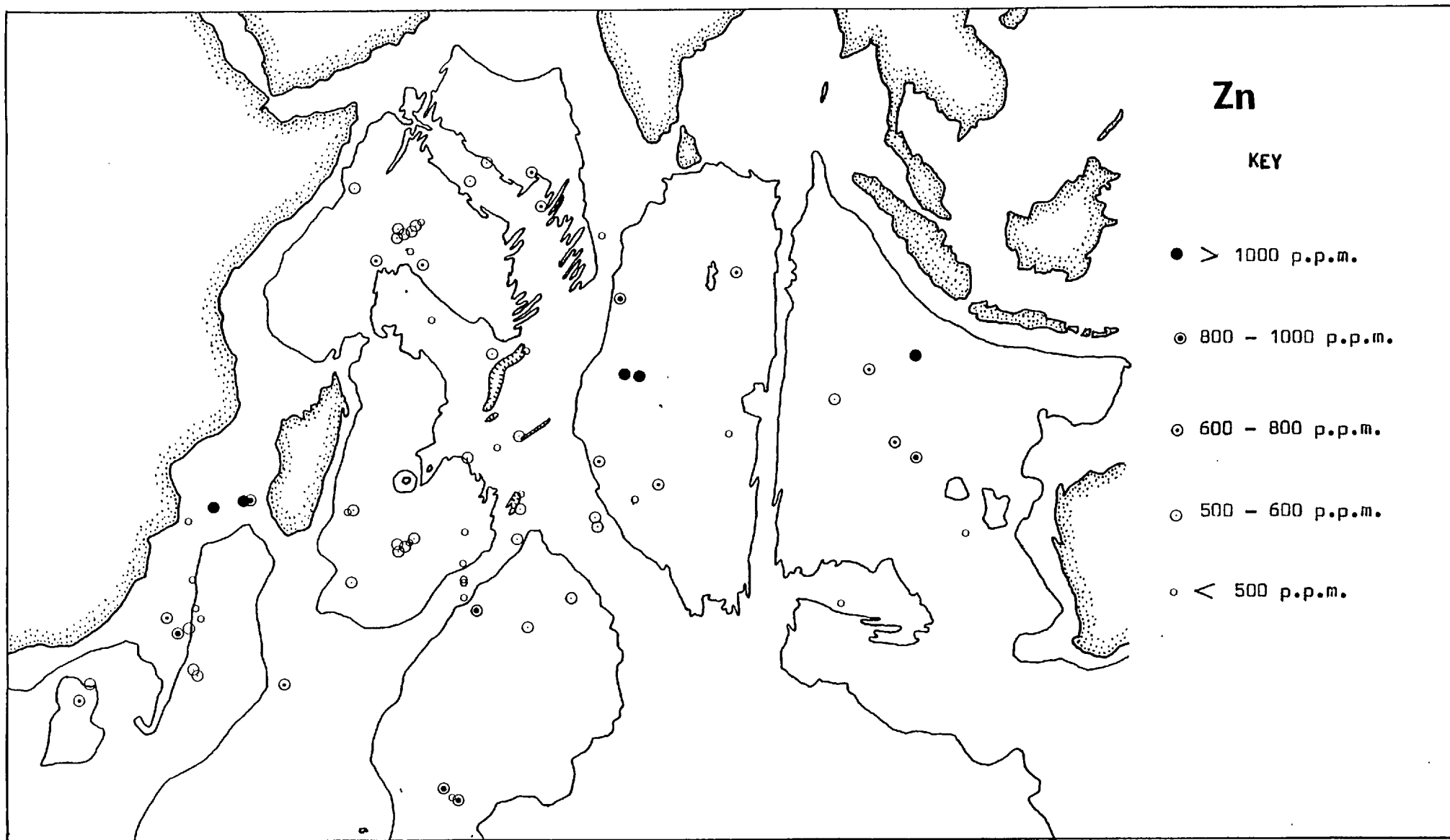


**FIGURE 67** Regional variations of Zn in Indian Ocean ferromanganese-oxide deposits.



Madagascar Basin samples are high in Co compared to other ocean basin areas and the average Co value of 2500 p.p.m. is above the whole ocean average. The plateaux off southern Africa are also characterized by samples with slightly above average Co values. Samples from the mid-ocean ridge system however, although from generally elevated sites, have average Co values of about 2000 p.p.m. and are thus below the Indian Ocean average. Sea-mount samples on the other hand are high in Co, particularly in the Somali Basin, and their average Co values are about twice the ocean average, almost 4500 p.p.m.

### Lead

Much less data is available for Pb than for Co but from that available it can be seen that this element shows roughly the same patterns of regional variation as Co, the amount of variation however being rather less extreme. The lowest Pb values occur in the Central Indian Basin and Mozambique Channel where average Pb levels are little more than half the Indian Ocean average of 1000 p.p.m. Slightly higher Pb values are found in the Somali and Wharton Basins, values averaging between 700 and 900 p.p.m.. Crozet and Madagascar Basin samples contain levels of Pb about that of the Indian Ocean average whilst Mozambique Basin samples are slightly enriched in Pb, averaging 1200 p.p.m. Samples from the plateau areas off southern Africa are similarly enriched in Pb but the greatest Pb enrichments are found in sea-mount samples, where Pb averages 1600 p.p.m., and may be as high as 2500 p.p.m. As is the case with Co, no Pb enrichment occurs in mid-ocean ridge samples even though these were from predominantly elevated areas. Average Pb values in mid-ocean ridge samples are in fact only a little over 900 p.p.m. and are therefore below the Indian Ocean average.

### Calcium

Calcium shows no marked regional trends and varies little from basin to basin (see figure 70). Of the basin areas however, the Crozet Basin tends to exhibit slightly higher Ca values than samples from other basins. Samples from this basin were recovered from an average depth of 4600m. This is only marginally below the lysocline at the latitudes occupied by this basin (see figure 9) and much nearer this boundary than many of the samples in other basins. Much of the Ca in these samples may therefore occur as carbonate.

The highest Ca values on average, occur in samples from the Mozambique Channel, southern Africa plateaux regions, isolated sea-mounts and the mid-ocean ridge system. These are elevated areas well above the lysocline and the enrichment of Ca in these samples may therefore be due to the inclusion in the samples of carbonate or calcium-rich phosphorite material, since these tend to occur characteristically in shallow water areas rather than deep water basins.

### Aluminium

Aluminium shows no regional trends, samples from all basin areas showing a wide range of Al values (see figure 71). However whilst samples with high Al contents occurred in all areas, those with very low Al contents were confined to elevated areas, particularly sea-mounts. Thus basin areas generally have average Al values above the Indian Ocean average and elevated areas have average Al values below the Indian Ocean average. The Al content of samples largely reflects the amount of diluting aluminosilicate material present in the samples which will be greatest in sediment-covered basins. It is therefore not surprising that Al does not show trends comparable with those of the other elements investigated, since these are incorporated

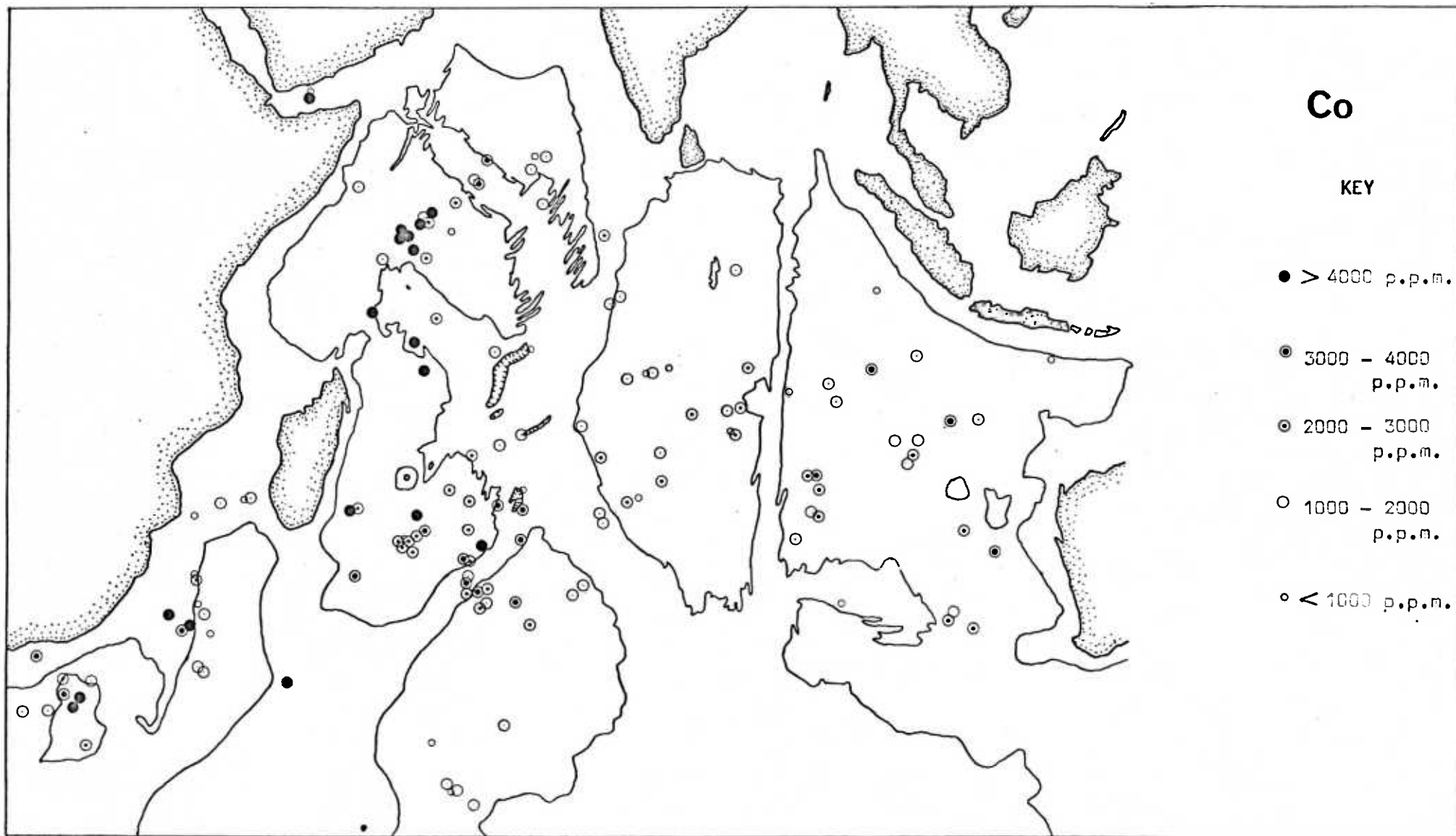


**FIGURE 69** Regional variations of Co in Indian Ocean ferromanganese-oxide deposits.

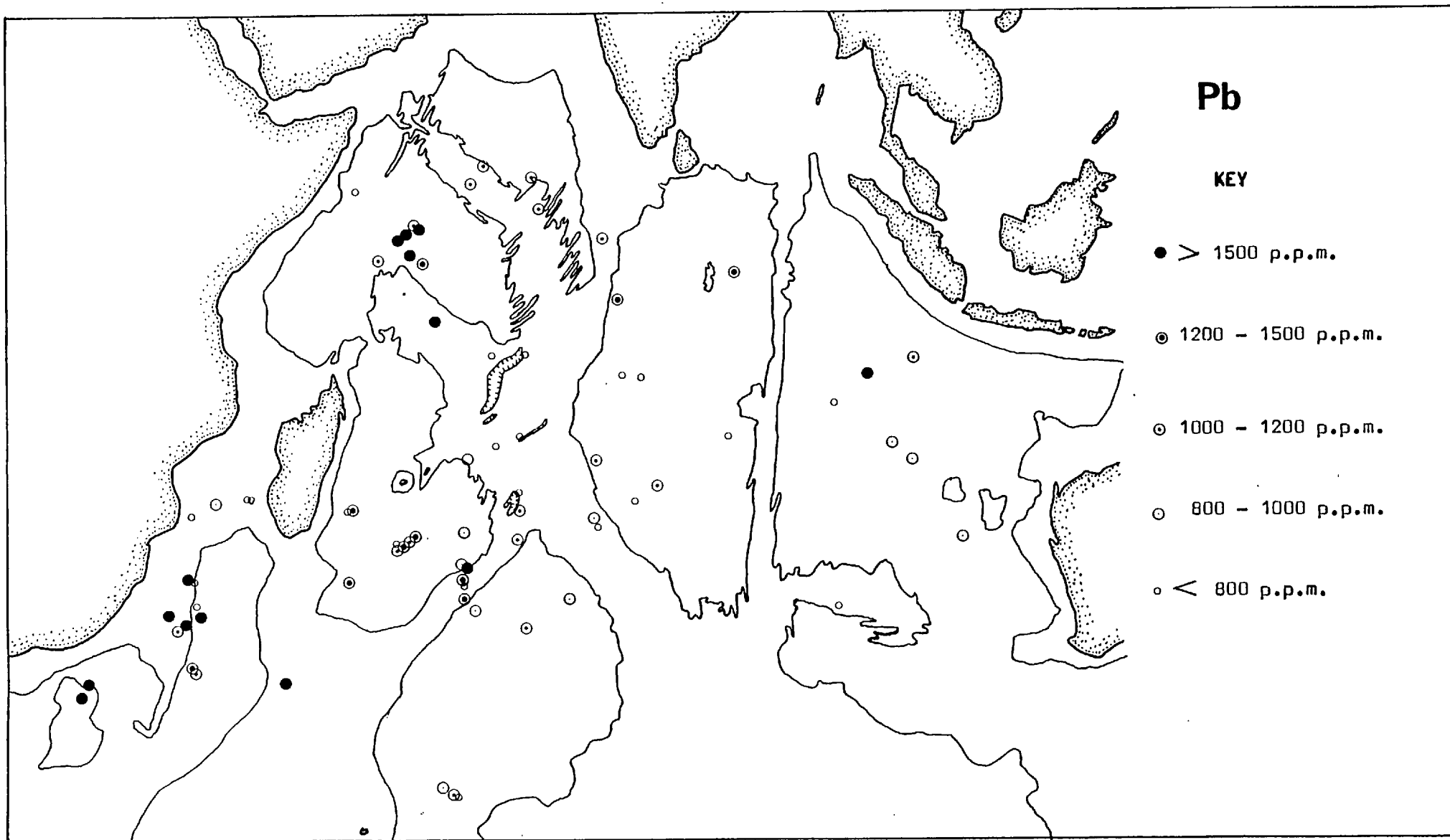
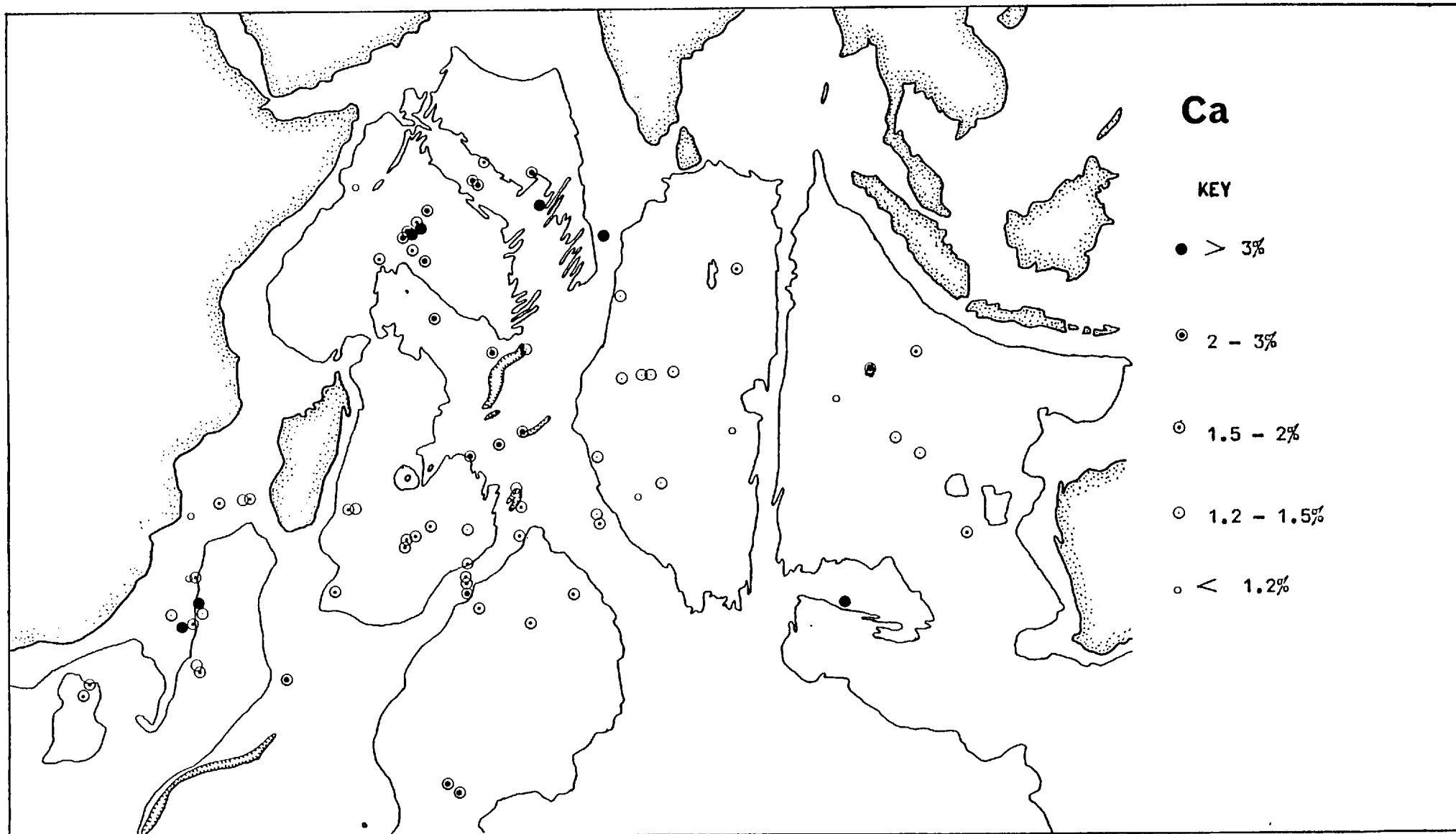
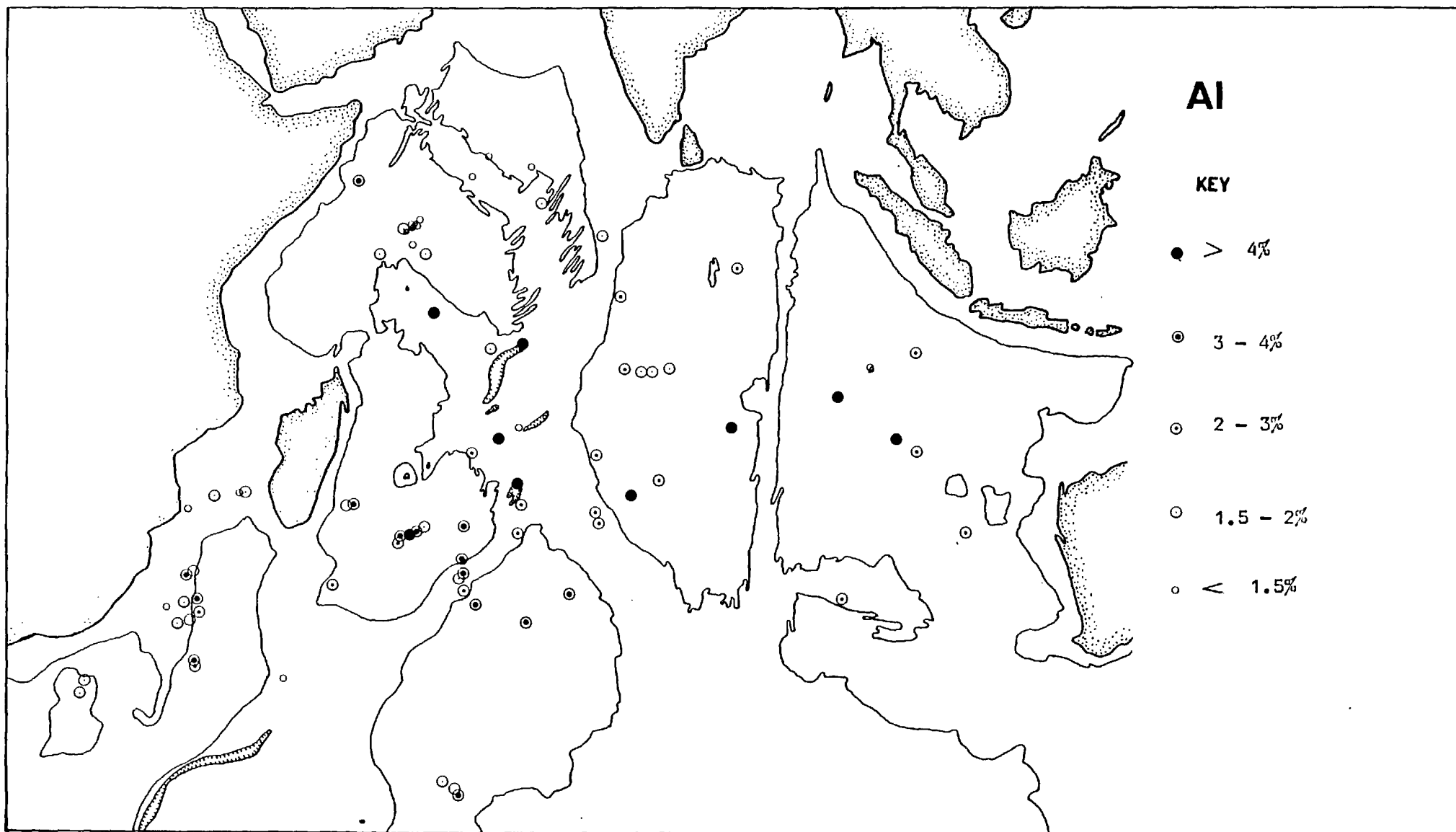


FIGURE 69 Regional variations of Pb in Indian Ocean ferromanganese-oxide deposits.



**FIGURE 70** Regional variations of Ca in Indian Ocean ferromanganese-oxide deposits.



**FIGURE 71** Regional variations of Al in Indian Ocean ferromanganese-oxide deposits.

predominantly in the authigenic oxide phases.

#### Cadmium, Chromium and Titanium

No realistic assessment of the regional variations of Cd, Cr or Ti could be carried out since only 27 samples from only two different basins were analysed for these elements. Some comparison between the two basins can be made however, using the data in Table 11. Cadmium and Cr tend to be higher on average in the Central Indian Basin than in the Madagascar Basin but the differences are rather too small to be ascribable to any particular cause. Madagascar Basin samples however contain an average of over 1% of Ti, over three times as much as the average Ti value of Central Indian Basin samples. The high Ti in Madagascar Basin samples is ascribable to the volcanic influence of the south-west Indian Ridge upon the bottom environment of this basin, as has already been discussed in Section 5.

## S E C T I O N 9

### DISCUSSION

In this section, various aspects of the work described will be discussed. These include the regional geochemistry of the major and minor elements in ferromanganese oxides, and the influence on nodule composition of element source together with that of the mineralogy of the oxide phases.

#### (i) REGIONAL GEOCHEMISTRY

It has already been shown that the minor elements Co, Ni, Cu, Zn and Pb are associated predominantly with the authigenic oxide phase of ferromanganese oxides, thus an understanding of the reasons for the regional variations in Mn and Fe content of these deposits is of primary importance in understanding the variation in overall composition.

#### (a) Major elements: Source Influences

In the marine environment Mn and Fe possess different degrees of



mobility (Krauskopf, 1957). Thus whilst these elements occur in intimate association in marine ferromanganese-oxides, their regional variation in these deposits is likely to be affected to different degrees by the proximity of deposits to major sources of these elements. The source of the Mn and Fe in marine ferromanganese-oxides has been a subject of controversy ever since these deposits were first discovered by the Challenger Expedition. Murray (Murray & Renard, 1891) considered that the Mn had a chiefly volcanic origin whilst Renard (op. cit.) suggested that most of the manganese was derived from continental run-off. Volcanism or alteration of the sea-floor basalts has been suggested as a metal source by Arrhenius et al, (1964), Arrhenius & Bonatti, (1965) and Bonatti & Nayudu, (1965), whilst Goldberg (1954) and Goldberg & Arrhenius, (1958) favoured a continental source for both major and minor elements.

Several workers have shown that Fe and Mn can be leached from hot basalts by sea-water, (Corliss, 1971; Wilkniss et al, 1971; Fein & Mergonstein, 1973). Bostrom & Peterson (1966) suggested that appreciable amounts of Fe may be supplied to the sea-floor by this process whilst Elderfield (1976) argued similarly for manganese. From investigations carried out on the East Pacific Rise, Lyle (1976) also argued that hydrothermal Mn introduced at oceanic spreading centres should be considered one of the major sources of Mn to the oceans. Such processes are thought to have given rise to the rapidly-precipitated Mn-rich and Fe-rich deposits which have been found associated with spreading centres in the Pacific and Atlantic oceans (Bonatti & Joensuu, 1966; Scott et al, 1974; Moore & Vogt, 1976; Burnett & Piper, 1977). However, this type of deposit, in which the Mn and Fe have precipitated out rapidly near the source of supply, appears to be fairly uncommon, and none have so far been reported from the Indian Ocean although such a deposit has been reported from the Gulf of Aden (Cann et al, 1977). Much of the Fe and Mn supplied from active ridge systems must therefore migrate greater distances before being re-precipitated. Iron is present in

much larger amounts in marine basalts than Mn and experimental leaching of basalts by sea-water produces solutions with an  $Fe/Mn$  ratio of 5 or greater (Wilkniss et al, 1971). A greater supply of Fe compared with Mn to the oceans at the ridges, combined with the lack of mobility of Fe compared with Mn in the marine environment, would explain the observation that Fe predominates over Mn in samples from the mid-Indian Ocean ridge system. Low  $Mn/Fe$  ratios were also observed in samples from sea-mounts and other elevated areas where extensive areas of basalt are exposed to ocean water indicating that Fe may be supplied to samples in such areas by submarine weathering of basalts. According to the above hypothesis, with increasing distance from the mid-ocean ridge a decrease in Fe content of samples and consequent increase in  $Mn/Fe$  ratio should occur. Samples from basin areas in the Indian Ocean do in fact have lower Fe contents and higher  $Mn/Fe$  ratio than samples from the ridge system (see figure 72). However, the variation in average Mn and Fe content and  $Mn/Fe$  ratio between the various basins is considerable and needs further explanation.

Price and Calvert (1970) and Calvert and Price (1977) suggest that diagenetic remobilisation of Mn is an important source of this element to growing nodules in several regions. In areas near the continents, undergoing fairly rapid sedimentation, large amounts of carbonaceous material are incorporated in the sediment column, producing reducing conditions at shallow depth and causing reduction and remobilisation of Mn within the sediment. In such environments nodules are considerably enriched in Mn and have high  $Mn/Fe$  ratios (Mero, 1965; Price & Calvert, 1970). In view of the particularly rapid sedimentation occurring in most continental margin areas of the Indian Ocean, nodules are likely to be rather uncommon there. Of those that have been recovered and analysed in this study only one displayed a high Mn content and  $Mn/Fe$  ratio. It appears therefore that the process of diagenetic enrichment of Mn in continental margin nodules, described by Price & Calvert may not be an important factor in many of the areas from which the nodules

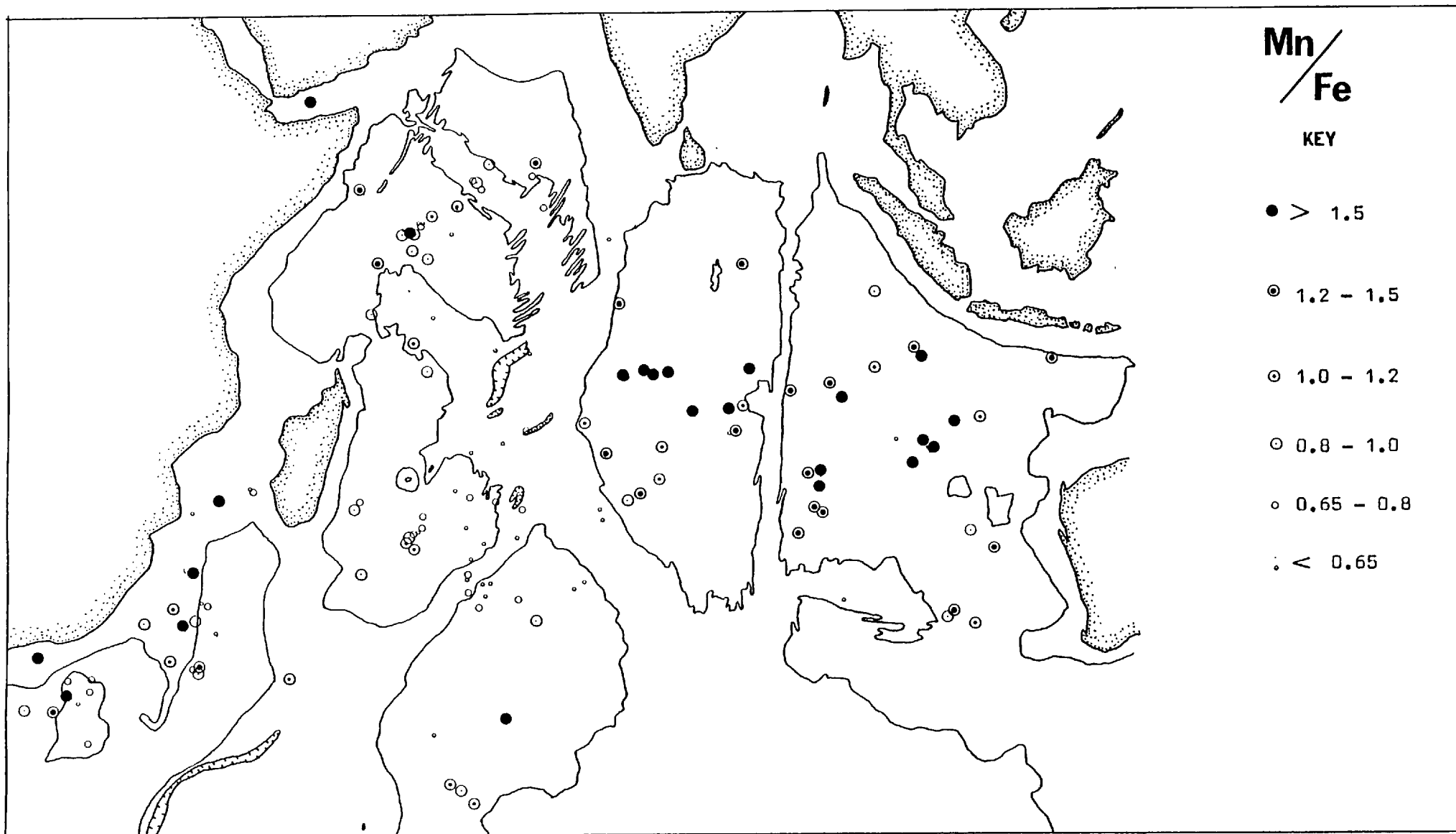


FIGURE 72  $Mn/Fe$  ratios of Indian Ocean ferromanganese-oxide deposits.

analysed in this study came. According to Price and Calvert (1970), diagenetic remobilisation also occurs in slowly accumulating sediments in pelagic areas which lie beneath regions of high surface biological productivity. This remobilisation is facilitated by the reduction of Mn in the sediment column by the comparatively large amounts of carbonaceous material which have become included in the sediment. According to these authors, the Mn - rich nodules in the equatorial north-east Pacific (Horn et al, 1973) have been enriched in Mn by this mechanism. However Bender (1971) and Elderfield (1976) have shown that remobilisation of Mn in the sediment column does not seem likely on the sort of scale and over the sort of distances which would appear necessary if the Price and Calvert theory of Mn enrichment of nodules is totally correct.

In the Indian Ocean an area of nodules of very similar composition to equatorial north-east Pacific samples occurs in the Central Indian Basin. Unfortunately, no buried sediment samples in this basin were analysed from sites at which surface nodules were also recovered. However a comparison of buried and surface sediment at two other sites in this basin revealed no marked increase in the Mn content of the surface sediment which would be expected if Mn were being remobilised and re-oxidised near the sediment-water interface.

Calvert and Price (1977) suggest that Pacific Ocean ferromanganese-oxides precipitated directly from sea-water have  $Mn/Fe$  ratios of approximately 1.0 and that nodules with a  $Mn/Fe$  ratio of greater than 1.5 have received substantial amounts of Mn from the underlying sediment by diagenetic remobilisation. Average  $Mn/Fe$  ratios in the Indian Ocean are generally lower than those of the Pacific. This is probably because Fe tends to predominate over Mn in volcanic areas, since it appears to be supplied in greater amounts by volcanic and hydrothermal sources, and volcanically active ridge areas are a much more prominent feature of the Indian Ocean than of the Pacific Ocean. Only three areas of the Indian Ocean were observed to have samples with an average  $Mn/Fe$  ratio much greater than 1.0, these were the Central Indian Basin,

the Somali Basin and the Wharton Basin. Only two samples were analysed from the Somali Basin. However both came from localities where sedimentation rates are fairly high, and at one of the sample sites (D.S.D.P. site 234) reducing conditions, indicated by the presence of pyrite, were present at fairly shallow depth (Fisher, Bunce et al, 1974). In the Wharton Basin again only one station was occupied at which information about the sediment at depth could be obtained. At this station, RC14/49, the composition of the buried sediment compared with that at the surface and the presence of a buried nodule indicate that if Mn is being remobilised at depth much of it must be re-oxidised well before it reaches the surface. Cores from D.S.D.P. sites elsewhere in the Wharton Basin all show well-oxidised sediments at depth (von der Borch and Sclater, 1974). Although very little data is available therefore, that which is available does not provide any evidence to indicate that Mn is being supplied to the surface sediments in this basin by remobilisation from depth in the sediment column. As already discussed, a similar conclusion was reached for Central Indian Basin sediments. In view of this and the more detailed work of Bender (1971) and Elderfield (1976) remobilisation of Mn from depth is not regarded as a significant source of Mn to Mn-enriched nodules, except perhaps in some continental margin areas.

If diagenetic remobilisation of Mn is not an important factor in influencing the composition of pelagic ferromanganese-oxide deposits then some other mechanism must be proposed. Greenslate et al (1973) suggest that marine organisms are an important source of Mn in areas of high surface biological productivity since these organisms are able to incorporate transition metals in their tests and/or soft parts. These metals are released into bottom waters when the organisms sink upon death and begin to decay and dissolve at depth. Piper and Williamson (1977) suggest that this biogenic supply of Mn has been a principal factor in the production of Mn-rich nodules beneath the equatorial zone of high biological productivity in the north-east Pacific. However Greenslate et al (1973) have shown that the Fe content of marine

organisms is at least an order of magnitude higher than their Mn content and if these organisms form the major supply of Mn to nodules in certain areas then some mechanism must be operating which inhibits the increased supply of iron. In fact an important factor of the equatorial Pacific Mn-rich nodules is that they are particularly low in iron (Mero, 1965; Cronan, 1967). Central Indian Basin Mn-rich nodules are also very low in Fe; and in the case of Somali and Wharton Basin samples Mn values are in fact only about the same as the Indian Ocean average and it is the low Fe values in these samples which give them high  $Mn/Fe$  ratios. In view of the fact that the chemical composition of ferromanganese-oxides, as usually expressed, forms an example of variables equalling a constant sum (Chayes, 1960), then a reduction in the supply of Fe to accreting samples will on its own partly account for higher Mn content.

A process whereby available Fe is actively removed from the bottom environment in certain areas must therefore be envisaged in order to account for the presence of manganese-rich nodules. Such a process was put forward by Lyle et al (1977) to explain the low Fe content of nodules from the Bauer Basin of the eastern equatorial Pacific. They suggested that ferromanganese oxides precipitate out from normal sea-water with an  $Mn/Fe$  ratio close to 1.0. These colloidal precipitates react with opaline silica in the accompanying sediment, leading to the formation of an Fe-rich smectite and liberating the Mn, which is incompatible with the smectite and which is therefore available for incorporation into nodules. Lyle et al (op. cit.) also suggest that trace metals such as Ni, Cu and Zn, which may occur in the biogenic opaline silica in relatively high amounts (Greenslate et al, 1973), may be released during this process and may subsequently become incorporated in the Mn phase of accreting nodules. The reaction process may be summarised thus:-



This process, which is thought to occur at or near the sediment-water interface could explain why Mn, Cu, Ni and Zn-rich nodules have been found in the Pacific Ocean concentrated on areas with a highly siliceous substrate. The largest areas of siliceous ooze sediment in the Indian Ocean occurs in the Central Indian Basin. Interestingly, the nodules from this siliceous ooze area are higher in Mn, Cu, Ni and Zn and lower in Fe than nodules from any other locality in the Indian Ocean and are very similar in composition to Pacific Ocean nodules lying on similar substrate. The Wharton Basin also contains areas of siliceous ooze sediment although its occurrence in the basin is rather more patchy than in the Central Indian Basin. As a consequence Cu and Ni values are appreciably higher and Fe values appreciably lower than the Indian Ocean average although these trends are not nearly so marked as those of Central Indian samples. Of the Wharton Basin samples analysed, only two were from localities with a highly siliceous substrate. The  $Mn/Fe$  ratio of these samples, 1.75, was noticeably higher than the average value for the whole basin (1.32). None of the Somali Basin samples had a siliceous substrate and Mn, Ni, Cu and Zn values were very near the Indian Ocean average in these samples.

The process outlined above could explain some of the compositional variations observed in nodules from basin areas of the Indian Ocean. However in the Crozet, Madagascar and to a lesser extent the Mozambique Basins nodules occur with  $Mn/Fe$  ratios appreciably less than 1.0 and whose compositions show more affinities with samples from the mid-ocean ridge system than the basin areas of the eastern Indian Ocean. This trend is most marked in samples from the Madagascar Basin. As already discussed, a marked feature of the bottom environment in this basin is the bottom current formed by the north-westerly movement of Antarctic Bottom Water. This current flows into the Madagascar Basin via the south-west branch of the mid-Indian Ocean Ridge and it is postulated that an extension of the Fe-rich ridge type of deposit has developed in the Madagascar Basin because of the ability of this current to

transport Fe-rich material, perhaps in colloidal form, from the ridge area down onto the basin area.

Although overall the Crozet Basin samples have a low  $Mn/Fe$  ratio they can be divided into two groups. The first consists of samples from the northern part of the basin near the mid-ocean ridge system (see figure 72). These have a low  $Mn/Fe$  ratio (0.70) and it seems this might be due to their proximity to the Fe-rich ridge environment. It must be pointed out however, that bottom currents in this area do not appear to be in a direction favourable to transport of material from the ridges to the basin floor, but rather in the opposite direction. Basalt may be exposed on the sea-floor, however, and be available for alteration. The other group of Crozet Basin samples come from the southern part of the basin, much further from the ridge. These samples have an  $Mn/Fe$  of 1.0 and do not show any indication of Fe-enrichment from volcanic sources.

The reason for the low  $Mn/Fe$  ratio of Mozambique Basin samples is less clear. Bottom currents in this basin flow in a direction which would seem to preclude any supply of Fe from ridge environments. However this basin receives much of its sediment from continental run-off and this material is much more enriched in Fe than Mn (Manheim, 1965). This may lead to enhanced amounts of available Fe in the bottom environment of this basin. The iron-rich nature of continental run-off and the observation of Krauskopf (1957) that Fe precipitates out before Mn as continental run-off enters the oceans could explain the extremely high Fe content and low  $Mn/Fe$  ratio of samples collected near the African coast in the Mozambique Channel. Similar observations and conclusions have been made for Pacific Ocean samples from comparable areas by Manheim (1965) and Mero (1965) and for the Atlantic Ocean by Cronan (1975).

(b) Major elements: Mineralogical Influences

According to Calvert and Price (1977) and Lyle et al (1977) "normal"



marine ferromanganese-oxide deposits consist of an intimate mixture of manganese and iron oxides with an overall  $Mn/Fe$  ratio of approximately 1.0 and with  $\delta$ - $MnO_2$  as the major Mn-bearing phase. In many cases, because of the high background fluorescence produced by the poorly crystalline material, it is not certain whether appreciable amounts of a discrete, crystalline Fe phase are present in samples where the  $Mn/Fe$  ratio is about 1.0. However in samples where the Fe content is appreciably higher than the Mn content goethite is often identified. According to Burns and Brown (1972) the presence of an active surface of  $FeOOH$  of small particle size acts as a catalyst to Mn oxidation and a ferromanganese-oxide deposit accumulates by deposition of  $Mn^{4+}$  oxides epitaxially intergrown with the Fe oxyhydroxides (Burns & Brown, *op. cit.*). These authors further suggest that abundant Fe in ferromanganese-oxides may reduce the capacity of the Mn-oxides to incorporate trace metals, destroying potential sites for these by "clogging" of the sites with  $FeOOH$ . As can be seen from Table 10, samples high in Fe tend to have much reduced trace metal contents.

According to Crerar & Barnes (1974) the more highly-oxidised Mn oxide,  $\delta$ - $MnO_2$  tends to occur mainly in samples from elevated areas such as the mid-ocean ridge system and sea-mounts, where sedimentation rates are low or zero and where conditions are thought to be highly oxidising. A similar observation was also made in the present study. If the hypothesis of Burns & Brown (1972) is correct, i.e. that active Fe oxyhydroxides catalyse the oxidation of divalent Mn, then this may explain the observation that  $\delta$ - $MnO_2$ -rich samples contain much more Fe on average than todorokite-rich samples (see Table 8) and that they occur predominantly in regions such as the mid-ocean ridge and sea-mounts where there is an abundant supply of iron. Thus the abundance of Fe may be equally as important a factor as the degree of oxidation of the environment in determining the mineralogy of the Mn phase. The importance of Fe in this respect was also noted by Lyle et al (1977), who suggested that in environments where the supply of Fe was much reduced, such as in areas with a

highly siliceous substrate far-removed from active ridge crest areas, abundant todorokite was able to develop. A similar observation was also made in the present study, the most todorokite-rich, Fe-poor samples being found on a siliceous substrate in the Central Indian Basin.

(c) Minor elements

The minor elements Co, Ni, Cu, Zn and Pb are associated predominantly with the authigenic oxide phase of marine ferromanganese oxide deposits. Thus whilst the sources of these metals will control the amounts which are available for incorporation into the deposits in a given area, the nature of the oxides themselves and their capacity to accept these metals must be a major influence on the minor metal content of marine ferromanganese-oxides.

The volcanic contribution of Co, Ni, Cu, Zn and Pb to the total budget of these metals in the oceans is not known. According to Corliss (1971), Co, Cu and Pb are all leached from basalt by sea-water and Bender et al (1972) found that much of the Pb in east Pacific Rise sediments was of volcanic origin. Sclater et al (1976) do not regard active ridges as being major suppliers of Ni to the oceans. Boyle (pers. comm.) has reached similar conclusions for Ni and for Cu, finding that in pelagic areas a major supply of Cu to the surface waters, thus to the total budget, is aeolian dust.

In the present study Co and Pb were not found to be enriched in mid-ocean ridge samples even though the mineralogy of the Mn phase in these samples is favourable for their enrichment. This indicates that active ridges may not be an important source of Co and Pb to ferromanganese-oxides. However, the low trace metal content of ridge samples may simply be due to their accumulation at a faster rate than samples from elsewhere in the ocean, this faster growth rate reducing the amount of scavenging of trace metals by the authigenic oxide phases.

The mineralogy of ocean ridge ferromanganese-oxide deposits, being

enriched in  $\delta$ - $\text{MnO}_2$  precludes any enrichment of Cu, Ni and Zn in these deposits even if these metals are being supplied extensively in ridge areas. The importance of such supply of these metals to the deposits cannot therefore be assessed readily. Whatever the ultimate source of Cu, Ni and Zn however, an important role in their cycle in the oceans and their transport to bottom waters is played by marine organisms (Sclater et al, 1976; Greenslate et al, 1973; Piper & Williamson, 1977).

The small amounts of trace metals which these organisms contain in their soft and hard parts are gradually released as the organisms sink and decay upon death. In the case of siliceous organisms, release of metals from the test is likely to be slow and may occur predominantly after the test has reached the sediment-water interface since siliceous organisms are much less soluble in deep ocean water than those with carbonate tests. Below the lysocline, carbonate organisms are likely to be extensively dissolved and areas below the carbonate compensation depth in areas of high biological productivity are likely to have bottom waters particularly enriched in metals from the dissolution of carbonate organisms. Large-scale fluctuations in the amounts of trace metals in bottom waters might thus occur from region to region.

Notwithstanding the possible importance of organisms in transporting metals to the sediment-water interface, over the Indian Ocean as a whole the variation in trace metal content of ferromanganese oxides can be accounted for mainly in terms of a mineralogical control. In Section 5, todorokite-rich nodules from the Indian Ocean were shown to be enriched in Mn, Ni, Cu and Zn compared with  $\delta$ - $\text{MnO}_2$  - rich samples, which are enriched in Fe, Co and Pb. The enrichment of Cu, Ni and Zn probably occurs at least partially because these metals are able to substitute for divalent Mn in the todorokite lattice. By contrast, Co can readily substitute for tetravalent Mn ions but not for divalent Mn, and is thus enriched in  $\delta$ - $\text{MnO}_2$ . Lead is also enriched in  $\delta$ - $\text{MnO}_2$  - rich samples but the mechanism of its incorporation is not known

since its large ionic radius makes it unlikely that it can readily substitute for tetravalent manganese.

It is evident from the preceding discussion that Cu, Ni and Zn enrichments are characteristic of nodules containing abundant todorokite and having a low Fe content. In areas where todorokite-rich, Fe-poor complexes are found and where Cu, Ni and Zn are being supplied in enhanced amounts then extreme enrichment of these elements occur. All these conditions are met in the siliceous ooze area of the Central Indian Basin and extreme enrichments of Cu, Ni and Zn occur in nodules from this area. In other areas of the Indian Ocean, where one or more of the above conditions is not met, enrichments of Cu, Ni and Zn are not marked. At the other extreme to Central Indian Basin nodules are samples which are rich in  $\delta\text{-MnO}_2$ . These are often recovered from sites where there is little or no sediment cover and where the supply of Fe is high. These deposits are depleted in Cu, Ni and Zn but are enriched in Co and Pb. Thus there is a continuous series of deposits occurring in the Indian Ocean with compositions ranging between the two extremes (Figures 19 - 27). This series is summarised in Table 19.

No attempt has been made in Table 19 to account for deposits from the several, limited areas mentioned in Section 8 where the behaviour of Ni and Cu differ substantially from normal. Taking into account the behaviour of Ni, Cu values are only about half of what would be expected, in the following regions; the Arabian Basin, the Mozambique Channel, Southern African Plateaux regions and isolated sea-mounts. With the exception of the Arabian Basin, these are all elevated areas with average depths of about 3000m. or less. In Section 5 a theory of biological fractionation of Cu from Ni was proposed to explain the lack of correlation of these metals in a suite of samples from the north-west Indian Ocean. This theory, that Cu is much lower in shallow water samples than would be expected because of its greater uptake into marine organisms, may account for the low Cu content of samples from all the anomalous areas except the Arabian Basin. The anomalous area in this Basin is

	3	2	1.5	1.2	1.0	0.8	0.6
Manganese Minerals							
Iron Minerals							
Type of Substrate	siliceous ooze	siliceous clay 'red' pelagic clay		nodules on pelagic clays and clay carbonates		No sediment, crusts on volcanic rock	
Trace Metal Enrichments	<p>Samples containing todorokite and plotting in this region show no Co or Pb enrichment</p>						
Characteristic Areas (Average Mn/Fe ratio in brackets) and observed authigenic minerals	Central Indian Basin (2.9)	Wharton & Somali Basins (both 1.3)	Southern African Plateaux (1.2)	Crozet & Mozambique Basins (0.83, 0.89)	Madagascar Basin (0.78)	Sea-Mounts (0.77)	Mid-Ocean Ridge (0.64)
	abundant todorokite	todorokite	some δ-MnO <sub>2</sub> but mainly no distinct Mn phase	no distinct Mn phase	δ-MnO <sub>2</sub> (some todorokite in Madagascar Basin)		δ-MnO <sub>2</sub> goethite

delineated entirely by samples analysed by other workers. Since no samples in the present study came from this area, no work was done on it and the reasons for the anomaly must therefore await future investigations. Some of the samples analysed in the present study do not follow the trends tabulated in Table 19. These samples all came from areas off the South African coast and from the Mozambique Channel. This area is characterised by nodules of highly variable composition. One sample was analysed which had a high  $Mn/Fe$  ratio, was rich in todorokite and yet depleted in trace metals. The high  $Mn/Fe$  ratio of this sample has already been described as being indicative of increased supply of Mn due to diagenetic remobilisation. Near the African coast, two samples were retrieved which had exceptionally low  $Mn/Fe$  ratios and which also had a very low trace metal content. Samples of similar composition have been found in the Pacific Ocean in continental borderland areas (Mero, 1965). Their very high Fe content is thought to be due to an enhanced supply of Fe from continental sources. All these samples depart from the series set out in Table 19 because one of the major elements, Mn or Fe, is supplied in very much greater amounts than the other. This increase in the amount supplied leads to growth rates an order of magnitude or more higher than those observed in pelagic deep-water samples (Ku & Glasby, 1972) and this rapid growth rate precludes the incorporation of large quantities of trace metals.

Table 19 can be expanded to incorporate deposits where rapid supply of Mn or Fe substantially modifies the composition of the accreting deposits. This has been done in Table 20. This Table summarises the main mineralogical and chemical variations observed in Indian Ocean ferromanganese-oxides and attempts to relate them to variations in several parameters such as sedimentation rate and type and element source. However, samples from the Mozambique Channel can still not be fitted into the diagram conveniently. Samples from this area contain todorokite in most cases, have rather variable  $Mn/Fe$  ratios with an average ratio of 1.0 and are high in Ni, Zn and to a

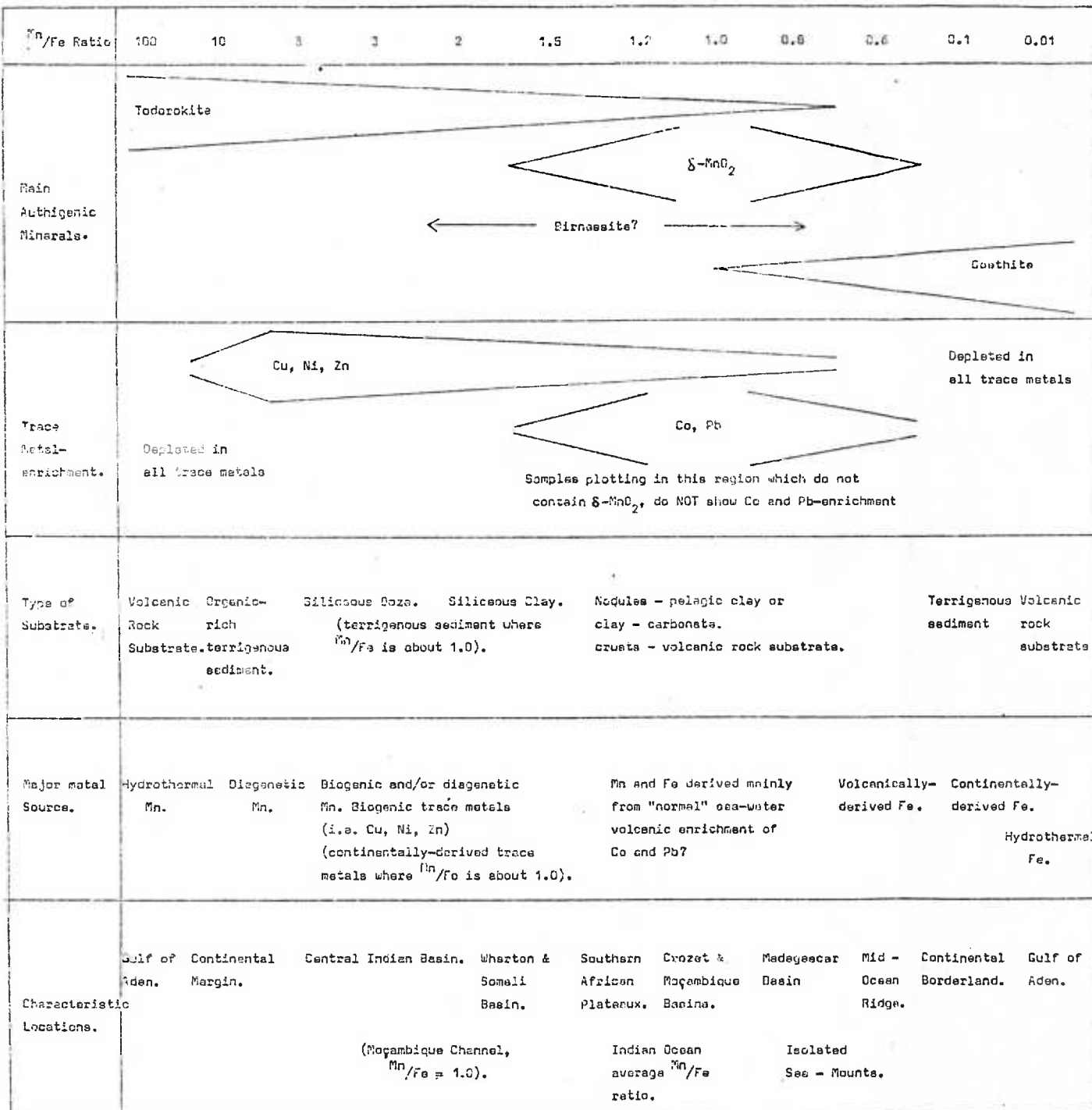


TABLE 20

Summary of compositional variability of Indian Ocean ferromanganese-oxide deposits in relation to mineralogy, element source and type of substrate.

lesser extent Cu; the samples rest on a carbonate-rich terrigenous clay sediment, and it is their high trace metal content which makes them anomalous. This anomaly might be explained in terms of a greatly increased supply of these metals to bottom waters in this area. Such supply may come from biological sources. However biological productivity does not appear to be particularly high in the waters above these sample sites, and the sites lie well above the lysocline in this region so there is likely to be little dissolution of carbonate organisms in the bottom water. Another possible supply of these metals is from continental sources, as adsorbed ionic species or organic complexes which might release metals into bottom waters. However, whilst the sediments supplied to this area are derived from rivers draining one of the most intensely mineralised regions of the earth's crust, doubt is cast upon this mechanism by the fact that there are almost no Ni deposits in southern Africa yet this metal is the most enriched in the nodule samples. No studies of the metal content of rivers draining into the Mozambique Channel have been carried out and the problem of the source of the Ni, Zn and Cu in the Mozambique Channel samples must therefore remain open. Because of this uncertainty these samples have been included in Table 20 only in brackets.

#### (ii) SUMMARY & CONCLUSIONS

This thesis has examined various aspects of Indian Ocean ferromanganese-oxide deposits and associated sediments, based on a large number of new analyses together with all previously published data accessible to the writer.

The distribution of ferromanganese-oxide deposits in the Indian Ocean is determined largely by sedimentation rates. Encrustations occur in rugged areas where sediment cannot accumulate and where exposed rock therefore forms the substrate. Nodules occur in areas floored by sediment but where, due to the very low rate of sediment supply or to the erosive action of bottom currents



rates of sediment accumulation are very low or zero. In areas of more rapid sedimentation, such as those above the lysocline or those receiving continental run-off, ferromanganese-oxide deposits are not common.

The mineralogy and chemical composition of the deposits varies in response to several complex interrelated parameters, the most important of which are element source and mobility and nature of the depositional environment. The behaviour of the elements Mn and Fe is of great importance in controlling the trace metal content of the deposits. A major source of Fe to marine ferromanganese-oxides is the mid-ocean ridge system and deposits on and near this feature reflect this in their higher Fe content. A high rate of supply of Fe coupled with the highly oxygenated conditions generally found in mid-ocean ridge environments, favours the growth of  $\delta$ - $\text{MnO}_2$  as the predominant Mn phase in the deposits.

In areas where available Mn is greatly in excess of Fe, samples rich in todorokite are found. Such areas tend to be those furthest removed from continental and submarine sources of Fe. Depending on their availability, Cu, Ni and Zn are more or less enriched in todorokite-rich samples. Particularly marked enrichments occur where the overlying surface waters support high biological productivity since marine organisms provide an important sink for these metals and the downward transport of these organisms after death leads to an enrichment of the bottom waters in Cu, Ni and Zn.

The different roles which parameters such as bottom currents, sediment type and sedimentation rate play in controlling the variation in distribution, morphology and composition of the deposits has been examined. Using presently available knowledge of the variations of these parameters over the Indian Ocean it has been possible to account reasonably well for many of the observed variations in mineralogy and chemical composition of the ferromanganese-oxide deposits analysed. However, exact relationships could not often be established and much detailed work remains to be done.

Summarising the regional variability of ferromanganese-oxide deposits,

the highest levels of Mn and the trace metals Ni, Cu and Zn are found in todorokite-rich nodules sitting on a siliceous ooze substrate in the Central Indian Basin. Manganese, Cu and Ni-enriched samples are also found in the Wharton Basin and in small isolated areas in the western Indian Ocean where the substrate is not necessarily highly siliceous. Iron exhibits roughly the reverse behaviour to that of Mn, being at its lowest in the Central Indian Basin and Wharton Basin and generally intermediate throughout much of the western Indian Ocean. The highest Fe values occur in mid-ocean ridge samples, with sea-mount samples also having Fe values above the whole ocean average. Many samples from both these types of locality are encrustations from a rock substrate. Cobalt and Pb behave in the opposite fashion to Ni and Cu, being at their lowest in the Central Indian and Wharton Basins, generally low in most basin areas, and at their highest in sea-mount samples, which also tend to be enriched in  $\delta\text{-MnO}_2$ . Cobalt values are also higher than average in the Madagascar Basin.

The regional variations in bulk composition of sediment samples analysed showed some similarity to the regional variations observed in ferromanganese-oxide samples. Thus Mn is highest and Fe lowest in Central Indian Basin samples, Co and Pb are higher in the western Indian Ocean than in the east, whilst Ni and Cu show the reverse trend, being higher in the eastern Indian Ocean basins. These regional trends were not nearly so marked as those observed in the ferromanganese-oxide deposits. However the fact that broadly similar trends do occur in both sample groups demonstrates that the processes and mechanisms influencing the composition of ferromanganese-oxide deposits are similar to those governing the overall composition of sediments. The fact that the trends observed in sediments do not exactly match those of the associated ferromanganese-oxide deposits may be explained by the fact that sediments are a much more complex mixture of material from many sources than are ferromanganese nodules.

PART TWO

## S E C T I O N 10

### SAMPLE LOCATION AND DESCRIPTION

#### (i) INTRODUCTION

Fourteen ferromanganese-oxide samples were collected from an area of the north-east Atlantic Ocean during a research cruise to this area in 1972 by R.R.S. Shackleton. These samples have been analysed in order to investigate the geochemical and mineralogical variations which might occur in this area and also to help provide a useful comparison with data obtained from the analysis of a much larger number of samples from the Indian Ocean, and which have been discussed in Part 1 of this thesis. This process of comparison was particularly important in the case of the partition analyses carried out on the nodule samples since there are virtually no published accounts of previous works of this nature.

#### (ii) (a) SETTING & GENERAL GEOLOGY

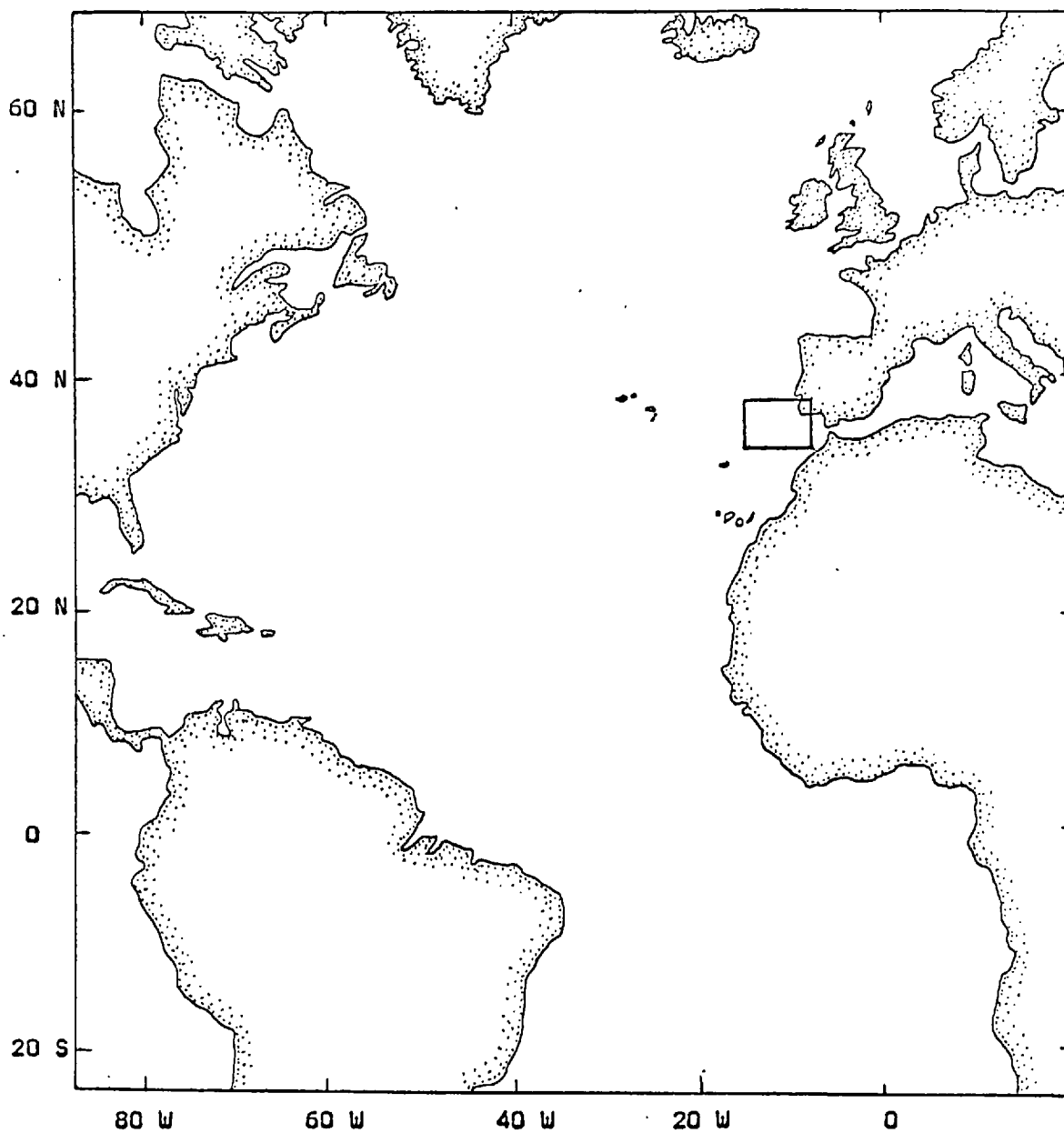
Figure 73 shows the part of the Atlantic Ocean in which the sample area is located, this area is shown in greater detail in figure 74. This region lies approximately 300 miles west-south-west of the southern tip of Portugal and to the east of the Madeira-Toré Rise. The structure of this

part of the north-east Atlantic Ocean is very complex and of considerable interest.

All the samples obtained were dredged from 5 localities on and around sea-mounts of the Horseshoe Sea-Mount Chain. This chain consists of a northern group (Hirondelle II, Gettysburg, and Ormonde sea-mounts) and a southern group (Unicorn, Ampère and Coral Patch sea-mounts) linked to each other in the west by sea-mounts of the Central section of the Madeira-Toré Rise, (Josephine and Lion Sea-Mounts). The Madeira-Toré Rise is interesting in that it straddles the actively spreading Azores Fracture Zone and the Horseshoe Sea-Mounts and Horseshoe Abyssal Plain to the east of this rise cover an area of complex plate tectonic activity. The Horseshoe Abyssal Plain lies on the Azores-Gibraltar plate boundary and is a seismically active area (Le Pichon et al, 1971).

McKenzie (1970, 1972) and Udias & Arroyo (1972) have suggested that the Horseshoe Sea-Mount area is in general one of compression and Fukao (1973) concluded that the oceanic crust was being thrust beneath the Gorringe Ridge in a north-north-westerly direction. Le Pichon et al (1970) have suggested that this ridge, which forms the Gettysburg and Ormonde Sea-Mounts, is not simply the result of a volcanic event but is a slab of oceanic crust uplifted during a fairly recent phase of compressive tectonics along the Azores-Gibraltar seismic zone. However, it may be that at least one, and possibly more, mini-plates may be involved in crustal structure in this region. The Hirondelle II and Josephine Sea-Mounts and the Ampère and Coral Patch Sea-Mounts to the south may be the result of normal volcanic activity or may be part of up-thrust mini-plates analagous to the Gorringe Ridge. A clearer picture of the structure and tectonics of this region however must await further investigation.

FIGURE 73 Map of Atlantic Ocean showing location of sample area.



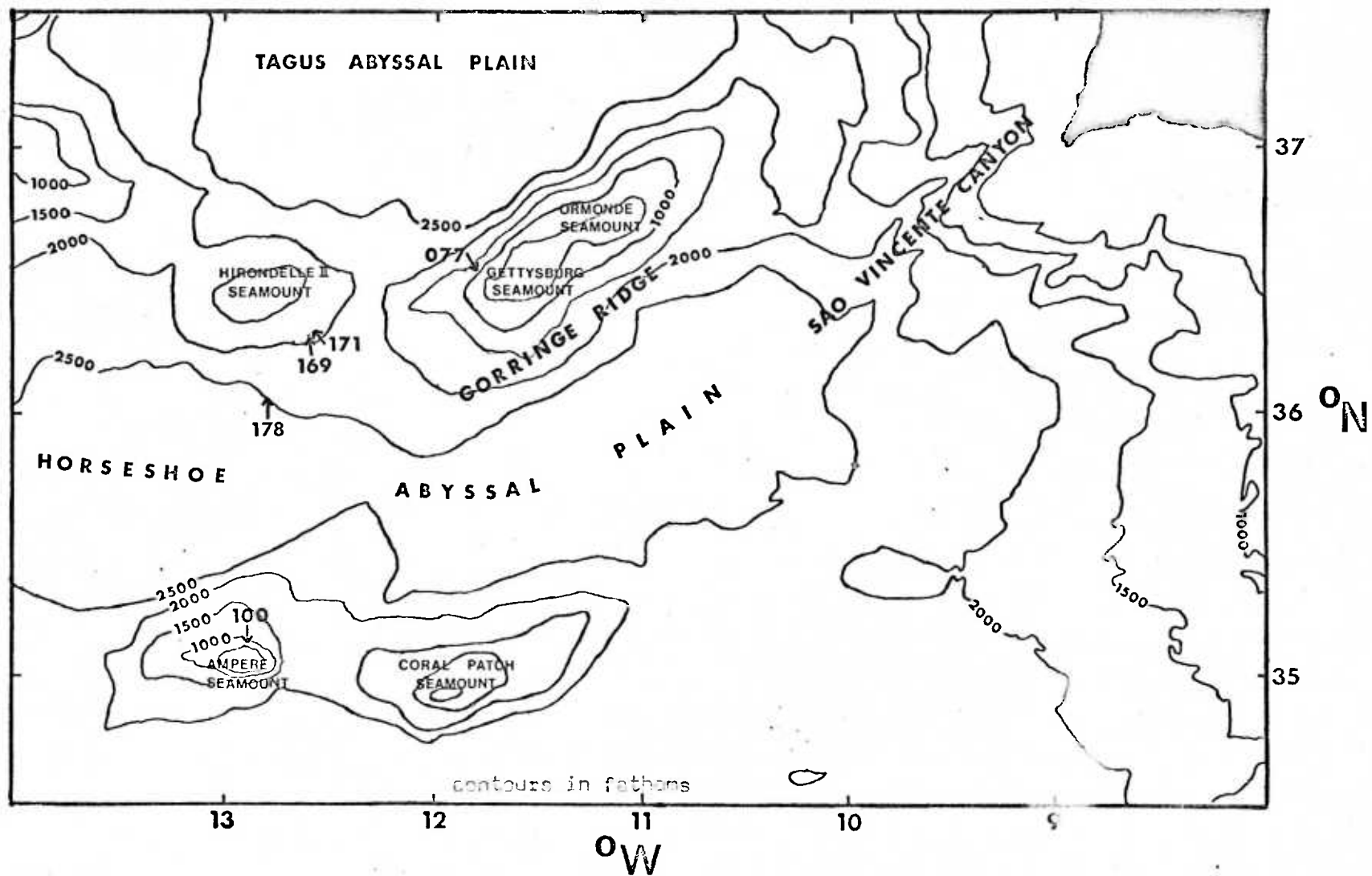


**FIGURE 74** Bathymetric map of Horseshoe Sea-Mount Area showing sampling localities (from Laughton et al, 1975).

## (ii)(b) SEDIMENTATION

The complex nature of the topography in the Horseshoe Sea-Mount area necessarily leads to a complex pattern of sedimentation. No sediments, other than tiny amounts adhering to the outer surface of some dredge samples, were recovered from any of the 5 stations occupied. Sediments in this area, however, have already been studied by several workers at other times. According to Le Pichon et al (1970) the Horseshoe Abyssal Plain is turbidite-floored and contains up to 9 kilometres of deformed sediments. Without this sediment infilling, Le Pichon et al suggest this area would be analogous to a Pacific Ocean-type trench. Horn, Ewing & Ewing (1972) state that the Horseshoe Abyssal Plain is filling with sediments brought in from the east. This material is presumably derived from the continental terrace off southern Portugal and Spain and is transported to the abyssal plain via the São Vicente and other canyons. This is borne out by the fact that there is a progressive decrease in the thickness and grain size of turbidites from east to west across the plain and a concomitant increase in the amounts of intercalated pelagic ooze. It is not clear to what extent, if any, slumping of sediments from the surrounding sea-mounts contributes to sediment accumulation on the abyssal plain. Certainly the steep flanks of many of the Horseshoe Sea-Mounts preclude their being covered by any great thickness of sediment although the more gentle upper slopes and summits may have a thicker sediment cover. According to Ryan et al (1973) the Gorringe Ridge is clear of sediment in some places, whilst in others there is a more or less uniform but relatively thin coating of sediment. Since the upper portions of these sea-mounts, at least, are well above the lysocline, their associated sediments might be expected to be carbonate-rich. This was confirmed by Ryan et al (1973) who found that surface sediments on the Gorringe Ridge consisted of a highly calcareous biogenic ooze rich in forams and coccoliths. This type of sediment is



therefore in marked contrast to the sediments on the floor of the abyssal plain which the sea-mounts encircle.

(ii) (c) SAMPLE LOCATION

The fourteen samples analysed were obtained from five dredge station sites located on and near various sea-mounts in the Horseshoe Sea-Mount Chain (see figure 74). Stations 169, 171 and 178 were occupied on the southern flanks of the Hironnelle II Sea-Mount. Stations 169 and 171 were separated by only about one mile whilst station 178 was occupied about 30 miles to the south-south-west at the foot of the sea-mount, on the northern edge of the Horseshoe Abyssal Plain. Station 077 was on the upper part of the northern slope of the Gettysburg Sea-Mount, about 50 miles to the east-north-east of stations 169 and 171. Station 100 was near the summit of the Ampère Sea-Mount, 80 miles south-south-west of stations 169 and 171 and on the southern side of the Horseshoe Abyssal Plain.

Since single dredge hauls can often traverse more than one type of bottom environment especially in areas of rugged topography, wherever more than one sample was obtained from a particular dredge haul, each was analysed separately, thus the samples analysed were as follows:-

Station 077:	2 samples - 1 nodule, 1 encrustation	(1600m. water depth)
Station 100:	2 samples - both encrustations	(1450m. water depth)
Station 169:	6 samples - 5 nodules, 1 encrustation	(3700m. water depth)
Station 171:	1 encrustation	(3800m. water depth)
Station 178:	3 samples - 3 separate nodules	(4600m. water depth)

### (iii) SAMPLE MORPHOLOGY AND STRUCTURE

Of the fourteen samples investigated, five were coatings or encrustations and nine were nodules or nodule fragments. The encrustations came from shallower average depths (2400m.) than the nodule samples (3766m.). The coatings and encrustations ranged in thickness from 1 mm. to 1 cm. Apart from sample 169.6, no idea of the overall size of the crusts could be gained since the material obtained had obviously been broken off a larger area of encrusted material on the sea-bed. Sample 169.5 was a thickly-coated basalt fragment which had a maximum diameter of 6 cm. and a minimum of 4.5 cm. The basalt fragment was appreciably altered especially at its contact with the encrustation but still extremely hard and had an irregular shape and surface. The ferromanganese coating on it was easily separated from the fragment, but was of very variable thickness, being absent in some places and reaching a maximum of 6 mm. in others. All the encrustations varied in colour from rich deep brown (171.15), through dark brown (169.6) to almost black (077.18, 100.2, 100.3). The colour of the samples seems to be linked to their Mn content, with the darkest samples containing more Mn (13%) than the browner samples (2.5% - 11%). The darker encrustations were also much harder and less porous than the browner material.

The thicker encrustations (100.2, 100.3) showed no evidence of internal laminations, being of very even colour. However, sample 171.15, and to a lesser extent 169.6, did show some evidence of very fine laminations. Both samples 100.2 and 100.3 were found on crushing to contain many small, angular, extremely hard fragments. It is likely that these fragments are either basalt fragments or detrital minerals such as rutile, from the weathering of basalt. It was not possible to remove these fragments during crushing.

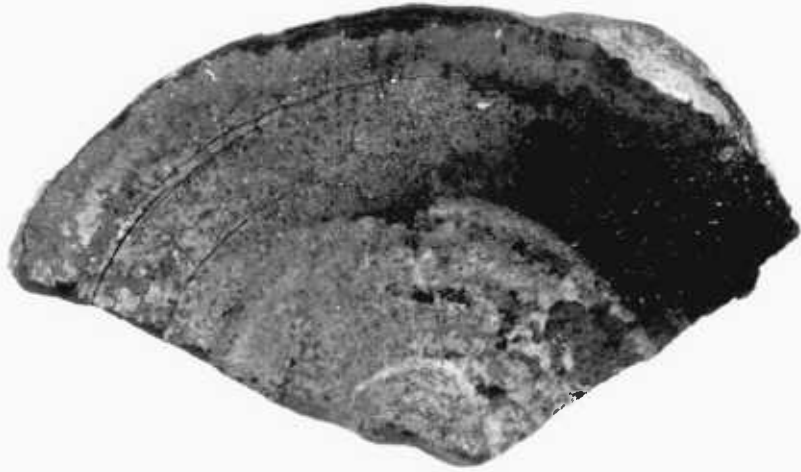
All the encrustations except samples 100.2 and 100.3 had a discontinuous thin coating of white to buff-coloured sediment on their outer surface which obscured the fine surface texture. It would seem, therefore, that samples 100.2 and 100.3 were the only samples which could have been actively accreting ferromanganese oxides at the present time. Except in the case of sample 169.6, already discussed, the substrate was not obtained with any of the samples and so no information could be gained of the type and condition of the encrusted material.

The nodules obtained were all fairly large in size, ranging from 5 cm. to 11 cm. in maximum diameter. Most nodules were spheroidal to spherical in shape. The three nodules from station 178 were all fairly large, averaging 8 cm in diameter, and very similar in overall size, shape and texture. Station 169 nodules were of more variable size and shape, and sample 169.3 was a polynucleate nodule, having two distinct cores.

All the nodules were fairly compact and of average density. Their surface shapes were all similar, being regular to sub-botryoidal. Their surface textures were all fairly similar, samples 077.33, 169.1 and 169.3 were smooth to microgranular whilst the other nodules from station 169 were fairly evenly microgranular. Station 178 nodules however tended to have a somewhat coarser macrogranular texture. Thus samples from deeper water appear to have a different, more granular surface texture which presumably indicates their growth in a somewhat different sedimentary environment to the other samples.

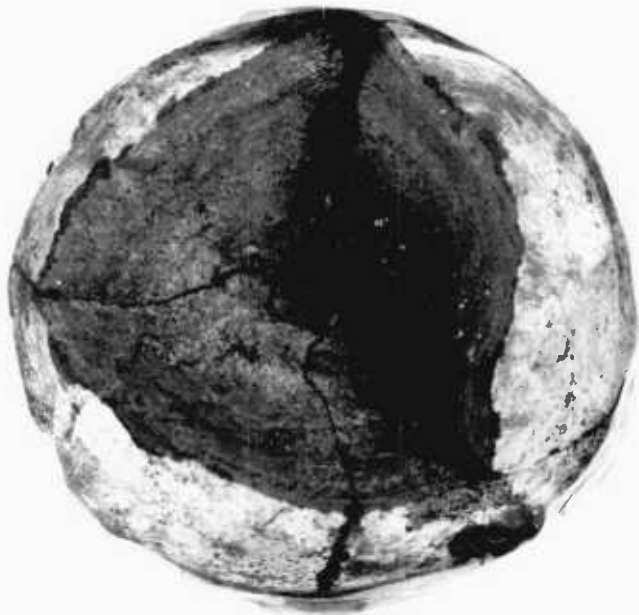
All nodules showed some evidence of internal structure although the laminations were often on a very fine scale and very unclear. All the samples from station 178 showed a tendency to fracture very easily on smooth concentric surfaces which presumably correspond to growth lines within the samples. This tendency has been accentuated due to the dehydration which has occurred during sample storage and is especially clear

SH73.178.4



CMS

SH 73 .178 .3



CMS

in sample 178.4 ( see plate 18).

There was little evidence in most samples to suggest that there had been any major breaks in nodule growth. However, sample 169.1 had an outer layer 4 to 5 mm. thick which was much darker and more ferromanganese-oxide-rich than the rest of the sample. This may represent a recent period of renewed growth. Sample 178.3 contained a small nodule with a weathered volcanic core, the whole of which appeared to form the nucleus for a second, much thicker growth stage, forming the rest of the nodule sample, (see plate 19).

None of the nodules had large or fresh-looking cores. Most in fact were highly altered and heavily indurated and replaced by ferromanganese-oxide material. Most cores were very irregular in shape but none had a largest diameter greater than 1.5 cm. All the cores had a similar appearance consisting of pale, buff-coloured clay-like material containing small hard fragments, probably palagonite and altered feldspar. All the cores were obviously of volcanic origin, as might be expected in view of the location of the samples in a region with a complex volcanic and tectonic history. All the samples had a thin, discontinuous coating of buff-coloured sediment on their outer surfaces indicating that active growth could not have been occurring at the present time, and that the samples may have been partly or wholly buried by sediment.

## SECTION 11

### MINERALOGY

#### (i) INTRODUCTION

Fourteen samples, collected from the 5 sites shown in figure 74 were analysed by X-Ray diffraction techniques on a Phillips diffractometer in order to investigate their mineralogical nature. Details of the techniques used are given in Appendix 2.

A brief history of research has been given in Section 4, together with a discussion of problems of identification and terminology of the authigenic Fe and Mn phases in marine ferromanganese-oxide deposits. It is sufficient here merely to summarise the conclusions reached. The three Mn phases identified with certainty in the samples analysed in this study gave the characteristic lines listed in Table 21. These were given the currently most-favoured names, todorokite, birnessite and  $\delta$ -MnO<sub>2</sub>. Samples in which none of these lines were definitely identifiable were regarded as containing a predominantly amorphous Mn phase.

Less work has been done on the Fe phases in ferromanganese-oxide deposits, probably mainly because even in samples with a high Fe content the iron phase often appears to be essentially amorphous. A discussion of the problems of identifying Fe phases in ferromanganese-oxide deposits has also been given in Section 4.

d(A)	I	PHASE
9.6 - 9.8	VS	Todorokite
4.6 - 4.8	S	"
2.46	M	"
2.39	M	"
7.0 - 7.2	VS	Birnessite
3.5 - 3.6	S	"
2.46	M	"
2.33	M	"
1.42	W	"
2.40 - 2.45	v. br. S	$\delta$ -MnO <sub>2</sub>
1.40 - 1.44	v. br. M	"

TABLE 21

Diffraction patterns of the manganese phases recognised in Atlantic Ocean ferromanganese-oxides

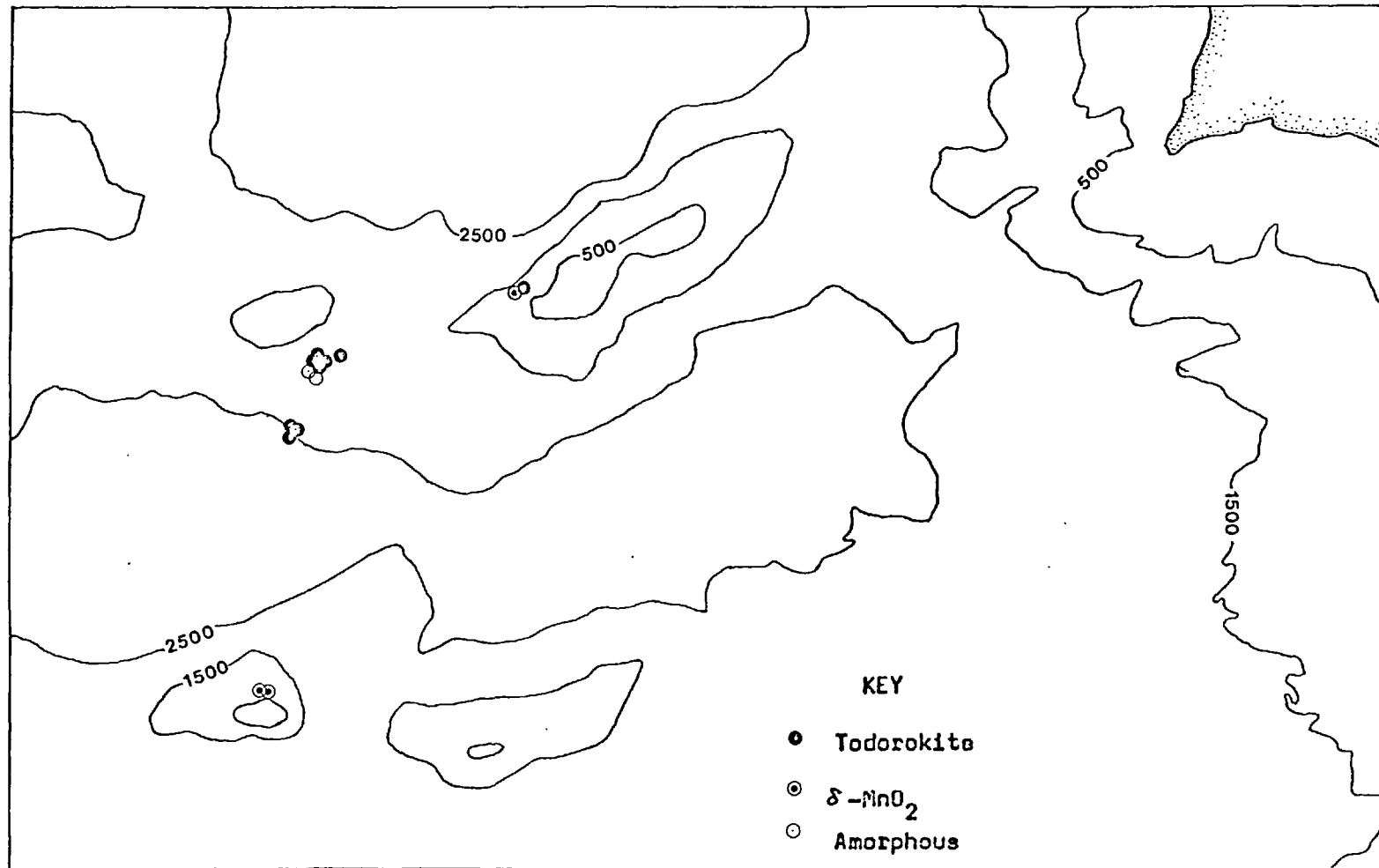


**FIGURE 75** Distribution of Mn minerals in north-east Atlantic Ocean samples.



Several Fe minerals have been reported as occurring in marine ferromanganese-oxides, however goethite was the only Fe mineral identified in the Atlantic Ocean samples except in one case, discussed later. Using Mossbauer techniques, discrete Fe phases have been identified by several workers (Johnson & Glasby, 1969; Hrynkiwicz et al, 1970; Brown, 1971) in nodules where no Fe phases were recognised by conventional X-Ray diffraction analysis. These workers found that in many of these samples, the mean particle diameter of the Fe phases was only of the order of 100Å. For the purposes of this study however, samples in which no peaks clearly assignable to an Fe mineral were seen, were regarded as containing an essentially amorphous phase.

#### (ii) MINERALOGY OF THE FERROMANGANESE PHASES

##### Mineralogy of the manganese phases

Table 22 gives the total number of samples in which the various manganese phases listed in Table 21 were recognised. As can be seen from Table 22, todorokite was the most abundant phase observed, occurring in almost three-quarters of the samples analysed. As can be seen from figure 75, samples containing  $\delta$ -MnO<sub>2</sub> only, were from the upper parts of sea-mounts, whereas nodules containing todorokite were from greater average depths. However, sample 077.33 from the upper part of the Gettysburg Sea-Mount was found to contain todorokite, although being collected from a depth of only 1600m.

Nodules which contained no identifiable manganese phase did not come from any particular characteristic depth environment or unique locality, being found in the same dredge haul as samples containing todorokite. The two samples in which the manganese phase was presumed to be essentially amorphous were very low in manganese, however the

MANGANESE PHASE	SAMPLES IN WHICH IDENTIFIED	TOTAL NO. OF SAMPLES	AVERAGE WATER DEPTH(m)	AVERAGE CONCENTRATION MN
Todorokite	077.33; 169.1; 169.3; 159.5; 169.20; 171.15 178.2; 178.3; 178.4	9	3780	8.1%
$\delta$ -MnO <sub>2</sub>	077.13; 100.2; 100.3	3	1550	13.3%
Birnessite		0		
Amorphous	169.14; 169.17	2	3700	7.4%

TABLE 22

Mineralogical composition of Atlantic Ocean nodules

average Mn content of samples containing identifiable todorokite was very little higher. This is in contrast to the behaviour of these sample types in the Indian Ocean where amorphous samples were much lower in Mn on average than in those containing todorokite. The recognition of diffraction lines due to todorokite in the samples may be more a factor of degree of crystallinity rather than the actual amount present.

#### Mineralogy of the iron phase

All the samples analysed were found to contain goethite. In some cases only the strongest line, at 4.18Å, was seen with certainty. However in some samples as many as 8 or 10 lines attributable to goethite were observed. Moreover, these lines were relatively sharp indicating that the goethite was well-crystalline and of comparatively large particle size. All the samples are comparatively high in iron (13% - 28%) and thus in those samples showing only one or two goethite peaks, much of the Fe must be present as an amorphous phase, or be extremely poorly crystalline. There did not appear to be any correlation between the Fe content of the samples and the height of the major goethite peaks. In four samples, 077.33, 169.3, 171.15, 178.4, the goethite appeared to be particularly well-crystalline and abundant, and sample 169.3 also contained traces of  $\gamma$ -Fe<sub>2</sub>O<sub>3</sub> (hematite).

#### (iii) OTHER MINERALS

A variety of authigenic and detrital minerals, other than the authigenic Fe and Mn oxides discussed above, have been reported as occurring in ferromanganese nodules and have been discussed in Section 4. All the samples, except 100.3 contained  $\alpha$ -quartz. In many of the samples, quartz was very abundant, the most intense peak at

3.34Å giving a full-scale deflection on the diffractometer trace.

Samples 100.2, 100.3, 169.1, 169.17 contained calcite but in the latter two there were only trace amounts. Station 100 was occupied in a water depth well above the lysocline. Most of the samples from stations 169, 171 and 178 contained small amounts of plagioclase feldspar and clay minerals. The main clay mineral appeared to be of montmorillonite type with a basal peak of about 14Å.

#### (iv) DISCUSSION

The small sample population and irregular sample distribution limits the conclusions which can be drawn from the mineralogical analyses. However, there are one or two noticeable trends. Todorokite occurs in samples which come from greater average depths than samples containing  $\delta$ -MnO<sub>2</sub>. This tendency has been found in nodules in other parts of the world's oceans (Barnes, 1967; Cronan & Tooms, 1969; Crerar & Barnes, 1974) and also in samples from throughout the Atlantic Ocean (Cronan, 1975). In general, the conclusions reached in the present study agree well with those observed by Cronan (1975) although the 7.1Å reflection observed in some samples by Cronan was not observed in any samples in this study.

Whilst the high average Fe content of Atlantic Ocean ferromanganese deposits has been noted by various authors (Mero, 1965; Cronan, 1972) virtually no work on the mineralogy of the Fe phase of these deposits appears to have been published. It is therefore not possible to assess whether the seemingly large amounts of relatively well-crystalline goethite in the samples analysed is a typical feature of Atlantic Ocean nodules from this type of environment. Certainly this behaviour has not been reported in samples from the Pacific or Indian Oceans.

Samples from the Nares Abyssal Plain in the North Atlantic, which were analysed by Smith et al (1968) were found to contain some goethite but this did not appear to be as abundant or as well-crystalline as that observed in this study. Goethite of very small particle size or amorphous  $\text{FeOOH}$  may re-crystallise with age within nodules to better crystalline goethite of fairly large particle size. Glasby (1970) has shown that the re-crystallisation within nodules of extremely fine-grained manganese-oxides to particles of larger size is thermodynamically favourable under marine bottom conditions and this may also be the case for the discrete iron oxide-hydroxide phase. As discussed earlier, several of the samples analysed were nodules of quite large size and therefore likely to be comparatively old. However, the samples had been stored dry at room temperature for two years prior to analysis and the effect which this may have had on the mineralogy is not known. According to Berner (1969) goethite is metastable under the conditions encountered on the deep-seafloor and ages to hematite. The identification of this mineral in one sample provides some evidence that ageing processes may have occurred within the iron phase of the samples before they were recovered.

SECTION 12GEOCHEMISTRY

## (i) INTRODUCTION

The fourteen ferromanganese-oxide samples from the five dredge stations shown in figure 74 were analysed for Mn, Fe, Co, Ni, Cu, Zn, Pb, Cd, Cr, Ca, Al and Ti. Analyses were carried out by atomic absorption spectrophotometry using the techniques described in Appendix 1. In addition to determining the bulk composition of the samples, selective chemical attacks were carried out in order to investigate the partitioning of elements between the various fractions released by the different attacks.

## (ii) COMPOSITIONAL VARIATION OF SAMPLES FROM SAME STATION

The type of material obtained for analysis was of fairly varied morphology, ranging from thin coatings on rock to nodules 11cm in diameter. Because of this wide variation in morphology, occasionally seen even in different samples from the same dredge haul, it was decided to analyse separately each type of sample obtained, even where several samples were obtained from the same dredge haul. In this way,

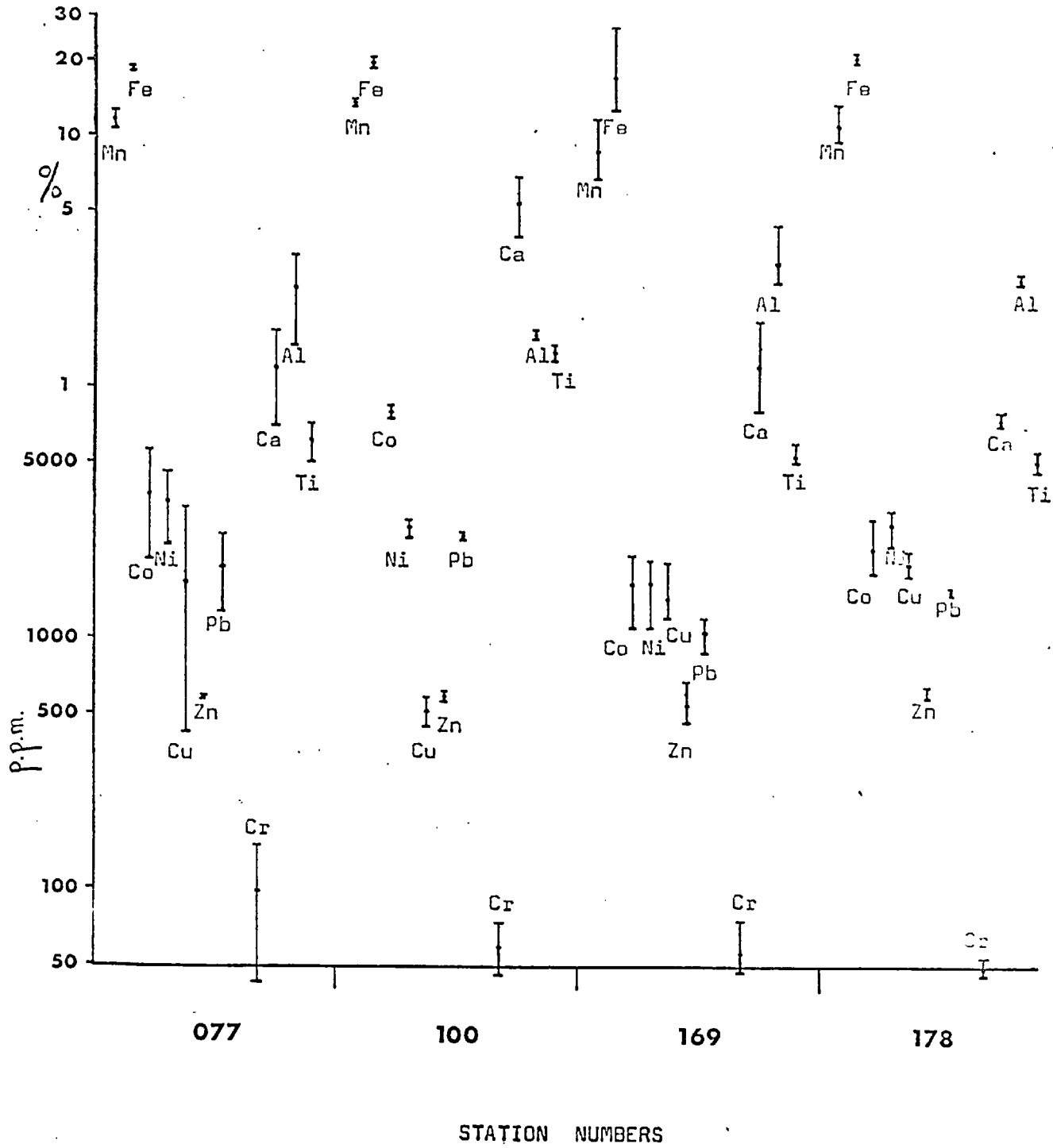
it was hoped to investigate whether significant morphological differences were reflected in significant compositional differences. The variation in composition of samples from each dredge station is summarised in figure 76. The station at the greatest depth, 178, contained material of fairly uniform size and morphology (see Section 10) and the three samples analysed show comparatively small variations in composition for both major and trace elements.

The six samples from station 169 were of slightly more varied type (see Section 10) and the variation in their composition is rather greater than that seen in station 178 samples. Both Mn and Fe have maxima which are slightly more than double their minima, whilst Ca shows a four-fold variation. Of the trace metals, Co Ni and Cu show a similar amount of variation to Mn and Fe. Zinc, Pb and Ti on the other hand show fairly uniform values.

Two samples were recovered from station 100. These were both encrustations on basalt of similar type and showed very little variation in composition for most elements. However, the concentration of Cr differs appreciably in the two samples and the Ca concentration also varies considerably between the two.

Material from station 077 consisted of a very thin crust and one large nodule. This marked morphological difference is reflected in the compositional variation of the samples. Whilst Mn and Fe show surprisingly little variation between the two samples, Co, Ni, Cu, Pb and Cr show very great variation. In the case of Cu this variation is extreme, the nodule containing eight times as much Cu as the thin crust. Of the trace metals, only Zn occurs at roughly the same concentration in both samples. A possible reason for the chemical variability of material from this station is discussed in Section 13. Cadmium levels in all the samples analysed were near the detection limit for this element. Because of this and the fact that very little variation seemed to occur in Cd values between

**FIGURE 76** Range in bulk composition of samples from the North-East Atlantic Ocean.





samples, Cd concentrations have not been plotted on figure 76.

Stations 077, 100, 169 were dredged on the flanks of large sea-mounts. These are areas of the sea-bed where, due to the rapidly changing nature of the bottom topography, considerable variations in bottom environment can occur even over the small distances traversed by a single dredge haul. This variation in bottom environment is reflected by the variation in ferromanganese-oxide morphology and composition, as has been observed by several workers (Cronan & Tooms, 1967; Glasby, 1970; Hubred, 1970; this study). The samples analysed in the present study, from the Horseshoe Sea-Mount Area of the Atlantic Ocean serve to confirm that the rapidly changing environmental conditions characteristic of major sea-mounts can cause significant variation in the composition of ferromanganese-oxides associated with the sea-mount.

### (iii) INTER-ELEMENT ASSOCIATIONS

Correlation matrices, using both normal and log-transformed data were calculated for the bulk compositional data using the same programme as that discussed in Section 5. The two matrices are given in Table 23, together with the minimum significant correlation coefficients at the 99% confidence level. Glasby, Tooms & Haworth (1974) have shown that even for comparatively large sample populations, the element correlations observed tend to be at least partially dependent on the characteristics of the sample population used. The only way to overcome this problem is to attempt to use as large a sample population from as many different types of bottom environment as possible. Only 14 samples were used in calculating the matrices given in Table 23 and these were from a limited range of environments hence the inter-element correlations obtained will not necessarily reflect those published in the literature using larger sample populations.

In general, the significant correlations using normal data agree with

	Depth	Mn	Fe	Co	Ni	Cu	Zn	Pb	Cd	Cr	Ca	Al	Ti	
Depth		-.39	-.02	-.65	-.43	.61	-.11	-.69	-.34	-.38	-.73	.69	-.78	L
Mn	-.42		-.42	.83	.61	-.38	.16	.58	.31	-.09	.62	-.45	.16	O
Fe	.06	-.39		-.28	.16	.17	.74	.29	-.76	.12	.66	-.35	.10	G
Co	-.74	.70	-.09		.45	-.71	.04	.79	-.36	.27	.74	-.64	.58	
Ni	-.38	.56	.06	.29		.11	.49	.54	-.15	-.17	.83	-.40	.06	T R
Cu	.35	-.32	.27	-.67	.46		.12	-.67	-.39	-.64	-.58	.71	-.84	A
Zn	-.05	.20	.69	.09	.39	.26		.47	-.58	-.01	.27	-.47	-.04	N
Pb	-.68	.68	.14	.93	.37	-.57	.35		-.07	.36	.69	-.93	.71	S
Cd	-.31	.16	-.74	.17	-.16	-.37	-.60	-.05		.18	-.32	.12	.33	F O
Cr	-.43	.05	.09	.41	-.15	-.54	.07	.48	.15		-.19	-.44	.54	R
Ca	-.63	.58	-.18	.82	.16	-.63	-.13	.70	.26	.07		-.59	.73	M
Al	.56	-.58	-.36	-.72	-.32	.42	-.55	-.88	.29	-.38	-.53		-.71	E
Ti	-.77	.35	.07	.87	.05	-.71	-.03	.82	.24	.47	.63	-.64		O

N O R M A L

TABLE 23

Correlation matrices for Atlantic Ocean ferromanganese-oxides. (Correlations significant at 99% confidence level are boxed. Number of samples used to calculate matrix = 14).

those observed using log-transformed data. However, there are one or two noticeable exceptions. For example, Cu correlates strongly positively with depth using log-transformed data but shows no significant correlation with depth using normal data. Similarly Fe and Ca, Ni and Ca, and Cu and Al show significant positive inter-correlations at the 99% confidence level using log-transformed data but do not show significant correlations using normal data.

Manganese correlates significantly positively with Co, Ni, Pb and Ca for both data sets whilst Fe correlates significantly positively with Zn and significantly negatively with Cd. However, the most significant correlations are those between the trace metals Co, Pb and Ti. These three elements all correlate positively with Ca, and Co, Pb, Ti and Ca all correlate strongly negatively with depth. Apart from the positive correlation with Ca, the behaviour of Co and Pb is similar to that observed for these elements in Indian Ocean nodules. As might be expected Al, which is associated predominantly with the diluting aluminosilicate phases in nodules, correlates significantly negatively with most of the metals associated with the authigenic phases, such as Mn, Co, Zn and Pb. However, Al correlates positively with Cu, although this correlation is only significant for log-transformed data. This is probably because in samples where Cu is particularly low in the samples as a whole, a substantial proportion of it may be associated with aluminosilicate material as was seen with several Indian Ocean samples in Section 5.

One striking feature of the correlation matrices is that they reveal no evidence of strong positive correlations between Cu, Ni, Zn and Cd or between these three elements and Mn. Nor is there a significant negative correlation between Mn and Fe. All these correlations have been observed in nodules from the Pacific and Indian Oceans (Cronan, 1967; Glasby, Tooms & Howarth, 1974; this study) and from the Atlantic Ocean (Cronan, 1975). The lack of correlation between elements which are known to be closely related in Pacific, Indian and other Atlantic Ocean nodules indicates that

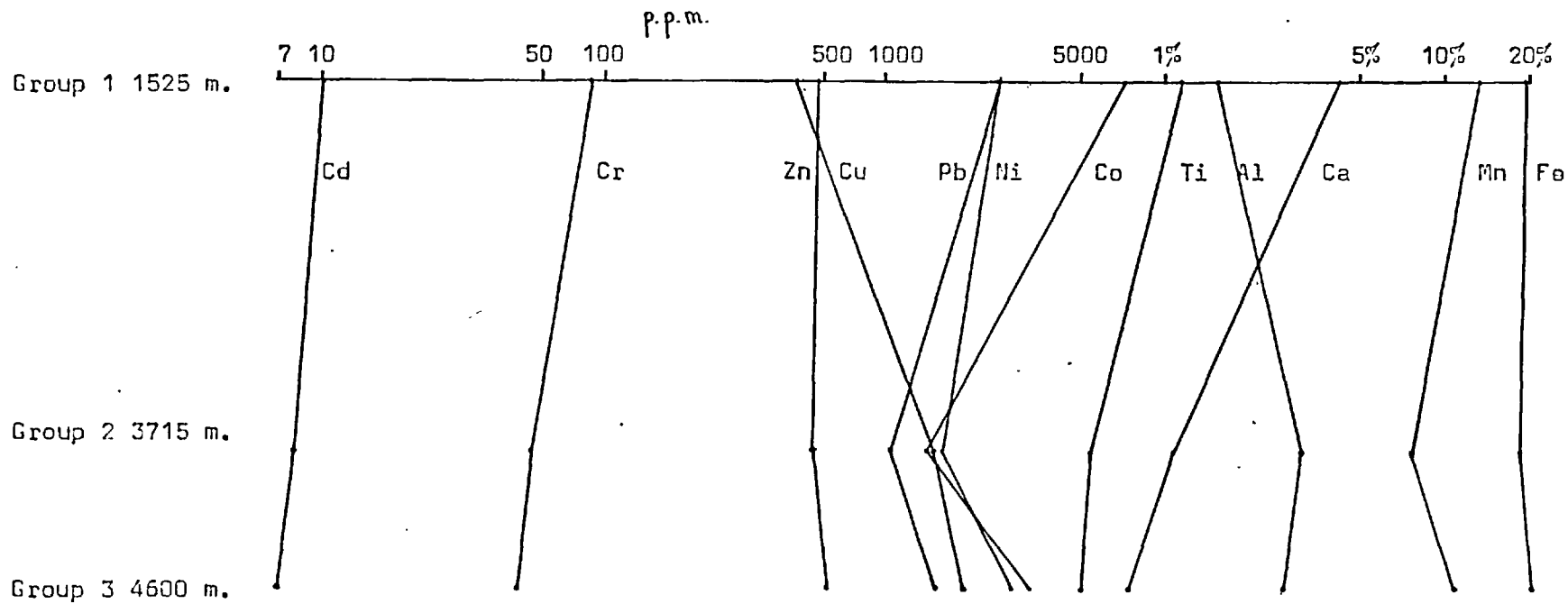


FIGURE 77 Element variation with depth in Atlantic Ocean ferromanganese-oxide samples.

the sample population studied here differs significantly from those studied by previous workers as a consequence of the small sample population used. The strong positive correlation between Co and Pb, on the other hand, and the negative correlations of these elements with depth is in agreement with the findings of previous workers (Cronan, 1967; Glasby Tooms & Haworth, 1974; Cronan, 1975). The positive correlations of Co and Pb with Ca and Ti are probably a result of the fact that all these elements correlate strongly negatively with depth. This depth correlation must be for different reasons, since selective chemical attacks on the samples have shown that Co and Pb are released predominantly in different fractions to Ca and Ti (see part (v) of this Section).

#### (iv) REGIONAL GEOCHEMISTRY

The fourteen samples studied were from only 5 separate sites, two of these being very close together. Furthermore, the sample stations were at 3 different depths on 3 different sea-mounts. This prevents an accurate comparison of nodule composition either at different depths on the same sea-mount or from similar depths on different sea-mounts. However, it is possible to divide the sample stations into 3 rough groups as follows:-

- Group 1. Stations from uppermost parts of sea-mounts:-  
stations 077, 100. (4 samples)
- Group 2. Stations from sea-mount flanks:-  
stations 169, 171. (7 samples).
- Group 3. Stations from the base of sea-mounts:-  
station 178. (3 samples).

The average composition of samples from each of these depth environments is summarised in figure 77. As already discussed in part (ii) of this Section, the two samples from station 077 are markedly different in morphology and composition. Since sample 077.33 was very different in morphology and composition from the other three samples in group 1 above,

it seems likely that it was dredged from a rather different environment perhaps lower down the sea-mount. It was therefore not included in the calculations when the average composition of group 1 samples was calculated and plotted on figure 77.

Several very clear trends are noticeable in the samples from different depth environments. Manganese is lowest in group 2 samples and is generally lower in the deeper water samples than in those of group 1. Aluminium shows a marked antipathetic correlation with Mn as might be expected in view of the presence of Al almost exclusively in the diluting aluminosilicate phase of the samples. Thus Al is generally higher in group 2 and 3 samples, which were presumably sitting on a sediment substrate, than in group 1 samples, which, being encrustations, are from a relatively sediment-free environment. By contrast, Ca is much higher in group 1 samples than in those of group 2 or 3. Most of the Ca in the samples is present as carbonate material (see part (v) of this Section) and it is likely that rates of supply of biogenic carbonate to the sea-bed are higher at shallow depths than at the depths from which group 2 and 3 were dredged, since the latter are from depths near to or perhaps even greater than the lysocline. Iron does not show any well-defined trend with depth.

Most of the trace metals Co, Ni, Cu, Zn, Pb, Cr and Ti also show marked changes in concentration with depth. With the single exception of Cu all these trace metals are lower in group 2 samples than in group 1 samples. These elements, with the exception of Cr and Ti, are incorporated predominantly in the authigenic ferromanganese-oxide phase and the lower trace metal content of group 2 samples may simply be a reflection of the lower Mn content of samples in this group. Lead and Co however, show a much greater fall in concentration than could be expected from this cause alone. As discussed in Section 11, samples from stations 077 and 100 contain  $\delta\text{-MnO}_2$  and Co and Pb are known to be enriched in ferromanganese-

oxides containing  $\delta\text{-MnO}_2$  (Barnes, 1967; Cronan & Tooms, 1969; Price & Calvert, 1970). This would explain the high Co and Pb contents of group 1 samples and also their negative correlation with depth.

In contrast to Co and Pb, Ni and Cu tend to be enriched in ferromanganese nodules from greater depths (Cronan, 1972; this study Section 5). This has been found to be the case for Atlantic Ocean nodules also (Cronan, 1975). The samples analysed in this study show a similar trend although for Ni the overall increase is very slight and group 2 samples actually show a decrease in Ni over group 1 samples. However as already explained, trace metal concentrations in group 2 samples are generally low.

Zinc and Cd show very little variation in concentration with depth, the variation in Cd values being within the limits of analytical precision obtained for this element.

Chromium and Ti are the only trace elements for which analysis was carried out which are not contained predominantly in the authigenic-oxide phases (see part (v)). Both these elements show a significant decrease in concentration with increase in depth. These 2 metals are present in basaltic rocks in comparatively high concentrations. Consequently, any small fragments of weathered or un-weathered basalt which become incorporated in ferromanganese-oxides are likely to appreciably increase the observed concentration of Cr and Ti in the sample. The incorporation of basalt fragments is especially likely where ferromanganese-oxide deposits are developing as encrustations directly on exposed rock. This was likely to be the case for all 3 samples in group 1, and in fact the samples from station 100 were found to contain minute fragments of material which were inferred to be basalt or its weathering products.

#### (v) PARTITION GEOCHEMISTRY

In addition to determining the bulk composition of the samples,

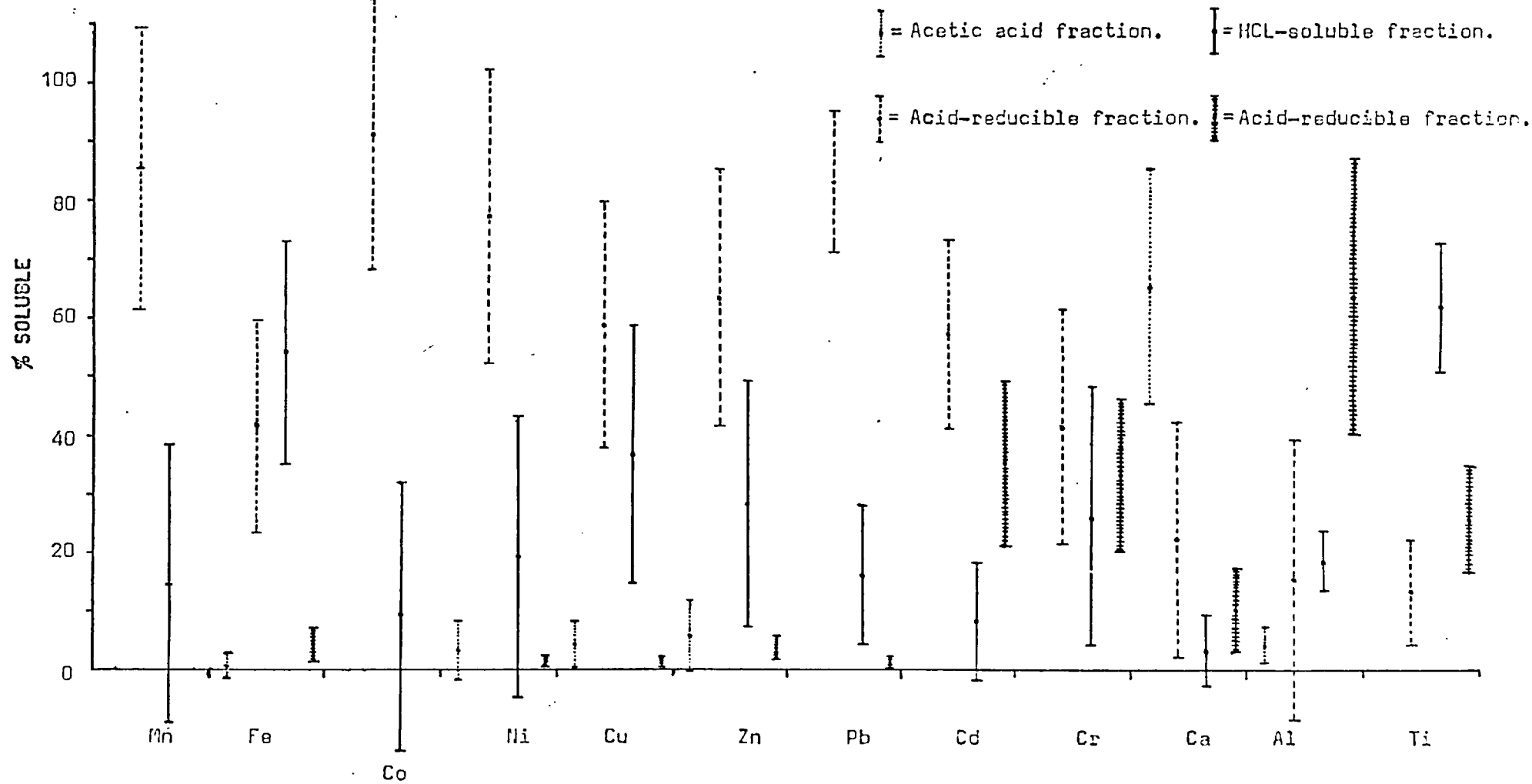


FIGURE 78 Mean partition values in Atlantic Ocean ferromanganese-oxide samples.



FIGURE 79 (a) & (b) Means and standard deviations of element partitions in Atlantic Ocean ferromanganese-oxides from different depth environments.

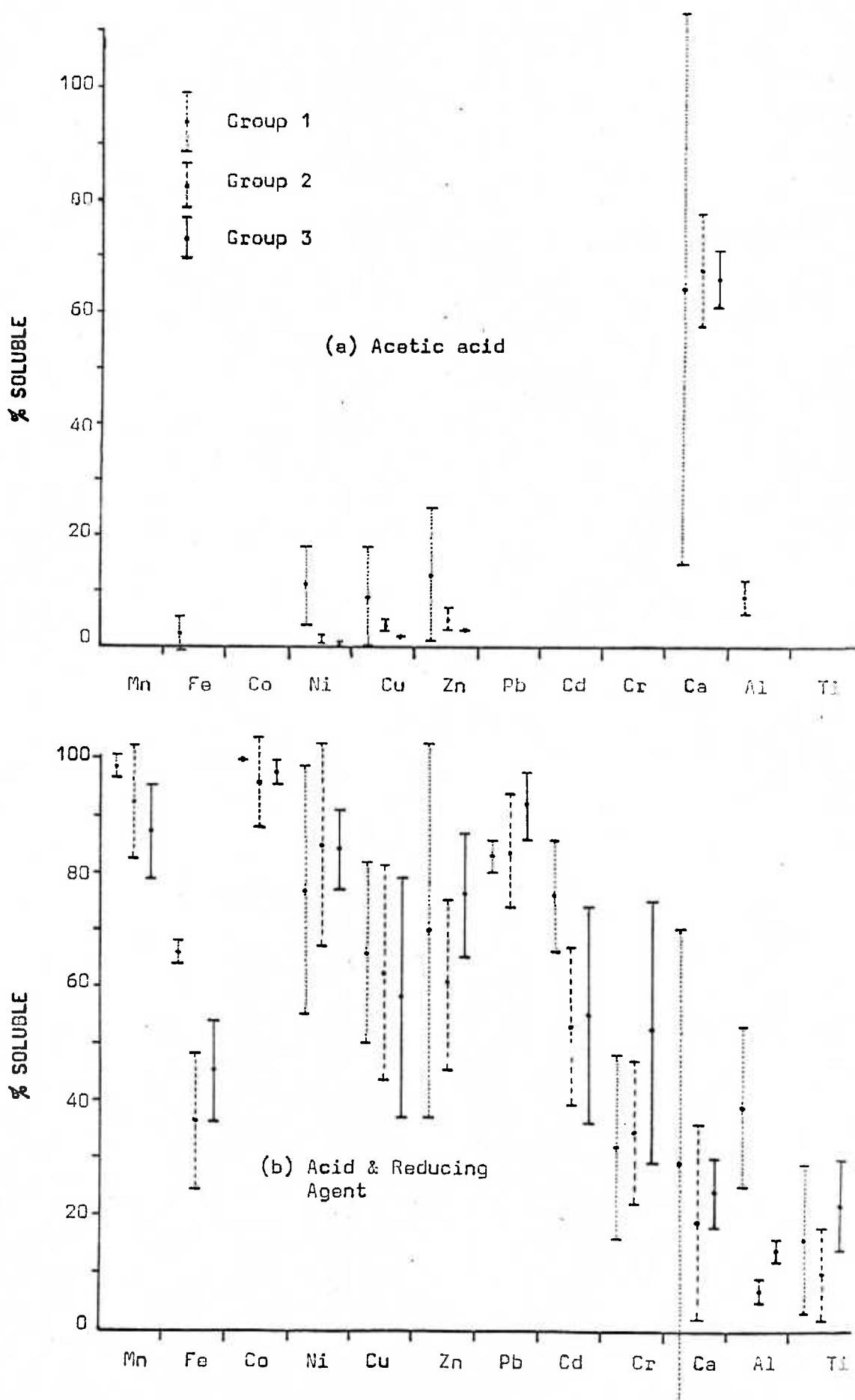
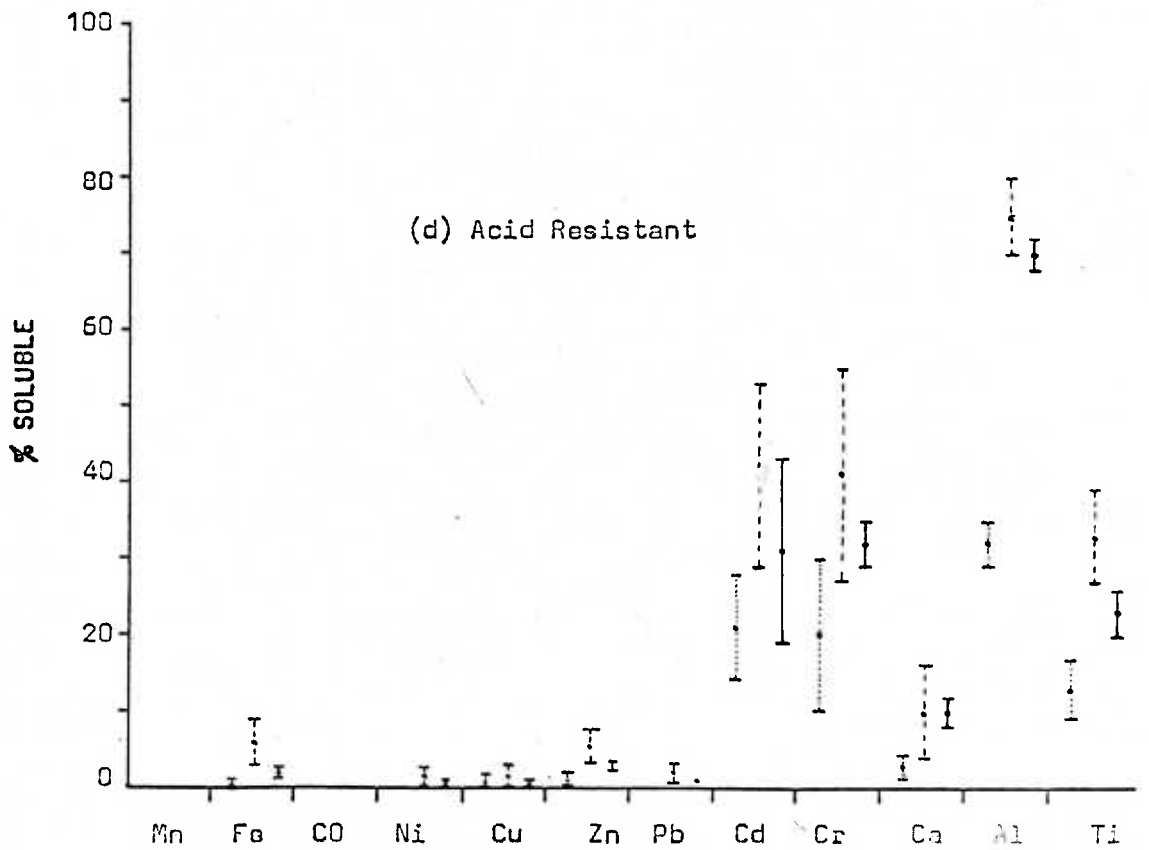
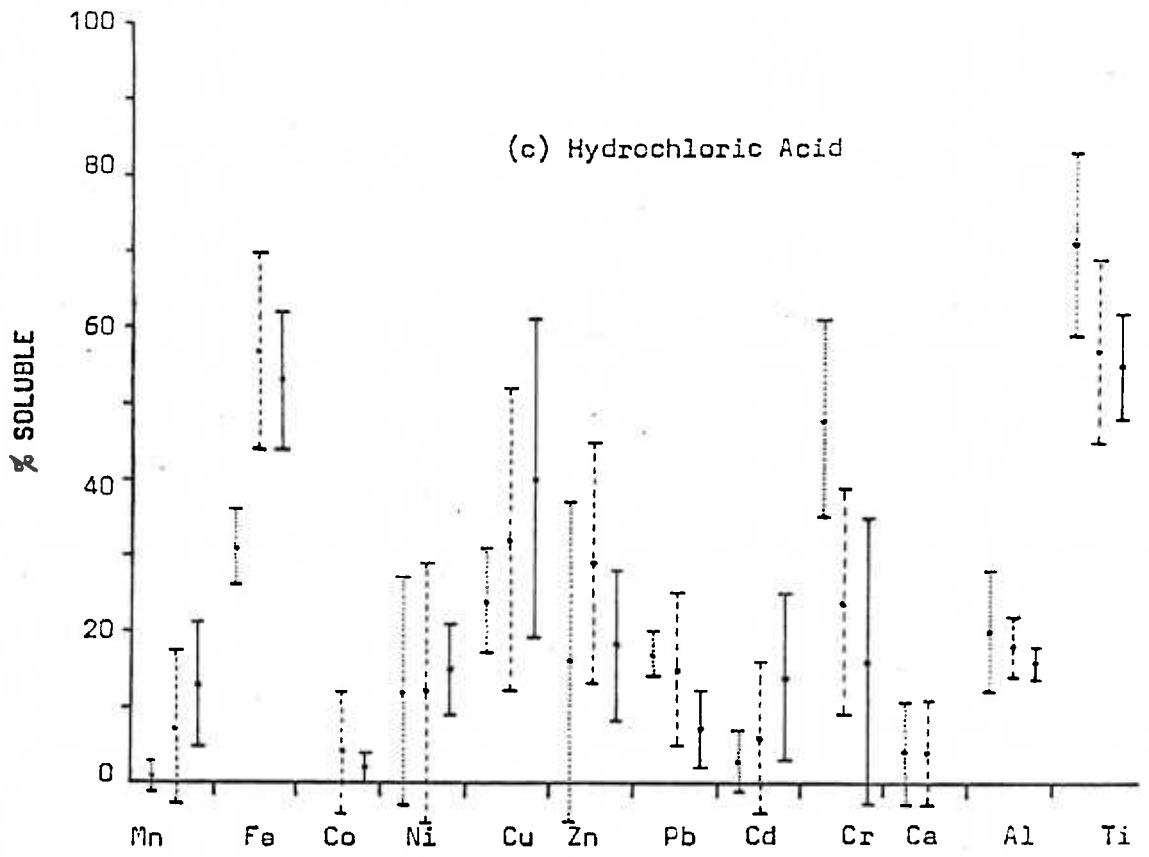


FIGURE 79 (c) & (d) Means and standard deviations of element partitions in Atlantic Ocean ferromanganese-oxides from different depth environments.



selective chemical attacks were carried out on each sample in order to investigate the distribution of the elements between the various phases liberated by each attack. The attacks used were an adaptation of the selective leach procedures developed by Chester & Hughes (1967) and are described in detail in Appendix 1. A detailed discussion of the phases present in marine ferromanganese oxides and which are likely to be selectively removed by each attack has been given in Section 7.

The attacks were carried out on separate sub-samples and the composition of each fraction calculated by subtraction as explained in Section 7. The mean value and standard deviation for each element released by each attack was calculated using the same method as before. The results are summarised in figure 78. The mean value and standard deviation for each element was also calculated for the 3 sample groups discussed above in order to investigate possible environmental effects on element partition. These results are summarised in figure 79.

(a) Average Partition Values in all samples -(Figure 78)

With the exception of Ca and Al, the largest proportion of all the elements for which analysis was carried out occur in either the acid-reducible or hydrochloric acid-soluble fraction but the partition values for most elements in these fractions show rather large standard deviations. This indicates that most elements are not present predominantly in the same fraction in all the samples analysed. However, it is still possible to see some major trends.

On average, 85% of the total Mn is present in the acid-reducible fraction indicating that the majority of the Mn in the samples is present as acid-reducible authigenic manganese oxides. In 4 samples, a substantial amount of the total Mn (more than 20%) was present in the hydrochloric acid-soluble fraction, and in sample 171.15 more than 90% of the total Mn

was in this fraction. In all the samples, essentially all the non-reducible Mn was in the HCL-soluble fraction, this amount averaging about 15% of the total Mn.

By contrast, Fe shows a more even distribution between the acid-reducible and HCL-soluble fractions, with slightly more in the latter than in the former. However, again the standard deviations about the mean values are large, the acid-reducible fraction for example, containing as little as 5% and as much as 67% of the total Fe content of samples. The acid-reducible Fe represents that Fe released from acid-reducible mixed iron-manganese-oxides and from amorphous iron oxyhydroxides (Chester & Hughes, 1967; Arrhenius, 1963). The non-reducible but HCL-soluble iron is probably present largely as crystalline goethite. This mineral was identified in all the samples analysed. This conclusion agrees with the observation that the four samples in which goethite appeared to be best-crystalline or most abundant (see Section 11) were also the four samples with the highest percentage of their total Fe content in the HCL-soluble fraction. A further interesting observation is that these 4 samples are the same 4 samples in which 20% or more of the total Mn was HCL-soluble. It would thus appear that goethite formed in this type of marine environment can incorporate a substantial amount of Mn without altering its susceptibility to chemical attack. The ability of hydrated Fe oxides to incorporate large amounts of Mn within their mineral structure rather than as adsorbed species has been proposed by Smith et al (1968) and demonstrated with synthetic preparations by Subramanian (1975).

The trace metals Co, Ni, Cu, Zn, Pb and Cd are all present predominantly in the acid-reducible fraction, and therefore are associated with the authigenic manganese and iron oxyhydroxides. Virtually all the Co and over three-quarters of the total Ni are present in this fraction on average, but only about 60% of the total Cu, Zn and Cd occur on average in this fraction. As might be expected in view of the large variations in the proportions of

Mn and Fe in this fraction, the standard deviation for all the trace metals in the acid-reducible fraction are also high. Virtually all the non-reducible Co, Ni, Cu, Zn and Pb is soluble in hydrochloric acid. However, the non acid-reducible Ca appears to be present in the acid-insoluble fraction rather than the HCL-soluble fraction. Small amounts of Ni, Cu and Zn are released by the acetic acid attack and are therefore probably present as loosely adsorbed cations. Chromium does not occur predominantly in any one fraction. On average, about 40% of the total is acid-reducible, the remainder being present in the HCL-soluble and acid-insoluble fractions, with slightly more in the latter than in the former. About two-thirds of the total Ca, on average, is present in the acetic acid-soluble fraction, indicating that most of the Ca in the samples is present as carbonate material. Most of the remaining Ca is present in the acid-reducible fraction and therefore presumably incorporated in the ferromanganese phases, whilst, on average, 10% of the total Ca appears to be acid-insoluble probably associated with resistant Ca-bearing silicates such as the plagioclase feldspars. By contrast, almost two-thirds of the total Al occurs in the acid-insoluble fraction associated with resistant silicates. A smaller but much less variable amount of Al (about 20%) is HCL-soluble and this probably represents Al released from the breakdown of clay minerals in the samples. An equally small but very variable amount of Al occurs in the acid-reducible fraction. This may represent that Al present in the samples as colloidal hydroxide material intimately intermixed with the acid-reducible ferromanganese phases. About two-thirds of the total Ti in the samples is HCL-soluble, whilst most of the rest is insoluble in HCL. This behaviour agrees well with the suggestion that most of the Ti in nodules is present as rutile or anatase (Arrhenius, 1963) which are only partly attacked by hydrochloric acid.

(b) Variation in element partition with depth

In view of the large standard deviations observed in the partition of most elements when all the samples were grouped together, the samples were split into the 3 groups discussed in part (iv) and the mean element partitions re-calculated together with their standard deviations. These results are summarised in figure 79. The partition of the elements in sample 171.15 was so different to any other sample that it was decided to exclude it from group 2 samples for the purposes of this study, since it would produce an unacceptably large bias on the averages calculated for group 2 samples.

Manganese occurs predominantly in the acid-reducible fraction in all 3 groups but the amount in this phase does decrease slightly with increasing depth, with a corresponding increase in the amounts which are HCL-soluble. Iron shows a similar trend to Mn but rather more marked, group 2 and 3 samples containing markedly less acid-reducible Fe (35 to 45%) than those from shallow depth (65%).

The trace metals Ni, Cu and Zn all show a very noticeable increase in the acetic acid-soluble fraction in samples from shallow depth. Copper and Cd increase markedly in the HCL-soluble fraction in samples from greater depth whilst Pb shows the reverse trend. Zinc shows a very marked increase in the HCL-soluble fraction in group 2 samples over the values found in this fraction in samples from both shallower and deeper waters. Chromium displays a rather complex behaviour with depth. There is a decrease in the percentage of Cr which is HCL-soluble at greater depths, whilst acid-reducible and acid-insoluble Cr show an overall increase with increasing depth. However, samples from the deepest environment (group 3 samples) do show a decrease in acid-insoluble Cr compared to group 2 samples.

Calcium, surprisingly, shows no distinct trends in partition with variation in depth even though, as has already been discussed, this element

correlates markedly negatively with depth in terms of bulk composition.

Aluminium shows a marked increase in resistance to chemical attack with depth. In group 1 samples, only about half the total Al is HCL-soluble or acid-insoluble whereas in group 2 and 3 samples amounts of Al in these two fractions form about 90% of the total Al. At shallow depth only about one-third of the total Al is acid-insoluble whereas in groups 2 and 3 samples about three-quarters of the total Al is acid-insoluble.

Titanium shows a decrease in the HCL-soluble fraction with increase in depth and there is an overall increase in the percentage of acid-insoluble Ti. Group 3 samples however, show an increase in acid-reducible Ti also.

S E C T I O N 13DISCUSSION

In spite of the limited number of samples from the north-east Atlantic Ocean which were available for investigation and their biased distribution both geographically and with depth, several noticeable features emerged from their analysis.

The major elements Mn and Fe show no systematic variation with depth but the trace metals associated with these major elements do, presumably in response to changes in depositional environment and element availability. Cobalt and lead are highest in samples from shallow depth whilst Ni and Cu tend to be enriched in samples from greater depths. This trend is complicated by the much lower Mn content of group 2 samples i.e. those from intermediate depth, this low Mn content tending also to depress values of all the trace metals associated with the authigenic Mn phase. All these group 2 samples came from the Hironnelle II Sea-Mount. The Al content of these samples indicates that the low Mn values may be due to dilution of the authigenic phase by larger than average amounts of aluminosilicate material.

The strong positive correlation between Co and Pb and their mutual



negative correlation with depth is in agreement with the findings of previous authors ( e.g. Cronan, 1972, 1975). The 3 samples with the highest Co and Pb values are also the 3 samples in which  $\delta\text{-MnO}_2$  was identified. The enrichment of Co and Pb in samples containing  $\delta\text{-MnO}_2$  has been observed by previous workers (Barnes, 1967; Price & Calvert, 1970; Calvert & Price, 1976; Cronan, 1975) and the possible reasons for this have been discussed in Part 1 of this thesis.

By contrast, Ni and Cu are higher in nodules from greater depth which were found to contain todorokite. The association of higher Cu and Ni values with nodules containing todorokite has also been noted by previous workers (Cronan & Tooms, 1969; Price & Calvert, 1970; Crerar & Barnes, 1974; Cronan, 1975). The reasons for this have also been discussed in Part 1 of the thesis.

Calcium and Titanium also show marked variation in concentration with depth, whilst the results of partition analysis show that these metals are not primarily associated with the ferromanganese-oxide phases. Calcium is present predominantly as carbonate material and shows a negative correlation with depth. This is probably due to the increased amounts of carbonate material reaching the sediment-water interface at shallow depths well above the lysocline. Highly calcareous sediments are known to occur at shallow depths in some parts of the area (Ryan et al, 1973) whilst at greater depths the sediments are lower in carbonate (Horn et al, 1972). Titanium also correlates negatively with depth and is especially high in the two samples from station 100. As already discussed, these samples were found to contain small rock fragments, probably of basalt or its weathering products, and these are likely to be comparatively rich in Ti. Where such fragments do occur in nodules from greater depths they are likely to be present in the nodule cores and therefore would have been removed prior to analysis.

Most samples from the same station show a limited range of composition

and morphology. However, the two samples from station 077 differ markedly in morphology, mineralogy and chemical composition. The nodule sample, 077.33, contained todorokite, was comparatively enriched in Cu and Ni compared to the encrustation sample 077.18, which contained  $\delta$ -MnO<sub>2</sub> and was rich in Co and Pb and very low in Cu. It is difficult to envisage how two samples can differ so much, chemically and mineralogically, unless they accreted under markedly different environmental conditions. In view of the marked association of  $\delta$ -MnO<sub>2</sub> and high Co and Pb values with oceanic nodules from shallow depth, it may be that sample 077.33 was picked up by the dredge much lower down the Gettysburg Sea-Mount and sample 077.18 near the summit. An alternative explanation may be that a less well-oxygenated environment, perhaps due to a pocket of ponded sediment, exists on the upper slopes of this sea-mount, in contrast to the conditions usually associated with this type of topographic feature. Such an environment would be favourable to the growth of nodules which would show more similarities in mineralogy and composition to sample 077.33 than to sample 077.18. However, there are no reports in the literature of similar occurrences in the Atlantic or other oceans.

Selective chemical attacks on the samples have shown that, on average, most of the manganese and about half the iron in the samples is present as acid-reducible oxides or oxyhydroxides. Much of the non-reducible Fe is probably present as goethite and the non-reducible, but HCL-soluble Mn and Mn-associated trace metals Co, Ni, Cu, Zn, Pb and Cd, may be associated with this phase. However, substantial amounts of these metals, and iron, may also be released by the breakdown of clays in the samples by HCL. The percentage of the total of these elements present in the HCL-soluble fraction tends to increase both with increase in total Al concentration and with increase in the percentage of HCL-soluble iron. However, a knowledge of the relative contributions of these two possible sources of HCL-soluble trace metals can probably only be gained by the development of a selective leach procedure

capable of releasing each of these phases separately from ferromanganese-oxide samples. Such a procedure was not attempted in this study and must await future development.

An interesting feature of the partition patterns of the trace elements is that Co, unlike the other authigenically-associated metals Ni, Cu, Zn, Pb and Cd, is present virtually exclusively in the acid-reducible fraction. This indicates that Co is not associated to any extent with the non-reducible iron phase, although it may be associated with an acid-reducible iron phase. Whilst this behaviour is in agreement with that observed in Indian Ocean nodules it does not agree with the results of Arrhenius (1963) who found that as much as 75% of the total Co in Pacific Ocean nodules was non-reducible. Electron microprobe work by Glasby (1970) and Burns & Brown (1972) has shown that Co is strongly enriched in manganese-rich areas and depleted in iron-rich areas within nodules. Calvert & Price (1977) have pointed out a general lack of agreement in the literature as to whether Co is associated with the Mn or Fe phase in nodules and suggest that the mineralogy of the Fe phase itself does not affect the concentration of Co or other trace metals in nodules. The results obtained in the present study are in agreement with this suggestion.

The often substantial, but highly variable amounts of Ni, Cu, Zn and Pb in the HCL-soluble fraction of Atlantic Ocean samples is in marked contrast to the behaviour of these metals in Indian Ocean nodules, where on average, less than 5% of their respective totals are HCL-soluble, and the standard deviations from the mean values in all the phases was very low. However, the Atlantic Ocean samples were on average much higher in iron (19%) than those from the Indian Ocean (11%), and more than 50% of the iron in the former was HCL-soluble whilst in the latter, HCL-soluble iron formed less than 30% of the total. Compared to Indian Ocean nodules therefore, a substantial amount of the authigenic phase of Atlantic Ocean nodules consists of a discrete non-reducible iron phase which may contain the minor elements in question.

Manganese shows a similar pattern to iron, with minimal amounts in the HCL-soluble fraction of Indian Ocean samples compared with an average of 15% of the total in the HCL-soluble fraction of Atlantic Ocean samples. In quantitative terms this represents a difference of between 5- and 10-fold. This manganese must be present within clays, within the iron phase or as a separate non-reducible manganese phase. A non-reducible manganese phase must consist essentially of divalent manganese ions. Since the  $Mn^{2+}$  ion is comparatively soluble in sea-water it is difficult to see how such a phase can occur, even as a product of a secondary reduction process within the concretion, since the products of such a process would simply be released into interstitial pore-waters and re-mobilised. A substantial amount of the non-reducible Mn may be present within clays, however the average Al content of Atlantic Ocean samples (2.7%) is even lower than that of Indian Ocean nodules (3.0%), in which very little Mn was HCL-soluble. Thus unless the clay minerals incorporated in Atlantic Ocean nodules are 5 to 10 times as rich in manganese as those in Indian Ocean samples, clay minerals cannot account on their own for the Mn released in the HCL-soluble fraction. It seems therefore that the HCL-soluble Fe phase must incorporate substantial amounts of Mn and, in view of their presence in the HCL-soluble fraction, probably of Ni, Cu, Zn and Pb also. Results of Mossbauer studies on nodules have shown that iron in nodules is present almost exclusively as the  $Fe^{3+}$  ion (Glasby, 1970; Burns & Brown, 1972). This has an ionic radius in goethite of 0.65 (Burns, 1976). Nickel and copper have ionic radii, in the divalent state in which they occur in sea-water, which are within 10% of that of  $Fe^{3+}$  and therefore may be able to substitute for this ion within the goethite lattice without too great a loss in crystal field stabilisation energy. The  $Mn^{4+}$  ion (0.54Å) however, is rather too small to substitute for  $Fe^{3+}$ , whilst the  $Mn^{2+}$  ion has an ionic radius of 0.82Å which makes it too large. It may be therefore that manganese enters the iron phase of nodules as  $Mn^{3+}$  which has an ionic radius identical to that of  $Fe^{3+}$ .

Whilst the  $Mn^{3+}$  ion appears to be stable in iron and manganese minerals in terrestrial soils (McKenzie, 1972) it has not been reported in marine ferromanganese-oxides. Subramanian (1975) was able to prepare synthetic iron hydroxides containing large amounts of Mn but he made no attempt to explain the structure of these phases or the oxidation states of the Mn and Fe within them. Smith et al (1968) argue that Mn is diadochic within the iron phase of manganese nodules but in view of the above arguments this is difficult to envisage unless much of the Mn is present as the  $Mn^{3+}$  ion. Where amounts of Mn in the sample are of the same order of magnitude as those of Fe, the manganese tends to occur as  $\delta$ - $MnO_2$  (i.e. as  $Mn^{4+}$ ) epitaxially intergrown with goethite (Burns, 1976). Where amounts of Mn are much smaller than those of Fe, however, much of it may well enter the goethite lattice as  $Mn^{3+}$ . A better understanding of the structure of substituted iron oxide-hydroxides and the valency states of the substituting ions must however await the outcome of future investigation.

Cobalt occurs as the  $Co^{3+}$  ion in marine sediments from oxidising environments (Goldberg, 1961; Burns, 1965.) This ion has a radius of 0.53Å which makes it too small to readily substitute for  $Fe^{3+}$  (Burns, 1976). The fact that Ni, Cu and Zn may under certain circumstances substitute for  $Fe^{3+}$  in lattice sites whilst Cobalt cannot readily do so may explain the unusual trace element composition of sample 171.15. Partition analysis has shown that the authigenic oxide phase of this sample consists almost entirely of an HCL-soluble iron phase with virtually no separate Mn phase. Bulk Cu, Ni and Zn values in this sample are similar to, or even higher than those in samples from station 169 nearby which does contain a separate Mn phase, whilst Co is extremely low (about 300 p.p.m. ), lower by a factor of 5 than average values in station 169 samples.

Comparison with previous studies

In view of the limited number of samples investigated and their limited geographical distribution, no attempt has been made to assess regional compositional trends. However, some comparisons can be made with reported compositions of samples from similar environments elsewhere in the Atlantic Ocean. Several workers have analysed small numbers of samples from various regions of the Atlantic Ocean (see Arrhenius, 1963; Ahrens et al, 1967; Maro, 1965; Smith et al, 1968; Kharin, 1973) and Cronan (1975) analysed 140 samples from sites throughout the Ocean. Table 24 shows a comparison of the data analysed in the present study with that obtained from similar environments by Cronan (1975). From this data it can be seen that samples from the upper parts of sea-mounts in the area studied (i.e. group 1 samples) are fairly close in average composition to those from sea-mounts in other areas of the ocean. However, cobalt concentrations in group 1 samples appear to be generally higher than those observed in sea-mount nodules by Cronan. No simple explanation can be put forward to account for this.

The group 3 samples analysed in this study were from the Horseshoe Abyssal Plain, which is separated from the north-east Atlantic Basin by the Madeira-Toré Rise. However, data from this basin are given for comparison with group 3 samples since it is the nearest abyssal area for which data are available. Data from Smith et al (1968) for samples from the Nares Abyssal Plain are also given. Compared with north-east Atlantic Basin samples, those from the Horseshoe Abyssal Plain (H.A.P.) are different in several respects. The most obvious difference is the much higher iron content of H.A.P. samples, together with rather higher Cu, Ni and Zn values and lower Co values than those observed in north-east Atlantic Basin (N.E.A.B.) samples. This difference in minor element composition could be due to a mineralogical control on nodule composition, since H.A.P. samples contained todorokite whilst in N.E.A.B. samples, todorokite was absent and in some cases  $\delta$ -MnO<sub>2</sub> was identified,

	Mn %	Fe %	Co p.p.m.	Ni p.p.m.	Cu p.p.m.	Zn p.p.m.	Ca %	Depth (m.)
Group 1 (3 samples) (this study)	14.1	20.6	7600	2780	515	620	4.43	1525
Atlantic Sea-Mounts (Cronan, 7 samples)	16.2	22.4	5390	2450	470	580	2.66	1227
Group 2 (7 samples) (this study)	13.8	33.0	2550	2860	2650	955	1.91	3715
Group 3 (3 samples) (this study)	15.9	29.7	3290	4080	2810	870	1.07	4600
North-East Atlantic Basin (Cronan, 13 samples)	19.8	18.5	4880	3610	1260	710	2.33	3107
Nares Abyssal Plain	18.4	30.0	4000	N.A.	1500	600	N.A.	5729

N.A. = Not analysed

All results are calculated on a detrital-free basis

TABLE 24

Comparison of average composition of Atlantic Ocean ferromanganese-oxide samples analysed in the present study with previously published data

(Cronan, 1975). As already discussed, todorokite-rich nodules tend to be enriched in Ni and Cu and depleted in Co compared to  $\delta$ - $MnO_2$ -rich samples. It seems likely therefore that the sedimentary environment, which governs nodule mineralogy, is rather different in the north-east Atlantic Basin to that found on the Horseshoe Abyssal Plain. A great amount of continentally-derived material is reaching the Horseshoe Abyssal Plain according to Horn et al (1974). Whilst comparatively little is known about sedimentation patterns in the north-east Atlantic Basin, it appears that much of it is occupied by turbidite-covered abyssal plains and thus also receives continental detritus. However, since the average water depth from which N.E.A.B. samples were recovered was only 3100m., it is obvious that many of these samples must have come from localities substantially elevated from the abyssal sea-floor, which averages about 4500m. water depth (see Laughton et al, 1975). Many of Cronan's (1975) samples therefore, may have come from localities receiving little or no continentally-derived material. This difference in sedimentary environment may account for the much higher Fe content and  $Fe/Mn$  ratios of H.A.B. samples, since according to Manheim (1965) continental run-off supplies a much greater amount of releasable Fe than Mn to the oceans. Nodules with very high Fe contents have been observed in continental borderland regions of the Pacific Ocean (Mero, 1965; Skorniyakova & Andrushchenko, 1970) and of the Indian Ocean (see Section 5) which are receiving continental run-off. In this respect it is interesting to note that nodules from near the continental borderland on the Nares Abyssal Plain have similar iron contents to those from the Horseshoe Abyssal Plain (see Table 24).

Nodules with high Fe contents and high  $Fe/Mn$  ratios have been observed from sea-mounts by various authors (Glasby, 1970; Cronan, 1972; Calvert & Price, 1976). Iron can be supplied to the sea-floor in substantial amounts by hydrothermal solutions and basalt weathering associated with submarine volcanic activity (Bostrom & Peterson, 1966; Corliea, 1971) and



precipitation of Fe-rich hydroxides in hydrothermally active areas has been observed in several localities (Zelenov, 1964; Bonatti et al, 1972; Smith & Cronan, 1975). Thus nodules from past or present volcanically-active areas such as sea-mounts might be expected to be enriched in iron. This theory might explain the very high Fe content of samples from the Hirondele II Sea-Mount (group 2 samples) although it must be stressed that this sea-mount is not known to be volcanically active at present. The rapid supply of Fe to these nodules may in turn account for the slightly depressed Mn, Ni and Co values compared with the other samples analysed.

REFERENCES

R E F E R E N C E S

- Ahrens, L.H., Willis, J.P. and Oethuizen, C.O. (1967). Further observations on the composition of manganese nodules with particular reference to some of the rarer elements. *Geochim. Cosmochim. Acta* 31, 2169 - 2180.
- Andrushchenko, P.F. and Skornyakova, N. (1969). The texture and mineral composition of ferromanganese concretions from the southern part of the Pacific Ocean. *Oceanol.* 9, 229 - 242.
- Arrhenius, G. (1963). Pelagic sediments. in "The Sea" (M.N. Hill, ed.), 3, 665 - 727. Interscience, New York.
- Arrhenius, G.O.S. and Bonatti, E. (1959). Uranium and thorium in marine minerals. Pre-prints 1st Int. Oceanogr. Congr. Am. Assoc. Adv. Sci., (M. Sears, ed.). 497.
- Arrhenius, G.O.S., Mero, J.L. and Korkish, J. (1964). Origin of oceanic manganese nodules. *Science* 144, 170.
- Aston, S., Chester, R., Griffiths, A. and Riley, J.P. (1972). Distribution of Cd in North Atlantic deep-sea sediments. *Nature* 239, 293.
- Aumento, F., Lawrence, D.E. and Plant, A.G. (1968). The ferromanganese pavement on the San Pablo sea-mount. *Geol. Surv. of Canada Prof. Paper*, 68, 32.
- Avraham, Z.B. and Bunce, E.T. (1977). Geophysical study of the Chagoe-Laccadive Ridge, Indian Ocean. *Jl. Geophys. Res.* 82(8), 1295 - 1305.
- Baas Becking, L.G.M., Kaplan, I.R. and Moore, D. (1960). Limits of the natural environment in terms of pH and oxidation-reduction potentials. *Jl. Geol.* 68, 243 - 284.
- Baker, B.H. (1963). Geology and mineral resources of the Seychelles Archipelago. *Geol. Surv. Kenya Memoir No. 3.*, Ministry of Commerce and Industry, Kenya.
- Baranov, V.I. and Kuzima, L.A. (1958). The rate of silt deposition in the Indian Ocean. *Geochemistry* 2, 131 - 140.

- Barnes, S.S. (1967). Minor element composition of ferromanganese nodules. *Science* 157, 63 - 65.
- Bé, W.H. and Tolderlund, D.S. (1971). Distribution and ecology of living planktonic foraminifera in surface waters of the Atlantic and Indian Oceans. in "Micropaleontology of the Oceans". (B.M. Funnell and W.R. Riedel, eds.). Cambridge University Press.
- Bender, M.L. (1971). Does upward diffusion supply the excess manganese in pelagic sediments? *Jl. Geophys. Res.* 76, 4212 - 4215.
- Bender, M.L. and Schultz, C. (1969). The distribution of trace metals in cores from a traverse across the Indian Ocean. *Geochim. Cosmochim. Acta* 33, 292 - 297.
- Bender, M.L., Broecker, W.S., Gornitz, V. et al (1971). Geochemistry of 3 cores from the East Pacific Rise. *Earth Plan. Sci. Lett.* 12, 425 - 433.
- Bergh, H.W. (1971). Sea floor spreading in the south-west Indian Ocean. *Jl. Geophys. Res.* 76, 6276 - 6282.
- Berner, R.A. (1969). Goethite stability and the origin of red-beds. *Geochim. Cosmochim. Acta* 33, 267 - 273.
- Bezrukov, P.L. (1963). Distribution of iron-manganese concretions on the floor of the Indian Ocean. *Okeanologiya* 2, 1014 - 1019, (in Russian).
- Bezrukov, P.L. (1963). Research in the Indian Ocean during the 35th voyage of the expeditional vessel "Vityaz". *Okeanologiya* 3, 540 - 549. (in Russian).
- Bezrukov, P.L. and Andrushchenko, P.F. (1973). Iron-manganese concretions of the Indian Ocean. *Int. Geol. Rev.* 15(3), 342 - 356.
- Bezrukov, P.L. and Andrushchenko, P.F. (1974). The Geochemistry of ferromanganese nodules from the Indian Ocean. *Int. Geol. Rev.* 16, 1044 - 1061.
- Bhat, S.G., Krishneswamy, S. and Lal, D. (1973). Radiometric and trace element studies of ferromanganese nodules. *Symposium on hydrogeochemistry and biogeochemistry, Vol. 1*, 443 - 462, Clarke Co., Washington.
- Bignell, R.D. (1975). The geochemistry of metalliferous brine precipitates and other sediments from the Red Sea. unpubl. Ph. D. thesis, Univ. London.
- Bonatti, E. and Joensuu, O. (1966). Deep sea iron deposits from the South Pacific. *Science* 154, 643.
- Bonatti, E. and Nayudu, Y. (1965). The origin of manganese nodules on the ocean floor. *Amer. Jl. Sci.* 263, 17 - 39.

- Bonatti, E., Kreemer, T. and Rydell, H. (1972). Cleveification and genesis of submarine iron-manganese deposits.  
in "Ferromanganese deposits on the ocean floor". (D.R. Horn, ed.). 149 - 165. Lemont Doherty Geol. Obs., Washington D.C.
- Bonatti, E., Honnorez, J., Joensuu, O. and Rydell, H.S. (1972). Submarine iron deposits from the Mediterranean Sea.  
in "Symposium on the sedimentation in the Mediterranean Sea". (D.S. Stanley, ed.). VIII Internat. Sediment. Congr., Heidelberg.
- von der Borch, C.C. and Rex, R.W. (1970). Amorphous iron-oxide precipitates in sediments cored during leg 5 of the Deep Sea Drilling Project.  
in "Initial Reports of the Deep Sea Drilling Project, Vol. V". (D.A. McMenus et al, eds.). Chap. 26, 541 - 544. U.S. Govt. Printing Office, Washington D.C.
- von der Borch, C.C. and Sclater, J.G. (1974). Initial Reports of the Deep Sea Drilling Project.  
Vol. XXII (von der Borch, C.C. and Sclater, J.G., eds.). U.S. Govt. Printing Office, Washington D.C.
- von der Borch, C.C., Nesteroff, W.D. and Galehouse, J.S. (1971). Iron-rich sediments cored during leg 8 of the Deep Sea Drilling Project.  
in "Initial Reports of the Deep Sea Drilling Project, Vol. VIII". (Tracey, Jr., J.I. ed.). U.S. Govt. Printing Office, Washington D.C. Chap. 17, 829 - 836.
- Bostrom, K. and Fisher, D.E. (1970). Volcanogenic U, V and Fe in Indian Ocean sediments.  
Earth and Plan. Sci. Lett. 11, 95 - 98.
- Boetrom, K. and Peterson, M.N.A. (1966). Precipitates from hydrothermal exhalations on the East Pacific Rise.  
Econ. Geol. 61, 1258 - 1265.
- Bricker, O.P. (1965). Some stability relations in the system  $MnO_2 - H_2O$  at  $25^\circ C$  and one atmosphere total pressure.  
Amer. Min. 50, 1296 - 1354.
- Brooke, J.N. (1968). The texture and hydrometallurgical processing of manganese nodules.  
unpubl. Ph. D. thesis Univ. London.
- Brown, B.A. (1972). A low temperature crushing technique applied to manganese nodules.  
Amer. Min. 57, 284 - 287.
- Burkle, L.H., Venkatarathnam, K. and Booth, J.D. (1974). Sediment transport by Antarctic Bottom Water in the western Indian Ocean.  
Eos (trans. Am. Geophys. Un.) 55(4), 312.
- Burnett, W.C. and Piper, D.Z. (1977). Rapidly formed ferromanganese deposit from the Hess Deep, Eastern Pacific.  
Nature 265, 596 - 600.

- Burns, R.G. (1965). Formation of  $\text{Co}^{3+}$  in the amorphous  $\text{Fe}(\text{OH})_2 \cdot n\text{H}_2\text{O}$  phase of manganese nodules.  
Nature 205, 999.
- Burns, R.G. (1976). The uptakes of cobalt into ferromanganese nodules, soils and synthetic Mn (IV) oxides.  
Geochim. Cosmochim. Acta 40, 95 - 102.
- Burns, R.G. and Brown, B.A. (1972). Nucleation and mineralogical controls on the composition of manganese nodules.  
in "Ferromanganese deposits on the ocean floor" (D.R. Horn, ed.). 51 - 60. Lamont Doherty Geol. Obs. Washington D.C.
- Burns, R.G. and Burns, V.M. (1974). Crystal chemistry of cobalt and nickel.  
in "Handbook of Geochemistry, Vol. II - IV" (K.H. Wedepohl, ed.). Chaps. 27A and 28A, Springer-Verlag, New York.
- Burns, R.G. and Burns, V.M. (1977). Mineralogy of ferromanganese nodules.  
in "Marine Manganese Nodules" (G.P. Glasby, ed.). Chap. 7 Elsevier, Amsterdam.
- Burns, R.G. and Fuerstenau, D.W. (1966). Electron-probe determination of inter-element relationships in manganese nodules.  
Am. Miners. 51, 895 - 902.
- Burns, R.G., Burns, V.M., Sung, W. and Brown, B.A. (1974). Ferromanganese nodule mineralogy: suggested terminology of the principal Mn oxide phases.  
Geol. Soc. Amer. Ann. Meet., Miami. Abstr. 6, 1069 - 1071.
- Buser, W. (1959). The nature of iron and manganese compounds in manganese nodules.  
Pre-prints Intern. Oceanog. Cong. Am. Assoc. Adv. Sci., (M. Sears, ed.). 962 - 964, Washington.
- Buser, W. and Grutter, A. (1956). Über die natur der manganknollen.  
Schweiz Min. Petrogr. Mitt. 36, 49 - 64.
- Buser, W., Graaf, P. and Feitknecht, W. (1954). Beitrag zur Kenntnis der Mangan (II) - manganite und des  $\delta\text{-MnO}_2$ .  
Helv. Chim. Acta 37, 2322 - 2333.
- Calvert, S.E. (1974). Deposition and diagenesis of siliceous marine sediments.  
Spec. Publ. Int. Ass. Sedimentologists 1, 273 - 299.
- Calvert, S.E. and Price, N.B. (1977). Geochemical variations in ferromanganese nodules and associated sediments from the Pacific Ocean.  
Mar. Chem. 5, 43 - 74.
- Cann, J.R., Winter, C.K. and Pritchard, R.G. (1977). A hydrothermal deposit from the floor of the Gulf of Aden.  
Min. Mag. 41, 193 - 199.
- Carpenter, R. and Wakeham, S. (1973). Mossbauer studies of marine and freshwater manganese nodules.  
Chem. Geol. 11, 109 - 116.

- Chayes, F. (1960). On correlation between variables of constant sum.  
Jl. Geophys. Res. 65, 4185 - 4193.
- Chester, R. and Hughes, M.J. (1967). A chemical technique for the separation of ferromanganese minerals and adsorbed trace elements from pelagic sediments.  
Chem. Geol. 2, 249 - 262.
- Chester, R. and Hughes, M.J. (1969). The trace element geochemistry of a north-Pacific pelagic clay core.  
Deep Sea Res. 16, 639 - 654.
- Cole, W.F., Wadeley, A.D. and Walkley, A. (1947). An X-Ray diffraction study of manganese dioxide.  
Trans. Electrochem. Soc. 92, 133 - 154.
- Corlies, J.B. (1971). The origin of metal-bearing submarine hydrothermal solutions.  
Jl. Geophys. Res. 76, 8128 - 8138.
- Crerar, D.A. and Barnes, H.L. (1974). Deposition of deep-sea manganese nodules.  
Geochim. Cosmochim. Acta 38, 279 - 300.
- Cronan, D.S. (1967). The geochemistry of some manganese nodules and associated pelagic deposits.  
unpubl. Ph. D. thesis, Univ. London 342 pp.
- Cronan, D.S. (1969). Chemical and mineralogical variations with depth in manganese nodules.  
Trans. Amer. Geophys. Union 50, 209.
- Cronan, D.S. (1972). Regional geochemistry of ferromanganese nodules in the World Ocean.  
in "Ferromanganese deposits on the ocean floor" (D.R. Horn, ed.). 19 - 30. Lamont Doherty Geol. Obs. New York.
- Cronan, D.S. (1975a). Manganese nodules and other ferromanganese oxide deposits from the Atlantic Ocean.  
Jl. Geophys. Res. 80, 3831 - 3837.
- Cronan, D.S. (1975b). Zinc in marine ferromanganese nodules.  
Trans. Inst. Min. Mett. 84, 1330 - 1332.
- Cronan, D.S. (1976a). Basal metalliferous sediments from the eastern Pacific.  
Bull. Geol. Soc. Am. 87, 928 - 934.
- Cronan, D.S. (1976b). Manganese nodules and other ferromanganese-oxide deposits.  
in "Marine Manganese Nodules (G.P. Glasby, ed.). Chap. 28, 217 - 263, Elsevier, Amsterdam.
- Cronan, D.S. and Toome, J.S. (1967). The geochemistry of manganese nodules from the north-west Indian Ocean.  
Deep Sea Res. 14, 239 - 249.
- Cronan, D.S. and Toome, J.S. (1968). A microscopic and electron probe investigation of manganese nodules from the north-west Indian Ocean.  
Deep Sea Res. 15, 215 - 223.

- Cronan, D.S. and Tooms, J.S. (1969). The geochemistry of manganese nodules and associated pelagic deposits from the Pacific and Indian Oceans.  
Deep Sea Res. 16, 335 - 359.
- Curray, J.R. and Moore, D.C. (1971). Growth of the Bengal deep-sea fan and denudation in the Himalayas.  
Bull. Geol. Soc. Am. 82, 563 - 572.
- Davies, T.A., Weser, O.E., Luyendyk, B.P. and Kidd, R.B. (1975). Unconformities in the sediments of the Indian Ocean.  
Nature 253, 15 - 19.
- Deer, W.A., Howie, R.A. and Zussman, J. (1966). An introduction to the rock-forming minerals.  
Longman, London.
- Dietz, R.S. and Holden, J.C. (1970). Reconstruction of Pangaea: Break-up and dispersion of continents Permian to Present.  
Jl. Geophys. Res. 75, 4939 - 4956.
- Dietz, R.S. and Holden, J.C. (1971). Pre-Mesozoic crust in the Eastern Indian Ocean, (Wharton Basin).  
Nature 229, 309 - 312.
- Dymond, J., Corliss, J.B. and Stillinger, R. (1976). Chemical composition and metal accumulation rates of metalliferous sediments from sites 319, 320 and 321.  
in "Initial Reports of the Deep Sea Drilling Project"  
(Yeats, R.S., Hart, S.R. et al, eds.). Chap. 50, U.S. Govt. Printing Office.
- Ehrlich, H.L. (1972). The role of microbes in manganese nodule genesis and degradation.  
in "Ferromanganese deposits on the Ocean Floor" (O.R. Horn, ed.). 63 - 70, Lamont Doherty Geol. Obs., Washington D.C.
- Ehrlich, H.L. (1975). The formation of ores in the sedimentary environment of the deep sea with microbial participation: The case for ferromanganese concretions.  
Soil Science 119, 36 - 41.
- Ehrlich, H.L., Ghiorae, W.C. and Johnson, G.L. (1972). Distributions of microbes in manganese nodules from the Atlantic and Pacific Oceans.  
Devel. Industr. Microbiol. 13, 57 - 65.
- Elderfield, H.L. (1976). Manganese fluxes to the oceans.  
Mar. Chem. 4, 103 - 132.
- Ewing, M., Aitken, T. and Eitrem, S. (1968). Giant ripples in the Madagascar Basin.  
Eos (Trans. Am. Geophys. Un.) 49, (1), 218.
- Ewing, M., Eitrem, S., Truchman, M. and Ewing, J.I. (1969). Sediment distribution in the Indian Ocean.  
Deep Sea Res. 16, (3), 231 - 248.
- Fein, C.D. and Morgenstein, M. (1973). Microprobe analysis of manganese crusts from the Hawaiian Archipelago.  
in "Ferromanganese deposits on the ocean floor" 85 - 92, unpubl. Phase I report, Seabed Assessment Program.  
I.D.O.E., N.S.F. Washington D.C.



- Feitknecht, W. and Marti, W. (1945). Über manganite und kunstlichen Braunstein.  
Helv. Chim. Acta 28, 148 - 156.
- Fisher, R.A. and Yates, F. (1963). Statistical tables for biological, agricultural and medical research.  
146pp, Oliver and Boyd, Edinburgh.
- Fisher, R.L., Sclater, J.G. and McKenzie, D.P. (1971). Evolution of the Central Indian Ridge, Western Indian Ocean.  
Bull. Geol. Soc. Am. 82, 553 - 562.
- Fisher, R.L., Bunce, E.T. et al (1974).  
in "Initial Reports of the Deep Sea Drilling Project",  
Vol. XXIV. U.S. Govt. Printing Office, Washington, D.C.
- Francis, T.S.G. and Raitt, R.W. (1967). Seismic refraction measurements in the southern Indian Ocean.  
Jl. Geophys. Res. 72, 3015 - 3042.
- Friedrich, G.H. (1976). Manganese micronodules in deep sea sediments and their relation to manganese nodule fields.  
in "Marine Geological Investigations in the south-west Pacific and adjacent areas" (G.P. Glasby and H.R. Katz, eds.).  
39 - 53, United Nations (C.C.O.P./S.O.P.A.C.) Tech. Bull. No. 2.
- Friedrich, G.H.W., Kunzendorf, H. and Plüger, W.L. (1974). Ship-borne geochemical investigations of deep sea manganese nodule deposits in the Pacific using a radioisotope energy dispersive X-Ray system.  
Jl. Geochem. Explor. 3, 303 - 317
- Frondel, C. (1971). New manganese-oxides: hydrohausmannite and woodruffite.  
Am. Min. 38, 761 - 769.
- Fuerstenau, D.W., Herring, A.P. and Hoover, M. (1973). Characterisation and extraction of metals from sea-floor manganese nodules.  
Trans. Soc. Min. Eng. (A.I.M.E.) 254, 205 - 211.
- Fujita, T. (1971). Concentrations of major chemical elements in marine plankton.  
Geochem. Jl. 4, 143 - 156.
- Fukao, Y. (1973). Thrust faulting at the lithospheric plate boundary. The Portugal Earthquake of 1969.  
Earth Plan. Sci. Lett. 18, 205 - 216.
- Giovanoli, R., Stahli, E. and Feitknecht, W. (1970a). Über Oxidhydroxide des vierwertigen Mangans mit Schichtengitter 1: Natriummangan (II, III) - Manganat (IV).  
Helv. Chim. Acta, 53, 209 - 220.
- Giovanoli, R., Stahli, E. and Feitknecht, W. (1970b). Über Oxidhydroxide des vierwertigen Mangans mit Schichtengitter 2: Mangan (III) - Manganat (IV).  
Helv. Chim., Acta, 53, 453 - 464.
- Giovanoli, R., Feitknecht, W. and Fisher, F. (1971). Über Oxidhydroxide des vierwertigen mit Schichtengitter 3: Reduktion von Mangan (III) - Manganat (IV) mit Zimtalkohol.  
Helv. Chim., Acta 54, 1112 - 1124.

- Giovanoli, R., Burki, F. and Scheise, P. (1973). Investigation of manganese nodules.  
re-print 33a, Univ. Berne Inst. Inorg. Anal. Phys. Chem. (unpub.).
- Glaeby, G.P. (1970). The geochemistry of manganese nodules and associated pelagic deposits from the north-west Indian Ocean.  
unpubl. Ph. D. thesis Univ. London, 629 p.p.
- Glasby, G.P. (1972a). The mineralogy of manganese nodules from a range of marine environments.  
Mar. Geol. 13, 57 - 72.
- Glaeby, G.P. (1972b). Influence of manganiferous fragments on the trace element geochemistry of pelagic sediments, north-west Indian Ocean.  
New Zealand Jl. Geol. Geophys. 15, 451 - 464.
- Glasby, G.P. (1973a). Manganese deposits in the south-west Pacific.  
in "Ferromanganese deposits on the ocean floor". 137 - 169.  
unpubl. Phase 1 report, Seabed Assessment Program. I.D.O.E. N.S.F. Washington D.C.
- Glaeby, G.P. (1973b). Manganese deposits of variable composition from north of the Indian Antarctic Ridge.  
Nature (Phys. Sci.) 242, 106 - 107.
- Glasby, G.P., Tooms, J.S. and Howarth, R.J. (1974). Geochemistry of manganese concretions from the north-west Indian Ocean.  
New Zealand Jl. Sci. 17, 387 - 407.
- Glemer, O., Gattow, G. and Meisek, H. (1961). Darstellung und Eigenschaften von Braunsteinen: I die - Gruppe der Braunsteine.  
Z. anorg. allg. Chem. 309, 1 - 19.
- Goldberg, E.D. (1954). Marine Geochemistry 1: Chemical scavengers of the sea.  
Jl. Geol. 62, 249 - 265.
- Goldberg, E.D. (1961). Chemistry of the Oceans.  
in "Oceanography" (M. Sears, ed.). 583 - 597. American Assoc. Adv. Science. New York.
- Goldberg, E.D. (1963). The oceans as a chemical system.  
in "The Sea" (M.N. Hill, ed.). 2, 3 - 25. Wiley - Interscience.
- Goldberg, E.D. (1965). Minor elements in sea-water.  
in "Chemical Oceanography" (J.P. Riley and G.W. Skirrow, eds.). 1, 163 - 196.
- Goldberg, E.D. and Arrhenius, G.D.S. (1958). Chemistry of Pacific pelagic sediments.  
Geochim. Cosmochim. Acta, 15, 153 - 212.
- Goldberg, E.D. and Koide, M. (1963). Rate of sediment accumulation in the Indian Ocean.  
in "Earth and Science and Meteorites" (J. Geise and E.D. Goldberg, eds.). 90 - 102. North-Holland, Amsterdam.
- Goldberg, E.D. and Griffin, J. (1970). The sediments of the northern Indian Ocean.  
Deep Sea Res. 17, (3), 513 - 538.

- Goodell, H.G., Meylan, M.A. and Grant, B. (1970). Ferromanganese deposits of the southern Pacific Ocean, Drake Passage and Scotia Sea. in "Antarctic Oceanology I" (J.L. Reid, ed.). Antarctic Res. Ser. 15, 27 - 92. Amer. Geophys. Union. Baltimore.
- Grant, J.B. (1970). A comparison of the chemistry and mineralogy with the distribution and physical aspects of marine manganese concretions of the southern Oceans. unpubl. M. Sc. thesis Florida State Univ. (Sed. Res. Lab. Geol. Dept.) Tallahassee, U.S.A. 94 p.p.
- Greenslate, J.L. (1974). Microorganisms participate in the construction of manganese nodules. *Nature* 249, 181 - 183.
- Greenslate, J.L., Frazer, J.Z. and Arrhenius, G. (1973). Origin and deposition of selected transition elements in the sea-bed. in "The origin and distribution of manganese nodules in the Pacific and prospects for exploration". (M. Morgenstein, ed.). 45 - 70, Hawaii Inst. Geophys. Honolulu, Hawaii.
- Griffin, J.J., Windom, H. and Goldberg, E.D. (1968). The distribution of clay minerals in the world oceans. *Deep Sea Res.* 15, 433 - 459.
- Grill, E.V., Murray, J.W. and MacDonald, R.D. (1968). Todorokite in manganese nodules from a British Columbia Fjord. *Nature (London)* 219, 358 - 359.
- Grutter, A. and Buser, W. (1957). Untersuchungen an Mangansedimenten. *Chimia* 11, 132 - 133.
- von Heimendahl, M., Hubred, G.L., Fuerstenau, D.W. and Thomae, G. (1976). A transmission electron microscope study of deep sea manganese nodules. *Deep Sea Res.* 23, 69 - 80.
- Heirtzler, J.R., Veevers, J.V., Bolli, H.M. et al. (1973). The age of the floor of the eastern Indian Ocean. *Science*, 180, 952 - 954.
- Herzenberg, C.L. and Riley, D. (1969). Interpretation of the Mosebauer spectra of marine iron-manganese nodules. *Nature*, 224, 259 - 260.
- Hewitt, D.F., Fleischer, N. and Conklin, N. (1963). Deposits of the manganese-oxides. *Econ. Geol.* 58, 1 - 51.
- Heye, D. (1975). Wachstumverhältnisse von Manganknollen. *Geol. Jahrb.* E5, 3 - 122.
- Heye, D. and Marchig, V. (1977). Relationship between the growth rate of manganese nodules from the central Pacific and their chemical constitution. *Mar. Geol.* 23, M19 - M25.
- Horn, D.R., Ewing, J.I. and Ewing, M. (1972). Graded bed sequences emplaced by turbidity currents north of 20°N in the Pacific, Atlantic and Mediterranean. *Sedimentology* 18, 247 - 275.

- Horn, D.R., Horn, B.M. and Delach, M.N. (1973). Copper and nickel content of ocean ferromanganese deposits and their relation to properties of the substrate.  
in "The origin and distribution of manganese nodules in the Pacific and prospects for exploration". (M. Morgenstein, ed.). 77 - 84. Hawaii Inst. Geophys. Honolulu, Hawaii.
- Horowitz A.J. (1974). Geochemical investigations of sediments associated with the mid-Atlantic Ridge.  
unpubl. Ph. D. thesis Univ. London, 247 p.p.
- Hryniewicz, A.Z., Sawicka, B.D. and Sawicki, J.A. (1970). The Mossbauer effect in Pacific Ocean ferromanganese nodules.  
phys. stat. sol. (a) 3, 1039 - 1045.
- Hubred, G.L. (1970). Relationship of morphology and transition metal content of Mn nodules to an abyssal hill.  
unpubl. M. Sc. thesis Univ. Hawaii.
- Johnson, B.D., Powell, C. McA. and Veevera, J.J. (1976). Spreading history of the eastern Indian Ocean and greater India's northward flight from Antarctica and Australia.  
Bull. Geol. Soc. Am. 87 (11), 1560 - 1566.
- Johnson, C.E. and Glasby, G.P. (1969). Mossbauer effect determination of particle size in microcrystalline iron-manganese nodules.  
Nature 222, 376 - 377.
- Jones, L.H.P. and Milne, A.A. (1956). Birnessite, a new manganese-oxide mineral from Aberdeenshire, Scotland.  
Min. Mag. 31, 235, 283 - 288.
- Kennett, J.P. and Thunnell, R.C. (1975). Global increase in Quaternary explosive volcanism.  
Science 187, 497 - 503.
- Kennett, J.P. and Watkins, N.D. (1975). Deep sea erosion and manganese nodule pavement development in the south and Indian Oceans.  
Science 188, 1011 - 1013.
- Kennett, J.P., Houtz, R.E. et al (1974). Development of the circum-Antarctic current.  
Science 186, 144 - 147.
- Kherin, G.S. (1973). Ferromanganese nodules on the flank of the mid-Atlantic Ridge.  
Dokl. Acad. Nauk. S.S.S.R. 212, 1440 - 1443 (in Russian).
- Kneuss, J.A. and Taft, B.A. (1964). Equatorial undercurrent of the Indian Ocean.  
Science 143, 354 - 356.
- Koblentz-Miehke, D.J., Volkovinsky, V.V. and Kabanova, J.G. (1970). Plankton primary production of the world ocean.  
in "Scientific Exploration of the South Pacific". (W.S. Wooster, ed.). 183 - 193. Nat. Acad. Sci. Washington D.C.
- Kolla, V., Bé, A.W.H. and Biscaye, P.E. (1976a). Calcium-carbonate distribution in the surface sediments in the Indian Ocean.  
Jl. Geophys. Res. 81, (15), 2605 - 2616.

- Kolla, V., Henderson, L. and Biaceys, P.E. (1976b). Clay mineralogy and sedimentation in the western Indian Ocean.  
Deep Sea Res. 23, 949 - 961.
- Kolla, V., Sullivan, L., Streeter, S.S. and Langeath, M.G.Jr. (1976c). Spreading of Antarctic Bottom Water and its effects on the floor of the Indian Ocean inferred from bottom water potential temperature, turbidity and sea-floor photography.  
Mar. Geol. 21, 171 - 189.
- Krauskopf, K.B. (1957). Separation of manganese from iron in sedimentary processes.  
Geochim. Cosmochim. Acta 12, 61 - 84.
- Krey, J. (1973). Primary production in the Indian Ocean.  
in "The Biology of the Indian Ocean". (B. Zitschel, ed.).  
115 - 126. Springer-Verlag, New York.
- Kriehnaswami, S., Somayajulu, B.L.K. and Moore, W.S. (1972). Dating of manganese nodules using Beryllium. - 10.  
in "Ferromanganese deposits on the ocean floor". (D.R. Horn, ed.)  
117 - 122. Lamont Doherty Geol. Obs. New York.
- Ku, T-L. and Broecker, W.S. (1969). Radiochemical studies on manganese nodules of deep sea origin.  
Deep Sea Res. 16, 625 - 637.
- Ku, T-L. and Glesby, G.P. (1972). Radiometric evidence for the rapid growth rate of shallow water continental margin manganese nodules.  
Geochim. Cosmochim. Acta 36, 699 - 704.
- Kutina, J. (1975). Tectonic development and Metallogeny of Madagascar with reference to the fracture pattern of the Indian Ocean.  
Bull. Geol. Soc. Am. 86, (4), 582 - 592.
- Laughton, A.S. (1967). Underwater photography of the Cerberus Ridge.  
in "Deep Sea Photography". (I.B. Hersey, ed.). 196 - 206.  
John Hopkins Press, Baltimore.
- Laughton, A.S., Matthews, D.H. and Fisher, R.L. (1971). The structure of the Indian Ocean.  
in "The Sea". (G. Maxwell, ed.). 4(2), 543 - 586.
- Laughton, A.S., McKenzie, D.P. and Sclater, J.G. (1972). The structure and evolution of the Indian Ocean.  
in "Proceedings 24th Int. Geol. Conf. Section 8, Mar. Geol. and Geophys.". 65 - 73. Montreal, Canada.
- Leatherland, T., Burton, J., McCartney, M. and Culkin, F. (1973). Concentrations of some trace metals in pelagic organisms and Hg in north-east Atlantic Ocean water.  
Deep Sea Res. 20, 679 - 683.
- Luyendyk, B.P. and Davies, T.A. (1974). Results of D.S.D.P. Leg 26 and the geologic history of the southern Indian Ocean.  
in "Initial Reports of the D.S.D.P., Leg XXVI". (T.A. Davies and B.P. Luyendyk, eds.). 909 - 943. U.S. Govt. Printing Office, Washington, D.C.

- Lyle, M. (1976). Estimation of hydrothermal manganese input to the oceans. *Geology* 4, 733 - 736.
- Lyle, M., Dymond, J. and Heath, G.R. (1977). Copper-nickel-enriched ferromanganese nodules and associated crusts from the Bauer Basin, northwest Nazca Plate. *Earth Plan. Sci. Lett.* 35, 55 - 64.
- Lynn, D. and Bonatti, E. (1965). Mobility of manganese in diagenesis of deep sea sediments. *Mar. Geol.* 3, 457 - 474.
- McElhinney, M.W. (1970). Formation of the Indian Ocean. *Nature*, 228, 977 - 979.
- McElhinney, M.W. and Luck, G.R. (1970). Palaeomagnetism and Gondwanaland. *Science* 168, 830 - 832.
- McKenzie, D.P. (1970). Plate tectonics of the Mediterranean region. *Nature (London)* 226, 239 - 246.
- McKenzie, D.P. and Sclater, J.G. (1971). The evolution of the Indian Ocean since the late Cretaceous. *Geophys. Jl. Roy. Astr. Soc.* 24, 437 - 528.
- McKenzie, R.M. (1971). The synthesis of birnessite, cryptomelane and some other oxides and hydroxides of manganese. *Min. Mag.* 38, 493 - 502.
- McKenzie, R.M. (1972). The sorption of some heavy metals by the oxides of Mn. *Geoderma* 8, 29 - 35.
- McMurdie, H.F. and Golovato, E. (1948). Study of the modifications of manganese dioxide. *Jl. Res. Nat. Bur. Stand.* 41, 589 - 600.
- Manheim, F.T. (1965). Manganese-iron accumulations in the shallow water environment. *Narragansett Mar. Lab. Occ. Publ.* 3, 217 - 276. Univ. Rhode Island.
- Margolis, S.V. and Burns, R.G. (1975). Pacific deep sea manganese nodules: their distribution, composition and origin. *Ann. Rev. Earth Plan. Sci.* 4, 229 - 263.
- Menard, H.W. (1967). Sea floor spreading, topography and the second layer. *Science* 157, 923 - 924.
- Mero, J.L. (1962). Ocean floor manganese nodules. *Econ. Geol.* 57, 747 - 767.
- Mero, J.L. (1965). *The Mineral Resources of the Sea*. Elsevier, Amsterdam.
- Meylan, M.A. (1974). Field Description and classification of manganese nodules. in "Ferromanganese deposits of the Ocean Floor". Cruise report Mn74 - 01. (J.E. Andrews et al, eds.). Hawaii Inst. Geophys. rep. HIG74 - 9, Honolulu, Hawaii. 193 p.p.

- Meylan, M.A. (1975). Regional variations in Pacific Ocean manganese nodule mineralogy. (Abstr.).  
Proc. Geol. Soc. Am. Ann. Meet. 1975.
- Monget, J.M., Murray, J.W. and Mascle, J. (1976). A world-wide compilation of published multicomponent analyses of ferromanganese concretions.  
I. D.O.E. Manganese nodules project, technical report no. 12.  
N.S.F., New York.
- Moore, W.S. and Vogt, P.R. (1976). Hydrothermal manganese crusts from two sites near the Galapagos spreading axis.  
Earth. Plan. Sci. Lett. 29, 349 - 356.
- Murray, J. and Renard, A.F. (1891). Report on the scientific results of the exploring voyage of H.M.S. Challenger.  
Vol. 3, 525 p.p., H.M.S.O. London.
- Nicholls, G.D., Curl, H.Jr. and Bowen, V.T. (1959). Spectrographic analysis of marine plankton.  
Limnol. Oceanogr. 4, 472 - 478.
- Opdyke, N.D. and Glaes, B.P. (1969). The palaeomagnetism of sediment cores from the Indian Ocean.  
Deep Sea Res. 16, 249 - 261.
- Pachadzhyanov, D.N., Bandurkin, G.A., Migdisov, A.A. and Girin, G.A. (1963). Data on the geochemistry of manganese nodules from the Indian Ocean.  
Geochim. Int. 5, 520 - 527.
- Panikkar, N.K. (1968). International Indian Ocean Expedition - Plankton Atlas. Vol. 1 (2) Maps of total zooplankton biomass in the Indian Ocean.  
Nat. Inst. Oceanog., C.S.I.R., New Delhi.
- Pautot, G. and Melguen, M. (1976). Deep bottom currents, sedimentary hiatuses and polymetallic nodules.  
in "Marine geological investigations in the south west Pacific and adjacent areas". 54 - 61. (G.P. Glæby and H.R. Katz, eds.).  
United Nations (C.C.O.P./S.O.P.A.C.) Technical Bull. no. 2.
- Payne, R.R. and Conolly, J.R. (1972). Pleistocene manganese pavement production: Its relationship to the origin of manganese in the Tasman Sea.  
in "Ferromanganese deposits on the ocean floor". 81 - 92. (D.R. Horn, ed.). Lamont Doherty Geol. Obs., New York.
- le Pichon, X. (1960). The deep water circulation in the south west Indian Ocean.  
Jl. Geophys. Res. 65, 4061 - 4074.
- le Pichon, X. and Heirtzler, J.R. (1968). Magnetic anomalies in the Indian Ocean and sea floor spreading.  
Jl. Geophys. Res. 73, 2101 - 2117.
- le Pichon, X. and Talwani, M. (1969). Regional gravity anomalies in the Indian Ocean.  
Deep Sea Res. 16, 263 - 274.

- le Pichon, X., Bonin, J. and Pautot, G. (1970). The Gibraltar end of the Azores-Gibraltar plate boundary: an example of compressive tectonics. (abstr.).  
Proc. Upper Mantle Committee Symposium, Flagstaff, Arizona.
- le Pichon, Z., Auzenda, J.M., Pautot, G., Monti, S. and Francheteau, J. (1971). Deep Sea photographs of an active seismic fault zone near Gibraltar Straits.  
Nature (London), 230, 110 - 111.
- Piper, D.Z. and Williamson, M.E. (1977). Composition of Pacific Ocean ferromanganese nodules.  
Mar. Geol. 23, 285 - 303.
- Presley, B.J., Brooks, R.R. and Kaplan, I.R. (1967). Manganese and related elements in the interstitial waters of marine sediments.  
Science 158, 906 - 910.
- Pricka, N.B. and Calvert, S.E. (1970). Compositional variations in Pacific Ocean Fe-Mn nodules and its relationship to sediment accumulation rates.  
Mar. Geol. 9, 145 - 171.
- Raab, W. (1972). Physical and chemical features of Pacific deep sea manganese nodules and their implications to the genesis of nodules.  
in "Ferromanganese deposits on the ocean floor". (D.R. Horn, ed.). 31 - 49. Lamont Doherty Geol. Obs. Washington, D.C.
- Rancitelli, L.A. and Perkins, R.W. (1973). Major and minor elemental composition of manganese nodules.  
in "Ferromanganese deposits on the ocean floor". 1 - 5.  
unpubl. Phase 1 report, Seabed Assessment Program I.D.O.E. N.S.F. Washington, D.C.
- Rao, T.S.S. (1973). Zooplankton studies in the Indian Ocean.  
in "The Biology of the Indian Ocean". (B. Zeitschel, ed.). 243 - 255. Springer-Verlag, New York.
- Rateev, M.A., Gorbunova, Z.N., Lisitzin, A.P. and Nosov, G.L. (1969). The distribution of clay minerals in the ocean.  
Sedimentology 13, 21 - 43.
- Rex, R.W. and Goldberg, E.D. (1958). Quartz content of pelagic sediments of the Pacific Ocean.  
Tellus 10, 153 - 159.
- Ryan, W.B.F., Heu, K.J. et al. (1973). Initial Reports of the Deep Sea Drilling Project, leg 13.  
Vol. XIII, U.S. Govt. Printing Office, Washington, D.C.
- Schlich, R. and Patriat, P. (1971). Anomalies magnétiques de la branch Est de la dorsale médio - Indienne entre les îles Amsterdam et Kerguelen.  
C.R. Acad. Sci. Paris 272, 773 - 776.
- Sclater, F.R., Boyle, E. and Edmond, J.M. (1976). On the marine geochemistry of Ni.  
Earth Plan. Sci. Lett. 31, 119 - 128.



- Scott, M.R., Scott, R.B. et al (1974). Rapidly accumulating manganese deposit from the median valley of the mid-Atlantic Ridge. *Geophys. Res. Lett.* 1, 355 - 359.
- Sharma, G.S. (1968). Some inferences on the equatorial undercurrent in the Indian Ocean based on the physical properties of the waters. *Jl. Mar. Biol. Assoc. India* 10, 224 - 236.
- Shterenberg, L.Ye., Stepanova, K.A. and Il'icheva, L.V. (1974). Detailed structure of iron manganese concretions from the Pacific. *Dokl. Acad. Nauk. S.S.S.R.* 219, 723 - 726.
- Skorniyakova, N.S. (1965). Dispersed iron and manganese in Pacific Ocean sediments. *Int. Geol. Rev.* 7, 2161 - 2174.
- Skorniyakova, N.S. and Andrushchenko, P.F. (1970a). The chemical composition of iron manganese concretions of the Pacific Ocean. *Okeanologiya* 2, 264 - 277.
- Skorniyakova, N.S. and Andrushchenko, P.F. (1970b). in "The Pacific Ocean". (P.L. Bezrukov, ed.). 6, 202 - 268. Nauka, Moscow.
- Skorniyakova, N.S., Bazilevskaya, E.S. and Gordeyev, V.V. (1975). Mineralogy and geochemistry of ferromanganese nodules in the Pacific Ocean. *Geochemistry International* 12, 83 - 95.
- Smith, A.G. and Hallam, A. (1970). The fit of the southern continents. *Nature* 225, 139 - 144.
- Smith, P.A. and Cronan, D.S. (1975). The dispersal of metals associated with an active submarine exhalative deposit. *Proc. 3rd Oceanol. Int. Conf. Brighton, U.K.*
- Smith, R.E., Gassaway, J.D. and Giles, H.N. (1968). Ferromanganese nodules from the Nares abyssal plain: geochemistry and mineralogy. *Science* 161, 780 - 781.
- Sorem, R.K. (1967). Manganese nodules: nature and significance of internal structure. *Econ. Geol.* 62, 141 - 152.
- Sorem, R.K. (1973). Manganese nodules as indicators of long-term variations in sea floor environment. in "The origin and distribution of manganese nodules in the Pacific and prospects for exploration". (M. Morgenstein, ed.). 151 - 165. Hawaii Inst. Geophys. Honolulu, Hawaii.
- Soram, R.K. and Foster, A.R. (1972). Internal structure of manganese nodules and implications in beneficiation. in "Ferromanganese deposits on the ocean floor". (D.R. Horn, ed.). 167 - 182. Lamont Doherty Geol. Obs. Washington, D.C.
- Sozanski, A.G. and Cronan, D.S. (1976). Environmental differentiation of morphology of ferromanganese oxide concretions in Shebandowan Lake, Ontario. *Limnol. Oceanog.* 21, 894 - 898.

- Starik, I.E., Kuznetsov, Yu.V., Grashchenko, S.M. and Frenklich, M.S. (1958).  
The ionium method of determination of age of marine sediments.  
Geochemistry 1, 1 - 15.
- Straczek, J.A., Horen, A., Ross, M. and Warsaw, C.W. (1960). Studies of the  
manganese oxides IV: todorokite.  
Am. Miner. 45, 1174 - 1184.
- Subramanian, V. (1975). Mossbauer effects in Fe-Mn precipitation.  
phys. stat. sol. (a) 27, 303 - 308.
- Sugimura, Y., Miyake, Y. and Yanagawa, H. (1975). Chemical composition and  
the rate of accumulation of ferromanganese nodules in the western  
north Pacific.  
Papers in Meteorology and Geophysics, Tokyo 26(2), 47 - 54.
- Swallow, J.C. (1964). Equatorial undercurrent in the western Indian Ocean.  
Nature 204, 436 - 437.
- Sykes, L.R. (1970). Seismicity of the Indian Ocean and a possible nascent  
island arc between Ceylon and Australia.  
Jl. Geophys. Res. 75, 5041 - 5055.
- Tooms, J.S., Summerhayes, C.P. and Cronan, D.S. (1969). Geochemistry of  
marine phosphate and manganese deposits.  
Oceanogr. Mar. Biol. 7, 49 - 100.
- Turekian, K.K. and Imbrie, J. (1966). The distribution of trace elements in  
deep sea sediments of the Atlantic Ocean.  
Earth Plan. Sci. Lett. 1, 161.
- Udias, A. and Arroyo, A.L. (1972). Plate tectonics and the Azores-Gibraltar  
region.  
Nature (Physical Science) 237, 67 - 69.
- Udintsev, G.B. et al (1975). Geological - Geophysical Atlas of the Indian  
Ocean.  
Pergamon Press, London.
- Venkatarathnam, K. and Biscaye, P.E. (1973). Clay mineralogy and sedimentation  
in the eastern Indian Ocean.  
Deep Sea Res. 20, 727 - 738.
- Vincent, E.S. (1972). Oceanography and late Quaternary planktonic foraminifera,  
southwestern Indian Ocean.  
unpubl. Ph.D. thesis, Univ. South. Calif. U.S.A. 353pp.
- El Wakeel, S.K. and Riley, J.P. (1961). Chemical and mineralogical studies of  
deep sea sediments.  
Geochim. Cosmochim. Acta 25, 110 - 146.
- Wangersky, P.J. (1967). Removal of soluble salts from air-dried sediments.  
Jl. Geol. 75, 733.
- Warren, B.A. (1974). Deep flow in the Madagascar and Mascarene Basins.  
Deep Sea Res. 21, 1 - 21.

- Watkins, J.D. and Kennett, J.P. (1973). Regional sedimentary disconformities and upper Cenozoic changes in bottom water velocities between Australasia and Antarctica.  
in "Antarctic Oceanology II" (D.E. Hayes, ed.). 273 - 293.  
Antarctic Res. Ser. 19.
- Watkins, N.D. and Kennett, J.P. (1977). Erosion of deep sea sediments in the southern Ocean between longitudes 70°E and 190°E and contrasts in manganese nodule development.  
Mar. Geol. 23, 103 - 112.
- Weiseel, J.K. and Hayes, D.E. (1971). Asymmetric sea floor spreading south of Australia.  
Nature 231, 518 - 522.
- Wilkins, P.E., Warner, T.B. and Carr, R.A. (1971). Some aspects of the geochemistry of F, Fe and Mn in coastal waters and in fresh-water springs on the south-east coast of Hawaii.  
Mar. Geol. 11, M39 - M46.
- Winterhalter, B. and Siivola, J. (1967). An electron microprobe study of the distribution of Fe, Mn, and P in concretions from the Gulf of Bothnia, northern Baltic Sea.  
Comptes Rend. Soc. géol. Fin. XXXIX, 161 - 172.
- Wyrski, K. (1971). Oceanographic Atlas of the International Indian Ocean Expedition.  
(K. Wyrski, ed.). U.S. National Science Foundation, Washington, D.C.
- Yoshimura, T. (1934). Todorokite, a new manganese mineral from the Todoroki mine, Hokkaido, Japan.  
Jl. Fac. Sci. Hokkaido Univ. Ser. 4, 2, 289.
- Zelenov, K.K. (1964). Iron and manganese in exhalations of the submarine Banu Wuhu volcano (Indonesia).  
Dokl. Acad. Sci. 155, 91 - 94.

A P P E N D I C E S

A P P E N D I X 1CHEMICAL ANALYTICAL TECHNIQUES(i) Sample Preparation

## (a) Ferromanganese-oxide samples.

The preparation of ferromanganese-oxide samples for analysis varied according to the nature of the samples. Those covered by adhering sediment were washed clean with de-ionised water and left to dry but in some cases this treatment was not necessary. Where possible, 10 to 15 g. of sample was taken for crushing. Where the whole sample weighed less than this, proportionately less was taken but in some cases the sample was so small that it all had to be taken for crushing. Large nodules and encrustation samples were sectioned using a hacksaw blade and a representative portion taken from substrate or core to outer surface. Contamination from the hacksaw was not regarded as being a problem since Cronan(1967) has shown that except for Cr, all the trace elements for which analysis was carried out were present at far lower levels in a hacksaw blade than their average values in the samples. Where core material was present in nodules it was separated out by hand, so far as possible, prior to crushing.

The samples were first crushed by hand with a porcelain pestle and mortar and then with an agate pestle and mortar until the powder passed

through an 80 mesh sieve. The sample powders were then transferred for storage into air-tight, clean, polythene or glass containers. Care was taken at all stages of the crushing procedure to avoid losing the finest fraction as dust to the atmosphere. After each sample had been crushed both pestles and mortars were thoroughly cleaned using HCL, de-ionised water and acetone. The hacksaw blade used for cutting up the larger samples was thoroughly cleaned in a similar manner between each sampling operation.

(b) Sediment samples.

All the sediment samples analysed had already been selected from their respective cores when they were received and some had already been dried. Treatment therefore consisted of taking a representative portion of each sample of about 10 g., (or all the sample where the total sample weight was less than 10 g.) placing it in a glass dish and freeze-drying it. The dried samples were then crushed in exactly the same way as the ferromanganese-oxide samples and stored in similar containers.

(ii) Bulk Chemical Attack

Approximately 250 - 300 mg. of each sample was weighed out accurately into separate numbered P.T.F.E. beakers which had previously been dried and weighed accurately. The beakers and their contents were then placed in dessicators and dried to constant weight, this usually taking 2 to 3 days. This preliminary dessication procedure was only required for ferromanganese-oxide samples, because of their tendency to absorb atmospheric moisture when in a finely divided state. After 2 ml. of 6M HCL had been added to the beakers, they were placed on

a hotplate and heated gently for about 2 hours to breakdown the Mn oxides prior to the addition of the main reagents. This pre-treatment was not necessary with sediment samples. The beakers were then cooled and the following reagents added to each; 8 ml. of 40% hydrofluoric acid, 6 ml. of 50 - 50 mixture of concentrated nitric and perchloric acids.

After addition of all the reagents the beakers were returned to the hotplate and evaporated to dryness overnight. When fuming finally ceased the beakers were removed from the heat, a further 2 ml. of the nitric and perchloric acid mixture added, and then the contents evaporated to dryness again. When fuming ceased the beakers were cooled but whilst still warm 5 ml. of 6M HCL was added to each to dissolve the small pellet of residue in the beaker. The resulting solutions, when cold, were transferred to separate, numbered 25 ml. volumetric flasks, the beakers were rinsed thoroughly with de-ionised water and the washings also transferred to the flask. The contents were then made up to 25 ml. with de-ionised water giving a final solution which was very nearly 1M HCL.

### (iii) Selective Leach Techniques

#### (a) Acetic acid attack

About half a gram of each sample (1 g. in the case of high-carbonate samples) was accurately weighed out into a conical 50 ml. flask fitted with a ground glass stopper and which had previously been dried and weighed. The flask and contents were then placed in a dessicator and dried to constant weight. This dessication procedure was only necessary for ferromanganese-oxide samples, as explained above.

After final weighing, 10 ml. of 25% (v/v) acetic acid was added to

each flask, the stoppers were replaced and the beakers placed in a mechanical shaker for 4 hours. The contents were then allowed to settle and then were filtered through a 0.45 $\mu$  membrane filter which had previously been weighed. The beaker and the residue were thoroughly washed with de-ionised water and the filtrate and washings were transferred to a 25 ml. volumetric flask. This was made up to the mark with de-ionised water giving a final solution containing about 5% acetic acid. The filter paper and residue were placed in a desiccator, allowed to thoroughly dry, and were then weighed. The weight percentage of each sample which was soluble in acetic acid was then calculated.

(b) Mixed acid and reducing agent attack

The initial weighing-out procedure for this attack was exactly the same as for the acetic acid attack. In this attack however the reagent used was a mixture of acetic acid and hydroxylamine hydrochloride in the following proportions:- 3 vols. of 35% (v/v) acetic acid to 7 vols. of 25% (w/w) hydroxylamine hydrochloride. To each sample was added 25 ml. of this mixed reagent and the flasks were then placed in a mechanical shaker for 4 hours. The contents were then filtered exactly as in the acetic acid attack but the filtrate and washings were placed in a 100 ml. beaker, covered with a watch glass and placed on a hot-plate. When the contents had evaporated down to about 10 ml. about 2 ml. of concentrated nitric acid was added drop by drop to the solution to break down the excess reagent. This addition was carried out away from the heat because of the tendency of the solution to boil violently during the addition if it was originally too hot. When the nitric acid had been added the beaker and watchglass were returned to the hotplate and evaporation of the contents was



continued until fumes of nitric acid were evolved. The beaker was then allowed to cool and the contents transferred to a 25 ml. volumetric flask. The beaker and watchglass were washed with 1M HCL and the washings also transferred to the volumetric flask, which was then made up to the mark with 1M HCL. The filter papers and residues were treated in the same manner as in the acetic acid attack and the weight percentage of each sample which was soluble in the mixed acid and reducing agent was then calculated.

(c) Hydrochloric acid attack.

The preliminary weighing-out procedure was exactly the same as for the acetic acid attack, except that the samples were placed in 50 ml. beakers rather than flasks. After the final weighing 5 ml. of 6M HCL was added to each beaker, a watchglass was placed over each and they were placed on a hotplate for 4 hours. The beakers were then removed from the heat, allowed to cool, and the contents filtered in the same way as for the acetic acid attack. The filtrate and washings were transferred to a 25 ml. volumetric flask and made up to the mark with de-ionised water. The filter papers and residues were treated in the same manner as in the acetic acid attack and the weight percentage of each sample calculated which was soluble in hydrochloric acid.

(iv) Analytical Precision and Accuracy

All the elements investigated were analysed in all samples by atomic absorption spectrophotometry using a Perkin Elmer 403 spectrophotometer in the Applied Geochemistry Research Group at Imperial College. All samples, except the solutions obtained from the acetic acid attack, were sprayed in the 1M HCL and compared against

internal standards made up in IM HCL. Solutions of samples subjected to the acetic acid attack contained 5% acetic acid and were therefore compared against standards made up in 5% acetic acid.

All determinations were carried out in duplicate and some in triplicate, except where the very small amount of sample available prevented this. An average value for each element in each sample was then calculated from these determinations. Each series of determinations constituted 30 to 50 samples of which at least 15% constituted blanks, standards and duplicates. The average precision and accuracy of the bulk attack are given in Table 1, based on the replicate analysis of 4 external nodule standards which were also analysed at 6 independent German laboratories. An accuracy of better than 6% was achieved for all elements except Pb and Ti for which the accuracies were 14% and 13% respectively.

The accuracy of the selective chemical leach analyses could not be established since no outside standard could be obtained which had been subjected to identical attacks. However the replicate sample precision for all elements for all three attacks was obtained using the same standards I to IV as were used for the bulk attack. The results are given in Table 2.

#### (v) Selective Attacks on Minerals and Synthetic Phases

In order to assess the susceptibility of various iron and manganese oxide phases to attack by the selective leach techniques described in Section (iii) of this appendix several synthetic oxide phases were prepared by rapid precipitation of the phases from aqueous solution. X-Ray diffraction studies of these phases showed them to be completely amorphous phases. Naturally occurring terrestrial samples of todorokite and goethite were also prepared using the

TABLE 1 Precision and accuracy of bulk chemical attack based on analysis of external standards

Standard	Number of Determinations	Result	Mn %	Fe %	Co %	Ni %	Cu %	Zn %	Pb %	Ca %	Al %	Cd %	Cr %	Ti %
I	6	Actual	29.5	5.2	1600	14600	14800	1570	350	1.78	3.18	n.d.	n.d.	0.37
		Found	28.6 +0.9 -0.9	5.22 +0.23 -0.23	1690 +70 -70	15100 +1100 -1100	14700 +600 -600	1450 +50 -50	390 +20 -20	1.64 +0.08 -0.08	3.28 +0.37 -0.37	25 +2 -2	23 +4 -4	0.42 +0.04 -0.04
		Accuracy (%)	3	1	6	3	1	8	11	8	3	-	-	14
II	5	Actual	22.3	13.2	2900	7600	5100	820	750	1.93	2.81	n.d.	n.d.	0.93
		Found	21.5 +1.0 -1.0	12.8 +0.4 -0.4	2920 +110 -110	7440 +410 -410	5110 +210 -210	800 +30 -30	870 +30 -30	1.79 +0.10 -0.10	2.74 +0.26 -0.26	17 +4 -4	43 +4 -4	0.99 +0.01 -0.01
		Accuracy (%)	4	3	1	2	1	2	15	7	2	-	-	6
III	6	Actual	19.1	6.7	1700	9500	8000	1010	490	1.45	4.98	n.d.	n.d.	0.50
		Found	18.9 +0.6 -0.6	6.67 +0.14 -0.14	1610 +90 -90	9550 +450 -450	8100 +100 -100	990 +60 -60	550 +70 -70	1.37 +0.12 -0.12	4.66 +0.28 -0.28	16 +1 -1	47 +4 -4	0.61 +0.05 -0.05
		Accuracy (%)	1	1	5	1	1	2	12	1	6	-	-	22
IV	6	Actual	31.8	4.6	1700	15200	15200	1580	330	1.66	2.81	n.d.	n.d.	0.30
		Found	31.4 +0.6 -0.6	4.56 +0.08 -0.08	1780 +30 -30	15100 +900 -900	15800 +200 -200	1640 +40 -40	400 +10 -10	1.56 +0.03 -0.03	2.74 +0.32 -0.32	30 +3 -3	20 +4 -4	0.33 +0.03 -0.03
		Accuracy (%)	1	1	5	1	4	4	20	6	2	-	-	10
Replicate sample Precision			+3% -3%	+3% -3%	+4% -4%	+5% -5%	+3% -3%	+4% -4%	+5% -5%	+6% -6%	+11% -11%	+11% -11%	+14% -14%	+9% -9%

Element Attack	Mn %	Fe %	Co %	Ni %	Cu %	Zn %	Pb %	Ca %	Al %	Cd %	Cr %	Ti %
Acetic Acid	$\begin{smallmatrix} + \\ - \end{smallmatrix} 15$	$\begin{smallmatrix} + \\ - \end{smallmatrix} 7$	*	$\begin{smallmatrix} + \\ - \end{smallmatrix} 16$	$\begin{smallmatrix} + \\ - \end{smallmatrix} 15$	$\begin{smallmatrix} + \\ - \end{smallmatrix} 11$	*	$\begin{smallmatrix} + \\ - \end{smallmatrix} 4$	$\begin{smallmatrix} + \\ - \end{smallmatrix} 12$	*	*	*
Mixed Acid & Reducing Agent	$\begin{smallmatrix} + \\ - \end{smallmatrix} 6$	$\begin{smallmatrix} + \\ - \end{smallmatrix} 5$	$\begin{smallmatrix} + \\ - \end{smallmatrix} 5$	$\begin{smallmatrix} + \\ - \end{smallmatrix} 4$	$\begin{smallmatrix} + \\ - \end{smallmatrix} 2$	$\begin{smallmatrix} + \\ - \end{smallmatrix} 9$	$\begin{smallmatrix} + \\ - \end{smallmatrix} 5$	$\begin{smallmatrix} + \\ - \end{smallmatrix} 3$	$\begin{smallmatrix} + \\ - \end{smallmatrix} 7$	$\begin{smallmatrix} + \\ - \end{smallmatrix} 14$	$\begin{smallmatrix} + \\ - \end{smallmatrix} 20$	$\begin{smallmatrix} + \\ - \end{smallmatrix} 25$
Hydrochloric Acid	$\begin{smallmatrix} + \\ - \end{smallmatrix} 2$	$\begin{smallmatrix} + \\ - \end{smallmatrix} 2$	$\begin{smallmatrix} + \\ - \end{smallmatrix} 4$	$\begin{smallmatrix} + \\ - \end{smallmatrix} 3$	$\begin{smallmatrix} + \\ - \end{smallmatrix} 3$	$\begin{smallmatrix} + \\ - \end{smallmatrix} 3$	$\begin{smallmatrix} + \\ - \end{smallmatrix} 5$	$\begin{smallmatrix} + \\ - \end{smallmatrix} 2$	$\begin{smallmatrix} + \\ - \end{smallmatrix} 11$	$\begin{smallmatrix} + \\ - \end{smallmatrix} 10$	$\begin{smallmatrix} + \\ - \end{smallmatrix} 12$	$\begin{smallmatrix} + \\ - \end{smallmatrix} 20$

\* - Element present at or below detection limit

TABLE 2 Precision of selective chemical attacks based on replicate analysis of nodule standards.

methods described in sub-section (i)(a) and these were subjected to the same selective leach techniques. The mineralogical purity of these samples was confirmed by X-Ray diffraction analysis. The results of these tests are given in Table 3.

(vi) Correction Procedure for Ca Interference

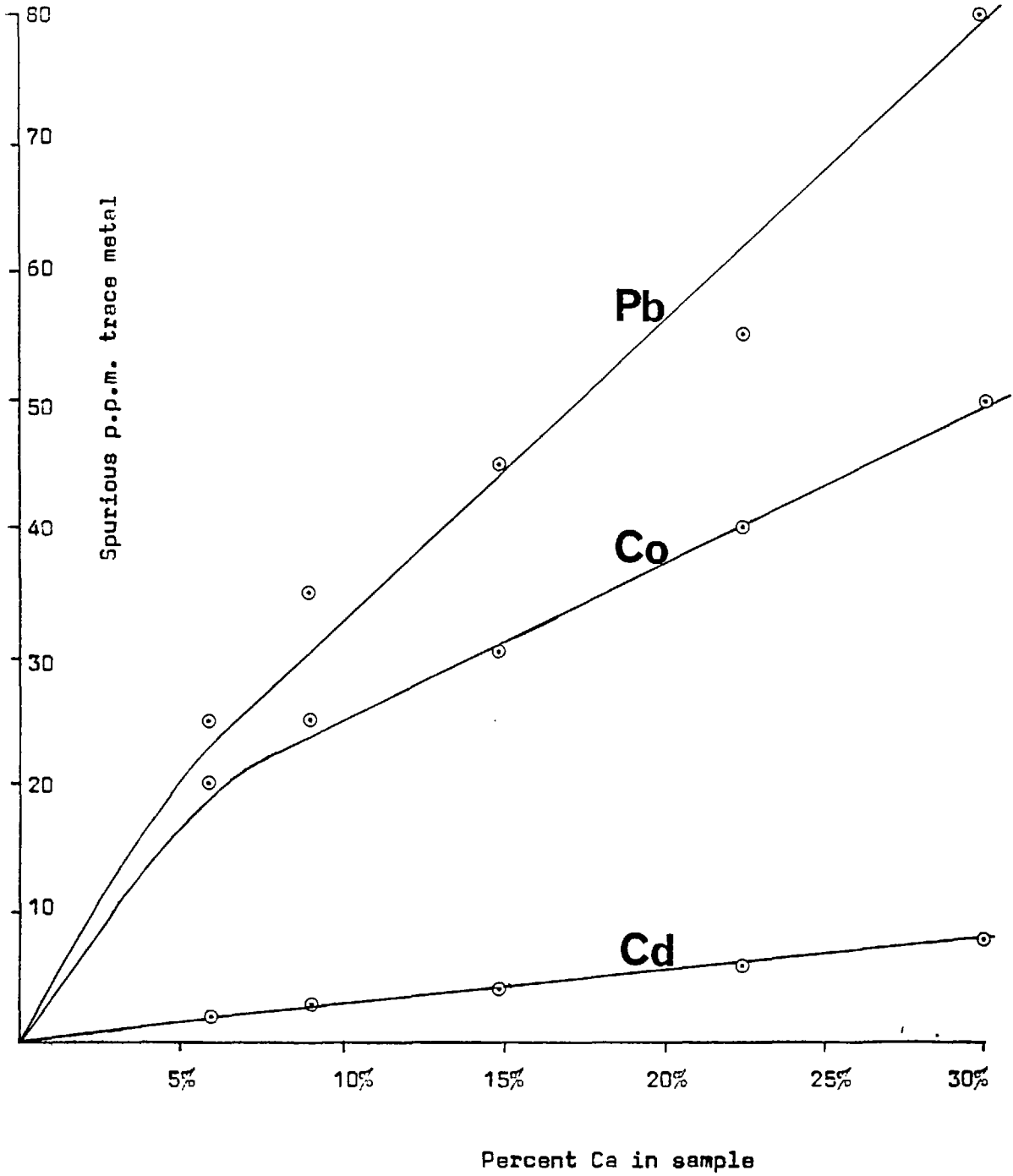
One disadvantage of analysis of samples by atomic absorption spectrophotometry is that several metals suffer interference effects when Ca is also present in the samples. This leads to spuriously high values of these metals being observed in samples where the Ca content is high. Calcium interference was only a major problem for the elements Pb, Cd and Co and only where these elements were present at low levels and Cs was present at high levels. Calcium interference was therefore not a problem in ferromanganese-oxide analysis. However levels of Pb and Co in many sediments were 100 p.p.m. or less and levels of Cd were an order of magnitude lower than this. Several sediments contained a high percentage of Cs as  $\text{CaCO}_3$  and in these sediments Ca interference caused spuriously high values of Co, Pb and Cd to be obtained. Although the interference phenomenon affected very few samples a correction procedure was adopted for the affected elements.

The correction procedure was carried out as follows. Standard solutions of 1M HCL were made up with increasing, accurately known, concentrations of Ca present in solution. These standard solutions were then sprayed on the spectrophotometer in turn using the lamp for Pb and readings taken of the concentration of Pb as determined by the instrument in each of the standard solutions. Since no Pb was actually present the reading obtained represented solely the interference produced by the calcium. A graph was drawn plotting the values of Pb thus obtained against the calcium concentrations used to obtain these values. This graph was

Phase Attack	Synthetic MnO <sub>2</sub>	Synthetic FeOOH	Synthetic co- precipitated Fe - Mn oxide	Todorokite	Goethite
Acetic acid (Amount soluble in wt. %)	1	1	1	1	1
Mixed acid and reducing agent (Amount soluble wt. %)	100	99	99	92	2
Hydrochloric acid (Amount soluble in wt. %)	100	100	100	100	98

TABLE 3 Susceptibility to chemical attack of various synthetic and naturally occurring Fe and Mn phases.

Figure 1 Graphs of Ca interference corrections.



then used to determine what proportion of the observed Pb concentrations in each sample was due to interference from the Ca which was also present. This value was then subtracted from the observed value in order to obtain the true Pb concentration in the sample. This procedure was repeated for Cd and Co also. Typical results are shown in figure 1.



A P P E N D I X 2MINERALOGICAL ANALYSIS(i) Sample Preparation

About 250 mg. of each sample, prepared as described in sub-section (i)(a) of Appendix 1, was placed in a small agate mortar and ground until the powder became quiet under the pestle. The pestle and mortar were thoroughly cleaned with dilute HCL and de-ionised water between each sample. The powders were then backloaded into cavity mounts.

Where insufficient material was available to use a cavity mount, 20 to 30 mg. of material was used to coat a fine glass capillary. This was then used in an 11.5 cm. Debye - Scherrer camera.

(ii) Analysis

The analyses were carried out on a Phillips model PW1010/80 diffractometer using Fe K radiation at a tube setting of 34KV at 28mA. The radiation was filtered using a Mn filter and passed through a 2<sup>o</sup> divergent slit and a 0.1<sup>o</sup> receiving slit. Counting was by means of a proportional counter. The samples were scanned at 1<sup>o</sup> per minute through a range of 2 $\theta$  from 4<sup>o</sup> to 65<sup>o</sup> and 80<sup>o</sup> to 90<sup>o</sup>. Samples analysed

by means of the Debye - Scherrer camera were exposed for between 4 hours and 12 hours depending on their degree of crystallinity.

The peaks obtained on the powder photographs and diffractograms were compared against those given for recognised minerals in the ASTM index.

(iii) Problems of Identification of  $\delta$ -MnO<sub>2</sub> in Samples containing Todorokite

$\delta$ -MnO<sub>2</sub> exhibits only two lines, the most intense of which is a broad peak at about 2.44Å. This corresponds to, and tends to overlap, the peaks of todorokite at 2.46Å and 2.39Å which are often faint and broad. The other  $\delta$ -MnO<sub>2</sub> line, at 1.42Å, also coincides with the 1.42Å peak of todorokite which again is often fairly faint and broad. Thus identification of  $\delta$ -MnO<sub>2</sub> in samples which also contain todorokite is made extremely difficult using the criteria of the simple presence or absence of peaks. In order to ascertain whether  $\delta$ -MnO<sub>2</sub> was present in samples in addition to todorokite a comparison of shape and intensity of peak heights was carried out in the following way.

Two samples were selected which from the nature of their diffractogram were assumed to contain abundant todorokite only. These were sample AB375G(b) (see Table 4 in Section 4) and a terrestrial sample of todorokite from Fiji. The shapes of the diffractograms of these samples at around 1.40Å - 1.50Å and 1.35Å - 1.45Å were then copied onto tracing paper for use as overlays. Similar tracings were made from two samples showing no lines other than at 2.45Å and 1.42Å, and therefore assumed to contain  $\delta$ -MnO<sub>2</sub> only (samples SH1301D(a) and SH1317D). By comparing the diffractograms of other samples with these four it was then possible to distinguish between the presence of todorokite only and of todorokite plus  $\delta$ -MnO<sub>2</sub>.